Freie Universität Berlin

Phosphinines as platforms for the design of new phosphorus-based ligands

Inaugural-Dissertation

to obtain the academic degree
Doctor rerum naturalium (Dr. rer. nat.)

submitted to the Department of Biology, Chemistry and Pharmacy
of Freie Universität Berlin

by

M. Sc. Massimo Rigo

from Trieste, Italy

June, 2017

The described work was carried out within the time period of November 2013 until May 2017 under the supervision of Prof. Dr. Christian Müller at the Freie Universität Berlin. The project is part of SusPhos: "A European Training Network for Sustainable Phosphorus Chemistry" funded under the Marie Curie Initial Training Network of the European Commission (Marie Curie ITN SusPhos, Grant Agreement No. 317404). Within this project, two secondments were undertaken in the groups of Prof. Dr. Hansjörg Grützmacher at ETH Zürich and Prof. Dr. Paul Pringle at the University of Bristol.

1. reviewer: Prof. Dr. Christian Müller

2. reviewer: Prof. Dr. Biprajit Sarkar

Date of the defense: 21.07.2017

To my brother

“This could really be a good life”

Emma Svensson Akusjärvi

Declaration

I herewith confirm that I have prepared this dissertation without the help of any impermissible resources. All citations are marked as such. The present thesis has neither been accepted in any previous doctorate degree procedure nor has it been evaluated as insufficient.

Massimo Rigo

Berlin, June 2017

Acknowledgements

This work would not have been possible without the help and support of various people.

First of all, I want to thank Prof. Dr. Christian Müller for giving me the opportunity to join his group at the end of 2013. In these years I learnt a lot about many things, and I am very grateful for his advice and support in any occasion. I had the freedom to try my own ideas and the support I needed when I was lost. The PhD was an incredible experience for me and I only have good memories about it.

I thank Prof. Dr. Biprajit Sarkar for being the second reviewer of this work and taking the time to read it. Also, I am grateful to him for the joint venture in the world of Au-catalysis.

Prof. Dieter Lentz and Dr. Simon Steinhauer are kindly acknowledged for sharing their deep understanding of crazy things and for always (unintentionally) reminding me how ignorant I am. Thanks to Dr. Adelheid Hagenbach, who sometimes helped me at the diffractometer.

Prof. Dr. Barbara Milani and Prof. Dr. Elisabetta Iengo are heartily acknowledged for luring me into doing a PhD.

Prof. Dr. Chady Irigo is kindly acknowledged for fruitful discussions.

Dr. Jelena Wiecko is gratefully acknowledged for being always there and shielding and protecting us like a mom.

To Antonia I am extremely thankful for many reasons. You shared with me this journey throughout the PhD more than anyone else. Thanks for hating bad food as much as I do and for being in the cooking group from the very beginning. Even now that everybody else left, we are still trying to cook and eat together. I will miss our lunches and long tea-breaks. Thanks as well for proof-reading the whole manuscript without complaining. You're the one to blame if there are typos left.

I'm thankful to Marlene for being part of the cooking group and for making me feel less lonely among all those Germans. Un beso a Matiaak!

Fanni is gratefully ackowledged for making me understand what "being professional" means, for being overly politically correct and for reminding me that greek food is heavy on my stomach.

Thanks to Julian, Marija, Gregor, Martin, Steven, Daniel, Friedrich, Cathérine and all the students and visiting students for the nice time spent in the group. Among these I want to mention Philipp, my first labmate. Thank you for helping me with my first steps in the lab, I guess you saved me from a couple of fires.

A big thanks goes to the students I supervised, and whose results are included in this manuscript: Nils, Florian, Je-Ryun and Brian. Special thanks goes to Merlin, a very brilliant student from whom I learned a lot of things I was supposed to know already. Please don't do a PhD in total synthesis, do something more cool.

I thank Markus and Dorian for helping with everyday issues and providing the group with huge amounts of $P(TMS)_3$. Manuela Weber is kindly acknowledged for solving almost all the crystal structures and for intruducing me to X-ray diffraction.

I am extremely grateful to Chris Slootweg for building up SusPhos. Besides funding my PhD position, this project allowed me to meet amazing people from all over the world and establish (hopefully) long-lasting friendships and collaborations. In fact, a big deal of this work has been possible only thanks to Susphos. Tetiana Krachko, Evi Habraken, Andreas Ehlers and Chris Slootweg are kindly acknowledged for performing the DFT calculations and Koyel Bhattacharyya and Nicolas Mézailles for synthetic input. Everybody in the Susphos family is gratefully acknowledged. In particular Paul Pringle and Hansjörg Grützmacher for hosting me in their groups for a little while. Riccardo Suter and Mark Bispinghoff are especially acknowledged for the good time in Zürich playing with sodium phosphaethynolate.

Of course I also want to thank all my friends and family.

A big thanks goes to Emma "Big Sven", for being amazing and sharing with me her deep interest and knowledge in beer drinking. Thanks also to Johannes and Liam for the good time we had together in Germany and Italy (coi controcazzi).

Thanks to all the italian crowd with which I had the pleasure to share amazing time, food and wine. Mostly wine (yes, Puppo, I'm talking about you). Thanks also to the Muloni vari, in particular to Enrico. In another life we will get married.

I want to thank all the flatmates that cheered me up when I got back from tough working days: Manu, Mazen, Kathrin, Imke, Chloe, Timo, Rick and Alex. However, Manu could have cleaned a bit more.

Friends in Trieste are kindly ackowledged for making an effort in partying harder when I was coming back home. Italo, te nomino solo a ti cussì te son contento.

Last but not least, vorrei ringraziare la mia famiglia. Grazie per essermi stati vicino in questi anni e per aver sopportato la mia sbadatezza nel farmi sentire al telefono. Vi voglio bene.

Ah si, grazie anche a Elena.

Abstract

This work has been carried out within the frame of the Susphos project. SusPhos: "A European Training Network for Sustainable Phosphorus Chemistry" is an Initial Training Network funded by the Marie Curie Actions of the European Commission. The explicit objective of SusPhos is the recycling, reuse and minimization of phosphorus waste by converting it back to the chemical feedstock. Each of the partners involved had to tackle this challenge according to its expertise. The main focus of the Müller group is the development of new phosphorus containing molecules, to be used in minute quantities as ligands in homogeneous catalysis. The longstanding experience of the group in phosphinine ligands spontaneously led to further exploration of the chemistry of these and related compounds.

In this respect an improved synthesis of phosphinines is presented at the beginning of the work, aimed at a more phosphorus-economic synthetic process. Starting from pyrylium salts, the use of a strong nucleophile in the O^+/P exchange in combination with salt elimination resulted in higher yields (Scheme 1).

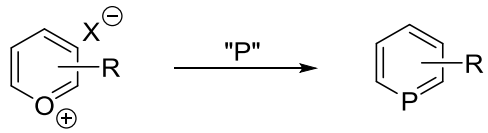

Scheme 1. O^+/P exchange of pyrylium salt to phosphinine.

New phosphabarrelene derivatives have been synthesized via [4+2] cycloaddition reaction between a phosphinine ring and an alkyne, namely hexafluoro-2-butyne or *in situ* generated benzyne (Scheme 2). Different benzyne precursors were tested, in order to establish new functional group tolerant pathways.

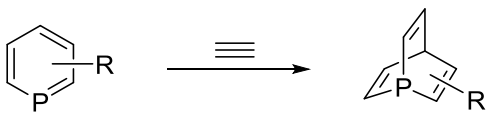

Scheme 2. [4+2] cycloaddition of a phosphinine to a phosphabarrelene.

Some phosphabarrelene derivatives showed to be prone to cycloreversion reactions, yielding new phosphinine derivatives. Among these, an electron-poor phosphinine was employed in the activation of small molecules at the low-coordinate P center.

New metal complexes have been obtained using phosphinine and phosphabarrelene ligands, expanding the rather unexplored coordination chemistry of these compounds.

5-Phosphasemibullvalene derivatives have been described for the first time, and were obtained by photoisomerization of phosphabarrelenes (Scheme 3). The mechanism of the reaction was investigated by means of DFT calculations and experimentally confirmed.

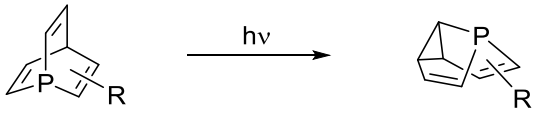

Scheme 3. Photoisomerization of phosphabarrelene to phosphasemibullvalene.

The substrate scope of the reaction and its selectivity have been investigated by changing the substituents on the ligand backbone.

An extensive characterization of the electronic and steric properties of phosphinines, phosphabarrelenes and phosphasemibullvalenes is presented. This is based on experimental data obtained from the infrared spectra of Ni(0) complexes and from theoretical calculations. Finally the three ligand classes have been employed for the first time in Au(I) catalyzed reactions. The catalytic cycloisomerization of propargyl amides was successfully achieved and the ligands proved to be suitable for the preparation of very active and selective catalysts.

Kurzbeschreibung

Diese Arbeit wurde im Rahmen des Susphos Projekts durchgeführt. Susphos: “A European Training Network for Sustainable Phosphorus Chemistry” ist ein von den Marie-Sklodowska-Curie-Maßnahmen der Europäischen Kommission gefördertes Ausbildungsnetzwerk, das die Wiederverwendung, das Recycling und die Reduzierung von Phosphor Abfallprodukten durch Umwandlung in das chemische Rohmaterial anstrebt. Die beteiligten Kooperationspartner sind dieser Herausforderung gemäß ihrer Kompetenzen angegangen. In der Arbeitsgruppe Müller liegt das Hauptaugenmerk auf der Entwicklung von neuen auf Phosphor basierenden Molekülen, die in minuziösen Mengen als Liganden in der homogenen Katalyse eingesetzt werden sollen. Die langjährige Erfahrung der Gruppe bezüglich der Phosphinin-Liganden führte spontan zur weiteren Untersuchung der Chemie dieser und ähnlicher Verbindungen.

In dieser Hinsicht soll zu Beginn der Arbeit eine verbesserte Synthese der Phosphinine präsentiert werden, in der die Reaktion durch Reduzierung der phosphorbasierenden Nebenprodukte ökonomischer wird. Ausgehend von Pyryliumsalzen führt die Verwendung von starken Nukleophilen in der O^+/P-Austauschreaktion, in Kombination mit einer Salzeliminierungsreaktion, zu höheren Ausbeuten (Schema 1).

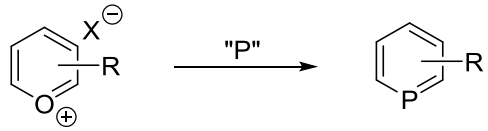

Schema 1. O^+/P-Austauschreaktion eines Pyryliumsalzes zum Phosphinin.

Neuartige Phosphabarrelen-Derivate wurden *via* einer [4+2]-Cycloadditions-Reaktion zwischen einem Phosphinin-Ring und einem Alkin (Hexafluoro-2-butin oder *in situ* gebildetes Arin) synthetisiert (Schema 2). Verschiedene Arin-Vorstufen wurden getestet, um neue Reaktionswege aufzustellen, die unterschiedliche funktionelle Gruppen tolerieren.

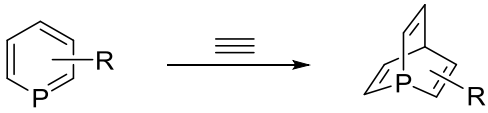

Schema 2. [4+2]-Cycloaddition eines Phosphinins zum Phosphabarrelen.

Einige Phosphabarrelen-Derivate zeigten eine Anfälligkeit für Cycloreversion-Reaktionen, die zu neuartigen Phosphinin-Verbindungen führte. Unter diesen wurde ein elektronenarmes

Phosphinin in der Aktivierung von kleinen Molekülen am niederkoordinierten Phosphorzentrum eingesetzt.

Die eher unerforschte Koordinationschemie der Phosphinin- und Phosphabarrelen-Liganden konnte durch die erfolgreiche Synthese entsprechender Metallkomplexverbindungen erweitert werden.

5-Phosphasemibullvalen-Derivate, die durch Photoisomerisierung von Phosphabarrelenen synthetisiert wurden, konnten erstmalig in dieser Arbeit beschrieben werden (Schema 3). Der Reaktionsmechanismus wurde mittels DFT-Berechnungen untersucht und konnte experimentell bestätigt werden.

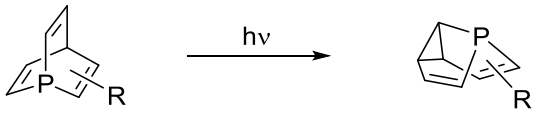

Schema 3. Photoisomerisierung eines Phosphabarralens zum Phosphasemibullvalen

Die Reaktivität und die Selektivität der Reaktion wurden untersucht, indem verschiedene Substituenten im Liganden eingebaut wurden.

Eine umfangreiche Charakterisierung der elektronischen und sterischen Eigenschaften der Phosphinine, der Phosphabarrelene und der Phosphasemibullvalene wird präsentiert. Diese basieren auf experimentelle Daten der infrarotspektroskopischen Untersuchungen von Ni(0)-Komplexen und auf theoretischen Berechnungen. Abschließend wurden die drei Ligandenklassen erstmals in Au(I) katalysierten Reaktionen eingesetzt. Die katalytische Cycloisomerisierung von Propargylamiden war erfolgreich und die Liganden erwiesen sich für die Darstellung von sehr reaktiven und selektiven Katalysatoren als geeignet.

List of Publications

"2,4,6-Triphenylphosphinine and 2,4,6-triphenylphosphabarrelene revisited: synthesis, reactivity and coordination chemistry" - M. Rigo, J. A. W. Sklorz, N. Hatje, F. Noack, M. Weber, J. Wiecko, C. Müller, *Dalton Trans.* **2016**, *45*, 2218.

"Expanding the Phosphorus-Carbon Analogy: Formation of an Unprecedented 5-Phosphasemibullvalene Derivative" - M. Rigo, M. Weber, C. Müller, *Chem. Commun.* **2016**, *52*, 7090.

"Phosphinines versus Mesoionic Carbenes: A Comparison of Structurally Related Ligands in Au(I)-Catalysis" - M. Rigo, L. Hettmancyzk, F. J. L. Heutz, S. Hohloch, M. Lutz, B. Sarkar, C. Müller, *Dalton Trans.* **2017**, *46*, 86.

Manuscripts in preparation

"Phosphinines, phosphabarrelenes and phosphasemibullvalenes: a comparison study on electronic properties and catalytic activity" - M. Rigo, M. Kleoff, M. Weber, J. A. W. Sklorz, E. R. M. Habraken, A. W. Ehlers, J. C. Slootweg, K. Bhattacharyya, N. Mézailles, C. Müller.

"Investigating the synthesis of 5-Phosphasemibullvalenes: an experimental and theoretical study" - M. Rigo, M. Kleoff, D. Frost, M. Weber, T. Krachko, E. Nicolas, K. Bhattacharyya, C. Slootweg, N. Mézailles, C. Müller.

Table of Abbreviations

Ac	Acetate
Ar	Aryl
δ	Chemical shift
d	doublet
DCM	Dichloromethane
DFT	Density functional theory
DMDA	Dimethyl acetylenedicarboxylate
DME	Dimethoxyethane
DMS	Dimethyl sulfide
ee	Enantiomeric excess
Et	Ethyl
exc	Excess
h	Planck constant
HOMO	Highest Occupied Molecular Orbital
HPLC	High Performance Liquid Chromatography
HSAB	Hard-Soft Acid-Base
Hz	Hertz
*i*Pr	*Iso*-Propyl
IR	Infrared
IUPAC	International Union of Pure and Applied Chemistry
J	Coupling Constant
λ	Wavelength
LUMO	Lowest Unoccupied Molecular Orbital
m	multiplet
m-	Meta

mbar	Millibar
Me	Methyl
MeCN	Acetonitrile
MHz	Megahertz
MO	Molecular Orbital
v	Frequency
*n*Bu	*n*-Butyl
NHC	N-heterocyclic carbene
NMR	Nuclear Magnetic Resonance
o-	Ortho
p-	Para
Ph	Phenyl
ppm	Parts per million
quin	Quintet
rt	Room temperature
s	singulet
t	triplet
*t*Bu	*tert*-Butyl
THF	Tetrahydrofuran
TEP	Tolman Electronic Parameter
Tf	Triflic
TMS	Trimethylsilyl
TOF	Turnover Frequency
TON	Turnover Number
Ts	Tosyl
UV	Ultra Violet
$\tilde{v}$	Wavenumber

Table of Contents

1. Introduction

1.1 Organophosphorus compounds

Organophosphorus compounds are organic molecules containing phosphorus. This molecule class is very wide, since phosphorus can adopt a variety of oxidation states and coordination numbers, and forms stable bonds with different atoms. Organophosphorus chemistry is a rather young discipline which had some major development in the last 50 years, together with the dramatic increase of phosphorus consumption. Most of organophosphorus compounds (mainly organophosphates) are employed in the agricultural and food industry as fertilizers or pesticides, while a minor part is employed in fine chemistry, in applications that are of most interest to scientists.[1]

In this respect, the principal area in which organophosphorus molecules have been employed is organometallic chemistry, specifically as ligands in homogeneous catalysis, and in the preparation of so-called molecular materials.[2–5]

The continuously growing importance of transition metal catalysis is evidenced by the recent awards of three Nobel prizes in 2001, 2005 and 2010. In these examples and generally in this field, phosphorus ligands are ubiquitous. Their electronic and steric properties can be finely tuned by choosing the right substituents on the phosphorus atom, making them extremely versatile platforms. Also, new and desirable characteristics such as redox-properties or chirality can be implemented in the ligand framework, resulting in unprecedented reactivity.[6,7] Nowadays, an incredible variety of these ligands is employed in any kind of catalytic process, from the megaton production of commodity chemical to the milligram quantities of natural products.[2,8,9] More recently, aside from metal-complexes, some phosphorus-containing molecules have been employed in (asymmetric) organocatalysis.[10–13]

However, organometallic chemistry is not limited to ligand synthesis and design. The development of new phosphorus-based systems to be employed in new electronic materials is an intriguing challenge. New, metal-free devices featuring conducting or light-emitting organic materials have been studied extensively in the last decades and are still a hot topic.[5,6,14] Many of these systems are based on molecules containing an extended π–system, which allow for high charge carrier mobility and a small HOMO-LUMO gap. At the same time, the incorporation of heavier main group elements in the π-framework is a winning strategy for the modification and enhancement of these properties. Following this principle, in

the last decades a large amount of phosphorus-containing organic emitters and optically active derivatives was synthesized.[14–21]

1.2 The phosphorus-carbon analogy

Phosphorus has been for long regarded as a chemical chameleon, thanks to its unique similarity to the adjacent atoms in the periodic table.[22] Although phosphorus is the higher homologue of nitrogen, some of its properties resemble more those of silicon,[23–25] some those of carbon[26] and some other are unique. Interestingly, the clearest resemblance is the one with carbon, with which there is a diagonal relationship. Carbon and phosphorus have similar Pauling electronegativity values (2.55 for C and 2.19 for P, respectively) and van der Waals radii (1.70 Å for C and 1.80 Å for P, respectively).[27] The similar chemical properties lead to strong covalent carbon-phosphorus bonds (bond dissociation energies; C-C 605 and P-C 507.5 $kJmol^{-1}$).[27] Therefore the reactivity of the two elements is much more similar than the reactivities of carbon and silicon.

This in mind, it appears clear why a common strategy for the synthesis of new phosphorus-containing compounds is to mimic the chemistry of carbon, which has been more widely explored in the last centuries. In fact, this analogy enables the synthesis of a great number of organophosphorus compounds, in which P-lone pair fragments substitute C-H moieties thanks to the isolobal equivalence between these two units (Figure 1).[26] The same applies to compounds having valence isoelectronic C or P^+ moieties.

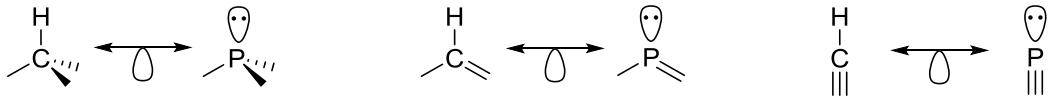

Figure 1. Isolobal analogy between C-H and P-lone pair fragments.

Even though the relationship has been mainly observed for molecules containing phosphorus in coordination numbers one and two (low-coordinate species), also examples with higher coordination numbers are reported.[26,28] This approach allowed for the synthesis of different organophosphorus molecules, a few examples are reported in Figure 2.[26]

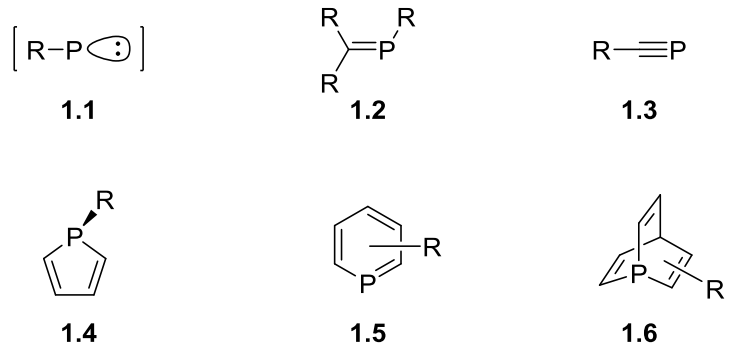

1.1 **1.2** **1.3**

1.4 **1.5** **1.6**

Figure 2. General structures of different linear and cyclic organophosphorus molecules.

Most of these molecule classes have been studied extensively and several publications describe their reactivity and their properties.[26] Phosphinidenes (**1.1**) are the phosphorus analogues of carbenes and nitrenes. They are transient species and have almost exclusively been trapped or stabilized by bulky groups, such as NHCs or metal fragments. [26,29,30] The first phosphinidene derivative which is stable at room temperature has been recently reported by Bertrand and co-workers.[31]

Phosphaalkenes and phosphaalkynes (**1.2** and **1.3**, respectively) also have an extremely rich chemistry. Their coordination properties and reactivity (mostly cycloadditions) mimic the one of alkenes and alkynes, as anticipated by the phosphorus-carbon analogy.[26,32–34] They have been used extensively as building blocks for the synthesis of phosphorus-containing heterocycles, such as phospholes (**1.4**) or larger ring systems.[22]

Phospholes are phosphorus-containing 5-membered rings and the higher homologues of pyrroles. These molecules sometimes exhibit peculiar optical properties thanks to the presence of the heteroatom. The coordination chemistry is quite rich, but mostly they found application in the preparation of monomeric and polymeric light-emitting materials.[16,28,35]

Also phosphinines (**1.5**) are known for many decades.[36] Among their properties, it is worth to mention the reactivity towards activated alkynes, which leads to the formation of phosphabarrelenes (**1.6**).[37] These two molecules are the phosphorus-containing analogues of benzene and barrelene. The presence of a lone pair on the heteroatom makes them potential ligands in organometallic chemistry and a few examples of phosphinine- and phosphabarrelene-based catalysts have been reported.[8,9] These two molecule classes, their properties, coordination chemistry and applications will be extensively introduced in the following chapters.

1.3 Scope of this Work

While the chemistry of phosphines and other P(III) species has been studied for a long time and these ligands have found application in many fields, the chemistry of phosphinines and phosphabarrelenes is much less explored. Even though they are known for decades, they have been regarded as chemical curiosities for a long time, and their organometallic chemistry has been only poorly investigated. For this reason, it is important to investigate the chemistry of these compounds, which has shown very unpredictable and surprising results.

Since the reaction pathways that lead to the formation of phosphinines are sometimes complex and have low yields, the first objective of this work is the improvement of the synthesis, in order to have easier access to larger amounts of phosphinines and phosphabarrelenes through a more atom-economic synthetic process.

These peculiar compounds have unprecedented characteristics and it has become of interest to study their electronic and steric properties, in order to better understand and predict their behavior as ligands in homogeneous catalysis. Phosphinines are expected to be strong π-acceptors, even though an in-depth study on their electronic properties is still missing in the literature. Even less is known about the electronic properties of phosphabarrelenes. An extensive study and a comparison between the electronic and steric properties of these related ligand classes is the objective of this study.

Finally, since only a few catalytic applications are reported for these ligands, it is important to extend the scope of their metal complexes by applying them in new catalytic reactions. The ligands will be used in the synthesis of [LAuCl] complexes, which will be tested as (pre)catalysts in cycloisomerization reactions. The supposedly strong π-accepting properties of these ligands are expected to be a crucial characteristic for the formation of a strongly electrophilic gold center, which is fundamental for the successful conversion of the substrates. The study of the electronic and steric properties is important for the understanding of the relationship between the electronic properties and the catalytic activity.

2. Phosphinines

Part of this chapter has been published in:

"2,4,6-Triphenylphosphinine and 2,4,6-triphenylphosphabarrelene revisited: synthesis, reactivity and coordination chemistry" - *M. Rigo, J. A. W. Sklorz, N. Hatje, F. Noack, M. Weber, J. Wiecko, C. Müller, Dalton Trans.* ***2016****, 45, 2218.*

2.1 Introduction

Phosphinines are aromatic, 6-membered heterocycles containing one phosphorus atom. These molecules are the first example in which a P=C double bond has been included in an aromatic system. Interestingly, they are among the first compounds to violate the double bond rule, which states that multiple bonds with elements of the third period or higher are not stable.[38] Usually they are referred to as $\lambda^3\sigma^2$-phosphinines according to the IUPAC nomenclature, where the descriptors λ and σ stand for the valency and the coordination number of the phosphorus atom, respectively.

The first derivative that has been described in the literature is 2,4,6-triphenylphosphinine **2.1**, which was synthesized in 1966 by Märkl.[36] The parent compound C_5H_5P **2.2** was reported a few years later in 1971 by Ashe III (Figure 3).[39]

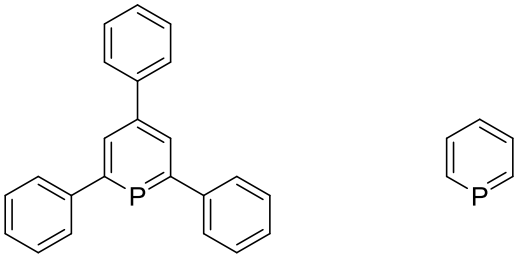

2.1 **2.2**

Figure 3. The first $\lambda^3\sigma^2$-phosphinine derivative (**2.1**) and the parent compound (**2.2**).

2.1.1 Electronic and Steric Properties

These heterocycles, also known as phosphabenzenes or phosphorins, are closely related to their carbon- and nitrogen-containing counterparts. In fact, similarly to benzene and pyridine, they are planar, aromatic and follow Hückel's rule. The aromaticity of phosphinine has been confirmed by theoretical investigations. In particular, according to bond separation methods, the aromaticity of phosphabenzene is as high as 88% of benzene, which was suggested by chemical hardness calculations.[40,41] Also Nuclear Independent Chemical Shift (NICS) calculations confirmed the aromaticity of the compound, resulting in a value of -10.2 (-11.5 and -10-6 for benzene and pyridine, respectively).[42]

These findings are endorsed by the structural characteristics of these compounds. As shown in the molecular structures of several derivatives, there is no alternation in the bond lengths between the C-C or the P-C bonds. In addition to this, the P-C bonds are elongated to about 1.75 Å, which lays in between the lengths of typical P–C single bonds (PPh_3: 1.83 Å) and P=C double bonds (diphenylmethylenephosphaalkene: 1.66 Å).[43] Experimentally, the aromaticity is confirmed by the NMR spectra, where all the resonances are typically found in the downfield area.

The poor ability of phosphorus to hybridize, together with the larger atomic radius, causes a decrease of the C-P-C angle to about 100°, closer to the angle of 90° between unhybridized p-orbitals, resulting in a distorted hexagon shape of the heterocycle.

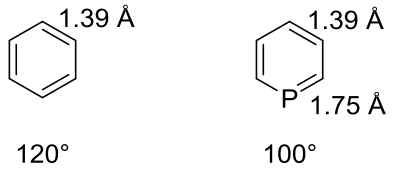

Figure 4. Average bond lengths and angles in benzene and phosphinine.

As phosphinines are the heavier homologues of pyridines, it is interesting to compare the respective electronic properties, which are summarized in the molecular orbital (MO) diagram (Figure 5).[44,45] The lone pair of the heteroatoms is best described by the HOMO in the case of pyridine and by the HOMO-2 in case of phosphinine. Also, the orbital on the phosphorus is more diffuse and less directional. This is reflected by the calculated value for the s-character of the lone pairs on the nitrogen and on the phosphorus atoms, which is 29.1% and 63.8%, respectively.[42] Consequently, phosphinines show a very low basicity in aqueous solutions with a pK_a ($C_5H_6P^+$) = 16.1 ± 1.0 (pK_a ($C_5H_6N^+$) = 5.23).[46] In addition to this, the LUMO of phosphinine, which has π-symmetry, is much lower in energy compared to its nitrogen counterpart. It follows that phosphinines are weaker σ-donors and stronger π- acceptors compared to pyridines. Finally, the HOMO and HOMO-1 of phosphinine can in principle contribute in π-donation due to their symmetry. By introducing electron-donating substituents on the periphery of the phosphinine ligand, this property can be enhanced.[47]

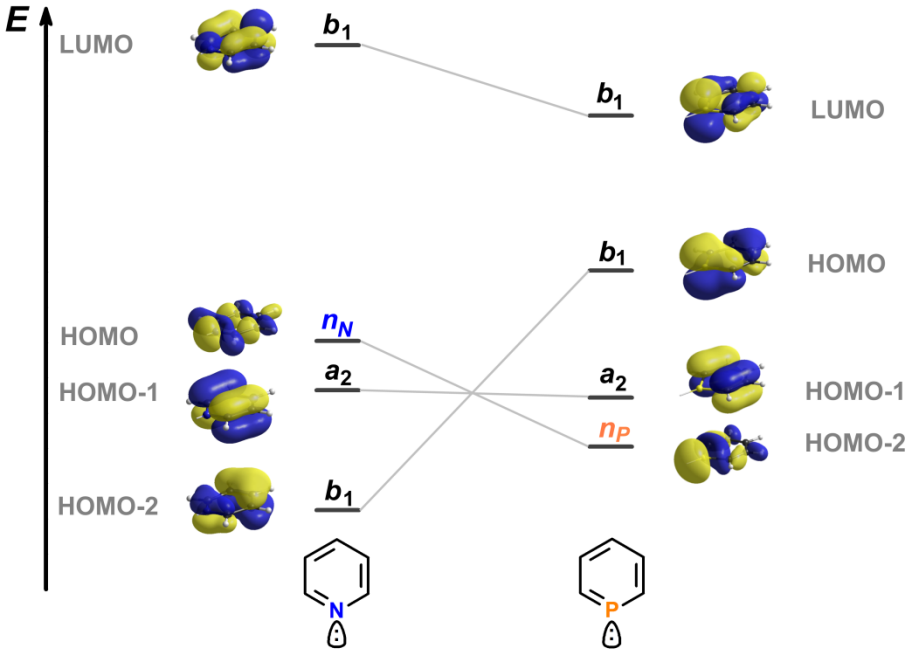

Figure 5. Simplified MO diagram of the frontier orbitals of pyridine (left) and phosphinine (right).[48]

Regarding the steric properties, phosphinines are quite different from classical P(III) ligands. Usually, the steric bulk of these compounds is evaluated using Tolman's cone angle θ. This is defined as the apex angle of a cylindrical cone, centered at 2.28 Å from the P atom, which just touches the van der Waals radii of the outermost atoms of the ligand.[49] Since phosphinines are rather flat heterocycles, a different descriptor is needed to better define their anisotropic steric demand. In this respect, the occupancy angles α and β are commonly used. These evaluate the steric bulk on the planes x and y, respectively (Figure 6).[49–51]

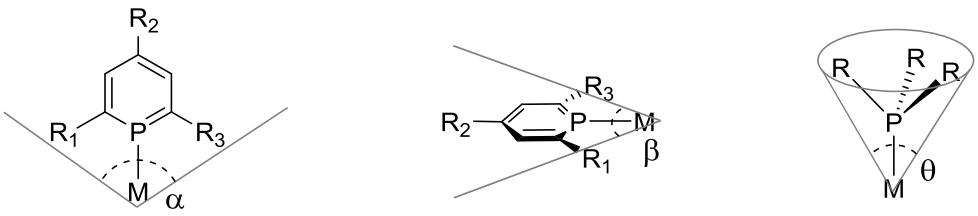

Figure 6. Steric bulk of phosphinines compared to common P(III) ligands.

2.1.2 Synthesis

Nowadays several procedures allow for the synthesis of a large variety of differently substituted phosphinines. Here only three methods will be introduced; the others are extensively described in the literature.[9,28,52]

The first methodology is the so-called pyrylium salt route, which was reported in 1966.[36] The reaction proceeds *via* O^+/P exchange performed by a phosphorus-containing nucleophile (Scheme 1). The first step is believed to be the attack of the phosphorus nucleophile to the α-carbon atom of the pyrylium salt with subsequent ring-opening. A rearrangement followed by a ring-closure completes the formation of the aromatic phosphorus-heterocycle.[53]

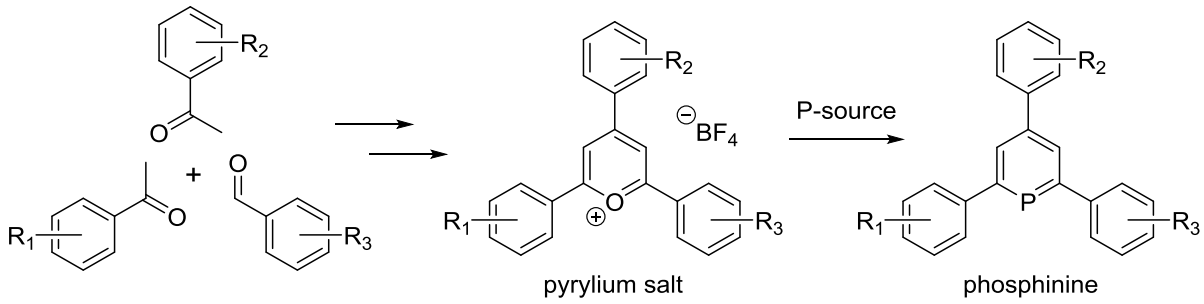

Scheme 1. Synthesis of pyrylium salts and phosphinines.

The first reported phosphinine **2.1** was prepared from 2,4,6-triphenylpyrylium tetrafluoroborate and $P(CH_2OH)_3$ in refluxing pyridine, and was obtained as a yellow air- and moisture-stable solid in 24-30% yield.[36] Alternatively, $P(TMS)_3$ in refluxing acetonitrile can be used as phosphorus source, leading to only slightly higher yields and to hexamethyldisiloxane (TMS-O-TMS) and Me_3SiBF_4 as byproduct.[53] Apparently, exchanging BF_4^- by I^- in the pyrylium salt leads to even higher yields (45%).[51] Despite its hazardous nature, pressurized PH_3 in an autoclave reaction gives pure **2.1** in 77% yield after recrystallization and only H_2O as by-product.[54–56] Similarly, performing the O^+/P exchange with PH_4I as *in situ* PH_3-source in butanol, **2.1** is obtained in 61% isolated yield.[57] PH_4I is, however, not commercially available anymore. For the preparation of the alkyl-substituted 2,4,6-tri-*tert*-butylphosphinine the salt $Li[P(SiMe_3)_2]$ was employed, yielding 75% of product.[58]

The advantage of this synthetic path is the versatility. Pyrylium salts have been deeply investigated in the past century and they can be easily prepared with different arylic and alkylic substituents on the pyrylium ring.[59]

A different pathway, useful to access low-substituted phosphinines, was reported for the first time by Regitz *et al.* in 1986.[60,61] Phosphaalkynes were employed as dienophiles in [4+2] cycloaddition reactions with cyclopentadienones or pyrones to obtain alkyl-substituted phosphinines after exclusion of CO or CO_2, respectively (Scheme 2).

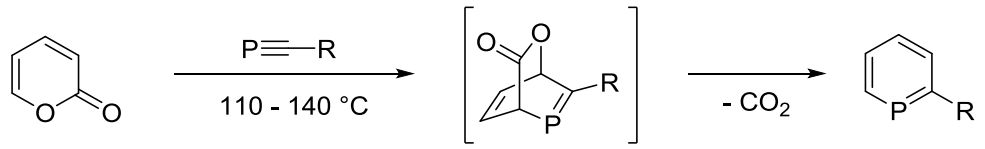

Scheme 2. [4+2] cycloaddition reaction between pyrone and a phosphaalkyne.

The same concept was applied by Grützmacher *et al.* using sodium phosphaethynolate (NaOCP) as dienophile, obtaining phosphinine-2-olate and 2-hydroxyphosphinine.[62] These have subsequently been used as platforms for the preparation of bidentate ligands.[63] Similarly, Müller *et al*. reported on the cycloaddition of TMS-C≡P with bromo-substituted pyrones to yield bromo-phosphinines, that can be used as substrates for cross-coupling reactions.[64] These reactions tend to have high yields, but as a drawback the number of available phosphaalkynes is rather limited.

The diazaphosphinine route was developed by Mathey *et al.* exploiting the peculiar reactivity of azaphosphinines such as **2.3**.[65–67] The reaction proceeds *via* two subsequent cycloaddition-cycloreversion steps, with the elimination of two equivalents of pivaloylcyanide (Scheme 3).

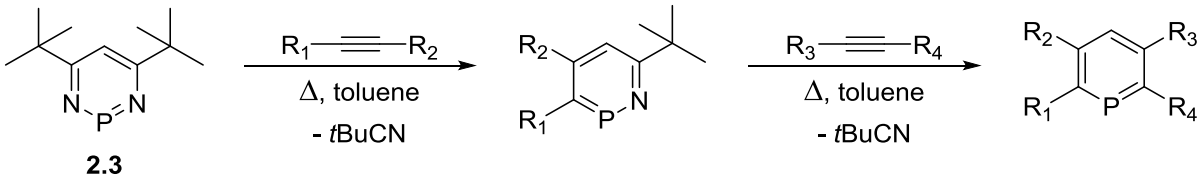

Scheme 3. Synthesis of phosphinines *via* the diazaphosphinine route.

As in the case of the pyrylium salt route, this reaction allows for the customized introduction of substituents on the phosphinine ring, since two different alkynes can be employed.

2.1.3 Reactivity

As stated above, phosphinines have rather different properties compared to their lighter homologues. Some reactions summarizing their peculiar reactivity are reported in Scheme 4.

Due to the low basicity, phosphinines can be protonated only by very strong, non-oxidizing acids with weakly coordinating anions. The only example reported in literature is **2.4**.[68] A large number of oxidized derivatives has been obtained. Phosphinine oxide has been detected but could not be isolated due to its high sensitivity.[69] Oxidation with H_2O_2 leads to the

formation of a 2-hydro-phosphinic acid derivative (**2.5**).[70] Oxidation with $Hg(OAc)_2$ in the presence of alcohols yields highly fluorescent λ^5-phosphinines like **2.6**. Diols and diamines can also be employed.[71,72] Moreover, several phosphinines have been oxidized by heating up their toluene solutions in the presence of elemental sulfur (**2.7**).[73,74] Phosphinine-selenides are, on the other hand, still unknown. The oxidation can also be achieved using halogens, obtaining products, such as **2.8** (X = Cl, Br).[75,76] One electron reduction and oxidation products have also been reported for phosphinines.[70,77–80]

The difference in electronegativity between carbon, phosphorus and nitrogen (Pauling electronegativities: 2.2 for P, 2.5 for C, and 3.0 for N)[27] results in an opposite charge distribution in pyridines and phosphinines, which present electrophilic character at the P atom. Hence, the reaction with strong nucleophiles, like Grignard or organolithium reagents, yields (1*R*)-phosphahexadienyl anions of the type **2.9** (also called λ^4-phosphinines).[81,82] Phosphininium cations, such as **2.10**, have been prepared by treating a λ^4-phosphinine with hexachloroethane and subsequently abstracting a chloride with $GaCl_3$.[83]

Finally, and most interestingly for this work, phosphinines also undergo [4+2] cycloadditions with activated alkynes to yield phosphabarrelenes, as in the case of **2.11**. This will be the topic of Chapter 3.

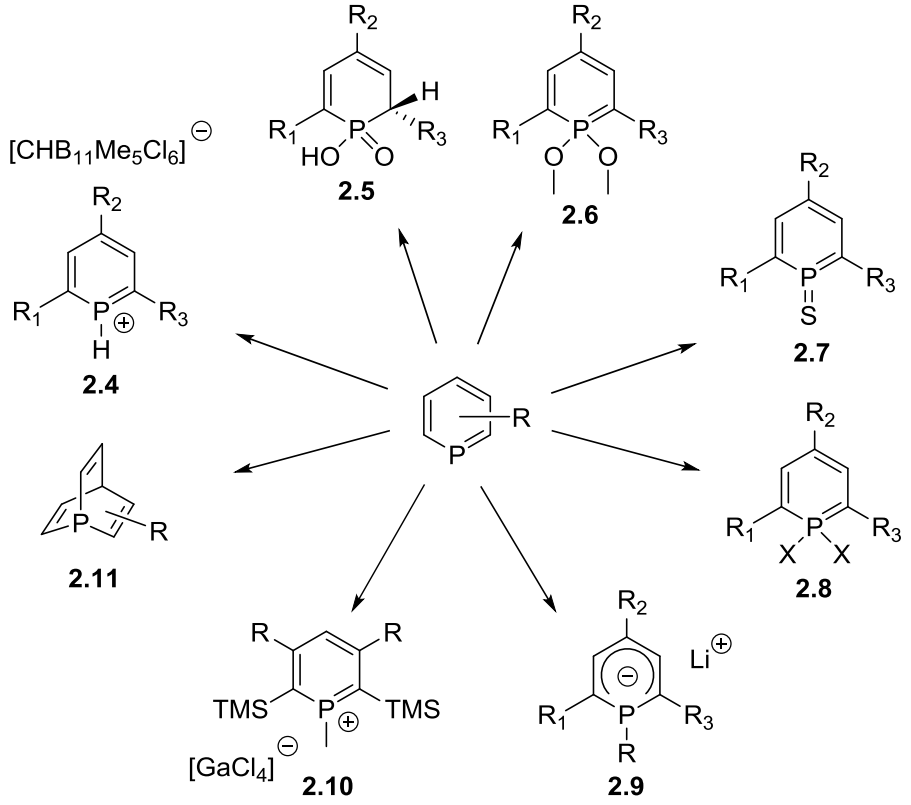

Scheme 4. Reactivity of phosphinines.

2.1.4 Coordination Chemistry

Thanks to their unique electronic and steric properties phosphinines show a rich coordination chemistry towards transition metals.[45,84–88] Interestingly, they are ambidentate ligands being able to coordinate to metal centers *via* the lone pair on the phosphorus atom or *via* the aromatic π-system. For this reason, different coordination modes and their combinations have been observed in transition metals complexes (Figure 7).

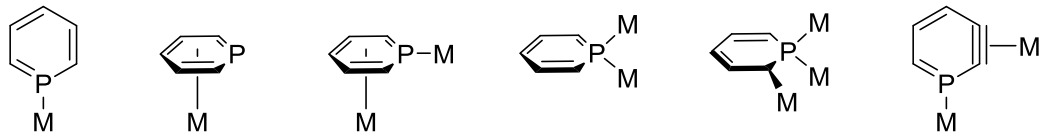

Figure 7. Coordination modes of $\lambda^3\sigma^2$-phosphinines.

The most common is the η^1-coordination *via* the phosphorus lone-pair and, since the seventies, several examples have been reported in literature.[89,90] The η^6-coordination *via* the π-system mainly occurs with early transition metals, and can be achieved by choosing the right metal-precursor or by using phosphinines bearing sterically encumbered groups on the α-carbons.[91–94] Combinations of these two coordination modes were also reported.[95]

Several examples of phosphinines bridging two or more metal centers are known, mainly in the presence of an additional donor moiety.[96–99] A similar example was described in which a phosphinine ligand bridges two osmium centers and coordinates to an additional metal center *via* the α-carbon under disruption of the aromaticity.[100] Finally also η^2-coordination was observed in a phosphabenzyne-zirconocene dimer.[101]

Remarkably, a common feature of these complexes is the decrease in the aromaticity of the heterocycle upon coordination to a metal center. This way the phosphinine tends to behave more like a phosphacyclohexatriene, being subjected to nucleophilic attacks at the P=C double bond.[98] Still, many interesting metal complexes have been prepared and characterized in the last decades, also showing interesting structures such as coordination polymers[96,102,103] or heterocubane clusters.[104]

2.1.5 Polydentate Phosphinines

In order to facilitate the coordination to a wider range of transition metals, additional donor moieties have been introduced in the phosphinine framework. Thanks to this strategy the stabilization of metal fragments in medium to high oxidation states was achieved, leading to a much broader scope of applications for phosphinines and their corresponding metal complexes.[48,105,106]

The most common combination of donor atoms in this respect is found in PN-hybrid ligands. The combination of a soft phosphorus atom and a hard nitrogen atom in the same chelating ligand has been extensively employed in coordination chemistry. Pyridyl-substituted phosphinines have been reported and metal complexes in both low- and high-oxidation states are known up to now. The first example of this family is the so-called NIPHOS (**2.12**, Figure 8), which was reported by Mathey and co-workers. Due to its sensitivity towards nucleophilic attacks, only a few coordination complexes have been reported.[98,107–109] A chiral version including an oxazoline moiety (**2.13**) was reported later on by Breit and co-workers.[110] Müller *et al*. reported on the synthesis of 2-pyridyl-4,6-diphenylphosphinine (**2.14**), which proved to be quite stable due to the presence of the phenyl group on the 6-position. A number of metal complexes bearing this ligand have been reported.[106,111–115] Similarly, the same group also reported on a PNP terpyridine derivative.[116]

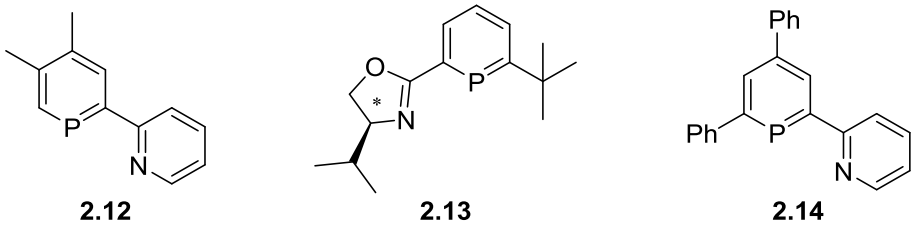

2.12 **2.13** **2.14**

Figure 8. PN-hybrid phosphinine ligands.

Bidentate phosphinines with an additional sulfur atom have also been reported. Thiophene-substituted ligands have been obtained *via* the pyrylium salt route,[106] and SPS pincer-type ligands were prepared *via* the diazaphosphinine route using alkynyl-substituted phosphanes and subsequently oxidizing with elemental sulfur. These derivatives were used in coordination chemistry as anionic ligands (**2.15**) and, interestingly, were able to activate alcohols and amines, likely in a sulfur-assisted mechanism (**2.16**, Scheme 5).[87–90]

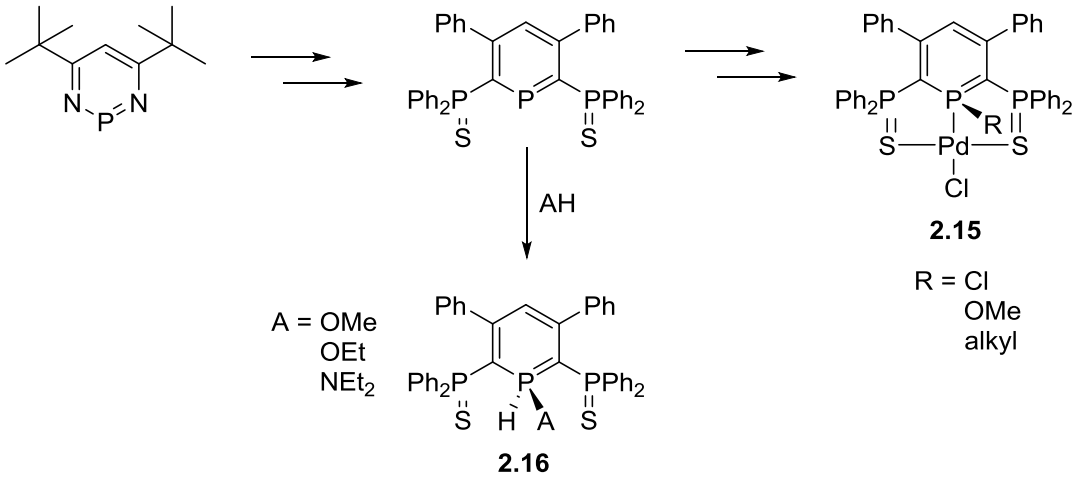

Scheme 5. Synthesis and reactivity of 2,6-bis(diphenylphosphanylsulfide)phosphinine.

Anionic PC-hybrid ligands have been obtained by C-H activation of 2-phenyl-substituted phosphinines (Figure 9). First the ligand coordinates in a η^1-fashion to the metal center and, upon addition of a base, the cyclometalation occurs. These anionic ligands are isoelectronic to the above mentioned PN ligands (**2.14**) and are able to stabilize metals in oxidation states 2 and 3.[121–124]

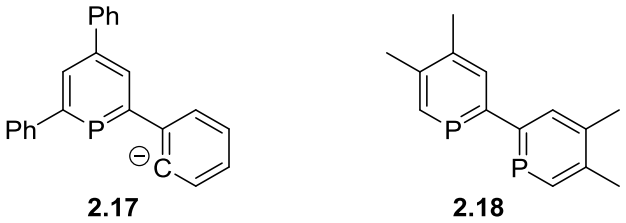

Figure 9. PC-hybrid phosphinine (left) and the first biphosphinine derivative (right).

Biphosphinines have also been reported (Figure 9). Bipyridines, the nitrogen analogs, are a well-established class of ligands, and their applications are ubiquitous in studies of electron and energy transfer, supramolecular and materials chemistry, and catalysis.[125] It is therefore interesting to investigate the properties of the phosphinine analogs, for which a few synthetic procedures have been reported in the last decades.

Most of these compounds have been obtained using 2-bromophosphinines as starting materials. Since in these species there is always a potential competition between the reactivity of the C-Br and P=C bonds, it is advisable to either protect the P=C bond or to activate the C-Br bond. In the first report concerning the synthesis of a biphosphinine, the P=C bond is protected by oxidation with sulfur followed by a [4+2] cycloaddition. A classical C-C-

coupling is subsequently performed and the biphosphinine is then obtained by desulfurization and cycloreversion.[126] A second procedure deals with the Pd-mediated activation of the C-Br bond, using stannylphosphinines as coupling partners in a Stille coupling reaction.[127] The simplest method known is the direct reductive coupling of 2-bromophosphinines with the bulky lithium tetramethylpiperidide (LiTMP).[128] Otherwise double ring expansion methods starting from a biphosphole have been reported. [129]

The most recent procedure to generate biphosphinine is a Ni(II)-promoted homocoupling of (2-phosphininyl)halogenozircocene complexes. In this synthetic approach, a two-step process first involves a double C-Zr to C-Ni bond metathesis, leading to an intermediate Ni(II) complex, followed by a classical reductive elimination favored by the imposed *cis* stereochemistry. Then hexachloroethane can be used to oxidize the Ni-complex, giving free biphosphinine with the concomitant release of [Ni(dppe)Cl_2].[130]

Even though several metal complexes in low oxidation states and metallates have been reported in the literature, a simple and versatile procedure for the synthesis of differently substituted biphosphinines still has to be implemented.[131–134]

2.2 Results and discussion

In this chapter the attempts to improve the synthesis of 2,4,6-triaryl-phosphinines will be presented. In addition to this, new insights in the coordination chemistry of these heterocycles will be given.

2.2.1 Synthesis of 2,4,6-triaryl-phosphinines

Among the reported derivatives with different substitution patterns, 2,4,6-triaryl-phosphinines are remarkably stable and are inert towards water, oxygen and many acids and bases, in contrast to less substituted ones. In addition to this, the pyrylium salt route is a modular approach which allows for the introduction of differently substituted aryl-rings in the phosphinine framework starting from cheap and readily available building blocks. In this

respect, the main drawback is the generally poor yield of the O^+/P exchange, although some progresses have been reported in literature.

To improve the yield of the O^+/P exchange, different phosphorus sources can be tested. According to the proposed mechanism, the reaction starts with a nucleophilic attack to the α-carbon. Consequently stronger phosphorus-nucleophiles, such as phosphides, could result in better yields.[53] At first a "*t*BuONa-coated" version of $NaPH_2$, reported by Grützmacher *et al.* was employed (Scheme 6, a). The reaction was performed in THF at T = -78 °C, and the solution was slowly heated up to room temperature. A ^{31}P NMR spectrum of the reaction mixture showed a quartet at approximately δ = -250 ppm, relative to the formation of PH_3.

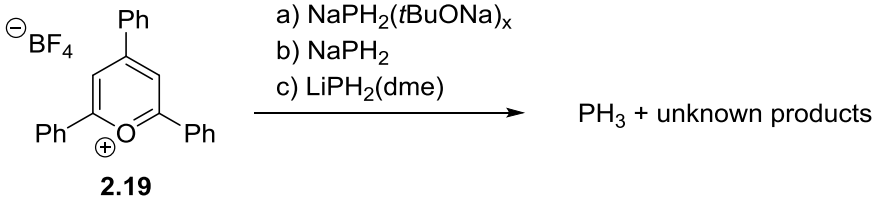

Scheme 6. Reaction between **2.17** and different phosphide sources.

Since the presence of the strong nucleophile *t*BuO$^-$ could affect the outcome of the experiment by reacting with the starting material or the product, the reaction was performed again using "naked" sources of PH_2^-, but unfortunately the same result was obtained (Scheme 6, b and c). It has to be mentioned here that the water formed during the possible reaction between **2.19** and a PH_2^- anion would react with MPH_2 itself, yielding PH_3 and MOH.

Finally, the phosphide sources have been tested with the desired product itself, to verify its stability towards their strong nucleophilicity (Scheme 7). Again, only PH_3 was detected in the reaction mixture by means of ^{31}P NMR spectroscopy.

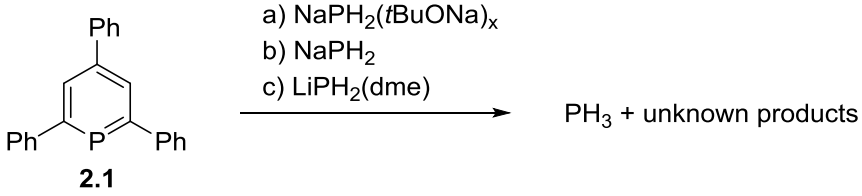

Scheme 7. Reaction between **2.1** and different phosphide sources.

This proves that these phosphides are too basic to be successfully used in this reaction, since they deprotonate and possibly decompose both substrate and product.

At this point, weaker nucleophiles have been employed. Sodium phosphaethynolate (NaOCP) was found to react in many cases as a weak, phosphorus-nucleophile.[135] A sample of **2.17** was treated with a slight excess of NaOCP in different solvents at T = -78 °C (Scheme 8).

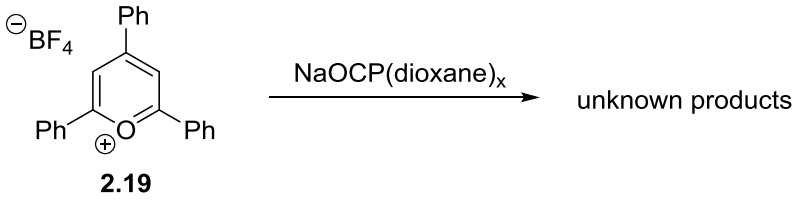

Scheme 8. Reaction of **2.17** with NaOCP.

Unfortunately no resonance was observed in the ^{31}P NMR spectra of the reaction mixture and in one case only an oxidation product of NaOCP was detected. The same reaction was then performed using slightly modified reagents, such as NaSCP and $Ph_3Sn(PCO)$.[135,136] Again, no product was observed in the reaction mixture.

Better results were obtained using $P(TMS)_3$ derivatives. At first $P(SnPh_3)_3$ was tested as a synthetic equivalent of $P(TMS)_3$ in the conversion of pyrylium salt **2.19** to phosphinine **2.1** (Scheme 9).

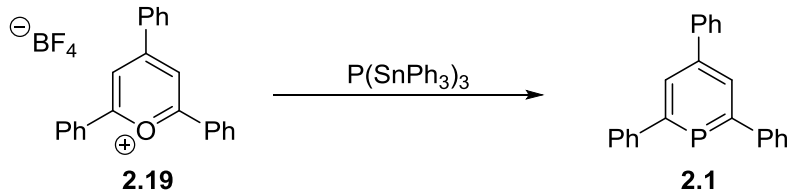

Scheme 9. Synthesis of **2.1** with $P(SnPh_3)_3$.

The reaction was performed in refluxing acetonitrile or THF. In both cases the resonance relative to the starting material slowly decreases while a new resonance rises at around δ = 180 ppm, confirming the formation of phosphinine **2.1**. The reaction seems to stop after 3 days, before full conversion is reached. Unfortunately, the difficult separation did not allow for the isolation of the product. In addition to this, the toxicity of Sn-containing compounds discouraged further attempts in this direction.

Another, more successful attempt was done using more nucleophilic derivatives such as $M[P(TMS)_2]$ (M = alkali metal). In fact, the formation of a MBF_4 salt precipitating from the reaction mixture should favour the formation of the desired heterocycle. $M[P(TMS)_2]$ salts

were prepared according to a literature procedure, by reacting $P(TMS)_3$ with different nucleophiles.[137,138]

An optimization of the conditions has been performed using **2.19** as substrate. The pyrylium salt and $M[P(TMS)_2]$ were put together in a Schlenk flask under an argon atmosphere; the solvent was added and the mixture was heated up for the given time. At the end, all volatiles were removed *in vacuo* and the crude product was eluted through a plug of neutral alumina to afford the pure product as a yellow solid.

The reaction was first examined using $Li[P(TMS)_2]$ in different solvents (Table 1). THF was found to be the most suitable one and reactions in DME and in the solid state also gave good results. MeCN could not be used because it reacted with $Li[P(TMS)_2]$, while **2.19** was completely insoluble in toluene.

Table 1. Choice of the solvent. Conditions: 1 eq. $Li[P(TMS)_2]$, refluxing for 6h.

Solvent	THF	MeCN	DME	Toluene	Solid state
Isolated yield	**56%**	**-**	**44%**	**-**	**48%**

Afterwards, the necessary reaction time was investigated, by running the conversion of **2.19** with $Li[P(TMS)_2]$ under the same conditions for 1 h, 6 h and 16 h, proving that a prolonged reaction does not significantly affect the outcome (Table 2).

Table 2. Choice of the reaction time. Conditions: 1 eq. $Li[P(TMS)_2]$, refluxing in THF.

Time	1 h	6 h	16 h
Isolated yield	33%	56%	55%

Different reaction temperatures have been investigated: an overnight reaction at room temperature and a shorter microwave reaction at T = 100 °C were performed, resulting in lower yields (Table 3).

Table 3. Choice of the temperature. Conditions: 1 eq. $Li[P(TMS)_2]$, THF.

Temperature	16 h, rt	6 h, reflux	3 h, 100 °C
Isolated yield	28%	56%	31%

Different ratios of pyrylium salt/Li[P(TMS)$_2$] were also tested, showing that a 2-fold excess of the phosphorus source results in the highest yield (Table 4).

Table 4. Choice of the ratio. Conditions: Li[P(TMS)$_2$], 6 h, refluxing THF.

Ratio	1 : 1	1 : 1.4	1 : 1.6	1 : 2
Isolated yield	56%	52%	54%	76%

Finally, a screening of the counterion was performed and different alkali metals (Li, Na, K) were employed, both in a 1:1 and 1:2 ratio. The comparison shows that reasonable yields are obtained with all three bis-trimethylsilylphosphides, although there is no significant difference between using one or two equivalents of Na[P(TMS)$_2$] and K[P(TMS)$_2$], in contrast to Li[P(TMS)$_2$] (Table 5).

Table 5. Choice of the counterion. Conditions: 6 h, refluxing THF.

	Li[P(TMS)$_2$]	**Na[P(TMS)$_2$]**	**K[P(TMS)$_2$]**
1 eq.	56%	45%	46%
2 eq.	76%	47%	51%

Finally it turned out that the optimal reaction time is 6 h, while the solvent of choice is THF under refluxing conditions. Interestingly, the use of 2 equivalents of Li[P(TMS)$_2$] has a beneficial effect on the yield of the reaction, as 76% of isolated 2,4,6-triphenylphosphinine could be obtained.

Next, the new procedure has been tested for the preparation of other 2,4,6-triarylphosphinines for which the isolated yields are normally rather low. The pyrylium salts which were chosen are precursors of phosphinines having particularly interesting properties (Figure 10). **2.20** is the precursor of 2-(2-pyridyl)-4,6-diphenyl-phosphinine (**2.14**),[48,106] which is a phosphorus-containing analog of bipyridine, while **2.21** is used to prepare 2,4-diphenyl-5-methyl-6-(2,3-dimethylphenyl)-phosphinine (**2.22**), an atropisomeric phosphinine with potential applications in asymmetric catalysis.[139,140]

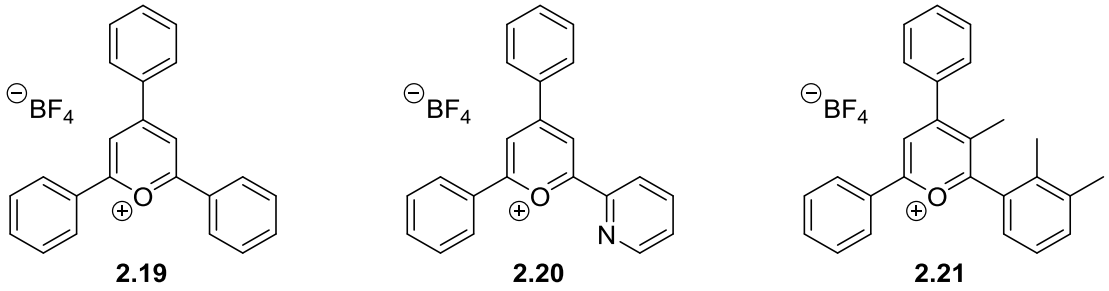

Figure 10. Different pyrylium salts screened in the O^+/P exchange.

Starting from the pyrylium salts and $P(TMS)_3$, **2.14** is usually obtained in an average yield of 25%, while **2.22** is typically isolated in only 10–15% yield. Interestingly it turned out that these compounds can be prepared in significantly higher yields under the same optimized conditions described for **2.19**, with which both ligands could be obtained in 37% isolated yield.

2.2.2 Coordination Chemistry

Even though phosphinines have been used as ligands in coordination chemistry for a long time and DFT calculations suggest them to be strong π-acceptors, an in-depth study on their electronic properties and a comparison with state-of-the-art ligands is still missing.

To examine their electronic properties as ligands, metal-carbonyl complexes were synthesized. In fact, metal-carbonyls can be used as probes for the evaluation and comparison of the electronic properties of a ligand, since the stretching frequency of the CO bands in the infrared spectra is proportional to the net-donation of electron density from the ligand to the metal center. More precisely, the higher the net-donation, the lower the frequency of the stretching vibration. For this reason the tungsten complex **2.23** was prepared by mixing equimolar amounts of **2.1** and the metal precursor $[(THF)W(CO)_5]$ in THF. The tungsten precursor was prepared by stirring a suspension of $[W(CO)_6]$ in THF for 2 h under UV light, according to a modified procedure described by Deberitz and Nöth.[89]

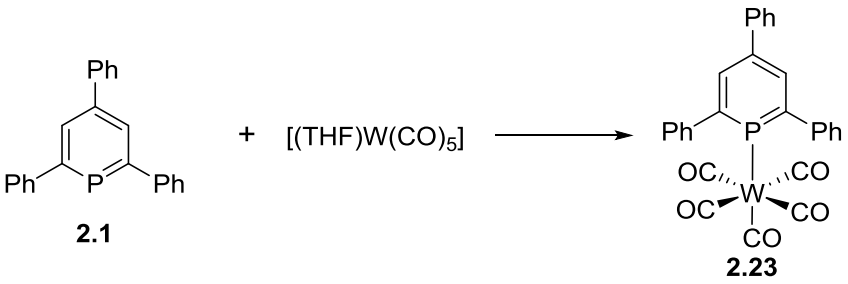

Scheme 10. Synthesis of complex **2.23**.

Within 30 minutes, the $^{31}P\{^{1}H\}$ NMR spectrum of the reaction mixture shows one single resonance at $\delta = 159.1$ ppm with characteristic satellites due to $^{1}J_{P\text{-}W}$ coupling. This is in agreement with the quantitative formation of **2.23**, which was characterized by means of NMR and IR spectroscopy. The IR spectrum of the obtained solid shows four CO stretching bands at $\tilde{\nu} = 2073$, 1992, 1932 and 1909 cm^{-1}. Single crystals suitable for X-ray diffraction analysis have been obtained by slow evaporation from a concentrated solution in pentane. The molecular structure in the crystal is depicted in Figure 11.

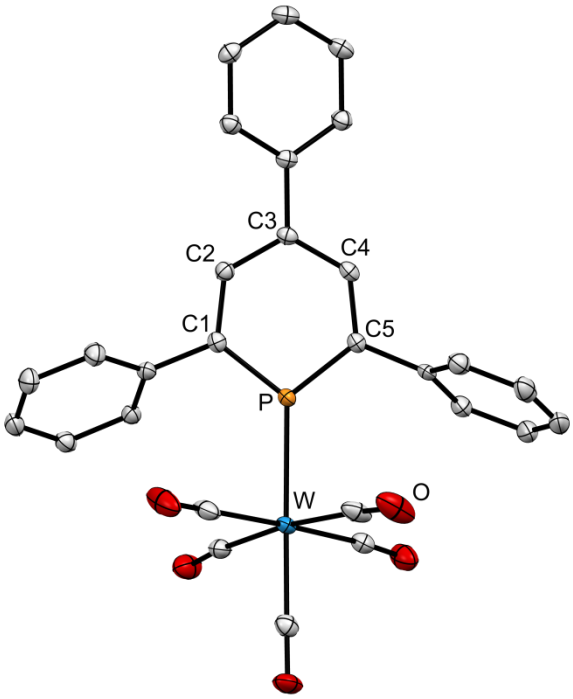

Figure 11. Molecular structure of **2.23** in the crystal. Displacement ellipsoids are shown at the 50% probability level. Hydrogen atoms are omitted for clarity. Selected bond lengths (Å) and angles (°): P–C1: 1.737(2); P–C5: 1.733(3); P–W: 2.5053(7); C1–C2: 1.390(4); C2–C3: 1.403(4); C3–C4: 1.390(3); C4–C5: 1.394(4); C1–P–C5: 103.6(1).

Similarly, another tungsten complex was prepared by mixing **2.1** and the metal precursor $[(MeCN)_2W(CO)_4]$ in a 2:1 ratio in THF (Scheme 11).

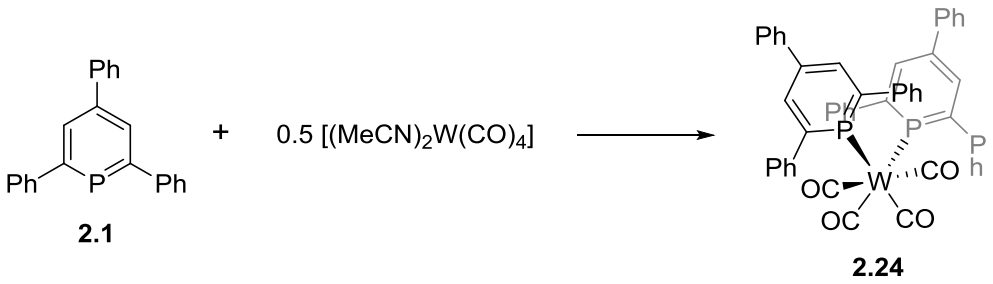

Scheme 11. Synthesis of complex **2.24**.

The product, that was also detected in traces as side-product in the previous reaction, has a chemical shift of δ = 169.9 ppm in the $^{31}P\{^{1}H\}$ NMR spectrum, with characteristic satellites due to $^{1}J_{P\text{-}W}$ coupling. IR and ^{13}C NMR spectra suggest the formation of a *cis*-complex, which was confirmed by single crystals X-ray diffraction analysis. The molecular structure in the crystal is depicted in Figure 12.

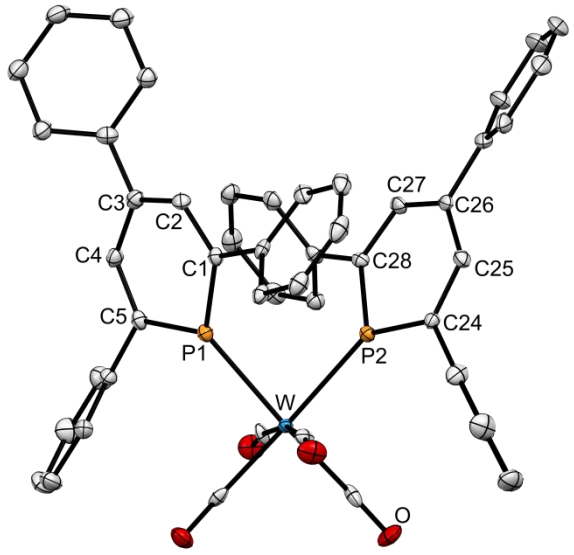

Figure 12. Molecular structure of **2.24** in the crystal. Displacement ellipsoids are shown at the 50% probability level. Hydrogen atoms and solvent molecules are omitted for clarity. Selected bond lengths (Å) and angles (°): P1–C1: 1.744(6); P1–C5: 1.744(6); P1–W: 2.494(2); C1–C2: 1.392(8); C2–C3: 1.397(8); C3–C4: 1.399(7); C4–C5: 1.385(8); P2–C24: 1.732(6); P2–C28: 1.746(5); P2–W: 2.500(1); C24–C25: 1.394(6); C25–C26: 1410(9); C3–C4: 1.39(1); C4–C5: 1.3918(7); C1–P–C5: 103.6(3); C24–P–C28: 104.0(3).

As will be discussed in Chapter 5, $[LNi(CO)_3]$ type complexes are the most suitable probes to investigate the electronic properties of a ligand. To prepare them, an excess of $[Ni(CO)_4]$ was

condensed at T = -196 °C onto a solution with the appropriate ligand in a J-Young NMR tube with a condensation line (Scheme 12).

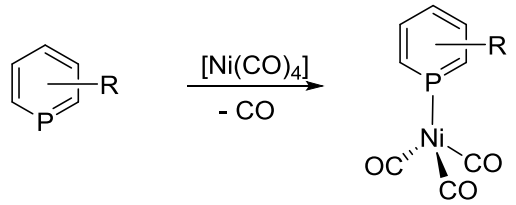

Scheme 12. Synthesis of nickel complexes of the type [LNi(CO)$_3$].

Upon thawing of the solution and shaking, a violent gas evolution was observed in the NMR tube. In the $^{31}P\{^{1}H\}$ NMR spectra, a downfield shift was observed, suggesting the formation of the respective nickel complexes. In Figure 13 are reported the ligands employed in this reaction. For ligand **2.22** the reaction was extremely fast and the corresponding complex turned out to be quite stable. For ligands **2.1**, **2.2** and **2.25**, it was necessary to degas the reaction mixture in order to eliminate the CO produced in the NMR tube during the reaction and to reach full conversion. Moreover these nickel complexes were not stable and decomposed under vacuum. In particular, **2.28** showed to be quite volatile. For the synthesis of this complex it has been necessary to carefully perform a stoichiometric reaction in DCM and directly measure the IR spectrum. Ligand **2.26** did not react at all with [Ni(CO)$_4$].

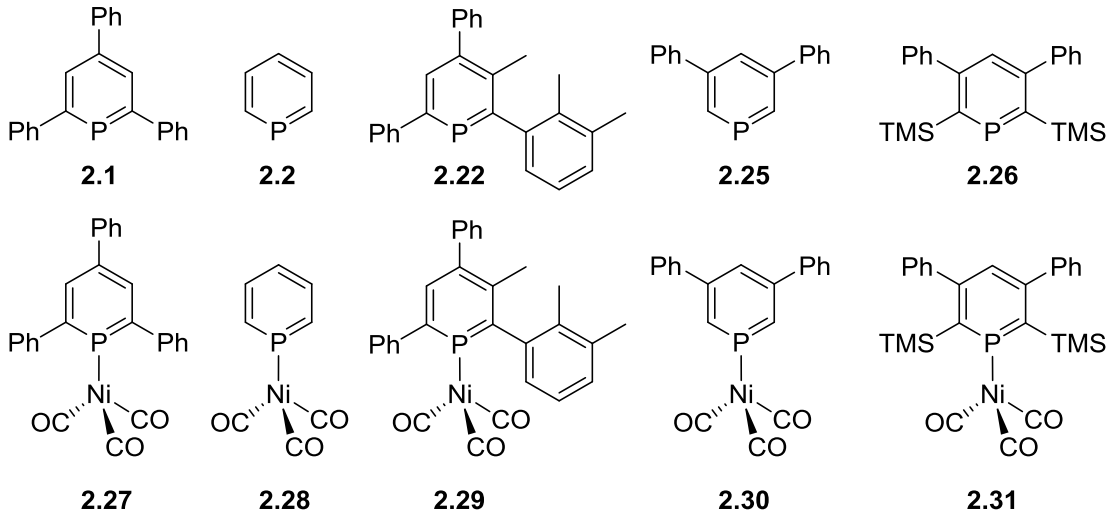

Figure 13. Phosphinine ligands employed in the reaction with [Ni(CO)$_4$] and corresponding metal complexes.

Evaporation of the volatiles yielded the compounds as grey solids, due to partial decomposition. The IR spectra were measured in DCM and showed the expected pattern for [LNi(CO)$_3$] type complexes. The spectra will be discussed in Chapter 5, as a comparison with phosphabarrelenes and phosphasemibullvalenes will be presented there.

In order to evaluate the properties of phosphinines as ligands in gold-catalyzed reactions, three [LAuCl] type complexes were synthesized starting from [AuCl(SMe_2)] in DCM at room temperature and a suitable ligand (**2.1** or **2.22** or **2.26**) (Scheme 12).

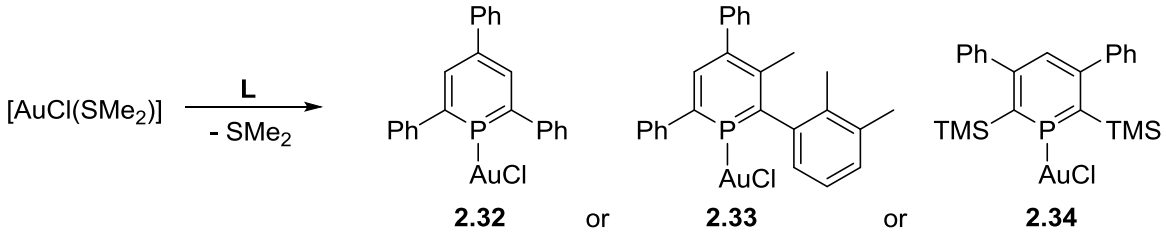

Scheme 13. Synthesis of complexes **2.32**, **2.33** and **2.34**.

Quantitative formation of complexes **2.32**, **2.33** and **2.34** was observed in the $^{31}P\{^{1}H\}$ NMR spectra, where a single upfield-shifted resonance was observed. Evaporation of the volatiles yielded the compounds as pale-yellow solids quantitatively. To completely remove dimethylsulfide it was necessary either to dissolve the complex again and remove the volatiles for a couple of times or to dissolve the complex in the smallest amount of DCM and precipitate it with diethyl ether or pentane. In this way the obtained pale-yellow solid could be more easily thoroughly dried in vacuum. If needed, washing with diethyl ether or pentane was helpful. Phosphinine-gold complexes are known for quite some time but have only recently been characterized crystallographically.[141] The molecular structure of **2.33** in the crystal (Figure 14).[142] interestingly reveals that the presence of the methyl groups causes a strong torsion of the xylyl ring compared to the phenyl ring (-77.6° *vs* -39.1°).

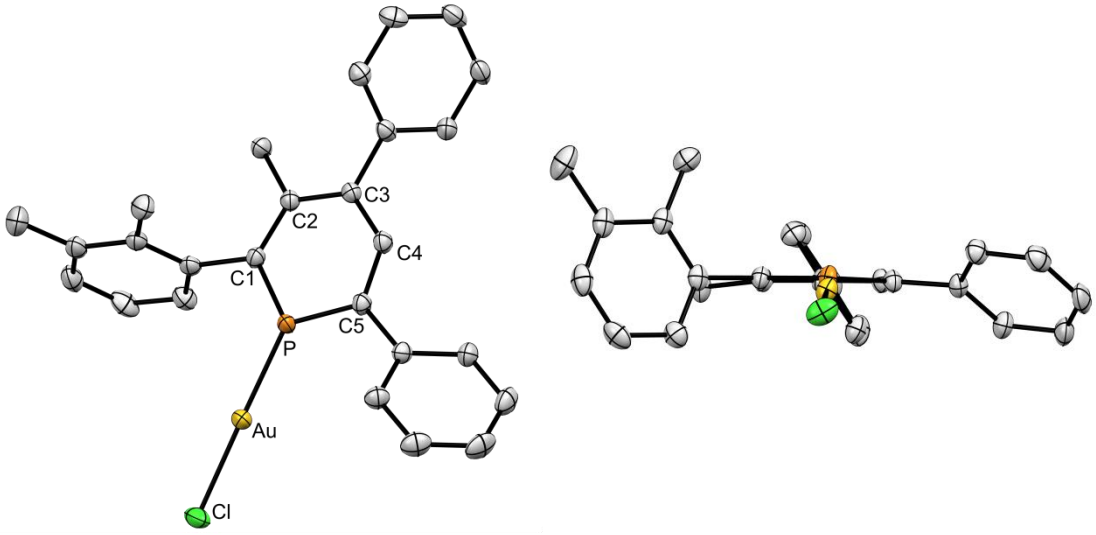

Figure 14. Molecular structure of **2.33** in the crystal: top view (left) and front view (right). Displacement ellipsoids are shown at the 50% probability level. Hydrogen atoms and a solvent molecule are omitted for clarity. Selected bond lengths (Å) and angles (°): P-Au: 2.2040(7), Au-Cl: 2.2674(8), P-C1: 1.715(3), P1-C5: 1.721(3), C1-C2: 1.391(4), C2-C3: 1.412(4), C3-C4: 1.399(4), C4-C5: 1.379(4), C1-P-C5: 107.26(14).

Single crystals of **2.34** suitable for X-ray diffraction were obtained by slow evaporation of DCM at T = -35 °C, and the molecular structure in the crystal is depicted in Figure 15.

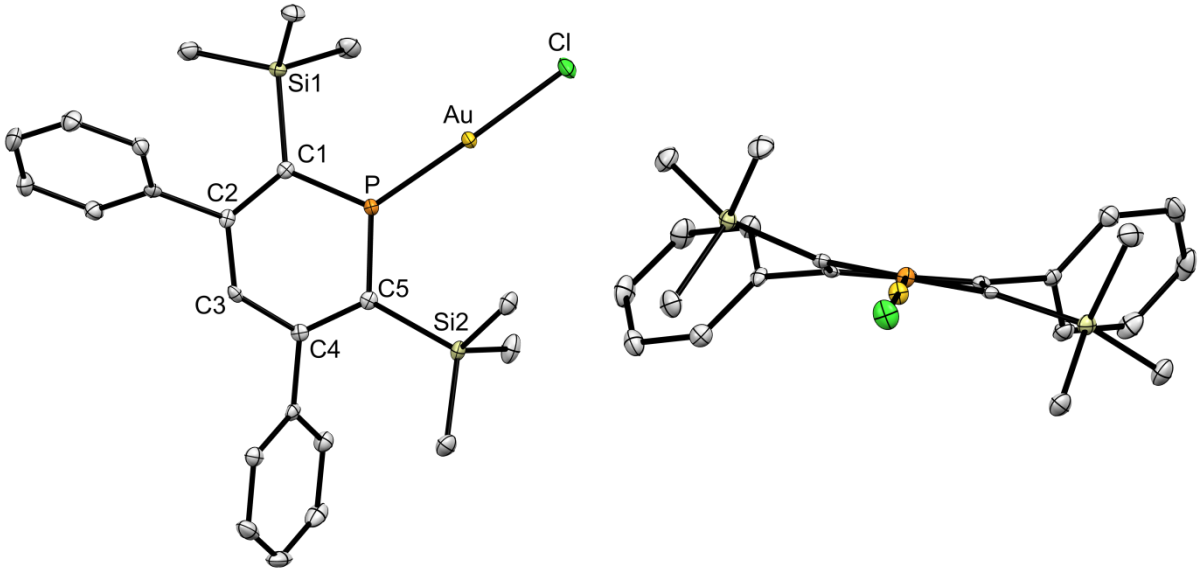

Figure 15. Molecular structure of **2.34** in the crystal. Displacement ellipsoids are shown at the 50% probability level. Hydrogen atoms are omitted for clarity. Selected bond lengths (Å) and angles (°): P–C1: 1.722(3); P–C5: 1.721(3); P–Au: 2.2082(9); Au–Cl: 2.2707(9); C1–C2: 1.410(4); C2–C3: 1.399(4); C3–C4: 1.401(4); C4–C5: 1.412(48); C1–Si1: 1.914(2); C5–Si2: 1.915(3); C1–P–C5: 112.0(1).

Interestingly, as observed in other reports, the PCP angle is surprisingly large compared to 2,4,6-triaryl-substituted phosphinine metal complexes (*ca*. 112° *vs* 106°).[143] This fact is ascribed to the high steric demand of the trimethylsilyl groups on the α-carbons. Moreover, this structure shows a rare distortion of the planarity of the phosphinine ring, for which a torsion angle (C3-C4-C5-P) of 13.8° is observed. This is not observed in the solid state structure of the free ligand,[144] and can be ascribed to the steric bulk originated by the TMS groups and the gold atom. This phenomenon has only been reported once for a similar ligand bearing ferrocenyl substituents in positions 3 and 5.[67]

2.3 Conclusions

An improved synthesis of 2,4,6-triarylphosphinines has been presented. To perform the O^+/P exchange a suitable nucleophile is needed. Phosphides are too strong bases and deprotonate the substrates forming PH_3, while NaOCP and derivatives lead to unidentified products. On the other hand, alkali metal salts of $P(TMS)_3$ turned out to be suitable reagents for this

reaction. The reaction conditions have been optimized. Parameters, such as time, temperature, solvent, stoichiometry and the nature of the counterion have been screened and the best reaction conditions have been found. Three different pyrylium salts have been tested in this reaction, resulting in higher yields and cleaner products compared to literature.

The obtained ligands have been used in the synthesis of metal-carbonyl complexes of W and Ni, in order to evaluate and compare their electronic properties. New gold complexes have been synthesized and fully characterized, in order to test them in Au(I)-catalyzed cycloisomerization reactions (see Chapter 5).

2.4 Experimental part

General Remarks

Unless otherwise stated, all experiments were performed under an inert argon atmosphere using modified Schlenk techniques or in a MBraun glovebox. All common chemicals were commercially available and were used as received. Dry or deoxygenated solvents were prepared using standard techniques or used from a MBraun solvent purification system. The NMR spectra were recorded on a JEOL ECX400 (400 MHz) spectrometer and chemical shifts are reported relative to the residual resonance in the deuterated solvents. IR spectra were measured on a Nicolet iS10 FTIR-ATR spectrometer by Thermo Scientific in the solid state and on a Vertex 70 FT-IR spectrometer by Bruker in dichloromethane. For reactions under UV irradiation, a UVP High intensity 100 Watt B-100AP Mercury Vapor Lamp without filter was used. The pyrylium salts[106,139] and $P(TMS)_3$[145] were prepared according to literature. The phosphides $LiP(TMS)_2$,[137] $NaP(TMS)_2$,[138] $KP(TMS)_2$,[138] $LiPH_2(DME)$,[146] $NaPH_2(tBuONa)_x$,[147] were prepared according to literature. Phosphaalkynes and derivatives like $NaOCP(dioxane)_y$,[62,148] NaSCP,[136] Ph_3SnPCO,[135] *t*BuCP[149] and TMSCP[150] were prepared following a literature procedure. The metal complexes $[(MeCN)_2W(CO)_4]$,[151] **2.32**[141,152] and **2.33**[153] were prepared as described in literature.

$NaPH_2$

Na_3P was prepared by stirring Na and P_{red} (3:1 ratio) in DME in the presence of naphthalene as catalyst (10 mol-%) for 16 h. 2 eq. of $Et_3N{\cdot}HCl$ were added and the mixture was stirred for t = 24 h. The black solid gradually became white. The volatiles were removed in vacuum and the solid thoroughly washed with pentane. The compound was used as such, as a mixture with NaCl.

^{31}P NMR (162 MHz, no solvent): δ = -290.1 (t, $^1J_{P\text{-}H}$ = 147 Hz) ppm

General procedure for the reaction of phosphides with pyrylium salts and phosphinines

The phosphide source was slurried in THF in a Schlenk tube and the mixture was cooled down to T = -78 °C. A slurry of the pyrylium salt (or the phosphinine) in THF was added dropwise at low temperature and the reaction mixture was slowly heated up to room temperature.

General procedure for the reaction of NaOCP and derivatives with pyrylium salts

The pyrylium salt was slurried in THF in a Schlenk tube and the mixture was cooled down to T = -78 °C. A slurry of NaOCP (or other derivative) in THF was added dropwise at low temperature and the reaction mixture was slowly heated up to room temperature.

2,4,6-triphenyl-phosphinine (2.1)

2,4,6-Triphenylpyrylium tetrafluoroborate (790 mg, 2.0 mmol) and $Li[P(TMS)_2] \times 0.5$ THF (870 mg, 2 eq.) were put together in a 50 mL Schlenk flask under an argon atmosphere. 25 mL of THF were added. Upon addition a dark reaction mixture was obtained which was heated to reflux for t = 6 h. Subsequently, all volatiles were removed *in vacuo* to obtain a yellow-brown oil. The crude product was eluted on air through a neutral alumina plug (8 cm) with toluene to afford the pure product as a yellow solid (490 mg, 76%).

The spectroscopic data match with the literature.[36]

2-(2-Pyridyl)-4,6-diphenyl-phosphinine (2.14)

2-(2-pyridyl)-4,6-diphenylpyrylium tetrafluoroborate (876 mg, 2.0 mmol) and $Li[P(TMS)_2] \times 0.5$ THF (870 mg, 2 eq.) were put together in a 50 mL Schlenk flask under an argon atmosphere. 25 mL of THF were added. Upon addition a dark reaction mixture was obtained which was heated to reflux for t = 6 h. Subsequently, all volatiles were removed *in vacuo* to obtain a red-brown solid. The crude product was purified by means of column chromatography over silica with hexane at first and hexane/ethyl acetate 9:1 to afford the product as a yellow solid (271 mg, 37%).

The spectroscopic data match with the literature.[106]

2,4-Diphenyl-5-methyl-6-(2,3-dimethylphenyl)phosphinine (2.22)

2,4-Diphenyl-5-methyl-6-(2,3-dimethylphenyl)pyrylium tetrafluoroborate (790 mg, 2.0 mmol) and $Li[P(TMS)_2] \times 0.5$ THF (870 mg, 2 eq.) were put together in a 50 mL Schlenk flask under an argon atmosphere. 25 mL of THF were added. Upon addition a dark reaction mixture was obtained which was heated to reflux for t = 6 h. Subsequently, all volatiles were removed *in vacuo* to obtain a yellow-brown solid. The crude product was purified by means of column chromatography over silica with hexane at first and then with hexane/ethyl acetate 9:1 to afford the product as a yellow solid (240 mg, 37%).

The spectroscopic data match with the literature.[139]

$[W(CO)_5(THF)]$

$[W(CO)_5 \cdot THF]$ was synthesized following a modified literature procedure.[154] A suspension of $[W(CO)_6]$ (50 mg, 0.14 mmol) in 2 mL THF was stirred for t = 2 h under UV light. The CO overpressure was released from time to time and the solution, which becomes yellow from colourless, was degassed after t = 1 h of exposition, to allow the CO to leave the reaction. Performing the reaction in a big vessel (100 mL flask) is also a good way to remove the CO from the reaction, but degassing is recommended.

[2,4,6-Triphenylphosphinine]-pentacarbonyltungsten(0) 2.23

The compound was synthesized following a modified literature procedure.[89] A solution of **2.1** (50 mg, 0.154 mmol) in 2 mL of dry THF was added dropwise to a solution of [$W(CO)_5$·THF] (1 eq.) in dry THF. The mixture was heated up to T = 60 °C for t = 1 h. Afterwards the solvent was removed *in vacuo* and the residue was washed with cold pentane, yielding the product as an orange powder (86%). Crystals suitable for X-ray analysis were obtained by slow evaporation from a pentane solution.

^{1}H NMR (400 MHz, CD_2Cl_2): δ = 7.41 (m, 1H, Ar-H), 7.50 (m, 12H, Ar-H), 7.66 (m, 2H, Ar-H), 8.12 (d, $^{3}J_{H\text{-}P}$ = 17.3 Hz, 2H, Ar-H) ppm.

^{13}C{^{1}H} NMR (101 MHz, CD_2Cl_2): δ = 128.0 (d, *J* = 3.0 Hz), 128.8 (d, *J* = 0.9 Hz), 128.9 (d, *J* = 2.1 Hz), 129.2 (d, *J* = 1.0 Hz), 129.7 (d, *J* = 0.9 Hz), 130.5 (d, *J* = 8.5 Hz), 136.5 (d, *J* = 11.6 Hz), 140.9 (d, *J* = 22.7 Hz), 141.4 (d, *J* = 5.3 Hz), 142.5 (d, *J* = 14.5 Hz), 168.9 (d, *J* = 12.0 Hz), 195.1 (d, $^{2}J_{C\text{-}P}$ = 9.0 Hz, with ^{183}W satellites, $^{1}J_{C\text{-}W}$ = 126.1 Hz, CO *cis*), 198.7 (d, $^{2}J_{C\text{-}P}$ = 32.0 Hz, CO *trans*) ppm.

^{31}P{^{1}H} NMR (162 MHz, CD_2Cl_2): δ = 159.1 (s, $^{1}J_{P\text{-}W}$ = 273 Hz) ppm.

IR (solid state): 2073 (w, CO), 1992 (w, CO), 1932 (shoulder), 1909 (s, CO) cm^{-1}.

***cis*-Bis-[2,4,6-triphenylphosphinine]-tetracarbonyltungsten(0) 2.24**

The compound was synthesized following a modified literature procedure.[89] A solution of **2.1** (37.8 mg, 0.116 mmol) in THF was added dropwise to a solution of [$W(CO)_4(CH_3CN)_2$] (0.5 eq.) in THF and the mixture was heated up to T = 60 °C for t = 1 h. Afterwards the solvent was removed *in vacuo* and the crude product was washed with small amounts of cold acetonitrile and pentane, yielding the product as a red powder (56%). Crystals suitable for X-ray analysis were obtained by recrystallization from hot acetonitrile.

^{1}H NMR (400 MHz, CD_2Cl_2): δ = 7.15 (d, 4H, *J* = 7.6 Hz), 7.29 (m, 4H), 7.40 (m, 3H), 7.50 (m, 2H), 7.49 (m, 6H, Ar-H), 7.67 (d, *J* = 7.7 Hz, 2H), 7.81 (m, 2H) ppm.

^{13}C{^{1}H} NMR (101 MHz, CD_2Cl_2): 127.8 (s), 128.1 (s), 128.5 (s), 128.7 (s), 129.7 (s), 130.5 (t, *J* = 4.4 Hz), 136.3 (t, *J* = 6.6 Hz), 139.7 (m), 141.8 (m), 142.8 (t, *J* = 7.0 Hz), 168.4 (t, *J* = 6.4 Hz), 197.5 (t, *J* = 8.6 Hz, CO_{cis}), 203.9 (m, CO_{trans}) ppm.

^{31}P{^{1}H} NMR (162 MHz, CD_2Cl_2): δ = 169.9 (s, $^{1}J_{P\text{-}W}$ = 263 Hz) ppm.

IR (solid state): 2024 (s, CO), 1915 (s, CO), 1884 (s, CO) cm^{-1}.

General procedure for the synthesis of [(L)Ni(CO)$_3$] complexes

Caution: [Ni(CO)$_4$] is highly toxic and potentially carcinogenic. It can be absorbed through the skin or inhaled due to its high volatility. Vapors of [Ni(CO)$_4$] can autoignite. All manipulations must be done with extreme care in a well-ventilated fumehood.

In a J-Young NMR tube 0.6 mL of THF containing the appropriate ligand were degassed by freeze and thaw technique. Afterwards, an excess of [Ni(CO)$_4$] was condensed in the same tube using a condensation line. The tube was slowly warmed up to room temperature, and the reaction progress was monitored by means of ^{31}P NMR spectroscopy, degassing the tubes until full conversion. The volatiles were removed *in vacuo*, yielding the product quantitatively. IR spectra were measured in DCM.

[2,4,6-Triphenylphosphinine]-tricarbonylnickel(0) 2.27

^{1}H NMR (400 MHz, THF-d_8): δ = 7.42 (m, 9H), 7.57 (m, 4H), 7.74 (d, *J* = 7.6 Hz, 2H), 8.21 (d, *J* = 14.3 Hz, 2H) ppm.

^{13}C{^{1}H} NMR (101 MHz, THF-d_8): δ = 128.0 (d, *J* = 3.0 Hz), 128.5 (d, *J* = 2.9 Hz), 129.0 (m), 129.5 (s), 130.0 (s), 130.2 (s), 130.3 (s), 135.8 (d, *J* = 12.6 Hz), 142.0 (d, *J* = 20.7 Hz), 142.2 (d, *J* = 1.5 Hz), 143.2 (d, *J* = 16.9 Hz), 166.8 (d, *J* = 1.5 Hz), 194.5 (d, *J* = 1.2 Hz, CO) ppm.

^{31}P{^{1}H} NMR (162 MHz, THF-d_8): δ = 181.8 ppm.

IR (dcm): 2079.2 (s), 2011.4 (s) cm^{-1}.

[Phosphinine]-tricarbonylnickel(0) 2.28

The compound is volatile or decomposes completely under vacuum. A stoichiometric reaction in DCM was needed to directly measure the IR spectrum. Extreme care is needed in order not to handle solutions containing [Ni(CO)$_4$] in excess.

^{31}P{^{1}H} NMR (162 MHz, no solvent): δ = 199.3 ppm.

IR (DCM): 2082.0 (s), 2011.6 (s) cm^{-1}.

[2,4-Diphenyl-5-methyl-6-(2,3-dimethylphenyl)phosphinine]-tricarbonylnickel(0) 2.29

$^{31}P\{^{1}H\}$ NMR (162 MHz, no solvent): δ = 187.9 ppm.

IR (DCM): 2077.0 (m), 2007.5 (bs) cm^{-1}.

[3,5-Diphenylphosphinine]-tricarbonylnickel(0) 2.30

$^{31}P\{^{1}H\}$ NMR (162 MHz, THF-d_8): δ = 198.9 ppm.

IR (DCM): 2081.6 (m), 2012.1 (bs) cm^{-1}.

General procedure for the synthesis of [(L)AuCl] complexes

A solution of the appropriate ligand (0.075 mmol) in 2 mL of DCM or THF was added dropwise to a solution of [AuCl(SMe_2)] (2 mL, 1 eq.) and stirred for t = 1 h at room temperature. Afterwards the solvent was removed, and the residue was dried thoroughly in high vacuum, yielding the product as a pale yellow solid in quantitative yield. To remove completely dimethylsulfide, the product was dissolved in the smallest amount of DCM and then precipitated using pentane, subsequently removing the volatiles and drying thoroughly.

[(3,5-Diphenyl-2,6-bis(trimethylsilyl)-phosphinine)AuCl] 2.33

^{1}H NMR (400 MHz, CD_2Cl_2): δ = 2.05 (s, 3H), 2.11 (s, 3H), 2.39 (s, 3H), 7.13 (m, 1H), 7.26 (m, 3H), 7.41 (m, 2H), 7.45 (m, 1H), 7.49 (m, 4H), 7.75 (m, 2H), 8.14 (d, $J_{H\text{-}P}$ = 20.3 Hz, 1H) ppm.

$^{13}C\{^{1}H\}$ NMR (400 MHz, CD_2Cl_2): δ = 17.2 (s), 20.9 (s) 21.1 (d, *J* = 6.1 Hz), 126.2 (d, *J* = 2.1 Hz), 128.4 (s), 128.6 (s), 128.7 (s), 128.8 (s), 129.1 (s), 129.4 (d, *J* = 6.1 Hz), 129.6 (d, *J* = 2.3 Hz), 129.8 (s), 131.0 (d, *J* = 2.8 Hz), 135.3 (d, *J* = 8.0 Hz), 138.4 (d, *J* = 1.8 Hz), 138.6 (d, *J* = 19.6 Hz), 139.1 (d, *J* = 10.1 Hz), 139.2 (d, *J* = 11.7 Hz), 142.4 (d, *J* = 4.6 Hz), 145.4 (d, *J* = 10.1 Hz), 146.0 (d, *J* = 26.5 Hz), 157.7 (d, *J* = 24.2 Hz), 162.1 (d, *J* = 29.9 Hz) ppm.

$^{31}P\{^{1}H\}$ NMR (400 MHz, CD_2Cl_2): δ = 164.3 ppm.

[(3,5-diphenyl-2,6-bis(trimethylsilyl)-phosphinine)AuCl] 2.34

^{1}H NMR (CD_2Cl_2, 400 MHz): δ = 0.28 (d, *J* = 0.8 Hz, 18H, TMS), 7.30 (m, 4H), 7.34 (d, *J* = 3.8 Hz, 1H), 7.43 (m, 6H) ppm.

^{13}C{^{1}H} NMR (CD_2Cl_2, 101 MHz): δ = 3.6 (d, *J* = 5.6 Hz), 128.8 (s), 129.0 (s), 129.3 (s), 133.0 (dd, *J* = 41.3, 7.5 Hz), 144.9 (d, *J* = 13.0 Hz), 155.4 (d, *J* = 14.6 Hz), 158.6 (d, *J* = 16.5 Hz) ppm.

^{29}Si{^{1}H} NMR (CD_2Cl_2, 79 MHz): δ = -0.5 (d, $^{2}J_{P\text{-}Si}$ = 19.4 Hz) ppm.

^{31}P{^{1}H} NMR (CD_2Cl_2, 162 MHz): δ = 210.6 (s, $^{2}J_{P\text{-}Si}$ = 19.4 Hz) ppm.

2.4.1 X-ray Crystal Structure Determination

X-ray crystal structure determination of 2.23 CCDC-1424312

Crystals suitable for X-ray diffraction were obtained by slow evaporation of a solution in pentane. *Crystallographic data*: $C_{28}H_{17}O_5PW$; *F*w= 648.23; 0.16×0.15×0.02 mm^3; yellow plate, monoclinic; *-P2yn*, *a* = 11.1311(4), *b* = 19.9977(7), *c* = 11.6468(4) Å; α = 90°, β = 109.4260(11), γ = 90°; *V* = 2444.95(15) Å^3; *Z* = 4; *D*x = 1.761 gcm^{-3}; μ = 4.827 mm^{-1}. 34007 reflections were measured by using a D8 Venture, Bruker Photon CMOS Detector (MoKα radiation; λ = 0.71073 Å)[155] up to a resolution of $(\sin\theta/\lambda)_{max}$= 0.67 Å^{-1} at a temperature of T = 100.00 K. 5320 reflections were unique (R_{int} =0.021). The structures were solved with SHELXS-2013 by using direct methods and refined with SHELXL-2013 on *F*2 for all reflections.[156] Non-hydrogen atoms were refined by using anisotropic displacement parameters. The positions of the hydrogen atoms were calculated for idealized positions. 316 parameter were refined with one restraint. R_1 = 0.021 for 5320 reflections with $I>2\sigma(I)$ and wR_2 = 0.044 for 6093 reflections, *S* = 1.055, residual electron density was between -0.85 and 1.80 eÅ^{-3}. Geometry calculations and checks for higher symmetry were performed with the PLATON program.[157]

X-ray crystal structure determination of 2.24 CCDC- 1424399

Crystals suitable for X-ray diffraction were obtained by cooling slowly down a hot saturated solution of **2.24** in acetonitrile. *Crystallographic data*: $C_{54}H_{40}N_2O_4P_2W$; *F*w = 1026.67;

0.28×0.2×0.03 mm^3; yellow plate, monoclinic; *C-2yc*; *a* = 29.1358(14), *b* = 11.5350(6), *c* = 15.4712(7) Å; α = 90°, β = 119.7420(10), γ = 90°; *V* = 4514.6(4) $Å^3$; *Z* = 4; *D*x = 1.510 gcm^{-3}; μ = 2.679 mm^{-1}. 32070 reflections were measured by using a D8 Venture, Bruker Photon CMOS Detector (MoKα radiation; λ = 0.71073 Å)[155] up to a resolution of $(\sin\theta/\lambda)_{max}$= 0.66 $Å^{-1}$ at a temperature of T = 100.00 K. 9315 reflections were unique (R_{int} = 0.029). The structures were solved with SHELXS-2013 by using direct methods and refined with SHELXL-2013 on *F*2 for all reflections.[156] Non-hydrogen atoms were refined by using anisotropic displacement parameters. The positions of the hydrogen atoms were calculated for idealized positions. 571 parameter were refined with one restraint. R_1 = 0.029 for 9315 reflections with $I>2\sigma(I)$ and wR_2 = 0.068 for 9939 reflections, *S* = 1.017, residual electron density was between -0.77 and 3.97 $eÅ^{-3}$. Geometry calculations and checks for higher symmetry were performed with the PLATON program.[157]

X-ray crystal structure determination of 2.34

Crystals suitable for X-ray diffraction were obtained from slow evaporation from a concentrated solution in DCM at T = -35 °C. *Crystallographic data*: $C_{23}H_{29}PAuCLSi_2$, *F*w = 625.03, 0.13×0.13×0.02 mm^3, colourless plate, monoclinic, $P2_1/c$, *a* = 12.7877(3), *b* = 10.3909(2), *c* = 19.4507(4) Å, α = 90°, β = 108.1687(7)°, γ = 90°; *V* = 2455.67(9) $Å^3$, *Z* = 4, *D*x = 1.691 gcm^{-3}, μ = 6.270 mm^{-1}. 32141 reflections were measured by using a Bruker-AXS smart CCD area detector diffractometer (MoKα radiation, λ = 0.71073 Å)[155] up to a resolution of $(\sin\theta/\lambda)_{max}$ = 0.61 $Å^{-1}$ at a temperature of T = 100 K. The reflections were corrected for absorption and scaled on the basis of multiple measured reflections by using the SADABS program[155] (0.56–0.75 correction range). 4164 reflections were unique (R_{int} = 0.046). Using ShelXle[158], the structures were solved with SHELXS-2014 by using direct methods and refined with SHELXL-2014 on *F*2 for all reflections.[156] Non-hydrogen atoms were refined by using anisotropic displacement parameters. The positions of the hydrogen atoms were calculated for idealized positions. 259 parameter were refined without restraints. R_1 = 0.018 for 4164 reflections with $I>2\sigma(I)$ and wR_2 = 0.039 for 4687 reflections, *S* = 1.028, residual electron density was between -0.65 and 0.43 $eÅ^{-3}$. Geometry calculations and checks for higher symmetry were performed with the PLATON program.[157]

3. Phosphabarrelenes

Part of this chapter has been published in:

"2,4,6-Triphenylphosphinine and 2,4,6-triphenylphosphabarrelene revisited: synthesis, reactivity and coordination chemistry" - *M. Rigo, J. A. W. Sklorz, N. Hatje, F. Noack, M. Weber, J. Wiecko, C. Müller, Dalton Trans.* ***2016****, 45, 2218.*

"Synthesis and characterization of phosphabarrelene-based complexes" – N. Hatje, Bachelor thesis.

"Zur Koordinationschemie von Phosphabarrelenen" – M. Kleoff, Bachelor thesis

3.1 Introduction

Phosphabarrelenes consist of two fused six-membered rings, in which one or more C-H fragment is substituted by a phosphorus atom bearing a lone pair in accordance with the isolobal analogy of these two moieties. The most common derivatives are 1-phosphabarrelenes, which have a phosphorus atom substituting one of the sp^3-hybridized carbon atoms of the bridgehead. Triptycenes are 1-phosphabarrelenes, in which the three unsaturated bridges are part of an aromatic ring (Figure 16).

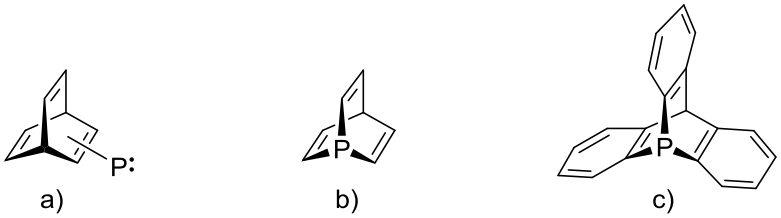

Figure 16. General formula of phosphabarrelene (a), 1-phosphabarrelenes (b) and phosphatriptycene (c).

3.1.1 1-Phosphabarrelenes

1-Phosphabarrelenes can be synthesized via [4+2] cycloaddition between a phosphinine ring and an alkyne, in which the heterocycle behaves as a diene. The first derivative was reported by Märkl *et al.* in 1968 and was obtained by reacting 2,4,6-triphenylphosphinine with hexafluoro-2-butyne at T = 100 °C in methylcyclohexane (Scheme 14).[37] Similarly, the same conversion has been performed for different pnictogen-containing 6-membered rings, such as arsa- and bismabenzene.[159]

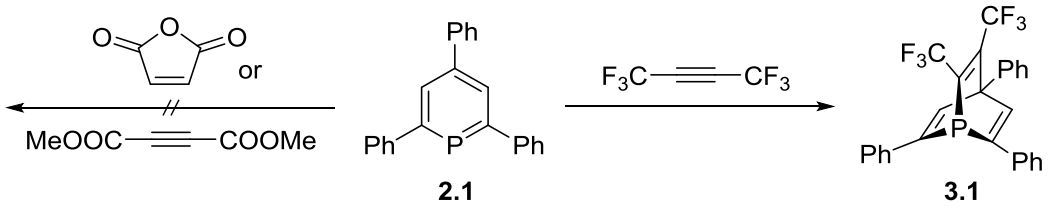

Scheme 14. Synthesis of **3.1**, the first 1-phosphabarrelene derivative.

Usually phosphinines do not easily undergo [4+2] cycloaddition, therefore very reactive alkynes are required for this reaction. In particular dienophiles bearing strong electron-withdrawing groups (*e.g.* -CF_3 or -CN) or strained cyclic alkynes (*e.g.* cyclooctyne or arynes)

are used. Less activated alkynes are in most of the cases not working (Scheme 14).[160,161] Besides this, the success of the cycloaddition reaction strongly depends on the substituents of the phosphinine ring. For example, some activated phosphinines bearing phosphino-sulfide substituents showed high reactivity towards fairly unreactive alkynes.[162]

A strategy to facilitate the cycloaddition reaction and extend the number of alkynes that can be employed is to increase the reactivity of the phosphinine by reducing its aromaticity. One way to do this is to oxidize the heterocycle. In fact, contrarily from their reduced counterparts, phosphinine sulfides proved to be reactive towards dimethyl acetylenedicarboxylate (DMAD) under mild conditions (Scheme 15).[163]

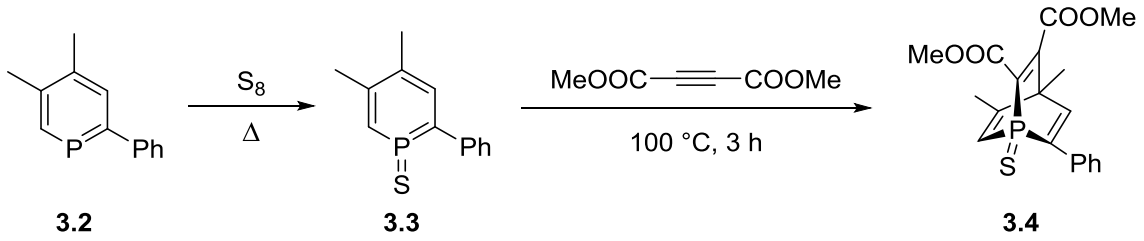

Scheme 15. Synthesis of phosphabarrelenes starting from phosphinine-sulfides.

This is supported by DFT calculations, that suggest a smaller energy barrier for the cycloaddition on the phosphinine sulfide together with a lower aromaticity of this λ^5-derivative.[73] Also, a concerted mechanism is proposed for this reaction.[164]

Similarly, the even lower aromaticity of a phosphininium cation allows for a cycloaddition to the phosphabarrelenium salt **3.5** using a poorly reactive alkyne, such as 4-octyne, at room temperature (Scheme 16).[73,83]

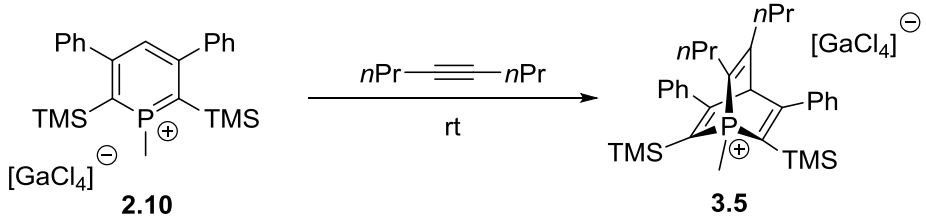

Scheme 16. Synthesis of the phosphabarrelenium salt **3.5**.

Other phosphabarrelene derivatives have been synthesized starting from thiaphosphole sulfides and alkynes. A cycloaddition yields a norbornadiene-like intermediate that rearranges to a putative phosphinine-sulfide. This can easily react regioselectively with DMAD or phenylacetylene.[165,166]

Likewise, the aromaticity of phosphinines can be decreased by coordination to a metal center. While alkenes, such as N-Phenylmaleimide or cyclopentadiene, and alkynes like DMAD do not usually react with phosphinines, the corresponding phosphabarrelenes (**3.7**) and dihydrophosphabarrelenes (**3.8**) can be obtained under mild conditions starting from [$LW(CO)_5$] metal complexes, as depicted in Scheme 17.[167,168]

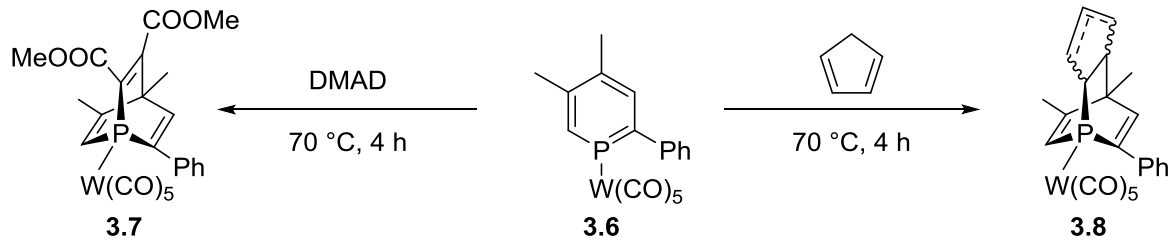

Scheme 17. Synthesis of phosphabarrelenes in the coordination sphere of a metal.

Similarly, gold(I) complexes of alkynyl-substituted phosphinines showed enhanced reactivity towards alkynes, yielding new species as shown in Scheme 18. Metal complex **3.9** is very reactive and upon concentration two alkynyl groups of two different phosphinines are involved in a [4+2] cycloaddition, yielding the dimer **3.10**, which was characterized crystallographically. If one equivalent of $(PhCC)_2SiMe_2$ is added to **3.9**, the symmetrical phosphabarrelene **3.11** is obtained instead.[143]

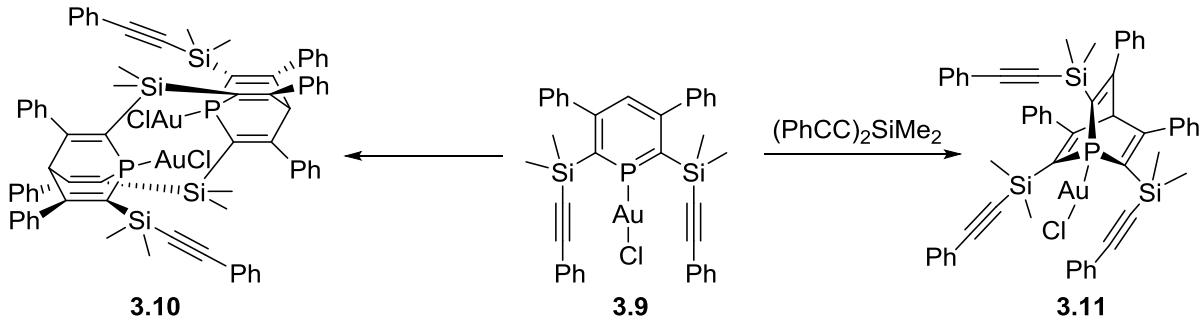

Scheme 18. Reactivity of **3.9** towards itself and $(PhCC)_2SiMe_2$.

Among other alkynes, the reaction with *in situ* generated arynes is particularly interesting. This yields benzo- or dibenzo-phosphabarrelenes, depending on the starting material which is employed.[160,161] The most common synthetic methodology for the *in situ* preparation of benzyne involves the oxidative addition of *o*-fluorobromobenzene to elemental magnesium in refluxing THF, and this approach has been extended to *o*-bromophenyl triflates.[169] Other precursors have been tested with scarce results.[160,170] In the past the groups of Märkl and Breit

investigated this reaction to assess whether it proceeds *via* a phosphahexadienyl anion intermediate (λ^4-phosphinine, see Chapter 2) or in a concerted fashion (Scheme 19).[160]

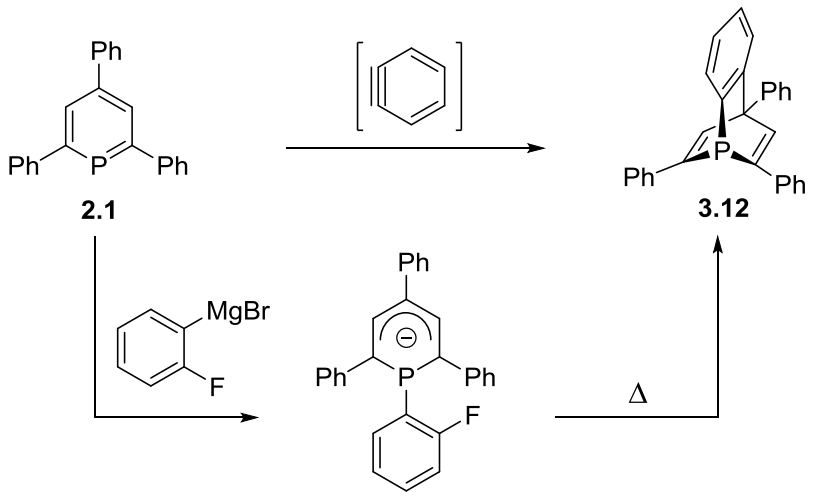

Scheme 19. Synthesis of benzo-phosphabarrelene **3.12**. Two possible pathways are depicted.

Initial findings suggesting a concerted mechanism have been confirmed experimentally by using an asymmetrically substituted aryne. If a phosphahexadienyl anion intermediate were to be involved in the process, only one product would be obtained. On the other hand, in the case of a concerted mechanism, two regioisomers would form in a 1:1 ratio. Since a 1:1 mixture of phosphabarrelenes **3.14** and **3.15** was observed after the reaction with the aryne, it was concluded that the mechanism is concerted (Scheme 20).[161,171]

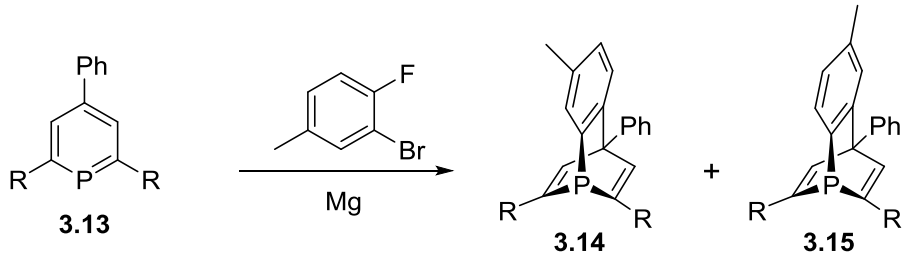

Scheme 20. Synthesis of phosphabarrelenes **3.14** and **3.15**, experimental proof for the concerted mechanism.

Different synthetic pathways have been developed for the synthesis of phosphatriptycenes. These derivatives have been obtained *via* ring closing reactions, usually starting from tripodal molecules.[172] Phosphatriptycenes bearing thiophene rings have been prepared using similar synthetic approaches.[173] The parent phosphatriptycene was prepared by Bickelhaupt *et al.* in 1974 by cyclization of 9-(*o*-chlorophenyl)-9,10-dihydrophosphaanthracene **3.16** using lithium diisopropylamide (Scheme 21).[174] Similar derivatives having one additional heteroatom at the bridgehead have also been reported.[175–177]

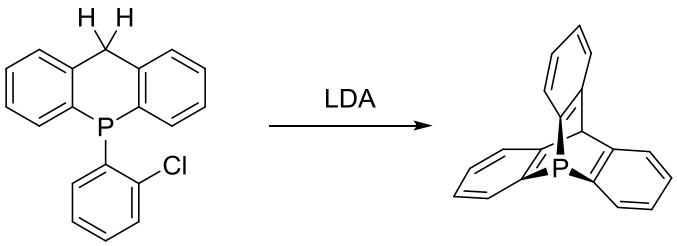

3.16 **3.17**

Scheme 21. Synthesis of phosphatriptycene **3.17**.

Oxidized phosphabarrelene derivatives have been reported and can be obtained in different ways. Some triptycenes can be synthesized as oxides, as the ring-closing reaction is performed on a symmetrically substituted phosphine-oxide and therefore the phosphorus is oxidized from the beginning of the reaction.[178–180] Similarly, some phosphabarrelenes have been obtained as sulfides as they are prepared *via* cycloaddition between an alkyne and a phosphinine sulfide, as in the case of **3.4**.

However, the most common pathway to access these derivatives is the direct oxidation, which can be performed similarly to classical phosphine ligands. In this way 1-phosphabarrelenes and triptycenes have been oxidized using simple peroxides under mild conditions.[173,176,181] Triptycene-sulfides have also been obtained, by oxidation of the starting materials with Lawesson's reagent or with elemental sulphur in the presence of a base.[173,178,179] Finally, also oxidation to the selenides has been achieved, by heating up a solution of the appropriate ligand in the presence of grey selenium.[169,173,177–179,182]

3.1.2 Coordination chemistry

Although these ligands are known for more than 40 years, the coordination chemistry of 1-phosphabarrelenes has not been explored extensively, and only a few metal complexes are described in the literature. Most of these examples involve η^1-coordination *via* the lone pair on the phosphorus atom. Only one example was reported in which the double bonds of the phosphabarrelene are involved in coordination to a second metal center.[169]

The first coordination compounds have been reported by Mathey and Märkl, prepared *via* cycloaddition of an alkyne with a phosphinine-tungsten complex. Consequently, the phosphabarrelene was obtained directly in the coordination sphere of the metal (*vide supra*, Scheme 17).[167,168] More complexes with group 6 metals have been synthesized. Edwards *et al.*

reported on a complex obtained by mixing equimolar amounts of the ligand and $[W(CO)_5THF]$, which was used to evaluate the electronic properties of phosphabarrelenes by comparing the $^1J_{P\text{-}W}$ coupling constant with other metal complexes.[183] Triptycene complexes of group 6 metals have also been shown for Mo and W. DTF calculations and experimental data suggest that these ligands are particularly weak σ-donors.[173,182]

The first coordination compound that has been characterized crystallographically is the gold(I)-complex **3.11**, which again was synthesized starting from a phosphinine-metal complex (*vide supra*, Scheme 18).[184] More derivatives with coinage metals have been prepared but not published yet.[169]

Rh(I) carbonyl complexes of the type $[L_2Rh(CO)Cl]$ using differently substituted phosphabarrelenes have been reported by the group of Breit (Scheme 22). The electronic properties of the ligands were evaluated by comparing the stretching frequency of the CO bands in the IR spectra of the metal complexes. According to the data obtained, the net-donation of phosphabarrelenes lays in between those of PPh_3 and 2,4,6-triphenylphosphinine. Some of these derivatives have been successfully employed in (asymmetric) hydrogenation and hydroformylation reactions.[171,181,185]

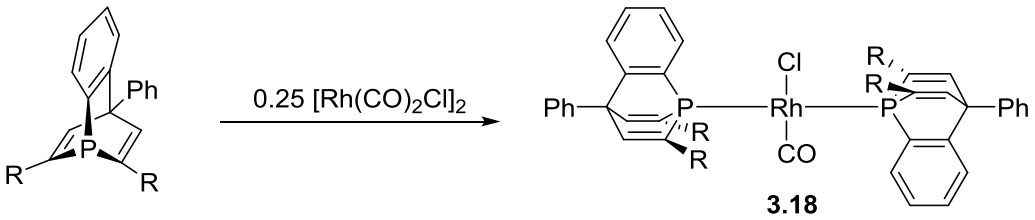

Scheme 22. Synthesis of Rh(I)-complex **3.18**.

Another Rh(I) complex has been prepared starting from a different metal precursor, yielding a complex of the type [L(cod)RhCl]. A similar reaction has been performed using an analogous Ir(I) precursor.[183]

Most of the known coordination compounds involve metals of group 10. The first Pd metal complexes have been reported by Müller *et al.* in combination with chiral phosphabarrelene derivatives.[139] The synthesis of a phosphabarrelene from the asymmetric, axially chiral phosphinine **2.20** leads to the formation of 4 different stereoisomers of **3.19**, as depicted in Figure 17. As these isomers are two pairs of enantiomers, the reaction with a chiral metal fragment forms in total four diastereomeric Pd complexes, which can easily be detected in the

NMR spectra of the mixture (Figure 17, right). This chiral ligand has been successfully employed in tandem-hydroformylation reactions.[186]

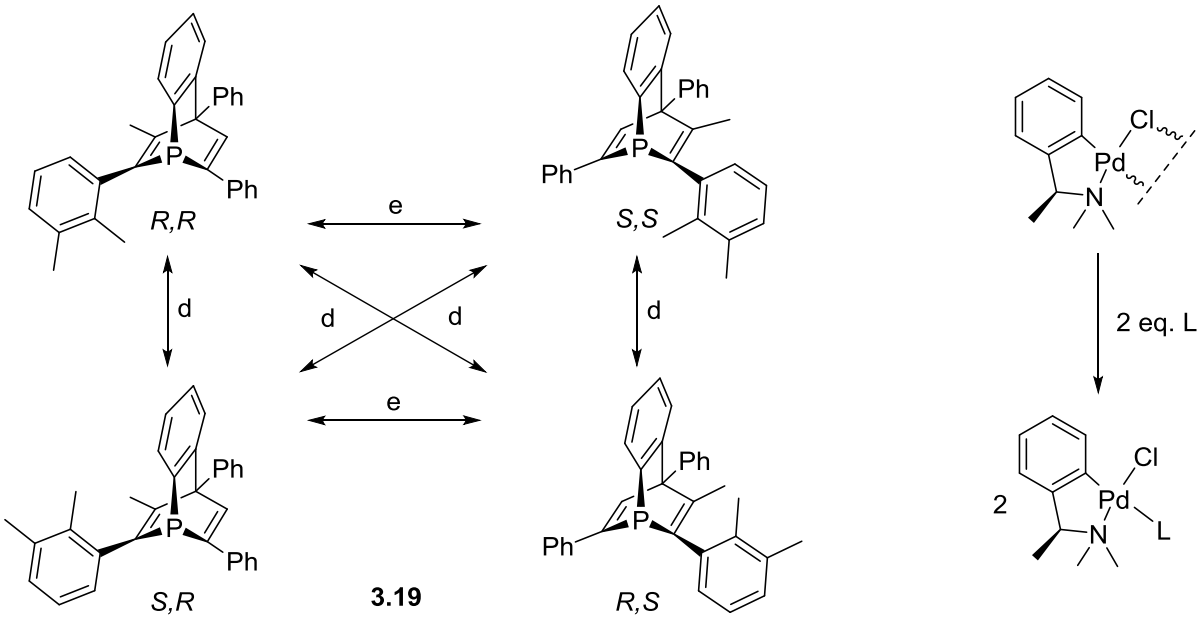

Figure 17. Different stereoisomers of **3.19** (left, e = enantiomers, d = diasteroisomers) and synthesis of diastereomeric Pd complexes (right).

Most of the phosphabarrelene-based chemistry of these metals has been investigated by the groups of Le Floch and Mézailles. Pd complexes in different oxidation states have been prepared using bulky phosphabarrelenes bearing trimethylsilyl groups in α-position to the phosphorus atom (**3.20**, Scheme 23). These complexes have been employed in catalytic cross coupling reactions, thus arousing interest in the molecular structure of the precatalysts and of the intermediates involved in these reactions. A Pd(II)-allyl complex of the type [LPd(allyl)Cl] (**3.21**) has been prepared starting from the $[Pd(allyl)Cl]_2$ dimer.[187] Compound **3.22** was obtained by reduction of **3.21** with Ar-ZnBr in the presence of one equivalent of free ligand or by reduction to Pd(0) with cobaltocene in the presence of two equivalents of **3.20**.[188] These Pd(0), 14-electron species are important precursors in cross coupling reactions, as the catalytic species is thought to be similar. The first species involved in the cycle has also been studied. By adding an equivalent of Ar-Br to **3.22**, a mixture of *cis*- and *trans*-**3.24** is formed, and the latter has been characterized crystallographically.[188] Finally, in a mechanistic study, the Pd(0) catalytic species has been trapped with a diene, yielding **3.25** and confirming the proposed mechanism.[189] The Pt-containing 14 valence electrons complex **3.23**, can be synthesized analogously to **3.22**, and was employed in hydrosilylation reactions. The complex can also be obtained starting from $[L_2Pt(H)Cl]$ and reducing in a nitrogen stream to eliminate

the HCl which is formed.[190] Finally, another Pt complex of the type $[L_2PtCl_2]$ has been reported by Edwards *et al.* in 2009.[183]

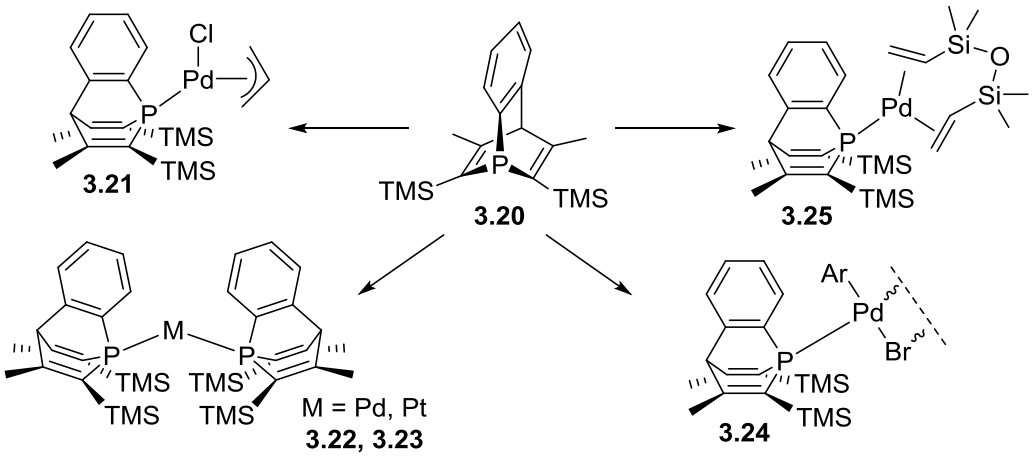

Scheme 23. Coordination chemistry of phosphabarrelene **3.20**.

In the same paper, the authors also report on the first Fe, Ru and Re phosphabarrelene-based metal complexes (Scheme 24). Coordination compound **3.27** has been prepared starting from $[Re(CO)_5Cl]$ under refluxing conditions in DCM and obtained as a yellow solid. Compounds **3.28** and **3.29** are the only half-sandwich complexes which have been reported and crystallographically characterized.[183]

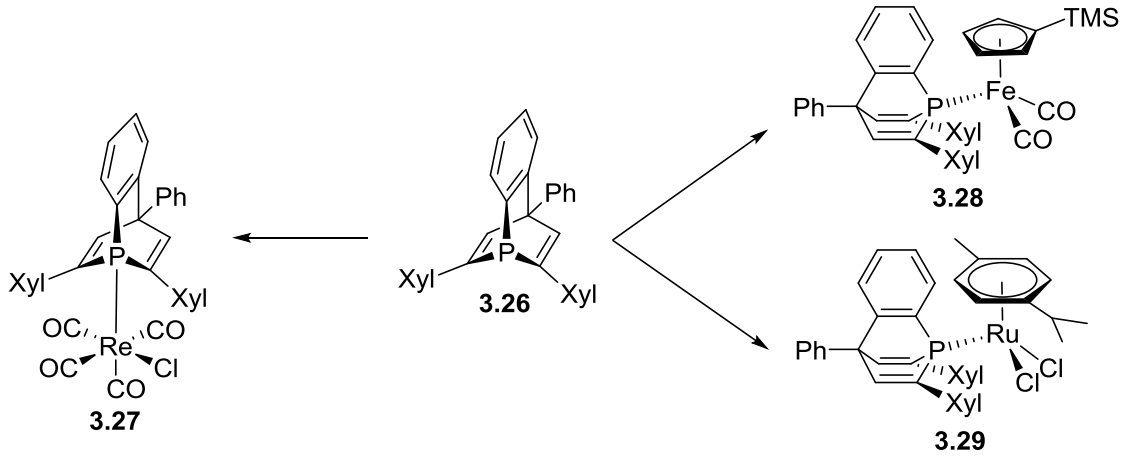

Scheme 24. Coordination chemistry of phosphabarrelene **3.26**.

An interesting metal-containing phosphabarrelene was reported by Le Floch and Mathey (Figure 18). This ferrocenyl-substituted phosphabarrelene was obtained starting from an alkynyl-substituted ferrocene and an azaphosphinine.[191]

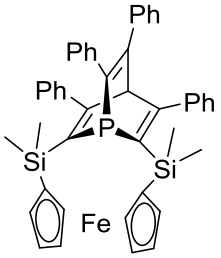

3.30

Figure 18. The ferrocenyl-substituted phosphabarrelene **3.30**.

Also polydentate phosphabarrelenes have been described in literature (Figure 19). The first were phosphino-sulfide substituted barrelenes, that can act as bi- or tridentate S-P hybrid ligands.[162] Ligand **3.31** can easily replace cyclooctadiene in the precursor $[Pd(cod)Cl_2]$ to form a stable Pd(II) complex. Starting from the dimer $[Pd(allyl)Cl]_2$ and abstracting a chloride ion with a silver salt, a Pd-allyl cationic complex is obtained. Similarly, the reaction of tridentate **3.32** with $[Pd(cod)Cl_2]$ leads to the formation of a cationic coordination compound with chloride as counterion. Bidentate phosphito-phosphabarrelenes have been reported by Breit and were employed in Rh-catalyzed hydrogenation reactions.[181] Very recently a chiral, pyridyl-substituted phosphabarrelene has been prepared by Müller *et al*. and some coordination compounds have been synthesized. **3.34** coordinates to a AuCl fragment only *via* the P atom, while the pyridyl moiety remains free for coordination to a second metal center. Starting from different precursors, two Rh complexes have been obtained where the phosphabarrelene acts as a chelating ligand. Finally one $[LW(CO)_4]$ complex has been synthesized in order to evaluate the electronic properties of the new compound, which showed to be a stronger donor compared to the phosphinine precursor.[99]

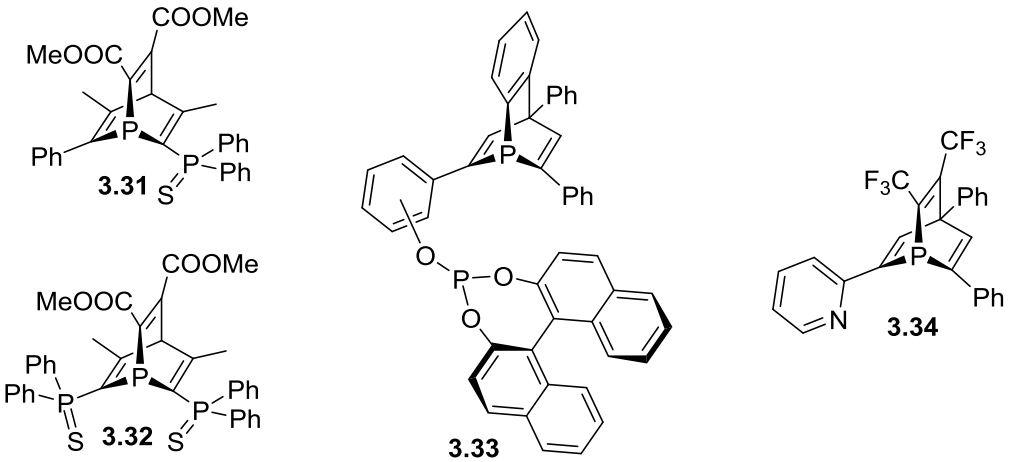

Figure 19. Polydentate phosphabarrelene ligands.

3.1.3 Other Phosphabarrelenes

Different 2-phosphabarrelene derivatives have been described by Regitz *et al.* in 1987. These were obtained *via* [4+2] cycloaddition between anthracene and a phosphaalkyne (Scheme 25).[192] Even though these compounds have been obtained in good yields, nothing is known about their coordination properties and reactivity.

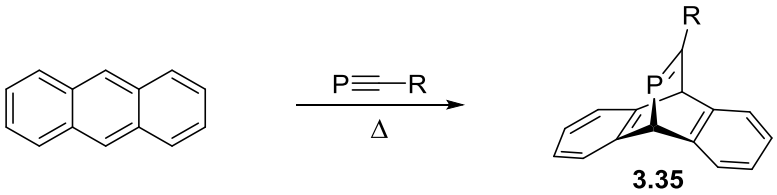

Scheme 25. Synthesis of 2-phosphabarrelenes of type **3.35**.

A few examples of phosphabarrelenes containing more than one phosphorus atom were also reported. Diphosphabarrelene **3.36** is the first derivative that can be found in literature (Figure 20, left). The compound was obtained by mixing hexafluoro-2-butyne and red phosphorus in the presence of a catalytic amount of iodine.[193,194] The reactivity of this compound towards diazocompounds, azides and dienes has been investigated.[195,196] Most interestingly, this compound has been used as precursor for the synthesis of the first diphosphabenzene **3.37** (Figure 20, right).[197]

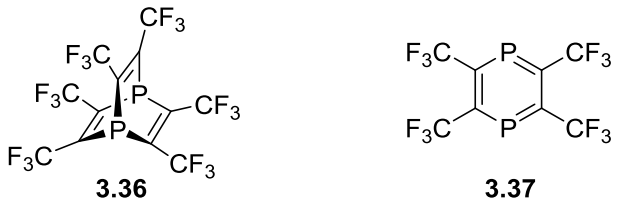

Figure 20. The first diphosphabarrelene and diphosphabenzene derivatives.

Triphosphabenzenes readily react with alkynes to unprecedented phosphorus-carbon cage compounds. These are the result of a Diels-Alder reaction and a fast, subsequent homo Diels-Alder reaction on the triphosphabarrelene intermediate of the type **3.38** (Scheme 26).[198] On the other hand, the reaction with alkenes smoothly proceeds to dihydrotriphosphabarrelene derivatives which do not further react with the dienophile. One of these derivatives was able to coordinate to a CoCp fragment *via* the two phosphaalkene moieties of the cage in a η^4 fashion.[199]

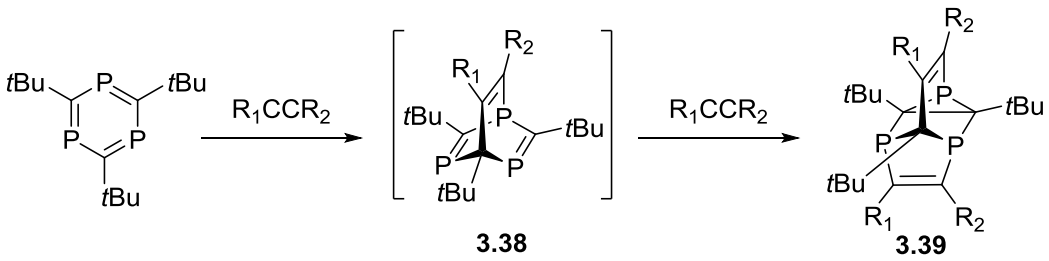

Scheme 26. Synthesis of cage compounds **3.39** *via* a triphosphabarrelene intermediate.

Tetraphosphabarrelenes are a more developed class of molecules. The first compound of this kind was described by Binger *et al.* as an oligomerization product of *t*Bu-C≡P. Four equivalents of the phosphaalkyne react stepwise in the coordination sphere of zirconium or hafnium, to yield a metal complex where the tetraphosphabarrelene is coordinated *via* two of the phosphaalkene moieties in a η^4 fashion. Oxidation with hexachloroethane yields the free tetraphosphabarrelene **3.40**, which was characterized crystallographically (Scheme 27).[200,201]

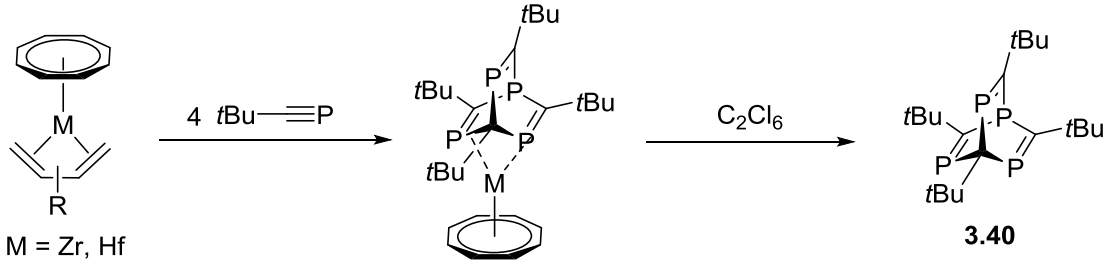

Scheme 27. Synthesis of tetraphosphabarrelene **3.40**.

Reacting one equivalent of phosphaalkyne with a triphosphinine sandwich complex led one more time to **3.40**, suggesting a stepwise formation of the trimer and the tetramer in this reaction. This is also enforced by DFT calculations run for a simplified system.[202,203] Using an excess of phosphaalkyne in this reaction leads to the formation of pentamers and other architectures.[204] A protonated version of **3.40** was obtained in the coordination sphere of cobalt during the vapour deposition of the corresponding phosphaalkyne on metallic cobalt. This molecule was characterized in a bimetallic complex of cobalt and tungsten.[205]

3.2 Results and discussion

This Chapter deals with the synthesis of new phosphabarrelene derivatives, the study of their reactivity and their employment in coordination chemistry.

3.2.1 Synthesis

As described in the introduction, very reactive alkynes are the best starting materials in the [4+2] cycloaddition with phosphinines. Consequently, the phosphabarrelenes reported in this work have been prepared using hexafluoro-2-butyne and *in situ* generated arynes as dienophiles.

As the reactions involving arynes generally have rather low yields,[171] an improvement of the synthetic route is desirable. Different pathways for the formation of arynes are known in the literature,[206–212] some of which have been employed in the preparation of phosphabarrelenes. The most common one involves the oxidative addition of *o*-fluorobromobenzene to elemental magnesium in refluxing THF.[160,171] Märkl and Breit suggested that the reaction between the aryne and the phosphinine ring is a concerted mechanism (see Scheme 19) and proved it using an asymmetrically substituted *o*-bromofluorobenzene as starting material (see Scheme 20).[160,171] Since the formation of the Grignard reagent is performed in boiling THF, it is to be expected that the elimination of FMgBr and concomitant formation of the aryne is almost instantaneous and uncontrolled under these conditions. The high rate of this intramolecular reaction does not allow for the formation of the λ^4-phosphinine intermediate that has been postulated. Hence, the mechanism *via* a concerted pathway may be the dominant under these conditions, but at low temperature another mechanism *via* a phosphadienyl anion is in principle possible. In addition to this, the high concentration of benzyne in this reaction could be a reason for the low yields, since this compound can react with itself and even with phosphabarrelenes.[213] Hence, a good strategy could be to keep the concentration of benzyne as low as possible to avoid undesired side reactions.

Among the known methodologies for the preparation of arynes, one is of most interest in this respect. Knochel and co-workers reported on the preparation of arynes *via* halogen-magnesium exchange on iodo-sulfonates.[214] Due to the electron-withdrawing effect of the

sulfonate group, the halogen-magnesium exchange can be conducted at low temperatures. Under these conditions, most functional groups are tolerated and it is even possible to perform selective iodine-magnesium exchange reactions in the presence of other halides.[215] Moreover, at these temperatures the Grignard reagent is stable in solution and the elimination of the magnesium salt and formation of the aryne only occur gradually when the solution is heated up to T = -10 °C approximately (Scheme 28).

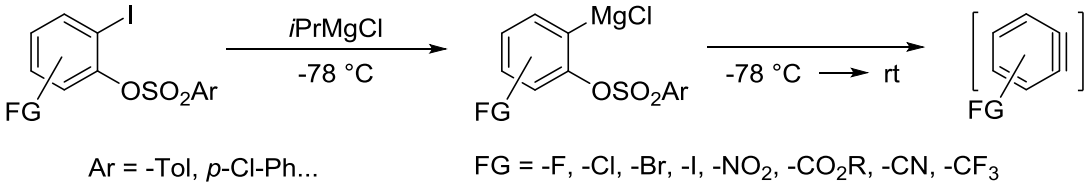

Scheme 28. Generation of benzyne via halogen exchange on iodo-tosylates.

Exploiting this route in the synthesis of phosphabarrelenes could be a way to ensure a stepwise reaction, proceeding *via* a nucleophilic attack of the Grignard reagent at the phosphorus atom to form the λ^4-phosphinine intermediate at low temperatures, followed by a ring-closing reaction upon heating (Scheme 29).

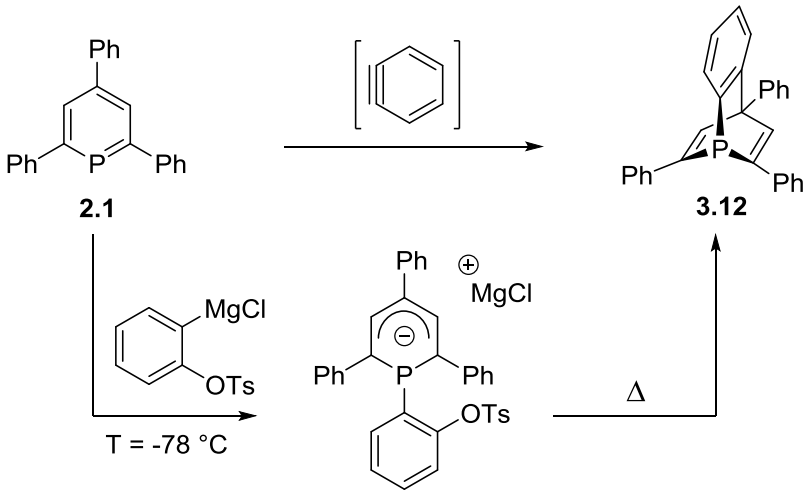

Scheme 29. Synthesis of benzo-phosphabarrelene **3.12**. Two possible pathways are depicted.

The benzyne precursor was prepared by stirring 2-iodophenoltosylate together with *i*PrMgCl at T = -90 °C for 1 h. A solution of the phosphinine was slowly added dropwise to prevent an increase in the temperature. When the phosphinine was added, the reaction mixture turned dark green immediately, which is the typical color for λ^4-phosphinine derivatives.[82] Afterwards, the reaction mixture was slowly warmed up to room temperature. During this process the green color disappeared at around T = -50 °C and the mixture became red/purple.

The $^{31}P\{^{1}H\}$ NMR spectrum of the crude product shows four resonances, including one at δ = -70.5 ppm, which can be assigned to phosphabarrelene **3.12**. After workup the product was obtained as a white solid (21% yield). The asymmetrically substituted phosphabarrelene **3.42** was prepared following the same procedure (Scheme 30), and obtained as a white powder after workup (7% yield).

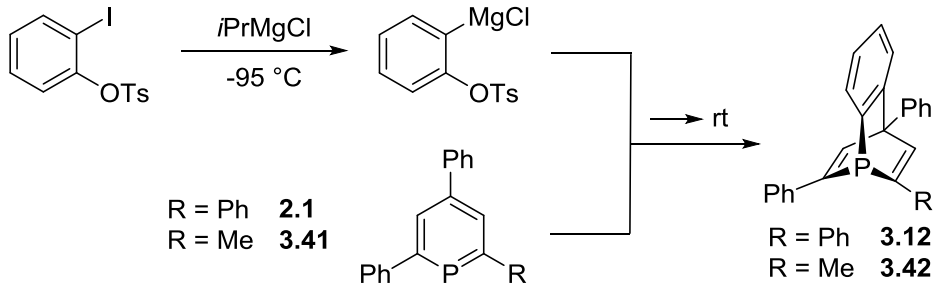

Scheme 30. Synthesis of phosphabarrelenes **3.12** and **3.42**.

Differently from **3.12**, **3.42** is relatively prone to oxidation if stored under air and for this reason additional care was required during the workup.

The same reaction has been tested by using organolithium or organozinc reagents. In the first case *t*BuLi was used instead of *i*PrMgCl, in order to form a more nucleophilic species that could react with **2.1** to form the λ^4-phosphinine. However, in the $^{31}P\{^{1}H\}$ NMR spectrum of the reaction mixture still a lot of starting material was detected together with an unidentified compound with a chemical shift of δ = 26 ppm. Similarly, the organozinc reagent obtained from the lithiated species and $ZnCl_2$ did not react with the substrate and no phosphabarrelene was found in the reaction mixture (Scheme 31).

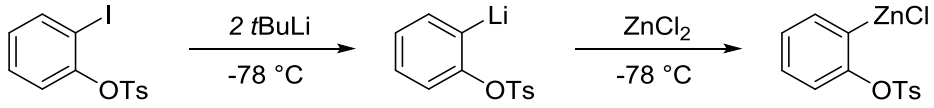

Scheme 31. Formation of organolithium and organozinc reagents.

In the end the Grignard route seems to be the most successful one. Even though the yields of this reaction are similar to the ones reported in the literature, this method proved to be successful for the preparation of phosphabarrelenes from arynes. Hoping that the low temperature reaction could lead to the products *via* a phosphadienyl anion intermediate, an asymmetric benzyne precursor was prepared and employed in the reaction (Scheme 32).

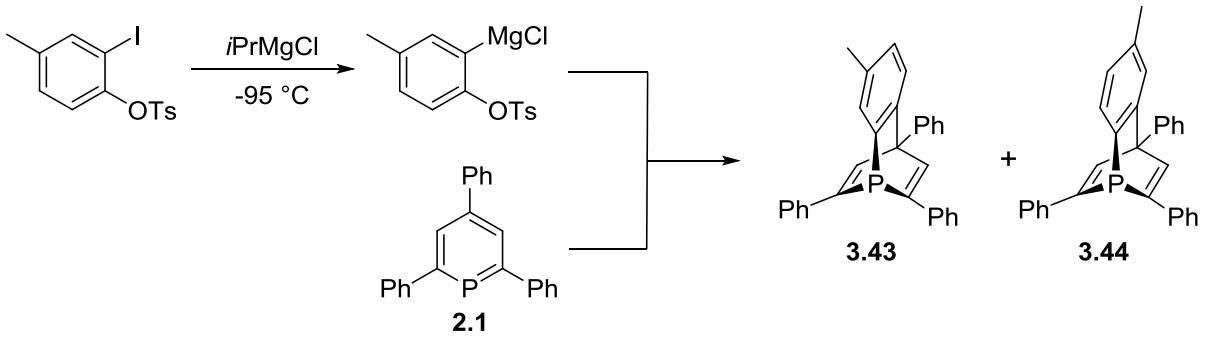

Scheme 32. Synthesis of phosphabarrelene **3.43** and **3.44**.

According to the stepwise mechanism, **3.43** was expected as only product. Surprisingly, in the $^{31}P\{^{1}H\}$ NMR spectrum of the reaction mixture, two resonances were detected around δ = -70 ppm, revealing the presence of both the compounds **3.43** and **3.44** in a 1:1 ratio. This can be considered as a definitive mechanistic proof for the concerted Diels-Alder reaction between benzyne and a phosphinine ring. Even though it has not been possible to regioselectively introduce substituents on the arynic bridge, this methodology has an advantage. In fact, different functional groups are tolerated and can in principle be introduced in the backbone of phosphabarrelenes by using iodosulfonates as precursors for arynes.[214]

The reaction of phosphinines with hexafluoro-2-butyne is in comparison more easy and straightforward, even though only three derivatives have been reported and scarcely characterized. Also, no transition metal complex or other derivative of any of these ligands is known.[37]

Using this procedure two different trifluoromethyl-substituted phosphabarrelenes have been prepared in this work, starting from phosphinines **2.1** and **2.26**. An excess of hexafluorobutyne was condensed in the reaction vessel, which was heated up to perform the Diels-Alder cycloaddition. The cycloaddition with phosphinine **2.1** is reported to lead to the formation of **3.1** (Scheme 14). A modified procedure for the workup of ligand **3.1** has been developed, resulting in an easier purification from unreacted 2,4,6-triphenylphosphinine. In addition to this, single crystals of this compound were grown and the molecular structure is depicted in Figure 21.

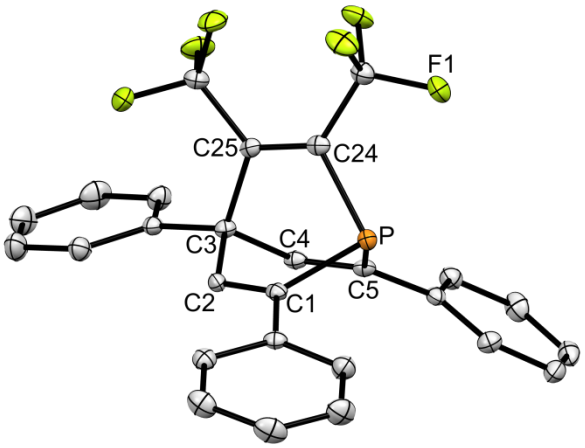

Figure 21. Molecular structure of **3.1** in the crystal. Displacement ellipsoids are shown at the 50% probability level. Hydrogen atoms are omitted for clarity. Selected bond lengths (Å) and angles (°): P–C1: 1.857(2); P–C5: 1.858(2); P–C24: 1.863(2); C1–C2: 1.335(3); C2–C3: 1.537(3); C3–C4: 1.542(3); C4–C5: 1.325(3); C24–C25: 1.335(3); C25–C3: 1.569(2); C1–P–C5: 95.71(9); C1–P–C24: 95.20(9); C5–P–C24: 91.97(9).

The second trifluoromethyl-substituted derivative which was synthesized is based on phosphinine **2.26**. Similarly, also the corresponding benzophosphabarrelene **3.45** was prepared (Scheme 33).[144]

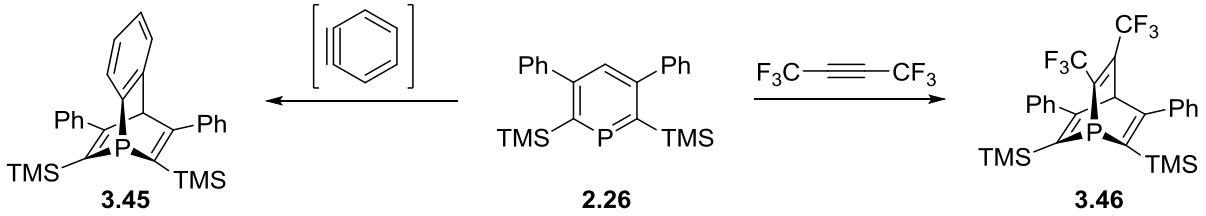

Scheme 33. Synthesis of phosphabarrelenes **3.45** and **3.46**.

Ligand **3.46** was obtained quantitatively by heating a toluene solution of **2.26** up to T = 60 °C for 16 h in the presence of an excess of hexafluoro-2-butyne. In the $^{31}P\{^{1}H\}$ NMR spectrum of the reaction mixture the resonance of the phosphinine at δ = 269.4 ppm disappeared and a quartet was detected at δ = -50.6 ppm, confirming the coupling between the phosphorus and three adjacent fluorine atoms. Recrystallization from methanol afforded pure product in high yields (85%). The isolated yield of this reaction is higher compared to the synthesis of **3.1** (51-54%).[37] The same has been observed also for the benzobarrelene **3.45**, which is prepared in higher yields compared to **3.12** (49% *vs* 26%).[144] This fact suggests that phosphinine **2.26** has a lower aromaticity compared to phosphinine **2.1**, and therefore the cycloaddition is favored.

Single crystals suitable for X-ray analysis were obtained for both the phosphabarrelene ligands and the molecular structures in the crystals are depicted in Figure 22.

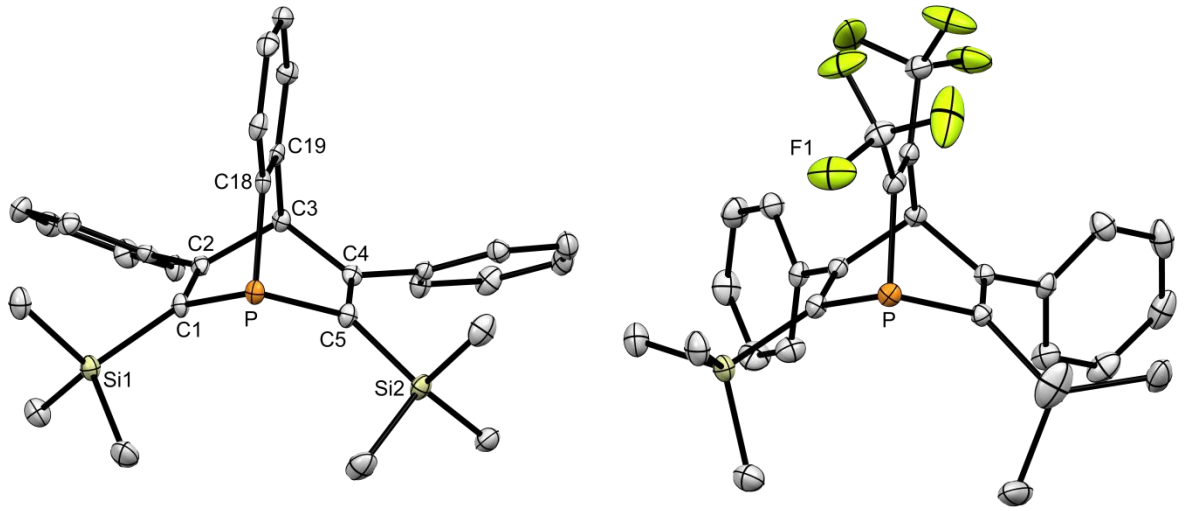

Figure 22. Molecular structure of **3.45** (left) and **3.46** (right) in the crystal. Displacement ellipsoids are shown at the 50% probability level. Hydrogen atoms are omitted for clarity. Only one molecule is shown in the case of **3.46**. Selected bond lengths (Å) and angles (°) for ligand **3.45**: P–C1: 1.869(2); P–C5: 1.869(3); P–C18: 1.842(3); C1–C2: 1.344(4); C2–C3: 1.538(4); C3–C4: 1.538(4); C4–C5: 1.343(4); C18–C19: 1.402(3); C19–C3: 1.517(3); Si1–C1: 1.874(3); Si2–C5: 1.880(3); C1–P–C5: 97.0(1); C1–P–C18: 94.9(1); C5–P–C18: 95.0(1). Selected bond lengths (Å) and angles (°) for ligand **3.46**: P–C1: 1.869(2); P–C5: 1.864(2); P–C18: 1.858(2); C1–C2: 1.341(3); C2–C3: 1.544(3); C3–C4: 1.544(3); C4–C5: 1.338(3); C18–C19: 1.328(3); C19–C3: 1.520(3); Si1–C1: 1.883(2); Si2–C5: 1.881(2); C1–P–C5: 96.75(9); C1–P–C18: 94.16(9); C5–P–C18: 95.53(9).

As reported by the group of Mézailles, it is possible to perform a protodesilylation on trimethylsilyl-substituted phosphabarrelenes using a fluoride source.[169] Several sources have been screened (aqueous HF, CsF, $Et_3N{\cdot}3HF$, PyHF, $NMe_4^+F^-$) but only tetrabutylammonium fluoride quantitatively transformed **3.45** into phosphabarrelene **3.47** (Scheme 34).

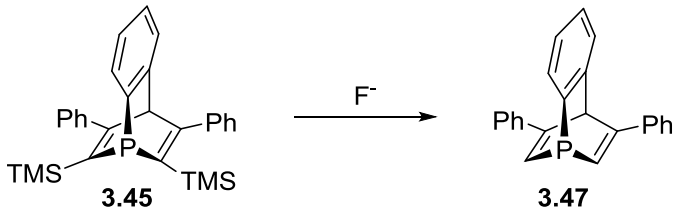

Scheme 34. Protodesilylation of phosphabarrelene **3.45** to compound **3.47**.

As in this work different phosphabarrelene derivatives have been crystallographically characterized, it is possible to compare the sum of their CPC angles (Σ_{CPC}) to evaluate the pyramidalization of the phosphorus atom. This method can be helpful to roughly estimate the basicity of a tertiary phosphine, since this value reflects the hybridization of the phosphorus atom.[216] A lower degree of pyramidalization at the phosphorus atom, related to a higher Σ_{CPC},

suggests a higher donation from the phosphorus lone pair. In Table 6 are reported the values of Σ_{CPC} for selected ligands.

Table 6. Σ_{CPC} values for selected phosphabarrelene ligands and PPh_3.

Ligand	Σ_{CPC} [°]
3.12	282.7[185]
3.1	282.9
3.45	286.9
3.46	286.4
PPh_3	307.2[169]

The Σ_{CPC} values are very similar for the two couples of ligands synthesized from the same phosphinine precursors. Aryl-substituted phosphabarrelenes **3.12** and **3.1** show a higher degree of pyramidalization compared to TMS-substituted **3.45** and **3.46**. This suggests that the latter are stronger σ-donors. A more accurate analysis of the electronic properties of these ligands is discussed in Chapter 5.

3.2.2 Cycloreversion reactions

Some phosphabarrelenes are prone to cycloreversion reactions, yielding phosphinines and alkynes (Scheme 35). This reaction is especially fast during the synthesis of phosphinines *via* cycloaddition on azaphosphinines, where nitrile molecules are eliminated instead of alkynes, and the phosphabarrelene intermediate has never been observed.[65,66,217] A similar example with a 2-phosphabarrelene reaction intermediate was reported by Bickelhaupt, in which a molecule of phosphaalkyne is excluded from a phosphanaphtalene.[218]

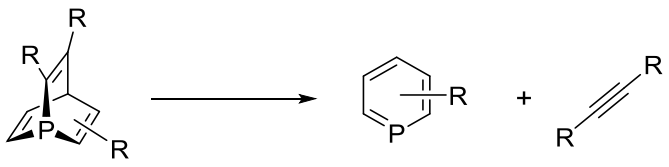

Scheme 35. Cycloreversion reaction of a phosphabarrelene to yield a phosphinine and an alkyne.

Thermolysis of benzophosphabarrelenes to phosphanaphtalenes has not been achieved, neither by heating up compound **3.20** in an oil bath nor in a microwave reactor under harsh conditions (T = 280 °C in toluene).[169] However, differently from other derivatives, trifluoromethyl-substituted phosphabarrelenes showed to be particularly prone to this kind of

reactions. The first example was reported for compound **3.34**, which yields back the starting materials when heated up to T = 100 °C.[99]

Interestingly, compound **3.46** showed a very diverse cycloreversion reactivity (Scheme 36).

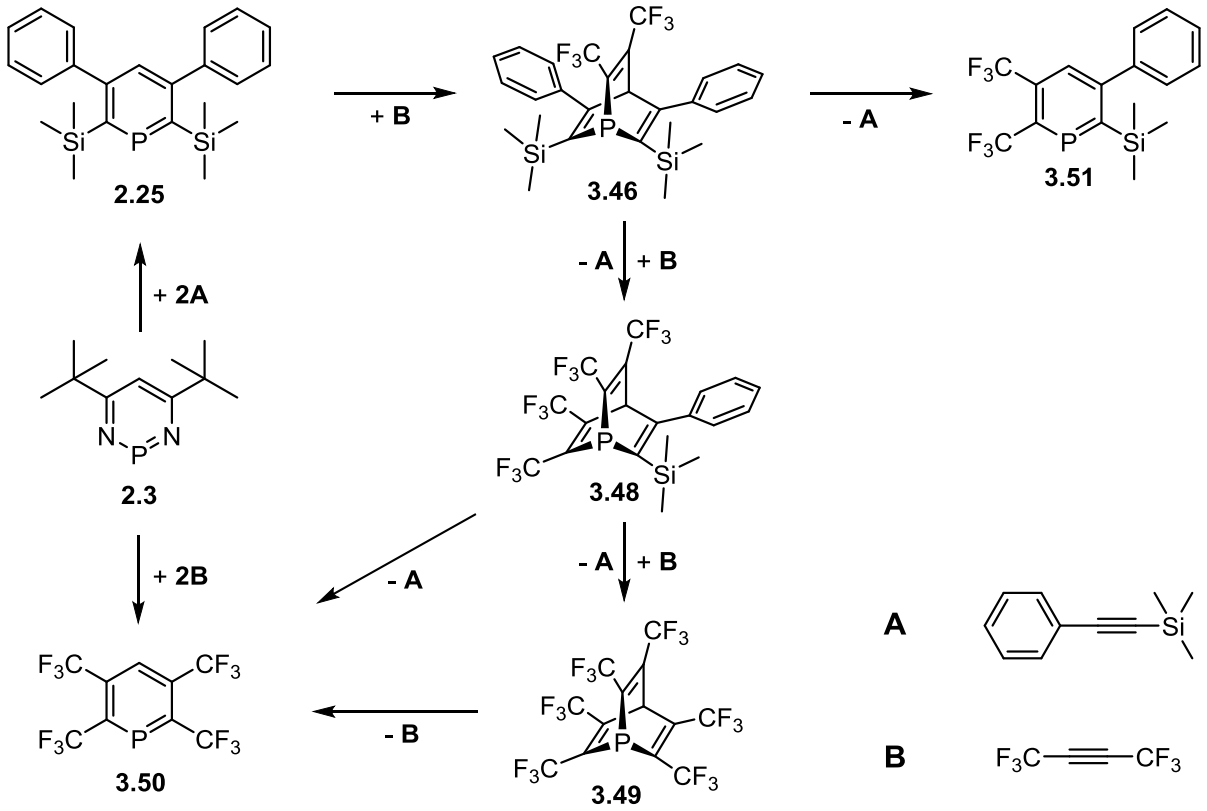

Scheme 36. Cycloaddition/cycloreversion reactions between trifluoromethyl-substituted phosphinines and phosphabarrelenes.

As stated above, phosphinine **2.25** reacts quantitatively to phosphabarrelene **3.46** at T = 60 °C in toluene in the presence of an excess of hexafluoro-2-butyne. Further heating to T = 85 °C does not result in any change according to the NMR spectra. However, when the temperature is raised to T = 100 °C for 16 h, a mixture of **3.46**, **3.48**, **3.50** and **3.51** is observed. These compounds could be identified by means of $^{31}P\{^{1}H\}$ NMR spectroscopy, since each substance has a characteristic chemical shift and coupling pattern between phosphorus and the fluorine atoms. Heating up to even higher temperatures (T = 120 °C) shifts the equilibrium towards **3.50**. Surprisingly, changing the solvent from toluene to methylcyclohexane modified the ratio of the products in the mixture, as after 72 h of heating at T = 100 °C **3.48** was the main product in a mixture with **3.46** and **3.49** (65% *vs* 30% *vs* 5%). With further heating at T = 120 °C for 16 h **3.46** was fully consumed and the resonance of **3.50** appeared, together with an increase in the amount of **3.49**. Interestingly, the latter is volatile and can be removed from the reaction mixture applying vacuum. However, the separation and full characterization of **3.48**

and **3.49** was not attempted. Heating up for longer time decreases the amount of **3.48** and increases the amounts of **3.49** and **3.50**. The latter can also be obtained directly by condensing an excess of hexafluoro-2-butyne on diazaphosphinine **2.3**. The first equivalent reacts in 10 minutes at room temperature, while the second cycloaddition/cycloreversion step is quantitatively performed by heating up to T = 60 °C for 16 h in toluene. Unfortunately, the high sensitivity of **3.50** did not allow for the isolation and purification of this compound, which decomposed upon contact with silica in the glovebox.

Similarly, in order to try to extrude an equivalent of trimethylsilyl-phenylacetylene (**A**) from **3.45** and substitute it with hexafluorobutyne, an excess of the gas was condensed in a closed vessel together with phosphabarrelene **3.45** and the mixture was heated up to T = 140 °C for 16 h. Unfortunately no change was detected in the $^{31}P\{^{1}H\}$ NMR spectrum.

On the other hand, if compound **3.46** is heated up to T = 140 °C for 16 h, a cycloreversion reaction yields phosphinine **3.51**, which can be purified by column chromatography under air. This molecule proved to have interesting properties for the activation of small molecules, similarly to a compound reported by Le Floch and co-workers.[119]

First of all, **3.51** is water stable, and can be heated in THF for 16 h in the presence of water without reacting (Scheme 37). On the other hand, it reacts with water in the presence of a base, and four different doublets are detected in the $^{31}P\{^{1}H\}$ NMR spectrum of the reaction mixture. This suggests a non-selective water addition at the P=C double bond, with the formation of the *syn* and *anti* products on both the α-carbons.

Interestingly, in the presence of methanol the phosphorus atom undergoes an oxidative addition, yielding compound **3.52** quantitatively (Scheme 37).

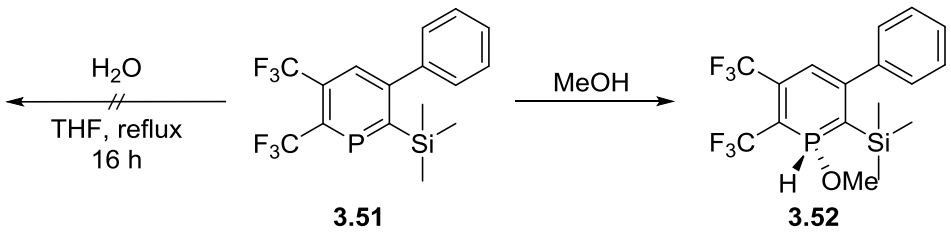

3.51 **3.52**

Scheme 37. Reactivity of **3.51** towards water and methanol.

The $^{31}P\{^{1}H\}$ NMR spectrum of this compound shows a doublet at δ = 21.2 ppm, with a coupling constant of $^{1}J_{P\text{-}H}$ = 570 Hz, comparable to literature known values.[119] Single crystals suitable for X-ray diffraction were obtained from a concentrated solution in methanol at

T = 4 °C and the molecular structure of **3.52** in the crystal is depicted in Figure 23. A similar compound was reported by Le Floch *et al.* (**2.16**), however, no crystallographic characterization was performed. Also, in this case the oxidative addition was thought to be facilitated by the presence of phosphino-sulfide groups.[119] The synthesis of phosphinine **3.52** proves wrong these hypotheses and suggests that the electronic properties of the phosphinine (most likely the low aromaticity) account for this peculiar behavior. Interestingly, this is a rare example of the activation of O-H bonds by main group elements.

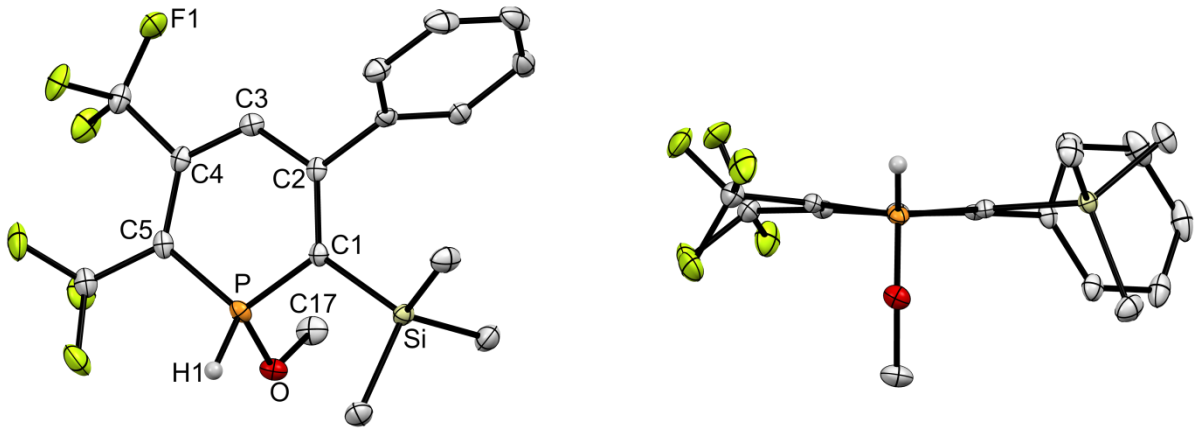

Figure 23. Molecular structure of **3.52** in the crystal: top view (left) and front view (right). Displacement ellipsoids are shown at the 50% probability level. Calculated hydrogen atoms are omitted for clarity. Selected bond lengths (Å) and angles (°): P1–C1: 1.732(2); P1–C5: 1.728(2); P1–O: 1.603(2); O–C17: 1.448(2); P–H1: 1.28(2); C1–C2: 1.388(3); C2–C3: 1.413(3); C3–C4: 1.376(3); C4–C5: 1.413(3); C1–Si: 1.900(2); C1–P–C5: 108.24(9); H1–P1–O: 95.7(9).

In addition to this, **3.51** shows an unusual reactivity towards HCl. Phosphinines are in general stable towards strong acids, but in this case upon addition of an excess of HCl a single resonance is visible in the $^{31}P\{^{1}H\}$ NMR spectrum at $\delta = 49$ ppm. Most likely, one equivalent of HCl performs a hydrodesilylation at the phosphinine ring[219] and a second equivalent adds at the P=C double bond, which was never observed before for $\lambda^3\sigma^2$-phosphinines. Reaction with $NH_3{\cdot}BH_3$, in the attempt of adding dihydrogen at the P center,[220] led to unidentified products.

Most interesting is the reaction with NH_3. Ammonia was condensed in a tube containing **3.51** which was then sealed under vacuum, and the solid ammonia was carefully thawed. The $^{31}P\{^{1}H\}$ NMR spectrum of the reaction mixture shows one doublet at $\delta = 2.1$ ppm with a coupling constant of $^{1}J_{P\text{-}H} = 498$ Hz, which confirms the presence of a direct P-H bond. Unfortunately, no additional characterization was possible, and it is not clear yet whether ammonia activation or, alternatively, an ammonia-catalyzed water addition was achieved in

this case. The fact that only one doublet is detected in the NMR spectrum is, however, a promising signal.

3.2.3 Oxidation

Like most phosphines, phosphabarrelenes are prone to oxidation with chalcogens. This can be achieved using well established procedures which have been reported in the introduction of this chapter (*vide supra*). Oxidation to the corresponding oxides can be easily achieved using hydrogen peroxide. To a solution of the appropriate ligand in DCM an excess of H_2O_2 is added and the mixture is stirred until full conversion, monitoring the reaction by means of $^{31}P\{^1H\}$ NMR spectroscopy. The excess of hydrogen peroxide can be removed by heating up the solution to the boiling point if in small quantities and the remaining white solid was dried thoroughly in vacuum. Oxidation with sulfur can be achieved by heating up the phosphabarrelene derivative together with elemental sulfur and DBU. A filtration over a short plug of silica gel affords the pure product in high yields (~ 90%). Finally oxidation with selenium is obtained by stirring the compound in refluxing toluene in the presence of an excess of grey selenium, which can be easily filtered out at the end of the reaction. In all these cases, a downfield shift was observed for the resonance of the phosphorus atom in the $^{31}P\{^1H\}$ NMR spectra.

Three oxidized derivatives have been prepared and fully characterized for phosphabarrelene **3.12**. The molecular structures in the crystal of the oxide **3.53**, sulfide **3.54** and selenide **3.55** are reported in Figure 24 and selected bond lengths (Å) and angles (°) are reported in Table 7.

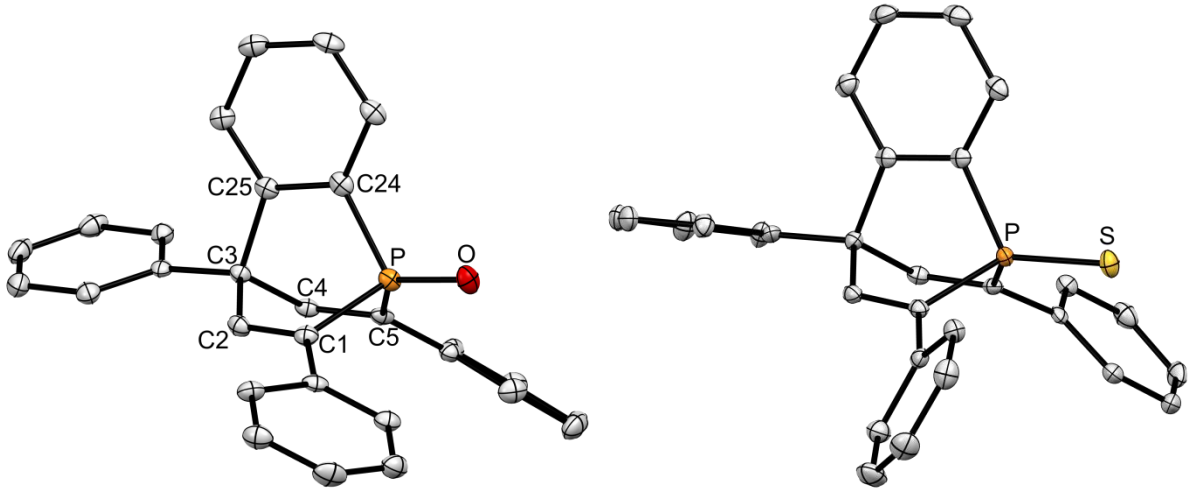

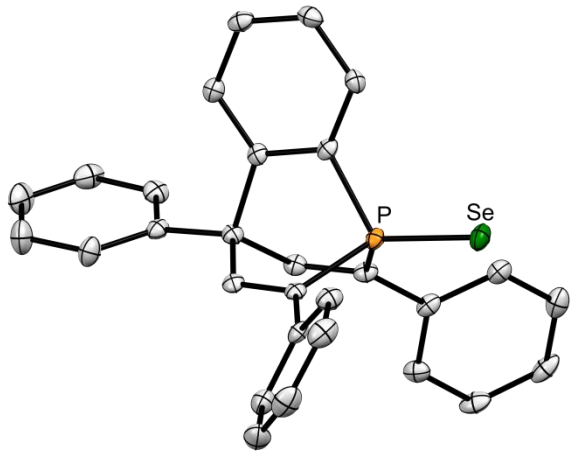

Figure 24. Molecular structure of **3.53**, **3.54** and **3.55** in the crystal. Displacement ellipsoids are shown at the 50% probability level. Hydrogen atoms and solvent molecules are omitted for clarity. Only one molecule is shown for each crystal structure. Selected bond lengths (Å) and angles (°) are reported in Table 7.

Table 7. Selected bond lengths (Å) and angles (°) of **3.53**, **3.54** and **3.55**, with E = O, S, Se, respectively.

Bond (Å) /angle (°)	**3.53**	**3.54**	**3.55**
P-C1	1.824(2)	1.831(2)	1.838(3)
P-C24	1.795(2)	1.810(2)	1.812(2)
P-C5	1.818(2)	1.830(2)	1.839(2)
P-E	1.476(1)	1.9365(6)	2.0924(7)
C1-C2	1.340(3)	1.333(2)	1.330(3)
C2-C3	1.539(3)	1.535(2)	1.531(3)
C3-C4	1.540(3)	1.538(2)	1.538(3)
C4-C5	1.334(3)	1.333(2)	1.333(4)
C24-C25	1.393(3)	1.398(2)	1.390(4)
C25-C3	1.557(2)	1.561(2)	1.563(3)
C1-P-C5	98.57(9)	98.87(8)	97.9(1)
C1-P-C24	98.65(9)	98.27(8)	97.4(1)
C24-P-C5	99.71(9)	97.01(8)	98.4(1)

Similarly, also phosphabarrelene **3.45** was oxidized with selenium to the derivative **3.56**. As in the case of **3.55**, after 16 h in refluxing toluene in the presence of grey selenium, the

$^{31}P\{^{1}H\}$ NMR spectrum shows only one resonance, with typical satellites due to the $^{1}J_{P\text{-}Se}$ coupling. The molecular structure in the crystal of **3.56** is depicted in Figure 25.

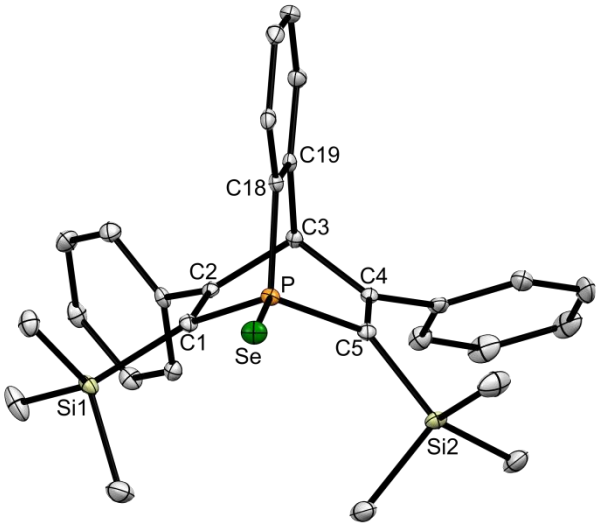

Figure 25. Molecular structure of **3.56** in the crystal. Displacement ellipsoids are shown at the 50% probability level. Hydrogen atoms are omitted for clarity. Selected bond lengths (Å) and angles (°): P–C1: 1.839(2); P–C5: 1.839(1); P–C18: 1.813(2); P–Se: 2.1010(5); Si1–C1: 1.903(2); Si2–C5: 1.899(2); C1–C2: 1.344(2); C2–C3: 1.547(2); C3–C4: 1.545(2); C4–C5: 1.349(2); C18–C19: 1.396(2); C19–C3: 1.524(4); C1–P–C5: 100.44(8); C1–P–C18: 98.94(8); C5–P–C18: 100.43(8).

The oxidation properties of phosphabarrelenes strongly depend on their substitution pattern. In fact, a different reactivity was observed for trifluoromethyl-substituted barrelenes **3.1** and **3.46**. None of these ligands reacted with grey selenium after prolonged heating in solution. In particular **3.46** started decomposing to phosphinine **3.51** before any oxidation could take place. While it still needs to be clarified whether oxidation with elemental sulfur is accessible, both these ligands could be easily oxidized to the corresponding oxides using H_2O_2 in DCM. In particular **3.57**, the oxide of **3.1**, was characterized crystallographically (Figure 26).

In an attempt to synthesize the elusive phosphinine-oxide, the oxide of phosphabarrelene **3.46** (**3.58**) was heated in toluene. Unfortunately, even though the reduced species underwent easy cycloreversions upon heating (see Scheme 36), this compound did not react after 16 h at T = 120 °C. Maybe even higher temperatures need to be reached, even though the unstable phosphinine-oxide could be affected by such harsh conditions.

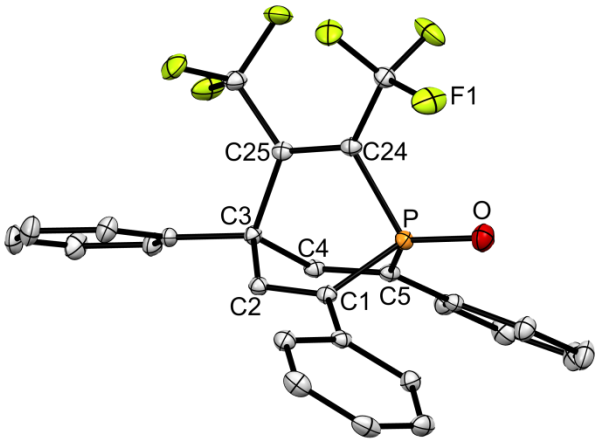

Figure 26. Molecular structure of **3.57** in the crystal. Displacement ellipsoids are shown at the 50% probability level. Hydrogen atoms are omitted for clarity. Selected bond lengths (Å) and angles (°): P–C1: 1.816(1); P–C5: 1.821(2); P–C24: 1.840(2); P–O: 1.460(1); C1–C2: 1.334(2); C2–C3: 1.552(2); C3–C4: 1.540(2); C4–C5: 1.339(2); C24–C25: 1.338(2); C25–C3: 1.570(2); C1–P–C5: 99.87(7); C1–P–C24: 96.10(7); C5–P–C24: 99.30(7).

3.2.4 Coordination chemistry

Even though phosphabarrelenes have been used as ligands in coordination chemistry for quite some time and partial studies on their electronic properties have been performed, an in-depth investigation and a comparison with state-of-the-art ligands is still missing.[171,187,221]

To examine their electronic properties, metal-carbonyl complexes of phosphabarrelenes were synthesized. In fact, metal-carbonyls can be used as probes for the evaluation and comparison of the electronic properties of a ligand, since the stretching of the CO bands in the infrared spectra is proportional to the net-donation of electron density from the ligand to the metal center. More precisely, the higher the net-donation, the lower the frequency of the stretching vibration. The results of the analysis on the electronic properties are reported in Chapter 5.

Various metal-carbonyl complexes have been synthesized in this work. First, group 6 metals have been used and the coordination compounds have been characterized by means of NMR and IR spectroscopy. Complexes **3.58**, **3.59** and **3.60** have been prepared starting from the corresponding $[M(CO)_5THF]$ precursors (M = Cr, Mo, W). Interestingly, **3.58** is the first phosphabarrelene-based chromium complex. The molecular structures in the crystal of these compounds are depicted in Figure 27, while selected bond lengths and angles are reported in Table 8.

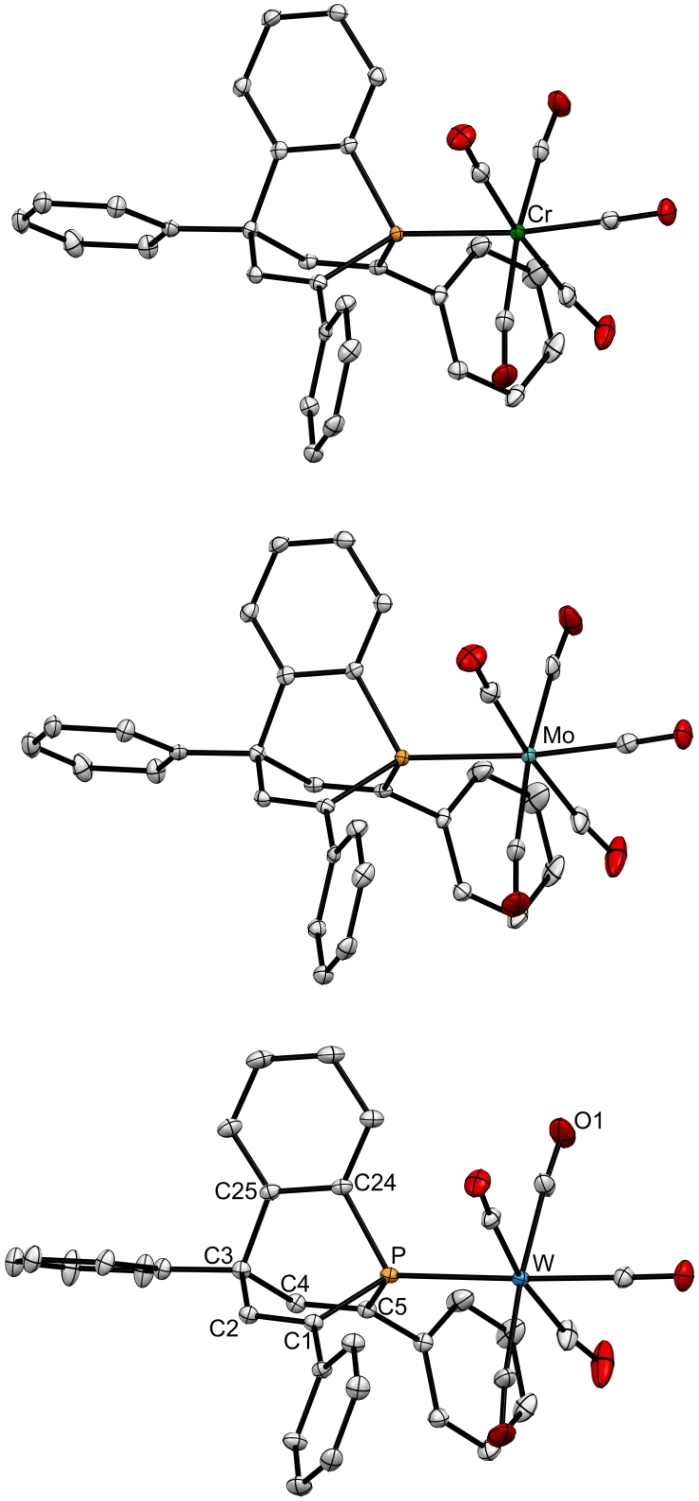

Figure 27. Molecular structure of **3.58**, **3.59** and **3.60** in the crystal. Displacement ellipsoids are shown at the 50% probability level. Hydrogen atoms are omitted for clarity. Selected bond lengths (Å) and angles (°) are reported in Table 8.

Table 8. Selected bond lengths (Å) and angles (°) of complexes **3.58**, **3.59** and **3.60**, with M = Cr, Mo, W respectively.

Bond (Å) /angle (°)	**3.58**	**3.59**	**3.60**
P-C1	1.849(1)	1.849(2)	1.853(1)
P-C24	1.837(2)	1.841(2)	1.833(1)
P-C5	1.853(2)	1.853(2)	1.845(1)
P-M	2.3769(5)	2.5216(6)	2.5275(2)
C1-C2	1.326(2)	1.330(3)	1.336(2)
C2-C3	1.529(2)	1.537(3)	1.532(2)
C3-C4	1.536(2)	1.534(3)	1.531(2)
C4-C5	1.328(2)	1.329(3)	1.337(2)
C24-C25	1.403(2)	1.399(3)	1.406(2)
C25-C3	1.552(2)	1.556(3)	1.551(2)
C1-P-C5	95.74(7)	95.84(9)	95.94(6)
C1-P-C24	95.94(7)	96.10(9)	95.90(6)
C24-P-C5	94.81(7)	94.95(9)	95.46(6)

In order to synthesize the corresponding complexes with trifluoromethyl-substituted phosphabarrelenes, **3.1** was also employed in analogous reactions, but did not react with any of the metal precursors. Exploiting the possibility to perform a [4+2] cycloaddition on a phosphinine which is in the coordination sphere of a metal, an excess of hexafluoro-2-butyne was condensed into a NMR J-Young tube containing a solution of the phosphinine-tungsten complex **2.23**. Surprisingly, the alkyne did react with the phosphinine, which left the coordination sphere upon reaction. Over 3 days in refluxing toluene, the resonance of the tungsten complex slowly disappears, while the signal of **3.1** rises at δ = -65.5 ppm. Finally, only the resonances of phosphabarrelene **3.1** and some side-products originated by light exposure (see Chapter 4) were observable in the $^{31}P\{^{1}H\}$ NMR spectrum (Figure 28). It can be concluded that the coordination properties of this ligand are very different compared to its benzophosphabarrelene analogue.

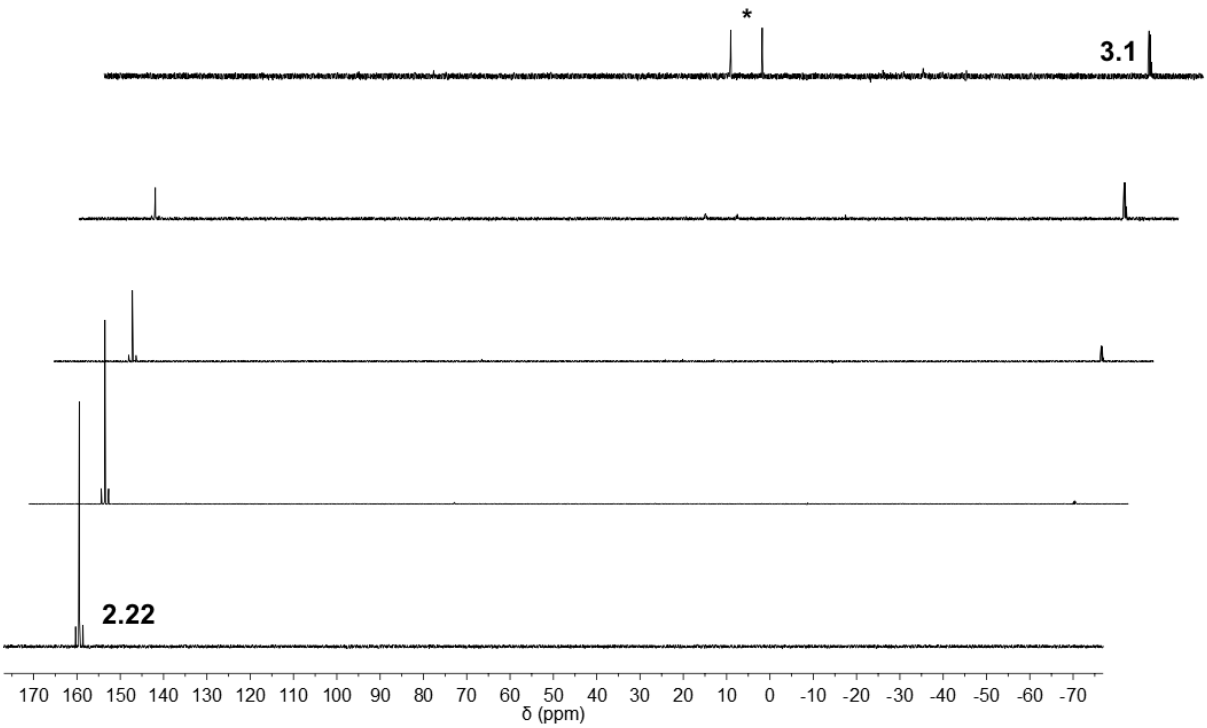

Figure 28. $^{31}P\{^{1}H\}$ NMR spectra of the reaction between **2.22** and hexafluoro-2-butyne. From bottom to top the consumption of **2.22** and the formation of **3.1** are observed. Side products in the top spectrum (*) are deriving from long light exposure (see Chapter 4).

Similarly, it was not possible to isolate a Rh complex of ligand **3.1**, since the reaction with $[Rh(CO)_2Cl]_2$ led to a rather unexpected result (see Chapter 4). The corresponding Rh complex featuring benzophosphabarrelene **3.12** instead has been prepared by Breit and co-workers, and its IR spectrum was used to estimate the electronic properties of the phosphabarrelene ligand.[171] Since the crystallographic characterization of this compound was still elusive, this complex (**3.61**) has been synthesized again. Single crystals suitable for X-ray analysis were grown from a concentrated solution in DCM and the molecular structure in the crystal was determined (Figure 29).

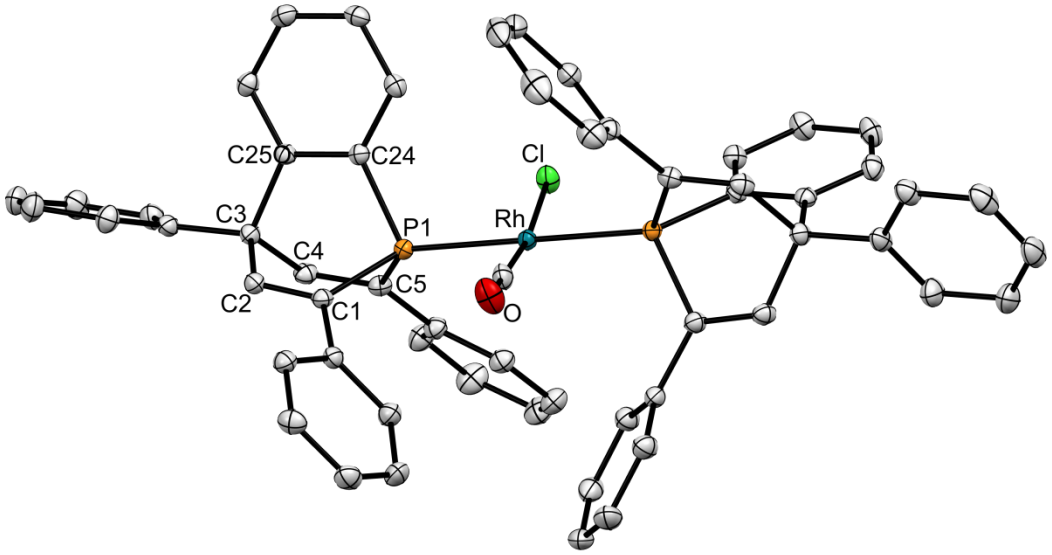

Figure 29. Molecular structure of **3.61** in the crystal. Displacement ellipsoids are shown at the 50% probability level. Hydrogen atoms are omitted for clarity. Selected bond lengths (Å) and angles (°): P1–C1: 1.841(2); P1–C5: 1.860(2); P1–C24: 1.823(2); P1–Rh: 2.3018(7); Rh–Cl: 2.3663(7); Rh–C30: 1.833(2); C30–O: 1.138(2); C1–C2: 1.335(3); C2–C3: 1.535(2); C3–C4: 1.538(3); C4–C5: 1.343(3); C24–C25: 1.393(3); C25–C3: 1.544(3); C1–P1–C5: 94.81(9); C1–P1–C24: 97.81(9); C5–P1–C24: 97.17(9).

As will be discussed in Chapter 5, [LNi(CO)$_3$] type complexes are the most common probes for the investigation of the electronic properties of a ligand. However, [LNi(CO)$_3$] complexes of phosphabarrelenes have so far not been reported in literature. To prepare them, an excess of [Ni(CO)$_4$] was condensed at T = -196 °C onto a solution with the appropriate ligand in a J-Young NMR tube using a condensation line (Scheme 38).

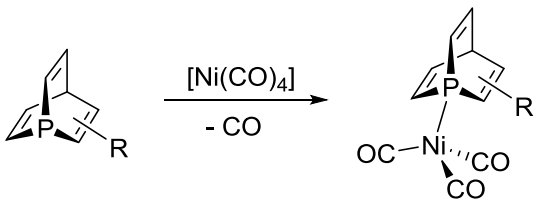

Scheme 38. Synthesis of [LNi(CO)$_3$] metal complexes.

Upon thawing of the solution and shaking, a violent gas evolution was detected in the NMR tube. In the $^{31}P\{^{1}H\}$ NMR spectrum, a downfield shift was observed, suggesting the formation of the respective nickel complexes. In Figure 30 the ligands employed in this reaction are illustrated. The reactions were generally fast but in some cases to reach full conversion it was necessary to degas the mixture in order to eliminate the CO produced in the NMR tube during the reaction. Unfortunately ligand **3.46** did not react at all with [Ni(CO)$_4$].

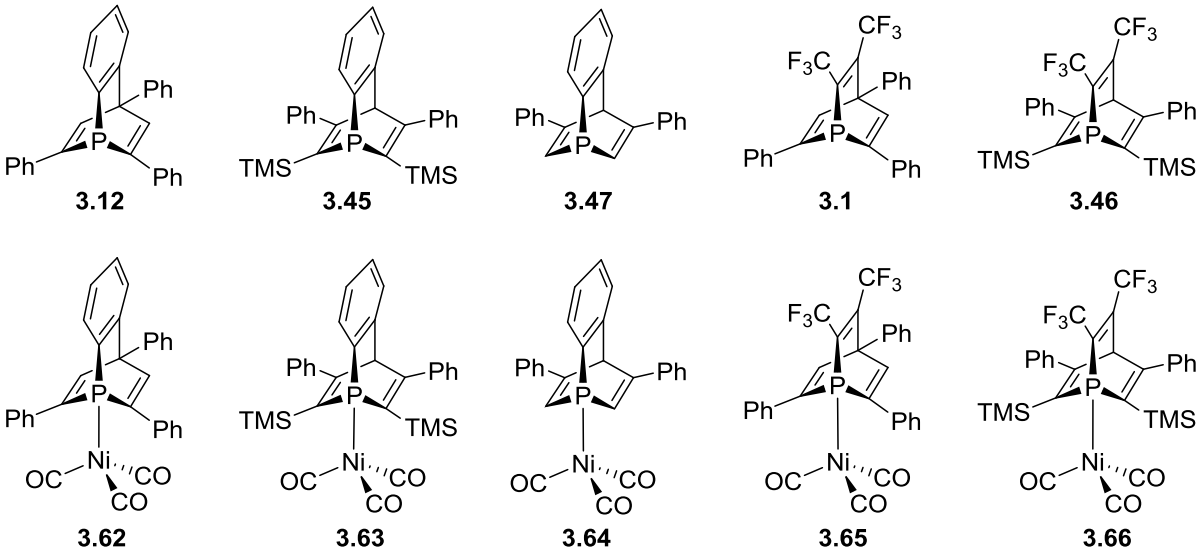

Figure 30. Phosphabarrelenes employed in the reaction with $[Ni(CO)_4]$ and corresponding metal complexes.

Evaporation of the volatiles yielded the compounds as off-white solids. The IR spectra were recorded in DCM and show the expected pattern for $[LNi(CO)_3]$ type complexes. The spectra will be discussed in Chapter 5. One of the derivatives (**3.62**) has been fully characterized and its molecular structure in the crystal is depicted in Figure 31. This is one of the few compounds of the type $[LNi(CO)_3]$ that has been characterized crystallographically.[222]

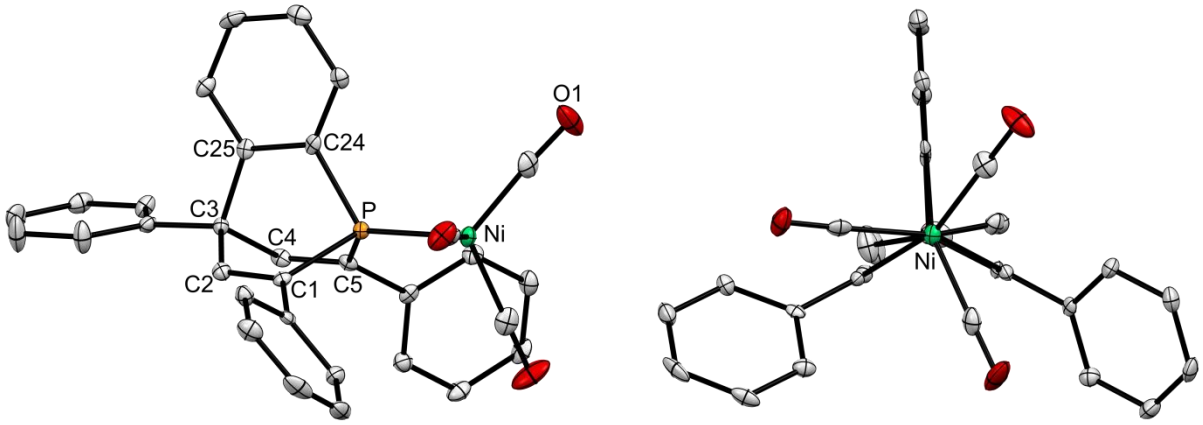

Figure 31. Molecular structure of **3.62** in the crystal. Displacement ellipsoids are shown at the 50% probability level. Hydrogen atoms are omitted for clarity. Selected bond lengths (Å) and angles (°): P–C1: 1.853(3); P–C5: 1.835(3); P–C24: 1.829(3); P–Ni: 2.1976(8); Ni–C(avg.): 1.798(4); C–O(avg.): 1.140(4); C1–C2: 1.328(4); C2–C3: 1.533(5); C3–C4: 1.537(4); C4–C5: 1.320(4); C24–C25: 1.401(3); C25–C3: 1.548(4); C1–P1–C5: 96.0(1); C1–P1–C24: 94.7(1); C5–P1–C24: 96.3(1).

In order to evaluate the properties of phosphabarrelenes as ligands in gold-catalyzed reactions, four [LAuCl] type complexes were synthesized starting from $[AuCl(SMe_2)]$ in DCM at room temperature using the suitable ligand (Figure 32).

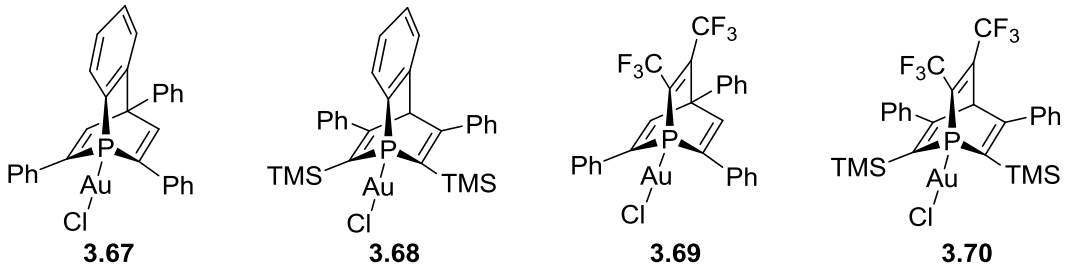

Figure 32. Phosphabarrelene-based gold(I) complexes.

Quantitative formation of complexes **3.67**, **3.68**, **3.69** and **3.70** was observed in the $^{31}P\{^{1}H\}$ NMR spectra, where a single downfield-shifted resonance was observed. Evaporation of the volatiles yielded the compounds as pale-yellow solids quantitatively. To completely remove dimethylsulfide it was necessary to either dissolve the complex again and remove the volatiles for a couple of times or dissolve the complex in the smallest amount of DCM and precipitate it with diethyl ether or pentane. In this way the obtained pale-yellow solid could be more easily thoroughly dried in vacuum. If needed, washing with diethyl ether or pentane was helpful. Single crystals of **3.67**, **3.68** and **3.69** suitable for X-ray diffraction were obtained by slow evaporation of DCM at T = -35 °C. The molecular structures are depicted in Figure 33, Figure 34 and Figure 35.

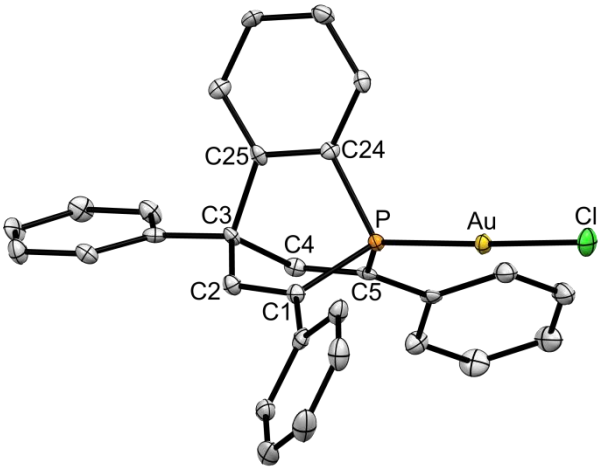

Figure 33. Molecular structure of **3.67** in the crystal. Displacement ellipsoids are shown at the 50% probability level. Only one molecule is shown. Hydrogen atoms and solvent are omitted for clarity. Selected bond lengths (Å) and angles (°): P–C1: 1.829(4); P–C5: 1.840(5); P–C24: 1.815(5); P–Au: 2.216(1); Au–Cl: 2.283(1); C1–C2: 1.333(5); C2–C3: 1.525(6); C3–C4: 1.540(5); C4–C5: 1.332(5); C24–C25: 1.403(6); C25–C3: 1.551(6); C1–P1–C5: 99.1(2); C1–P1–C24: 98.3(2); C5–P1–C24: 95.9(2).

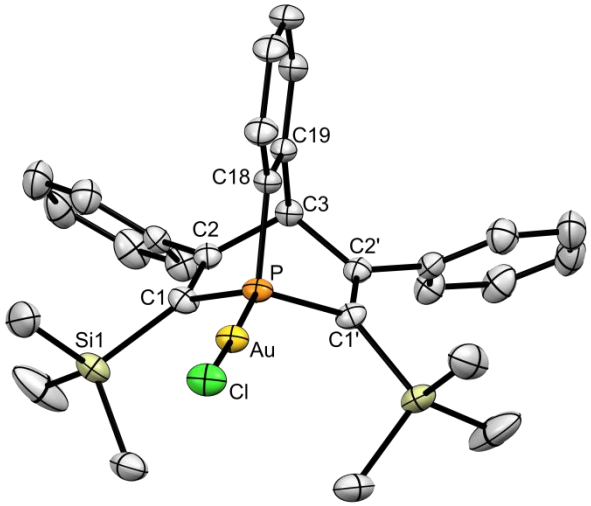

Figure 34. Molecular structure of **3.68** in the crystal. Displacement ellipsoids are shown at the 50% probability level. Hydrogen atoms and solvent are omitted for clarity. Selected bond lengths (Å) and angles (°): P–C1: 1.836; P–C18: 1.816; P–Au: 2.229; Au–Cl: 2.283; Si1–C1: 1.890(4); C1–C2: 1.345(5); C2–C3: 1.535; C18–C19: 1.399; C19–C3: 1.533; C1–P–C1′: 100.8; C1–P–C18: 99.1.

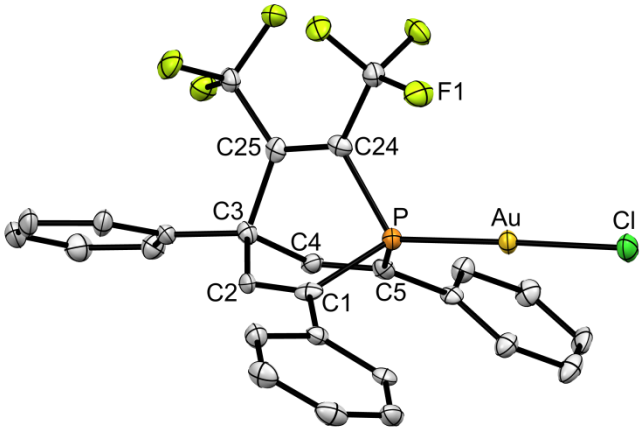

Figure 35. Molecular structure of **3.69** in the crystal. Displacement ellipsoids are shown at the 50% probability level. Hydrogen atoms are omitted for clarity. Selected bond lengths (Å) and angles (°): P–C1: 1.847(6); P–C5: 1.827(5); P–C24: 1.854(5); P–Au: 2.210(1); Au–Cl: 2.270(1); C1–C2: 1.291(8); C2–C3: 1.558(7); C3–C4: 1.540(6); C4–C5: 1.326(7); C24–C25: 1.320(8); C25–C3: 1.579(8); C1–P–C5: 99.6(2); C1–P–C24: 94.9(3); C5–P–C24: 97.1(2).

Phosphinine-containing copper complexes have been reported and some of them showed interesting optical properties.[63,104] Hence, it is interesting to investigate the properties of the analogous phosphabarrelene complexes. However, no copper complex containing phosphabarrelene ligands has been published in peer-reviewed journals so far.[169]

First, ligand **3.12** was mixed with anhydrous CuCl in DCM in equimolar amounts. The product is barely soluble and a white precipitate was observed in the reaction vessel. The $^{31}P\{^{1}H\}$ NMR spectrum shows a broad signal, which suggest the successful coordination to copper, since its quadrupolar moment typically gives rise to broad resonances. The ^{1}H NMR

spectrum shows a single set of signals, suggesting the quantitative formation of a single species. Surprisingly, the molecular structure in the crystal shows the formation of the 2:1 complex **3.71**, which has a distorted trigonal planar geometry (Figure 36). Repeating the experiment with a 2-fold amount of ligand resulted in the same species according to the NMR spectra, suggesting that 0.5 equivalents of unreacted CuCl were still present in the solution.

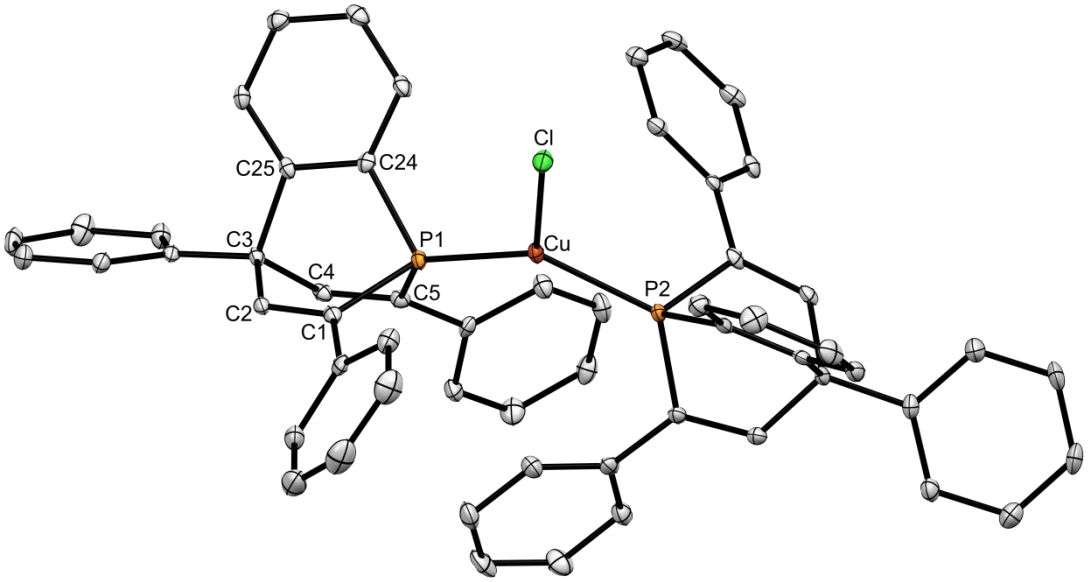

Figure 36. Molecular structure of **3.71** in the crystal. Displacement ellipsoids are shown at the 50% probability level. Hydrogen atoms are omitted for clarity. Selected bond lengths (Å) and angles (°): P1–C1: 1.846(2); P1–C5: 1.838(2); P1–C24: 1.829(2); P1–Cu: 2.2340(6); Cu–Cl: 2.2475(8); P2–Cu: 2.2256(8); C1–C2: 1.330(3); C2–C3: 1.537(3); C3–C4: 1.532(4); C4–C5: 1.340(3); C24–C25: 1.404(3); C25–C3: 1.553(4); C1–P1–C5: 95.8(1); C1–P1–C24: 96.1(1); C5–P1–C24: 97.2(1); P1–Cu–P2: 134.42(3); P1–Cu–Cl: 108.08(3); P2–Cu–Cl: 117.38(3).

To obtain a 1:1 adduct, it was necessary to switch to a more strongly coordinating solvent. The same reaction performed in refluxing acetonitrile yielded crystalline **3.72**, whose molecular structure is depicted in Figure 37. Interestingly, only one molecule of acetonitrile is found in the asymmetric unit, probably due to steric reasons. Consequently, one of the copper centers has a tetrahedral geometry, while the other one is arranged in a distorted trigonal planar fashion. Due to its extremely low solubility, the characterization in solution is limited to the ^{1}H NMR spectrum. This complex appeared to be only stable in acetonitrile. When the crystals were dissolved in DCM, the ^{1}H NMR spectrum looked equal to the one of **3.71**.

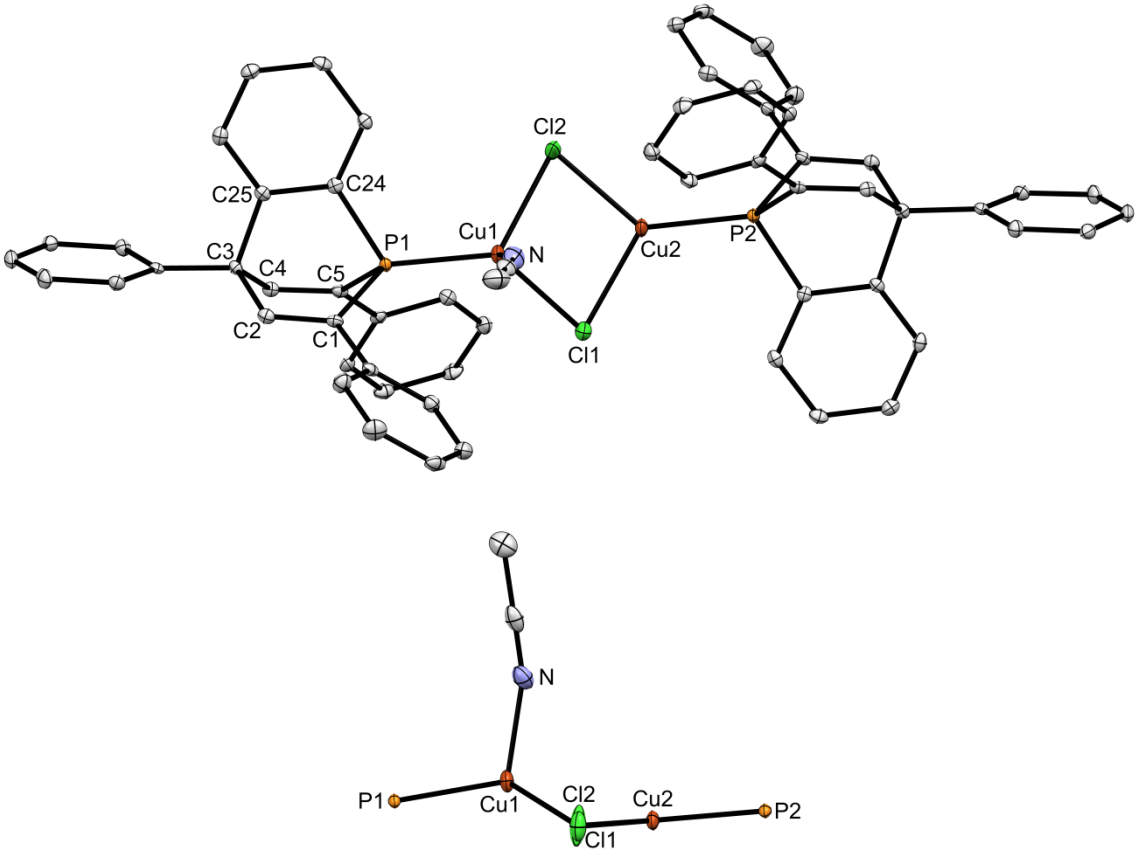

Figure 37. Molecular structure of **3.72** in the crystal (top) and side view of the metal's coordination sphere (bottom). Displacement ellipsoids are shown at the 50% probability level. Hydrogen atoms are omitted for clarity. Selected bond lengths (Å) and angles (°): P1–C1: 1.849(2); P1–C5: 1.850(2); P1–C24: 1.828(2); P1–Cu1: 2.2027(7); Cu1–Cl1: 2.3864(8); Cu1–Cl2: 2.4014(8); Cu1–N: 2.023(2); Cu2–Cl1: 2.2892(7); Cu2–Cl2: 2.2659(7); P2–Cu2: 2.1715(6); C1–C2: 1.331(3); C2–C3: 1.541(3); C3–C4: 1.540(3); C4–C5: 1.332(3); C24–C25: 1.404(3); C25–C3: 1.552(3); C1–P1–C5: 95.2(1); C1–P1–C24: 96.4(1); C5–P1–C24: 96.1(1); P1–Cu1–Cl1: 123.51(3); P1–Cu1–Cl2: 116.56(3); P1–Cu1–N: 108.84(7); P2–Cu2–Cl1: 125.75(3); P2–Cu2–Cl2: 132.72(3); Cl1–Cu2–Cl2: 101.52(3).

3.3 Conclusions

A new strategy for the formation of phosphabarrelenes was presented, which uses arynes prepared at low temperature from iodosulfonates. Even though the isolated yields are not higher than the reported ones, this could be a good methodology for the insertion of functional groups on the phosphabarrelene backbone. A definitive mechanistic proof has been found for the concerted Diels-Alder reaction of an aryne with a phosphinine ring. No λ^4-phosphinine intermediate is involved in this process.

The oxidation of phosphabarrelenes was investigated. Oxidized benzophosphabarrelene derivatives with O, S, Se have been synthesized, fully characterized and structurally compared. Trifluoromethyl-substituted phosphabarrelenes are more difficult to oxidize and only oxides were obtained.

The cycloreversion reactivity of a trifluoromethyl-substituted phosphabarrelene has been investigated. An asymmetrically substituted phosphinine was obtained in high yields starting from this phosphabarrelene derivative. This compound shows interesting properties for the activation of small molecules.

The coordination chemistry of phosphabarrelenes has been further explored. Complexes of Cr, Mo, W and Rh with benzophosphabarrelenes have been synthesized and fully characterized. At the same time trifluoromethyl-substituted ligands showed different reactivity with the same metal precursors. Ni complexes of the ligands were prepared in order to compare their electronic properties (see Chapter 5). The coordination chemistry with Cu was investigated and the first complexes were reported. New gold complexes have been synthesized and fully characterized, in order to test them in Au(I)-catalyzed cycloisomerization reactions (see Chapter 5).

3.4 Experimental part

General Remarks

Unless otherwise stated, all the experiments were performed under an inert argon atmosphere using modified Schlenk techniques or in a MBraun glovebox. All common chemicals were commercially available and were used as received. Dry or deoxygenated solvents were prepared using standard techniques or used from a MBraun solvent purification system. The NMR spectra were recorded on a JEOL ECX400 (400 MHz) spectrometer and chemical shifts are reported relative to the residual resonance in the deuterated solvents. IR spectra were measured on a Nicolet iS10 FTIR-ATR spectrometer by Thermo Scientific in the solid state and on a Vertex 70 FT-IR spectrometer by Bruker in dichloromethane. For reactions under UV irradiation, a UVP High intensity 100 Watt B-100AP Mercury Vapor Lamp without filter was used. Iodophenyltosylate derivatives,[223,224] pyrylium salts[225] and phosphinines[51,66] have been prepared according to the literature.

[4,6,7-triphenyl-2,3-bis(trifluoromethyl)-1-phosphabicyclo[2.2.2]octa-2,5,7-triene], (3.1)

The compound was synthesized according to a modified literature procedure.[37] 18 mL of dry methylcyclohexane were added to triphenylphosphinine (1.00 g, 3.09 mmol) in a 100 mL Schlenk bomb. After degassing completely the reaction vessel, hexafluorobutyne was condensed into the solution (2.5 g, 15.45 mmol). The reaction mixture was then heated up to T = 100 °C and stirred for t = 48 h. Afterwards the volatiles were removed and the crude mixture was absorbed on silica gel (*ca*. 10 g). The loaded silica was stored under air for one week. Subsequently the adsorbate was eluted through another pad of silica gel (*ca*. 8 cm) with hexane. The dark crude mixture obtained was then recrystallized from EtOH/water, yielding the pure product as a white powder (631 mg, 51%). Single crystals suitable for X-ray analysis were obtained by slow evaporation from a diethyl ether solution.

Caution: vessel under pressure!

$^{1}H\{^{19}F\}$ NMR ($CDCl_3$, 400 MHz): δ = 7.37 (m, 6H), 7.49 (m, 1H), 7.55 (m, 2H), 7.63 (m, 4H), 7.80 (d, 2H, *J* = 7.2 Hz), 8.06 (d, 2H, *J* = 6.5 Hz) ppm.

$^{13}C\{^{1}H,^{19}F\}$ NMR ($CDCl_3$, 101 MHz): δ = 66.7 (d, *J* = 5.3 Hz), 121.3 (s), 123.5 (d, *J* = 27.7 Hz), 126.2 (d, *J* = 13.5 Hz), 128.5 (s), 128.8 (d, *J* = 1.8 Hz), 128.9 (s), 129.0 (s), 129.3 (s), 137.0 (d, *J* = 26.4 Hz), 139.1 (s), 148.3 (d, *J* = 3.6 Hz), 148.9 (d, *J* = 34.1 Hz), 152.4 (d, *J* = 19.7 Hz), 159.1 (d, *J* = 3.9 Hz) ppm.

$^{31}P\{^{1}H\}$ NMR ($CDCl_3$, 162 MHz): δ = -65.5 (q, *J* = 37.2 Hz) ppm.

$^{19}F\{^{1}H\}$ NMR ($CDCl_3$, 376 MHz): δ = -54.5 (dq, *J* = 38.9, 13.1 Hz), -54.1 (q, *J* = 13.1 Hz) ppm.

General procedure for the synthesis of benzophosphabarrelenes *via* iodosulphonates

To a solution of 2-iodophenyl-4-methylbenzenesulfonate (1.6 g, 4.3 mmol, 1.4 eq) in THF (25 mL) at T = -95 °C isopropylmagnesium chloride (2.2 mL, 4.4 mmol, 1.4 eq; 2.0 M solution in THF) was added dropwise. The resulting pale brown to grey solution was stirred for t = 1 h. Subsequently, a solution of phosphinine (3.1 mmol, 1.0 eq.) in THF (8 mL) was added dropwise at T = -95 °C. The solution immediately turned dark green and was allowed to warm to room temperature overnight in the cooling bath (approximately 8 h). During the process, the color of the solution turned to dark red. The reaction mixture was quenched in air with NH_4Cl (sat. aq., 100 mL) and diluted with DCM (100 mL). The aqueous layer was extracted with DCM (2 × 20 mL) and the combined organic fractions were dried over anhydrous

$MgSO_4$ and concentrated under reduced pressure. The violet residue was purified by flash chromatography (silica gel, hexanes/DCM (5:1) + 1 vol% Et_3N), yielding the product as a colorless solid.

[2,4,10-triphenyl-4H-1,4-ethenophosphinoline], (3.12)

The spectroscopic data were consistent with those reported in the literature.[171] Yield: 21%.

[2,4-diphenyl-10-methyl-4H-1,4-ethenophosphinoline], (3.42)

The obtained yellow fraction was recrystallized under argon from EtOH/H_2O (3:1), yielding the product as a colorless solid (7%).

^{1}H NMR (THF-d_8, 400 MHz): δ = 2.13 (ddd, *J* = 13.4, 1.8, 1.0 Hz, 3H), 6.45 (m, 1H), 6.92 (m, 2H), 7.20 (m, 1H), 7.29 (m, 2H), 7.44 (m, 1H), 7.56 (m, 2H), 7.67 (m, 2H), 7.79 (m, 2H), 8.05 (dd, *J* = 5.9, 1.0 Hz, 1H) ppm.

^{13}C{^{1}H} NMR (THF-d_8, 101 MHz): δ = 20.9 (d, *J* = 36.7 Hz), 63.5 (d, *J* = 1.2 Hz), 123.5 (d, *J* = 12.9 Hz), 123.7 (d, *J* = 1.2 Hz), 125.7 (d, *J* = 13.2 Hz), 126.6 (d, *J* = 1.7 Hz), 127.2 (m), 128.2 (d, *J* = 1.2 Hz), 128.8 (d, *J* = 20.2 Hz), 131.1 (d, *J* = 38.2 Hz), 138.9 (d, *J* = 24.1 Hz), 141.6 (s), 141.8 (d, *J* = 12.0 Hz), 146.9 (dd, *J* = 12.6, 5.1 Hz), 148.7 (d, *J* = 16.3 Hz), 152.6 (d, *J* = 16.3 Hz), 155.6 (d, *J* = 4.0 Hz) ppm.

^{31}P{^{1}H} NMR (THF-d_8, 162 MHz): δ = -64.3 (s) ppm.

[3,9-diphenyl-2,10-bis(trimethylsilyl)-4H-1,4-ethenophosphinoline], (3.45)

The compound was synthesized according to a modified literature procedure.[187] 1-Bromo-2-fluorobenzene (0.39 mL, 3.57 mmol) was slowly added to a mixture of phosphinine **2.25** (1.00 g, 2.55 mmol) and magnesium turnings (93.1 mg, 3.83 mmol) in THF (20 mL) at room temperature. The reaction mixture was stirred for t = 12 h at room temperature. The solvent was evaporated, and the resulting residue was extracted with hexanes (3 x 5 mL). The resulting powder was rinsed with methanol (3 x 5 mL). After evaporation of the solvent, the title compound was obtained as an off-white crystalline solid in 49% yield (580 g, 1.24 mmol).

^{1}H NMR (C_6D_6, 400 MHz): δ = 0.12 (s, 18H), 5.70 (s, 1H), 7.45 (m, 14H) ppm.

$^{13}C\{^{1}H\}$ NMR (101 MHz, $CDCl_3$): δ = -0.1 (CH_3, d, *J* = 8.5 Hz), 71.9 (d, *J* = 4.2 Hz), 121.8 (s), 124.3 (s), 124.4 (s), 127.0 (d, *J* = 0.8 Hz), 127.8 (s), 130.7 (d, *J* = 32.6 Hz), 139.4 (d, *J* = 52.3 Hz), 142.9 (d, *J* = 22.1 Hz), 144.5 (d, *J* = 3.1 Hz), 148.0 (d, *J* = 3.0 Hz), 172.6 (d, *J* = 2.5 Hz) ppm.

$^{29}Si\{^{1}H\}$ NMR (79 MHz, $CDCl_3$): δ = -4.2 (d, *J* = 36.6 Hz) ppm.

$^{31}P\{^{1}H\}$ NMR (C_6D_6, 162 MHz): δ = -58.8 (s) ppm.

[5,8-diphenyl-6,7-bis(trimethylsilyl)-2,3-bis(trifluoromethyl)-1-phosphabicyclo[2.2.2]octa-2,5,7-triene], (3.46)

A solution of phosphinine **2.25** (392.6 mg, 1.0 mmol) in 10 mL of toluene in a 25 mL Schlenk bomb was degassed by pump and thaw. Subsequently, hexafluoro-2-butyne (roughly 4 eq.) was condensed in the vessel using a condensation line. Afterwards the mixture was allowed to warm up to room temperature and stirred at T = 65 °C overnight. The volatiles were removed and the crude mixture was recrystallized from hot methanol (then cooled to T = -20 °C), yielding the product as colourless crystals (471 mg, 85%). Crystals suitable for X-ray analysis were obtained during the recrystallization process.

^{1}H NMR (400 MHz, $CDCl_3$): δ = -0.03 (d, *J* = 1.1 Hz, 18H), 5.74 (m, 1H), 7.00 (m, 4H), 7.30 (m, 6H) ppm.

$^{13}C\{^{1}H,^{19}F\}$ NMR (101 MHz, $CDCl_3$): δ = -0.3 (CH_3, d, *J* = 7.0 Hz), 70.1 (d, *J* = 4.2 Hz), 121.8 (s), 123.3 (d, *J* = 27.5 Hz), 127.1 (s), 128.3 (s), 128.5 (s), 141.7 (d, *J* = 3.6 Hz), 141.8 (d, *J* = 54.9 Hz), 146.7 (d, *J* = 46.6 Hz), 148.8 (d, *J* = 4.2 Hz), 171.7 (d, *J* = 1.9 Hz) ppm.

^{19}F NMR (377 MHz, $CDCl_3$): δ = -60.9 (qd, *J* = 12.0, 1.1 Hz), -56.1 (dq, *J* = 29.5, 12.1 Hz) ppm.

$^{29}Si\{^{1}H\}$ NMR (79 MHz, $CDCl_3$): δ = -2.8 (d, *J* = 37.8 Hz) ppm.

$^{31}P\{^{1}H\}$ NMR (162 MHz, $CDCl_3$): δ = -50.6 (q, *J* = 29.4 Hz) ppm.

[3,9-diphenyl-4H-1,4-ethenophosphinoline], (3.47)

The compound was synthesized according to a literature procedure.[169] To a solution of phosphinine **3.45** (32.8 mg, 0.070 mmol) in THF 3 eq. of tetrabutylammonium fluoride hydrate [$(Bu_4N)F{\cdot}H_2O$, TBAF] were added and the solution was heated up to T = 60 °C for t = 1 h. Afterwards the volatiles were evaporated and the residue was dissolved in toluene. The solution was extracted with water three times and the organic phase was dryed over

anhydrous $MgSO_4$. Finally the toluene solution was eluted through a short plug of silica (6 cm, in a pipette) with toluene and the product was obtained as first fraction as a white solid after evaporation of the solvent (11.8 mg, 52%).

^{1}H NMR (400 MHz, THF-d_8): δ = 6.17 (m, 1H), 6.96 (m, 1H), 7.01 (m, 1H), 7.08 (m, 2H), 7.25 (m, 2H), 7.32 (m, 4H), 7.51 (m, 4H), 7.63 (m, 2H) ppm.

^{13}C{^{1}H} NMR (101 MHz, THF-d_8): δ = 60.1 (d, *J* = 2.4 Hz), 125.4 (d, *J* = 11.9 Hz), 125.9 (d, *J* = 1.1 Hz), 126.2 (s), 127.7 (d, *J* = 1.4 Hz), 129.0 (s), 129.4 (s), 131.7 (d, *J* = 21.3 Hz), 131.9 (d, *J* = 36.6 Hz), 140.0 (d, *J* = 2.5 Hz), 143.8 (d, *J* = 12.5 Hz), 150.8 (d, *J* = 4.2 Hz), 164.9 (d, *J* = 6.1 Hz) ppm.

^{31}P NMR (162 MHz, THF-d_8): δ = -78.6 (tdd, *J* = 51.9, 8.2, 2.2 Hz) ppm.

General procedure for the oxidation to phosphabarrelene oxides

To a solution of the appropriate phosphabarrelene in DCM (0.075 mmol), an excess of H_2O_2 (> 20-fold) was added and the solution was stirred until full conversion. The progress of the reaction was monitored by means of ^{31}P{^{1}H} NMR spectroscopy. Afterwards the solvent and the excess of H_2O_2 were removed by boiling the reaction mixture and the remaining white solid was dried thoroughly under vacuum. The reactions are quantitative. Crystals suitable for X-ray analysis were obtained by slow evaporation of a toluene solution.

[2,4,10-triphenyl-4H-1,4-ethenophosphinoline] oxide, (3.53)

^{1}H NMR ($CDCl_3$, 400 MHz): δ = 6.51 (dd, *J* = 7.7, 5.0 Hz, 1H), 7.09 (m, 1H), 7.23 (m, 1H), 7.32 (m, 2H), 7.38 (m, 4H), 7.54 (m, 1H), 7.64 (m, 2H), 7.76 (m, 6H), 8.01 (d, *J* = 31.8 Hz, 2H), 8.10 (m, 1H) ppm.

^{13}C{^{1}H} NMR ($CDCl_3$, 101 MHz): δ = 55.7 (d, *J* = 28.7 Hz), 124.1 (s), 125.06 (s), 127.0 (s), 128.2 (s), 128.6 (s), 129.2 (s), 129.4 (s), 133.3 (s), 134.1 (s), 134.2 (s), 134.2 (s), 139.4 (s), 144.6 (s), 145.4 (s), 148.8 (s), 152.1 (d, *J* = 4.3 Hz) ppm.

^{31}P{^{1}H} NMR ($CDCl_3$, 162 MHz): δ = 12.7 (s) ppm.

[4,6,7-triphenyl-2,3-bis(trifluoromethyl)-1-phosphabicyclo[2.2.2]octa-2,5,7-triene] oxide, (3.57)

^{1}H{^{19}F} NMR (acetone-d_6, 400 MHz): δ = 7.43 (m, 6H), 7.52 (m, 1H), 7.60 (m, 2H), 7.87 (m, 4H), 8.07 (d, 2H, *J* = 7.6 Hz), 8.36 (d, 2H, *J* = 33.2 Hz) ppm.

$^{13}C\{^{1}H,^{19}F\}$ NMR (acetone-d_6, 101 MHz): δ = 57.0 (d, *J* = 35.7 Hz), 121.7 (m), 122.9 (m), 128.4 (d, *J* = 6.1 Hz), 129.4 (s), 129.5 (s), 129.7 (s), 129.8 (s), 130.1 (s), 133.7 (d, *J* = 7.4 Hz), 139.1 (s), 142.4 (d, *J* = 69.8 Hz), 144.7 (d, *J* = 82.7 Hz), 151.0 (s), 159.8 (s) ppm.

$^{31}P\{^{1}H,^{19}F\}$ NMR (acetone-d_6, 162 MHz): δ = 9.8 (s) ppm.

$^{19}F\{^{1}H\}$ NMR (acetone-d_6, 376 MHz): δ = -55.1 (q, *J* = 13.8 Hz), -55.8 (q, *J* = 13.7 Hz) ppm.

[5,8-diphenyl-6,7-bis(trimethylsilyl)-2,3-bis(trifluoromethyl)-1-phosphabicyclo[2.2.2]octa-2,5,7-triene] oxide, (3.58)

^{1}H NMR (400 MHz, $CDCl_3$): δ = 0.08 (d, *J* = 0.9 Hz, 18H), 5.33 (d, *J* = 8.3 Hz, 1H), 6.99 (m, 4H), 7.34 (m, 6H) ppm.

$^{13}C\{^{1}H,^{19}F\}$ NMR (101 MHz, $CDCl_3$): δ = -0.1 (CH_3, d, *J* = 1.9 Hz), 61.9 (d, *J* = 52.8 Hz), 121.2 (d, *J* = 13.6 Hz), 126.7 (d, *J* = 1.2 Hz), 128.6 (s), 129.0 (s), 137.3 (d, *J* = 42.4 Hz), 138.4 (d, *J* = 61.9 Hz), 140.3 (d, *J* = 17.7 Hz), 147.8 (d, *J* = 4.4 Hz), 171.1 (d, *J* = 4.9 Hz) ppm.

^{19}F NMR (377 MHz, $CDCl_3$): δ = -60.5 (q, *J* = 12.4 Hz), -55.8 (dq, *J* = 12.4, 2.4 Hz) ppm.

$^{29}Si\{^{1}H\}$ NMR (79 MHz, $CDCl_3$): δ = -1.6 (d, *J* = 9.6 Hz) ppm.

$^{31}P\{^{1}H\}$ NMR (162 MHz, $CDCl_3$): δ = 24.1 (q, *J* = 2.4 Hz) ppm.

General procedure for the oxidation to phosphabarrelene sulfides

To a solution of the appropriate ligand in toluene, 1.1/8 eq. of S_8 and a drop of DBU were added. The reaction was then heated up to reflux for t = 5 h. Afterwards the volatiles were removed and the product was purified by column chromatography over a short plug of silica, using a DCM/pentane 3:2 mixture as eluent. The volatiles were once more removed yielding the product as a white solid in good yields.

[2,4,10-triphenyl-4H-1,4-ethenophosphinoline] sulfide, (3.54)

Yield: 71%.

^{1}H NMR ($CDCl_3$, 400 MHz): δ = 6.60 (dd, *J* = 7.6, 4.9 Hz, 1H), 7.15 (tt, *J* = 7.6, 1.2 Hz, 1H), 7.38 (m, 7H), 7.59 (m, 5H), 7.76 (m, 2H), 8.01 (d, *J* = 30.0 Hz, 2H), 8.21 (ddd, *J* = 14.4, 7.2, 1.3 Hz, 1H) ppm.

$^{13}C\{^{1}H\}$ NMR ($CDCl_3$, 101 MHz): δ = 57.4 (d, *J* = 24.5 Hz), 124.1 (d, *J* = 6.9 Hz), 125.2 (d, *J* = 12.9 Hz), 128.3 (s), 128.3 (s), 128.4 (s), 128.4 (s), 128.4 (s), 128.5 (s), 128.5 (s), 134.1 (d, *J* = 8.2 Hz), 135.0 (d, *J* = 77.0 Hz), 139.3 (s), 146.3 (d, *J* = 61.1 Hz), 149.8 (s), 151.5 (d, *J* = 1.6 Hz) ppm.

$^{31}P\{^{1}H\}$ NMR ($CDCl_3$, 162 MHz): δ = 16.0 (s) ppm.

General procedure for the oxidation to phosphabarrelene selenides

To a solution of the appropriate phosphabarrelene in toluene or THF, an excess of grey selenium was added and the solution was heated up to reflux until full conversion. The progress of the reaction was monitored by means of $^{31}P\{^{1}H\}$ NMR spectroscopy. Afterwards the solution was filtered over celite and the solvent was removed *in vacuo*, yielding the product as a white powder quantitatively. Crystals suitable for X-ray analysis were obtained by slow evaporation of a toluene solution.

[2,4,10-triphenyl-4H-1,4-ethenophosphinoline] selenide, (3.55)

^{1}H NMR (THF-d_8, 400 MHz): δ = 6.56 (dd, *J* = 7.6, 4.7 Hz, 1H), 7.13 (td, *J* = 7.5, 1.2 Hz, 1H), 7.29 (m, 7H), 7.58 (m, 7H), 7.88 (d, *J* = 7.2 Hz 2H), 8.07 (d, *J* = 28.8 Hz, 2H), 8.14 (m, 1H) ppm.

$^{13}C\{^{1}H\}$ NMR (THF-d_8, 101 MHz): δ = 59.8 (d, *J* = 22.2 Hz), 124.9 (d, *J* = 6.4 Hz), 125.8 (d, *J* = 13.4 Hz), 128.7 (s), 129.0 (s), 129.0 (s), 129.3 (d, *J* = 3.4 Hz), 129.7 (d, *J* = 5.6 Hz), 129.8 (s), 130.2 (s), 130.2 (d, *J* = 11.2 Hz), 135.6 (d, *J* = 9.6 Hz), 135.8 (d, *J* = 67.6 Hz), 140.6 (d, *J* = 1.5 Hz), 146.2 (d, *J* = 52.1 Hz), 150.9 (s), 152.6 (s) ppm.

$^{31}P\{^{1}H\}$ NMR (THF-d_8, 162 MHz): δ = 6.6 (s, $^{1}J_{P\text{-}Se}$ = 833.9 Hz) ppm.

[3,9-diphenyl-2,10-bis(trimethylsilyl)-4H-1,4-ethenophosphinoline] selenide, (3.56)

^{1}H NMR (400 MHz, THF-d_8): δ = 0.06 (bs, 18H), 5.34 (d, *J* = 4.3 Hz, 1H), 7.02 (bm, 4H), 7.23 (m, 1H), 7.31 (m, 8H), 8.11 (m, 1H) ppm.

$^{13}C\{^{1}H\}$ NMR (101 MHz, THF-d_8): δ = 0.8 (CH_3, d, *J* = 1.4 Hz), 68.9 (dd, *J* = 39.9, 2.0 Hz), 125.3 (d, *J* = 12.2 Hz), 127.0 (s), 128.0 (s), 128.2 (s), 128.8 (d, *J* = 10.3 Hz), 134.8 (s), 135.5 (s), 135.9 (d, *J* = 12.1 Hz), 142.2 (d, *J* = 15.6 Hz), 143.5 (d, *J* = 1.9 Hz), 172.5 (d, *J* = 8.1 Hz) ppm.

$^{29}Si\{^{1}H\}$ NMR (79 MHz, THF-d_8): δ = -1.4 (d, $^{2}J_{P\text{-}Si}$ = 14.5 Hz) ppm.

$^{31}P\{^{1}H\}$ NMR (162 MHz, THF-d_8): δ = 5.3 (s, $^{2}J_{P\text{-}Si}$ = 14.9 Hz, $^{1}J_{P\text{-}Se}$ = 779.8 Hz) ppm.

[2,4,10-triphenyl-4H-1,4-ethenophosphinoline]-pentacarbonylchromium(0), (3.58)

A solution of phosphabarrelene **3.12** (30 mg, 0.075 mmol) in THF was added dropwise to a solution of $[Cr(CO)_5{\cdot}THF]$[154] (1 eq.) in THF and heated at T = 80 °C for t = 3 h. Afterwards the solvent was removed *in vacuo* and the residue washed thoroughly with cold pentane, yielding the product as a white powder (55%). Crystals suitable for X-ray analysis were obtained by slow evaporation of a THF solution.

^{1}H NMR (400 MHz, $CDCl_3$): δ = 6.64 (dt, *J* = 7.5, 1.3 Hz, 1H), 7.11 (m, 5H), 7.27 (m, 1H), 7.33 (m, 6H), 7.50 (m, 1H), 7.57 (m, 2H), 7.67 (m, 2H), 7.85 (d, *J* = 15.9 Hz, 2H), 8.14 (ddd, *J* = 10.8, 7.4, 1.2 Hz, 1H) ppm.

$^{13}C\{^{1}H\}$ NMR ($CDCl_3$, 101 MHz): δ = 61.4 (d, *J* = 8.6 Hz), 124.9 (d, *J* = 11.9 Hz), 125.2 (bs), 127.7 (s), 128.1 (s), 128.3 (s), 128.8 (s), 129.4 (s), 130.8 (d, *J* = 18.7 Hz), 138.6 (d, *J* = 27.8 Hz), 139.0 (d, *J* = 15.4 Hz), 139.8 (s), 151.2 (bs), 152.3 (m), 215.6 (d, CO_{cis}, *J* = 13.8 Hz), 220.4 (bs, CO_{trans}) ppm.

$^{31}P\{^{1}H\}$ NMR (162 MHz, $CDCl_3$): δ = 25.5 ppm

IR (solid state): 2062 (CO), 1986 (w, CO), 1935 (shoulder), 1915 (s, CO) cm^{-1}.

[2,4,10-triphenyl-4H-1,4-ethenophosphinoline]-pentacarbonylmolibdenum(0), (3.59)

A solution of phosphabarrelene **3.12** (30 mg, 0.075 mmol) in THF was added dropwise to a solution of $[Mo(CO)_5{\cdot}THF]$, prepared by irradiating a suspension of $[Mo(CO)_6]$ (2.5 eq.) with UV light in THF for t = 5 h. An excess of metal precursor was needed since the dissociation of the CO molecule from the metal center is not complete. The solution was then refluxed overnight. Afterwards the solvent was removed under vacuum and the residue was dissolved in toluene and filtered over a plug of neutral aluminum oxide. Removing the volatiles yielded the product as a white powder (46%). Crystals suitable for X-ray analysis were obtained by slow evaporation from a pentane solution.

^{1}H NMR (400 MHz, $CDCl_3$): δ = 6.57 (d, 1H, *J* = 7.6 Hz), 7.03 (m, 4H), 7.24 (m, 4H), 7.49 (m, 4H), 7.62 (d, 3H, *J* = 7.1 Hz), 7.79 (d, 3H, *J* = 15.5 Hz), 8.05 (m, 2H) ppm.

$^{13}C\{^{1}H\}$ NMR ($CDCl_3$, 101 MHz): δ = 61.8 (d, *J* = 8.2 Hz), 124.9 (d, *J* = 12.4 Hz), 125.1 (d, *J* = 3.2 Hz), 127.8 (d, *J* = 12.4 Hz), 128.1 (s), 128.3 (d, *J* = 2.1 Hz), 128.6 (d, *J* = 4.1 Hz), 128.7 (d, *J* = 1.4 Hz), 128.8 (s), 129.4 (s), 131.2 (d, *J* = 21.4 Hz), 139.1 (d, *J* = 16.8 Hz), 139.5 (d, *J* = 27.2 Hz), 139.9 (s), 150.8 (d, *J* = 3.8 Hz), 152.2 (d, *J* = 16 Hz), 152.5 (d, *J* = 3.8 Hz), 204.6 (d, CO_{cis}, *J* = 9.5 Hz), 208.7 (d, CO_{trans}, *J* = 27.6 Hz) ppm.

$^{31}P\{^{1}H\}$ NMR ($CDCl_3$, 162 MHz): δ = 7.6 (s) ppm.

IR (solid state): 2073 (s, CO), 1993 (w, CO), 1941 (shoulder, CO), 1914 (s, CO) cm^{-1}.

[2,4,10-triphenyl-4H-1,4-ethenophosphinoline]-pentacarbonyltungsten(0), (3.60)

A solution of phosphabarrelene **3.12** (30 mg, 0.075 mmol) in THF was added dropwise to a solution of [$W(CO)_5$·THF] (1 eq.) in THF and heated at T = 80 °C for t = 3 h. Afterwards the solvent was removed *in vacuo* and the residue washed with cold pentane, yielding the product as a white powder (85%). Crystals suitable for X-ray analysis were obtained by slow evaporation of a pentane solution.

^{1}H NMR (400 MHz, $CDCl_3$): δ = 6.64 (d, *J* = 7.8 Hz, 1H), 7.11 (m, 5H), 7.28 (m, 1H), 7.35 (m, 6H), 7.50 (t, *J* = 7.2 Hz, 1H), 7.58 (t, *J* = 7.8 Hz, 2H), 7.68 (d, *J* = 7.8 Hz, 2H), 7.88 (d, *J* = 16.9 Hz, 2H), 8.09 ppm (dd, *J* = 7.3 Hz, J = 12.3 Hz, 1H) ppm.

^{13}C{^{1}H} NMR (101 MHz, $CDCl_3$): δ = 61.8 (d, *J* = 9.7 Hz), 124.9 (d, *J* = 12.7 Hz), 125.2 (m), 128.0 (s), 128.2 (s), 128.4 (s), 128.8 (s), 129.4 (s), 131.8 (d, *J* = 5.3 Hz), 131.9 (d, *J* = 5.3 Hz), 138.9 (d, *J* = 15.4 Hz), 138.9 (d, *J* = 32.8 Hz), 139.8 (bs), 151.0 (bs), 152.2 (d, *J* = 21.3 Hz), 152.4 (d, *J* = 3.6 Hz), 195.3 (d, $^2J_{C\text{-}P}$ = 7.6 Hz, $^1J_{C\text{-}W}$ = 125.5 Hz, CO *cis*), 197.31 (d, $^2J_{C\text{-}P}$ = 26.7 Hz, CO *trans*) ppm.

^{31}P{^{1}H} NMR (162 MHz, $CDCl_3$): δ = -8.5 ppm (s, $^1J_{P\text{-}W}$ = 266 Hz).

IR (solid state): 2071 (w, CO), 1989 (w, CO), 1930 (shoulder), 1907 (s, CO) cm^{-1}.

***trans*-[Rh(2,4,10-triphenyl-4H-1,4-ethenophosphinoline)$_2$Cl(CO)], (3.61)**

The compound was synthesized following a literature procedure.[171] Crystals suitable for X-ray analysis were obtained from a concentrated solution of the complex in DCM at RT.

^{1}H NMR (700 MHz, CD_2Cl_2): δ = 6.58 (d, *J* = 7.8 Hz, 2H), 7.08 (t, *J* = 7.5 Hz, 2H), 7.13 (t, *J* = 7.6 Hz, 2H), 7.31 (t, *J* = 7.4 Hz, 4H), 7.36 (t, *J* = 7.6 Hz, 8H), 7.53 (t, *J* = 7.5 Hz, 2H), 7.63 (t, *J* = 7.8 Hz, 4H), 7.70 (d, *J* = 7.1 Hz, 8H), 7.78 (d, *J* = 7.8 Hz, 4H), 7.97 (t, *J* = 9.5 Hz, 4H), 8.66 ppm (m, 2H).

^{13}C{^{1}H} NMR (176 MHz, CD_2Cl_2): δ = 62.4 (t, *J* = 6.3 Hz), 124.8 (t, *J* = 6.4 Hz), 125.1 (m), 128.3 (m), 128.5 (m), 128.6 (s), 129.3 (s), 129.8 (s), 135.2 (t, *J* = 9.5 Hz), 137.7 (t, *J* = 19.1 Hz), 139.2 (m), 140.6 (s), 150.5 (t, *J* = 14.5 Hz), 151.6 (s), 153.2 (s), 183.6 ppm (CO).

^{31}P{^{1}H} NMR (162 MHz, CD_2Cl_2): δ = -10.9 ppm (d, $^1J_{Rh\text{-}P}$ = 144 Hz).

IR (solid state): 1995 cm^{-1}.

General procedure for the synthesis of [(L)Ni(CO)$_3$] complexes

Caution: [Ni(CO)$_4$] is highly toxic and potentially carcinogenic. It can be absorbed through the skin or inhaled due to its high volatility. Vapors of [Ni(CO)$_4$] can autoignite. All manipulations must be done with extreme care in a well-ventilated fumehood.

In a J-Young NMR tube 0.6 mL of THF containing the appropriate ligand were degassed by freeze and thaw technique. Afterwards, an excess of [Ni(CO)$_4$] was condensed in the same tube using a condensation line. The tube was slowly warmed up to room temperature, and the reaction progress was monitored by means of $^{31}P\{^1H\}$ NMR spectroscopy, degassing the tubes until full conversion. The volatiles were removed *in vacuo*, yielding the product quantitatively. IR spectra were measured in DCM.

[2,4,10-triphenyl-4H-1,4-ethenophosphinoline]-triscarbonylnickel(0), (3.62)

Crystals suitable for X-ray analysis were obtained by slow evaporation of a concentrated solution in THF.

^1H NMR (400 MHz, THF-d_8): δ = 6.63 (d, *J* = 7.6 Hz, 1H), 7.08 (m, 1H), 7.15 (m, 1H), 7.21-7.35 (m, 10H), 7.49 (m, 1H), 7.60 (t, *J* = 7.7 Hz, 2H), 7.85 (m, 3H), 8.02 ppm (d, *J* = 14.6 Hz, 2H)

$^{13}C\{^1H\}$ NMR (101 MHz, THF-d_8): δ = 63.4 (d, *J* = 7.5 Hz), 125.5 (d, *J* = 13.4 Hz), 125.6 (d, *J* = 3.1 Hz), 128.6 (d, *J* = 1.9 Hz), 128.7 (d, *J* = 2.0 Hz), 128.8 (s), 128.9 (s), 129.0 (s), 129.0 (d, *J* = 0.8 Hz), 130.1 (d, *J* = 10.2 Hz), 131.4 (d, *J* = 25.4 Hz), 139.4 (d, *J* = 17.6 Hz), 140.3 (d, *J* = 26.5 Hz), 141.5 (s), 151.0 (d, *J* = 4.6 Hz), 152.4 (d, *J* = 17.6 Hz), 154.3 (d, *J* = 4.0 Hz), 196.2 (bs, CO).

$^{31}P\{^1H\}$ NMR (162 MHz, THF-d_8): δ = -5.5 ppm.

IR (DCM): 2075.0 (m), 2001.0 (bs) cm^{-1}.

[3,9-diphenyl-2,10-bis(trimethylsilyl)-4H-1,4-ethenophosphinoline]-triscarbonylnickel(0), (3.63)

^1H NMR (400 MHz, THF-d_8): δ = -0.03 (bs, 18H), 5.46 (d, *J* = 2.4 Hz, 1H), 7.04 (bs, 4H), 7.15 (m, 1H), 7.22 (m, 2H), 7.31 (m, 6H), 7.93 (m, 1H) ppm.

$^{13}C\{^1H\}$ NMR (101 MHz, THF-d_8): δ = 2.1 (CH_3, d, *J* = 3.2 Hz), 73.2 (d, *J* = 21.9 Hz), 125.7 (d, *J* = 2.7 Hz), 126.1 (d, *J* = 12.2 Hz), 128.4 (s), 128.8 (s), 129.0 (s), 129.4 (s), 131.9 (d,

J = 22.7 Hz), 139.2 (d, *J* = 20.0 Hz), 140.5 (d, *J* = 23.8 Hz), 144.6 (d, *J* = 8.1 Hz), 147.4 (d, *J* = 3.0 Hz), 174.4 (d, *J* = 9.0 Hz), 197.5 (bs, CO) ppm.

$^{29}Si\{^{1}H\}$ NMR (79 MHz, THF-d_8): δ = -2.8 (d, $^{2}J_{P\text{-}Si}$ = 27.5 Hz) ppm.

$^{31}P\{^{1}H\}$ NMR (162 MHz, THF-d_8): δ = -17.5 (s, with ^{29}Si satellites, $^{2}J_{P\text{-}Si}$ = 27.4 Hz) ppm.

IR (DCM): 2069.5 (m), 1992.5 (bs) cm^{-1}.

[3,9-diphenyl-4H-1,4-ethenophosphinoline]-triscarbonylnickel(0), (3.64)

$^{31}P\{^{1}H\}$ NMR (162 MHz, THF-d_8): δ = -30.2 ppm.

IR (DCM): 2073.2 (m), 1998.6 (bs) cm^{-1}.

[(4,6,7-triphenyl-2,3-bis(trifluoromethyl)-1-phosphabicyclo[2.2.2]octa-2,5,7-triene)$Ni(CO)_3$], (3.65)

^{1}H NMR (THF-d_8, 400 MHz): δ = 7.20 (m, 4H), 7.37 (m, 7H), 7.50 (m, 2H), 7.86 (d, *J* = 7.7 Hz, 2H), 8.05 (d, *J* = 14.7 Hz, 2H) ppm.

$^{13}C\{^{1}H, ^{19}F\}$ NMR (THF-d_8, 101 MHz): δ = 65.8 (d, *J* = 6.0 Hz), 122.7 (s), 124.2 (d, *J* = 19.0 Hz), 127.1 (d, *J* = 14.3 Hz), 129.3 (m), 129.3 (s), 129.4 (m), 129.8 (d, *J* = 6.7 Hz), 137.5 (d, *J* = 19.1 Hz), 140.1 (s), 148.4 (s), 152.2 (d, *J* = 4.5 Hz), 152.5 (d, *J* = 14.3 Hz), 160.1 (d, *J* = 6.1 Hz), 194.8 (d, *J* = 0.7 Hz) ppm.

$^{31}P\{^{1}H\}$ NMR (THF-d_8, 162 MHz): δ = -3.4 (q, *J* = 18.0 Hz) ppm.

$^{19}F\{^{1}H\}$ NMR (THF-d_8, 376 MHz): δ = -54.9 (dq, *J* = 18.1, 13.7 Hz), -54.2 (q, *J* = 13.9 Hz) ppm.

IR (DCM): 2081.2 (m), 2010.5 (bs) cm^{-1}.

General procedure for the synthesis of [(L)AuCl] complexes

A solution of the appropriate ligand (0.075 mmol) in 2 mL of DCM or THF was added dropwise to a solution of [$AuCl(SMe_2)$] (2 mL, 1 eq.) and stirred for t = 1 h at room temperature. Afterwards the solvent was removed, and the residue was dried thoroughly in high vacuum, yielding the product as a pale yellow solid in quantitative yield. To remove dimethylsulfide completely, the product was dissolved in the smallest amount of DCM and then precipitated using pentane, subsequently removing the volatiles and drying thoroughly. If

needed, washing with diethyl ether or pentane was helpful. Crystals suitable for X-ray analysis were obtained by slow evaporation of a DCM solution.

[(2,4,10-triphenyl-4H-1,4-ethenophosphinoline)AuCl], (3.67)

^{1}H NMR (THF-d_8, 400 MHz): δ = 6.66 (dd, *J* = 7.7, 3.0 Hz, 1H), 7.16 (m, 1H), 7.24 (m, 1H), 7.38 (m, 6H), 7.55 (m, 1H), 7.66 (m, 2H), 7.79 (dd, *J* = 8.1, 1.2 Hz, 4H), 7.93 (d, *J* = 8.4 Hz, 2H), 8.07 (dd, *J* = 14.9, 7.2 Hz, 1H), 8.36 (d, *J* = 22.1 Hz, 2H) ppm.

^{13}C{^{1}H} NMR (THF-d_8, 101 MHz): δ = 63.4 (d, *J* = 17.1 Hz), 126.1 (d, *J* = 14.4 Hz), 126.4 (d, *J* = 5.0 Hz), 128.1 (d, *J* = 8.4 Hz), 129.1 (s), 129.5 (d, *J* = 1.6 Hz), 129.6 (s), 129.8 (s), 130.2 (s), 130.2 (d, *J* = 2.3 Hz), 133.0 (d, *J* = 20.4 Hz), 135.0 (d, *J* = 53.3 Hz), 137.3 (d, *J* = 13.5 Hz), 140.1 (d, *J* = 0.8 Hz), 147.4 (d, *J* = 42.5 Hz), 151.9 (d, *J* = 3.5 Hz), 153.3 (d, *J* = 2.1 Hz) ppm.

^{31}P{^{1}H} NMR (THF-d_8, 162 MHz): δ = -3.9 (s) ppm.

[(3,9-diphenyl-2,10-bis(trimethylsilyl)-4H-1,4-ethenophosphinoline)AuCl], (3.68)

^{1}H NMR (400 MHz, THF-d_8): δ = 0.12 (bs, 18H), 5.63 (d, *J* = 3.9 Hz, 1H), 7.04 (m, 4H), 7.33 (m, 8H), 7.49 (m, 1H), 8.00 (m, 1H) ppm.

^{13}C{^{1}H} NMR (101 MHz, THF-d_8): δ = 1.1 (CH_3, d, *J* = 3.4 Hz), 72.0 (dd, *J* = 34.0, 1.8 Hz), 126.5 (s), 126.9 (d, *J* = 14.0 Hz), 128.1 (s), 129.5 (s), 130.5 (s), 131.9 (d, *J* = 18.1 Hz), 135.6 (d, *J* = 51.1 Hz), 136.0 (d, *J* = 1.6 Hz), 143.3 (d, *J* = 12.9 Hz), 146.5 (d, *J* = 1.4 Hz), 175.3 (d, *J* = 9.7 Hz) ppm.

^{29}Si{^{1}H} NMR (79 MHz, THF-d_8): δ = -2.8 (d, $^{2}J_{P\text{-}Si}$ = 20.6 Hz) ppm.

^{31}P{^{1}H} NMR (162 MHz, THF-d_8): δ = -10.0 (s, $^{2}J_{P\text{-}Si}$ = 20.9 Hz) ppm.

(4,6,7-triphenyl-2,3-bis(trifluoromethyl)-1-phosphabicyclo[2.2.2]octa-2,5,7-triene)AuCl], (3.69)

^{1}H NMR (THF-d_8, 400 MHz): δ = 7.48 (m, 7H), 7.56 (m, 2H), 7.76 (m, 4H), 7.96 (d, *J* = 7.7 Hz, 2H), 8.44 (d, *J* = 21.9 Hz, 2H) ppm.

^{13}C{^{1}H, ^{19}F} NMR (THF-d_8, 101 MHz): δ = 66.0 (d, *J* = 18.3 Hz), 122.3 (d, *J* = 8.57 Hz), 123.1 (d, *J* = 15.6 Hz), 128.6 (d, *J* = 8.7 Hz), 130.0 (m), 130.5 (m), 135.9 (d, *J* = 14.9 Hz), 138.7 (s), 144.1 (d, *J* = 33.7 Hz), 147.1 (d, *J* = 39.3 Hz), 152.9 (m), 162.1 (d, *J* = 5.6 Hz) ppm.

^{31}P{^{1}H} NMR (THF-d_8, 162 MHz): δ = -5.4 (m) ppm.

^{19}F{^{1}H} NMR (THF-d_8, 376 MHz): δ = -54.68 (m) ppm.

[(5,8-diphenyl-6,7-bis(trimethylsilyl)-2,3-bis(trifluoromethyl)-1-phosphabicyclo[2.2.2]octa-2,5,7-triene)AuCl], (3.70)

^{1}H NMR (400 MHz, $CDCl_3$): δ = 0.16 (d, *J* = 0.6 Hz, 18H), 5.81 (d, *J* = 5.5 Hz, 1H), 6.99 (m, 4H), 7.37 (m, 6H) ppm.

$^{13}C\{^{1}H\}$ NMR (101 MHz, $CDCl_3$): δ = 0.8 (CH_3, d, *J* = 3.6 Hz), 69.3 (d, *J* = 38.5 Hz), 121.7 (d, *J* = 8.4 Hz), 122.0 (m), 127.4 (s), 129.5 (s), 130.0 (s), 135.1 (d, *J* = 4.3 Hz), 139.7 (d, *J* = 30.0 Hz), 140.5 (d, *J* = 12.7 Hz), 151.0 (d, *J* = 2.7 Hz), 174.8 (d, *J* = 10.9 Hz) ppm.

^{19}F NMR (377 MHz, $CDCl_3$): δ = -60.2 (q, *J* = 12.9 Hz), -55.8 (dq, *J* = 12.4, 13.1 Hz) ppm.

$^{29}Si\{^{1}H\}$ NMR (79 MHz, $CDCl_3$): δ = -0.5 (d, *J* = 22.0 Hz) ppm.

$^{31}P\{^{1}H\}$ NMR (162 MHz, $CDCl_3$): δ = -8.9 (q, *J* = 14.0 Hz) ppm.

[1-(trimethylsilyl)-2-phenyl-4,5-bis(trifluoromethyl)-phosphinine], (3.51)

A solution of phosphabarrelene **3.46** (320 mg, 0.81 mmol) in 15 mL of toluene was heated up in a Schlenk bomb at 140 °C overnight. Subsequently the volatiles were evaporated and the oily residue was dried thoroughly. The crude product was purified by means of flash chromatography on silica using hexane as eluent, yielding the product as a colourless oil (73%).

^{1}H NMR (400 MHz, CD_2Cl_2): δ = 0.13 (d, *J* = 1.8 Hz, 9H), 7.29 (m, 2H), 7.47 (m, 3H), 7.81 (s, 1H) ppm.

$^{13}C\{^{1}H,^{19}F\}$ NMR (101 MHz, $CDCl_3$): δ = 1.7 (CH_3, d, *J* = 10.7 Hz), 122.7 (s), 125.2 (d, *J* = 23.9 Hz), 128.4 (s), 128.7 (s), 130.7 (d, *J* = 14.3 Hz), 134.1 (d, *J* = 12.5 Hz), 143.5 (d, *J* = 4.3 Hz), 153.0 (d, *J* = 73.9 Hz), 157.1 (d, *J* = 10.1 Hz), 173.4 (d, *J* = 84.8 Hz) ppm.

^{19}F NMR (377 MHz, CD_2Cl_2): δ = -60.6 (q, *J* = 14.7 Hz), -53.7 (dq, *J* = 53.1, 14.7 Hz) ppm.

$^{29}Si\{^{1}H\}$ NMR (79 MHz, CD_2Cl_2): δ = -0.3 (d, *J* = 39.5 Hz) ppm.

$^{31}P\{^{1}H\}$ NMR (162 MHz, CD_2Cl_2): δ = 248.9 (q, *J* = 53.0 Hz) ppm.

[(2,4,10-triphenyl-4H-1,4-ethenophosphinoline)$_2$CuCl], (3.71)

Compound **3.12** (24 mg, 0.060 mmol) and anhydrous CuCl (0.5 eq.) were mixed together in THF (0.6 mL) and the reaction mixture was heated to reflux for t = 1 h. Due to the poor solubility of the product in THF, a white solid is formed and precipitates. The pure compound was quantitatively obtained by removing the volatiles.

^{1}H NMR (THF-d_8, 400 MHz): δ = 6.55 (d, *J* = 7.8 Hz, 1H), 7.04 (m, 2H), 7.19 (m, 6H), 7.50 (m, 1H), 7.62 (t, *J* = 7.8 Hz, 2H), 7.77 (d, *J* = 7.5 Hz, 4H), 7.90 (d, *J* = 7.4 Hz, 2H), 8.16 (d, *J* = 10.7 Hz, 2H), 8.30 (b, 1H) ppm.

^{13}C{^{1}H} NMR (THF-d_8, 101 MHz): δ = 63.50 (s), 123.92 (d, *J* = 13.0 Hz), 124.12 (d, *J* = 1.3 Hz), 125.97 (d, *J* = 12.0 Hz), 127.05 (s), 127.35 (s), 128.19 (s), 128.79 (s), 128.91 (s), 131.80 (d, *J* = 34.5 Hz), 138.22 (d, *J* = 22.3 Hz), 140.99 (s), 147.89 (s), 151.28 (s), 154.85 (s) ppm.

^{31}P{^{1}H} NMR (THF-d_8, 162 MHz): δ = -65.0 (bs) ppm.

[(2,4,10-triphenyl-4H-1,4-ethenophosphinoline)CuCl]$_2$·MeCN, (3.72)

Compound **3.12** (24 mg, 0.060 mmol) and anhydrous CuCl (1 eq.) were mixed together in MeCN-d_3 (0.6 mL) and the reaction mixture was heated to reflux for t = 1 h. The product is insoluble in acetonitrile and decomposed to **3.71** in the presence of THF or DCM. Single crystals suitable for X-ray analysis were found in the reaction mixture.

^{1}H NMR (MeCN-d_3, 400 MHz): δ = 6.54 (m, 1H), 7.13 (m, 2H), 7.38 (m, 6H), 7.55 (m, 1H), 7.63 (m, 6H), 7.89 (m, 2H), 8.04 (m, 1H), 8.13 (d, *J* = 11.6 Hz, 2H) ppm.

3.4.1 X-ray Crystal Structure Determination

X-ray Crystal Structure Determination of 3.1

Crystals suitable for X-ray diffraction were obtained from slow evaporation from a concentrated solution in diethyl ether. *Crystallographic data*: $C_{27}H_{17}F_6P$, *F*w = 486.38, 0.45×0.29×0.19 mm^3, yellow block, monoclinic, $P2_1/c$, a = 10.5596(2), b = 22.6126(7), c = 9.5917(3) Å, α = 90°, β = 108.6424(9)°, γ = 90°, V = 2170.14(10) Å^3, Z = 4, Dx = 1.489 gcm^{-3}, μ = 0.192 mm^{-1}. 26264 reflections were measured by using a Bruker-AXS smart CCD area detector diffractometer (MoKα radiation, λ = 0.71073 Å)[155] up to a resolution of $(\sin\theta/\lambda)_{max}$ = 0.63 Å^{-1} at a temperature of T = 100 K. The reflections were corrected for absorption and scaled on the basis of multiple measured reflections by using the SADABS program[155] (0.83–0.94 correction range). 3444 reflections were unique (R_{int} = 0.073). Using ShelXle[158], the structures were solved with SHELXS-2014 by using direct methods and refined with SHELXL-2014 on *F*2 for all reflections.[156] Non-hydrogen atoms were refined by using anisotropic displacement parameters. The positions of the hydrogen atoms were

calculated for idealized positions. 307 parameter were refined without restraints. R_1 = 0.043 for 3444 reflections with $I>2\sigma(I)$ and wR_2 = 0.105 for 4436 reflections, S = 1.043, residual electron density was between -0.43 and 0.48 eÅ^{-3}. Geometry calculations and checks for higher symmetry were performed with the PLATON program.[157]

X-ray Crystal Structure Determination of 3.45

Crystals suitable for X-ray diffraction were obtained from slow evaporation of a solution of **3.45** in methanol. *Crystallographic data*: $C_{29}H_{33}PSi_2$, *F*w = 468.70, 0.08×0.08×0.03 mm^3, colourless platelet, triclinic, $P\bar{1}$, a = 9.8992(1), b = 10.4958(1), c = 13.0431(1)Å, α = 78.8106(6)°, β = 89.5035(6)°, γ = 86.4333(6)°, V = 1326.84(2) Å^3, Z = 2, Dx = 1.173 gcm^{-3}, μ = 1.876 mm^{-1}. 13949 reflections were measured by using a Bruker-AXS smart CCD area detector diffractometer (CuKα radiation, λ = 1.54178Å)[155] up to a resolution of $(\sin\theta/\lambda)_{max}$ = 0.60 Å^{-1} at a temperature of 100 K. The reflections were corrected for absorption and scaled on the basis of multiple measured reflections by using the SADABS program[155] (0.84–0.92 correction range). 3417 reflections were unique (R_{int} = 0.058). Using ShelXle[158], the structures were solved with SHELXS-2014 by using direct methods and refined with SHELXL-2014 on $F2$ for all reflections.[156] Non-hydrogen atoms were refined by using anisotropic displacement parameters. The positions of the hydrogen atoms were calculated for idealized positions. 296 parameter were refined without restraints. R_1 = 0.048 for 3417 reflections with $I>2\sigma(I)$ and wR_2 = 0.108 for 4688 reflections, S = 1.047, residual electron density was between -0.32 and 0.39 eÅ^{-3}. Geometry calculations and checks for higher symmetry were performed with the PLATON program.[157]

X-ray Crystal Structure Determination of 3.46

Crystals suitable for X-ray diffraction were obtained from slow evaporation of a concentrated solution in methanol. *Crystallographic data*: $C_{27}H_{29}PF_6Si_2$, *F*w = 554.65, 0.28×0.28×0.14 mm^3, colourless block, triclinic, $P\bar{1}$, a = 10.78717(8), b = 15.23382(3), c = 18.26277(13)Å, α = 97.4263(3)°, β = 103.9082(3)°, γ = 99.6371(3)°, V = 2826.62(4) Å^3, Z = 4, Dx = 1.303 gcm^{-3}, μ = 2.159 mm^{-1}. 29818 reflections were measured by using a Bruker-AXS smart CCD area detector diffractometer (CuKα radiation, λ = 1.54178 Å)[155] up to a resolution of $(\sin\theta/\lambda)_{max}$ = 0.60 Å^{-1} at a temperature of T = 100 K. The reflections were

corrected for absorption and scaled on the basis of multiple measured reflections by using the SADABS program[155] (0.60–0.71 correction range). 8562 reflections were unique (R_{int} = 0.035). Using ShelXle[158], the structures were solved with SHELXS-2014 by using direct methods and refined with SHELXL-2014 on *F*2 for all reflections.[156] Non-hydrogen atoms were refined by using anisotropic displacement parameters. The positions of the hydrogen atoms were calculated for idealized positions. 661 parameter were refined without restraints. R_1 = 0.038 for 8562 reflections with $I>2\sigma(I)$ and wR_2 = 0.088 for 9977 reflections, S = 1.051, residual electron density was between -0.36 and 0.36 eÅ^{-3}. Geometry calculations and checks for higher symmetry were performed with the PLATON program.[157]

X-ray Crystal Structure Determination of 3.52

Crystals suitable for X-ray diffraction were obtained from slow evaporation of a concentrated solution in methanol. *Crystallographic data*: $C_{17}H_{19}PF_6OSi$, *F*w = 412.38, 0.28×0.21×0.09 mm^3, colourless block, triclinic, $P\bar{1}$, a = 8.9992(4), b = 10.1647(3), c = 11.3907(3)Å, α = 99.1849(3)°, β = 91.1844(10)°, γ = 112.8005(9)°, V = 944.31(4) Å^3, Z = 2, Dx = 1.450 gcm^{-3}, μ = 0.269 mm^{-1}. 14905 reflections were measured by using a Bruker-AXS smart CCD area detector diffractometer (MoKα radiation, λ = 0.71073Å)[155] up to a resolution of $(\sin\theta/\lambda)_{max}$ = 0.63 Å^{-1} at a temperature of T = 100 K. The reflections were corrected for absorption and scaled on the basis of multiple measured reflections by using the SADABS program[155] (0.93–0.96 correction range). 3092 reflections were unique (R_{int} = 0.046). Using ShelXle[158], the structures were solved with SHELXS-2014 by using direct methods and refined with SHELXL-2014 on *F*2 for all reflections.[156] Non-hydrogen atoms were refined by using anisotropic displacement parameters. The positions of the hydrogen atoms were calculated for idealized positions. 243 parameter were refined without restraints. R_1 = 0.039 for 3092 reflections with $I>2\sigma(I)$ and wR_2 = 0.088 for 3879 reflections, S = 1.018, residual electron density was between -0.33 and 0.36 eÅ^{-3}. Geometry calculations and checks for higher symmetry were performed with the PLATON program.[157]

X-ray Crystal Structure Determination of 3.53

Crystals suitable for X-ray diffraction were obtained from slow evaporation of a concentrated solution in toluene. *Crystallographic data*: $C_{29}H_{21}OP$, *F*w = 416.43, 0.43×0.30×0.06 mm^3,

colourless platelet, orthorhombic, *Pbcn*, a = 29.6409(5), b = 7.4094(1), c = 19.1055(3) Å, V = 4195.97(11) Å^3, Z = 8, Dx = 1.318 gcm^{-3}, μ = 0.15 mm^{-1}. 23744 reflections were measured by using a Bruker-AXS smart CCD area detector diffractometer (MoKα radiation, λ = 0.71073 Å)[155] up to a resolution of $(\sin\theta/\lambda)_{max}$ = 0.60 Å^{-1} at a temperature of T = 100 K. The reflections were corrected for absorption and scaled on the basis of multiple measured reflections by using the SADABS program[155] (0.61–0.97 correction range). 2980 reflections were unique (R_{int} = 0.066). Using ShelXle[158], the structures were solved with SHELXS-2014 by using direct methods and refined with SHELXL-2014 on $F2$ for all reflections.[156] Non-hydrogen atoms were refined by using anisotropic displacement parameters. The positions of the hydrogen atoms were calculated for idealized positions. 280 parameter were refined without restraints. R_1 = 0.041 for 2980 reflections with $I>2\sigma(I)$ and wR_2 = 0.10 for 3702 reflections, S = 1.033, residual electron density was between -0.42 and 0.31 eÅ^{-3}. Geometry calculations and checks for higher symmetry were performed with the PLATON program.[157]

X-ray Crystal Structure Determination of 3.54

Crystals suitable for X-ray diffraction were obtained by slow evaporation of a concentrated solution in toluene. *Crystallographic data*: $C_{29}H_{21}PS$, Fw = 432.49, 0.41×0.16×0.06 mm^3, colourless platelet, monoclinic, $P2_1/c$, a = 9.7691(1), b = 14.6930(3), c = 15.2033(2) Å, α = 90°, β = 96.5699(8)°, γ = 90°, V = 2167.92(6) Å^3, Z = 4, Dx = 1.325 gcm^{-3}, μ = 0.24 mm^{-1}. 18563 reflections were measured by using a Bruker-AXS smart CCD area detector diffractometer (MoKα radiation, λ = 0.71073 Å)[155] up to a resolution of $(\sin\theta/\lambda)_{max}$ = 0.63 Å^{-1} at a temperature of T = 100 K. The reflections were corrected for absorption and scaled on the basis of multiple measured reflections by using the SADABS program[155] (0.88–0.96 correction range). 3660 reflections were unique (R_{int} = 0.048). Using ShelXle[158], the structures were solved with SHELXS-2014 by using direct methods and refined with SHELXL-2014 on $F2$ for all reflections.[156] Non-hydrogen atoms were refined by using anisotropic displacement parameters. The positions of the hydrogen atoms were calculated for idealized positions. 280 parameter were refined without restraints. R_1 = 0.036 for 3660 reflections with $I>2\sigma(I)$ and wR_2 = 0.088 for 4455 reflections, S = 1.031, residual electron density was between -0.31 and 0.32 eÅ^{-3}. Geometry calculations and checks for higher symmetry were performed with the PLATON program.[157]

X-ray Crystal Structure Determination of 3.55 CCDC- 1424313

Crystals suitable for X-ray diffraction were obtained by slow evaporation of a saturated solution of in toluene. *Crystallographic data*: $C_{29}H_{21}PSe$; *F*w = 479.39; 0.38×0.29×0.17 mm^3; colourless block, triclinic; P -1; *a* = 9.8524(2), *b* = 12.4381(2), *c* =18.8967(3) Å; α = 87.80(7)°, β = 89.78(8), γ = 75.57(6)°; *V* = 2240.98(7) $Å^3$; *Z* = 4; *D*x = 1.421 gcm^{-3}; μ = 1.761mm^{-1}. 76227 reflections were measured by using a D8 Venture, Bruker Photon CMOS Detector (MoKα radiation; λ = 0.71073 Å)[155] up to a resolution of $(\sin\theta/\lambda)_{max}$= 0.62 $Å^{-1}$ at a temperature of T = 100.0 K. 7511 reflections were unique (R_{int} = 0.073). The structures were solved with SHELXS-2013 by using direct methods and refined with SHELXL-2013 on *F*2 for all reflections.[156] Non-hydrogen atoms were refined by using anisotropic displacement parameters. The positions of the hydrogen atoms were calculated for idealized positions. 559 parameter were refined with one restraint. R_1 = 0.036 for 7511 reflections with $I>2\sigma(I)$ and wR_2 = 0.083 for 9231 reflections, *S* = 1.066, residual electron density was between -0.53 and 0.75 $eÅ^{-3}$. Geometry calculations and checks for higher symmetry were performed with the PLATON program.[157]

X-ray Crystal Structure Determination of 3.56

Crystals suitable for X-ray diffraction were obtained from slow evaporation of a concentrated solution in toluene. *Crystallographic data*: $C_{29}H_{33}PSeSi_2$, *F*w = 547.66, 0.24×0.16×0.08 mm^3, colourless platelet, triclinic, $P\bar{1}$, *a* = 11.2328(2), *b* = 11.5305(2), *c* = 12.5506(2)Å, α = 97.0293(5)°, β = 99.6595(5)°, γ = 116.5661(5)°, *V* = 1396.92(7) $Å^3$, *Z* = 2, *D*x = 1.302 gcm^{-3}, μ = 1.502 mm^{-1}. 24191 reflections were measured by using a Bruker-AXS smart CCD area detector diffractometer (MoKα radiation, λ = 0.71073 Å)[155] up to a resolution of $(\sin\theta/\lambda)_{max}$ = 0.61 $Å^{-1}$ at a temperature of T = 100 K. The reflections were corrected for absorption and scaled on the basis of multiple measured reflections by using the SADABS program[155] (0.61–0.70 correction range). 4975 reflections were unique (R_{int} = 0.027). Using ShelXle[158], the structures were solved with SHELXS-2014 by using direct methods and refined with SHELXL-2014 on *F*2 for all reflections.[156] Non-hydrogen atoms were refined by using anisotropic displacement parameters. The positions of the hydrogen atoms were calculated for idealized positions. 304 parameter were refined without restraints. R_1 = 0.022 for 4975 reflections with $I>2\sigma(I)$ and wR_2 = 0.055 for 5299 reflections, *S* = 1.062, residual electron

density was between -0.36 and 0.30 eÅ^{-3}. Geometry calculations and checks for higher symmetry were performed with the PLATON program.[157]

X-ray Crystal Structure Determination of 3.57

Crystals suitable for X-ray diffraction were obtained by slow evaporation of a concentrated solution in diethyl ether. *Crystallographic data*: $C_{27}H_{17}PF_6O$, *F*w = 502.38, 0.31×0.18×0.10 mm^3, colourless prism, monoclinic, $P2_1/c$, a = 10.6007(2), b = 22.9575(4), c = 9.5515(2) Å, α = 90°, β = 109.5693(6)°, γ = 90°, V = 2190.24(7) Å^3, Z = 4, Dx = 1.523 gcm^{-3}, μ = 0.196 mm^{-1}. 39950 reflections were measured by using a Bruker-AXS smart CCD area detector diffractometer (MoKα radiation, λ = 0.71073 Å)[155] up to a resolution of $(\sin\theta/\lambda)_{max}$ = 0.63 Å^{-1} at a temperature of T = 100 K. The reflections were corrected for absorption and scaled on the basis of multiple measured reflections by using the SADABS program[155] (0.94–0.97 correction range). 4022 reflections were unique (R_{int} = 0.043). Using ShelXle[158], the structures were solved with SHELXS-2014 by using direct methods and refined with SHELXL-2014 on $F2$ for all reflections.[156] Non-hydrogen atoms were refined by using anisotropic displacement parameters. The positions of the hydrogen atoms were calculated for idealized positions. 317 parameter were refined without restraints. R_1 = 0.033 for 4022 reflections with $I>2\sigma(I)$ and wR_2 = 0.083 for 4480 reflections, S = 1.046, residual electron density was between -0.34 and 0.38 eÅ^{-3}. Geometry calculations and checks for higher symmetry were performed with the PLATON program.[157]

X-ray Crystal Structure Determination of 3.58

Crystals suitable for X-ray diffraction were obtained by slow evaporation of a concentrated solution in THF. *Crystallographic data*: $C_{34}H_{21}CrO_5P$, *F*w = 592.48, 0.24×0.10×0.07 mm^3, colourless platelet, monoclinic, $P2_1/c$, a = 11.0446(2), b = 12.6960(2), c = 19.9868(3) Å, α = 90°, β = 91.205(1)°, γ = 90°, V = 2801.97(8) Å^3, Z = 4, Dx = 1.405 gcm^{-3}, μ = 0.508 mm^{-1}. 59409 reflections were measured by using a Bruker-AXS smart CCD area detector diffractometer (MoKα radiation, λ = 0.71073 Å)[155] up to a resolution of $(\sin\theta/\lambda)_{max}$ = 0.63 Å^{-1} at a temperature of T = 100 K. The reflections were corrected for absorption and scaled on the basis of multiple measured reflections by using the SADABS program[155] (0.71–0.75 correction range). 5101 reflections were unique (R_{int} = 0.044). Using

ShelXle[158], the structures were solved with SHELXS-2014 by using direct methods and refined with SHELXL-2014 on *F*2 for all reflections. [156] Non-hydrogen atoms were refined by using anisotropic displacement parameters. The positions of the hydrogen atoms were calculated for idealized positions. 370 parameter were refined without restraints. R_1 = 0.029 for 5101 reflections with $I>2\sigma(I)$ and wR_2 = 0.078 for 5757 reflections, S = 1.037, residual electron density was between -0.42 and 0.35 eÅ^{-3}. Geometry calculations and checks for higher symmetry were performed with the PLATON program.[157]

X-ray Crystal Structure Determination of 3.59

Crystals suitable for X-ray diffraction were obtained from slow evaporation of evaporation of a solution of **3.59** in pentane. *Crystallographic data*: $C_{34}H_{21}MoO_5P$, *F*w = 636.42, 0.31×0.22×0.14 mm^3, colourless block, monoclinic, $P2_1/c$, a = 11.2067(2), b = 12.8656(2), c = 19.9607(5) Å, α = 90°, β = 91.1287(8)°, γ = 90°, V = 2877.39(10) Å^3, Z = 4, Dx = 1.469 gcm^{-3}, μ = 0.553 mm^{-1}. 29939 reflections were measured by using a Bruker-AXS smart CCD area detector diffractometer (MoKα radiation, λ = 0.71073 Å)[155] up to a resolution of $(\sin\theta/\lambda)_{max}$ = 0.63 Å^{-1} at a temperature of T = 100 K. The reflections were corrected for absorption and scaled on the basis of multiple measured reflections by using the SADABS program[155] (0.76–0.85 correction range). 4924 reflections were unique (R_{int} = 0.049). Using ShelXle[158], the structures were solved with SHELXS-2014 by using direct methods and refined with SHELXL-2014 on *F*2 for all reflections.[156] Non-hydrogen atoms were refined by using anisotropic displacement parameters. The positions of the hydrogen atoms were calculated for idealized positions. 370 parameter were refined without restraints. R_1 = 0.029 for 4924 reflections with $I>2\sigma(I)$ and wR_2 = 0.066 for 5859 reflections, S = 1.058, residual electron density was between -0.46 and 0.40 eÅ^{-3}. Geometry calculations and checks for higher symmetry were performed with the PLATON program.[157]

X-ray Crystal Structure Determination of 3.60 CCDC-1424314

Crystals suitable for X-ray diffraction were obtained by slow evaporation of a solution of **3.60** in pentane. *Crystallographic data*: $C_{34}H_{21}O_5PW$; *F*w=724.33; 0.23×0.14×0.11 mm^3; colourless chunk, monoclinic; *-P2yn*; a = 11.5473(2), b = 12.8913(2), c = 19.8913(3) Å; α = 90°, β = 102.46, γ = 90°; V = 2891.29(8) Å^3; Z = 4; Dx = 1.156 gcm^{-3}; μ = 1.837 mm^{-1}.

12965 reflections were measured by using a D8 Venture, Bruker Photon CMOS Detector (MoKα radiation; λ = 0.71073 Å)[155] up to a resolution of $(\sin\theta/\lambda)_{max}$= 0.98 Å^{-1} at a temperature of T = 100 K. 18773 reflections were unique (R_{int} = 0.029). The structures were solved with SHELXS-2013 by using direct methods and refined with SHELXL-2013 on *F*2 for all reflections.[156] Non-hydrogen atoms were refined by using anisotropic displacement parameters. The positions of the hydrogen atoms were calculated for idealized positions. 370 parameter were refined with one restraint. R_1 = 0.029 for 18773 reflections with $I>2\sigma(I)$ and wR_2 = 0.070 for 22892 reflections, *S* = 1.057, residual electron density was between -2.51 and 4.54 eÅ^{-3}. Geometry calculations and checks for higher symmetry were performed with the PLATON program.[157]

X-ray Crystal Structure Determination of 3.61

Crystals suitable for X-ray diffraction were obtained by slow evaporation of a concentrated solution in DCM. *Crystallographic data*: $C_{59}H_{42}CLOP_2Rh$, *F*w = 967.23, 0.42×0.40×0.14 mm^3, yellow block, monoclinic, *C2/c*, *a* = 35.9111(19), *b* = 10.1730(5), *c* = 29.3914(15) Å, α = 90°, β = 112.5356(13)°, γ = 90°, *V* = 9917.5(9) Å^3, *Z* = 8, *D*x = 1.296 gcm^{-3}, μ = 0.502 mm^{-1}. 56830 reflections were measured by using a Bruker-AXS smart CCD area detector diffractometer (MoKα radiation, λ = 0.71073 Å)[155] up to a resolution of $(\sin\theta/\lambda)_{max}$ = 0.63 Å^{-1} at a temperature of T = 100 K. The reflections were corrected for absorption and scaled on the basis of multiple measured reflections by using the SADABS program[155] (0.81–0.93 correction range). 200466 reflections were unique (R_{int} = 0.082). Using ShelXle[158], the structures were solved with SHELXS-2014 by using direct methods and refined with SHELXL-2014 on *F*2 for all reflections.[156] Non-hydrogen atoms were refined by using anisotropic displacement parameters. The positions of the hydrogen atoms were calculated for idealized positions. 577 parameter were refined without restraints. R_1 = 0.037 for 11459 reflections with $I>2\sigma(I)$ and wR_2 = 0.087 for 12549 reflections, *S* = 1.076, residual electron density was between -0.62 and 1.95 eÅ^{-3}. Geometry calculations and checks for higher symmetry were performed with the PLATON program.[157]

SQUEEZE RESULTS (APPEND TO CIF)[226]
Note: Data are Listed for all Voids in the P1 Unit Cell
i.e. Centre of Gravity, Solvent Accessible Volume,
Recovered number of Electrons in the Void and
Details about the Squeezed Material

```
  _platon_squeeze_void_nr
  _platon_squeeze_void_average_x
  _platon_squeeze_void_average_y
  _platon_squeeze_void_average_z
  _platon_squeeze_void_volume
  _platon_squeeze_void_count_electrons
  _platon_squeeze_void_content
   1  0.000  0.603  0.250      163       39 ' '
   2  0.500  0.103  0.250      163       39 ' '
   3  0.250  0.283  0.250      222       38 ' '
   4  0.750  0.783  0.250      222       38 ' '
   5  0.000  0.397  0.750      163       39 ' '
   6  0.500  0.897  0.750      163       39 ' '
   7  0.250  0.715  0.750      222       38 ' '
   8  0.750  0.215  0.750      222       38 ' '
_platon_squeeze_details
```

The general procedure has been described in more detail as the "BYPASS procedure".[227]

X-ray Crystal Structure Determination of 3.62

Crystals suitable for X-ray diffraction were obtained from slow evaporation of a concentrated solution in THF. *Crystallographic data*: $C_{32}H_{21}NiO_3P$, *F*w = 543.17, 0.15×0.09×0.04 mm^3, colourless block, monoclinic, *P 21/c*, *a* = 11.9762(7), *b* = 11.8806(6), *c* = 18.6899(10) Å, α = 90°, β = 92.959(4)°, γ = 90°, *V* = 2655.7(2) $Å^3$, *Z* = 4, *D*x = 1.358 gcm^{-3}, μ = 0.822 mm^{-1}. 29858 reflections were measured by using a Bruker-AXS smart CCD area detector diffractometer (MoKα radiation, λ = 0.71073Å)[155] up to a resolution of $(\sin\theta/\lambda)_{max}$ = 0.62 $Å^{-1}$ at a temperature of T = 100 K. The reflections were corrected for absorption and scaled on the basis of multiple measured reflections by using the SADABS program[155] (0.84–0.92 correction range). 6595 reflections were unique (R_{int} = 0.1672). Using ShelXle[158], the structures were solved with SHELXS-2014 by using direct methods and refined with SHELXL-2014 on *F*2 for all reflections. [156] Non-hydrogen atoms were refined by using anisotropic displacement parameters. The positions of the hydrogen atoms were calculated for idealized positions. 334 parameter were refined without restraints. R_1 = 0.0623 for 3945 reflections with $I>2\sigma(I)$ and wR_2 = 0.1027 for 6595 reflections, *S* = 1.015, residual electron density was between -0.51 and 0.44 $eÅ^{-3}$. Geometry calculations and checks for higher symmetry were performed with the PLATON program.[157]

X-ray Crystal Structure Determination of 3.67

Crystals suitable for X-ray diffraction were obtained by slow evaporation of a concentrated solution in DCM at T = -35 °C. *Crystallographic data*: $(C_{29}H_{21}PAuCL)_2$,CH_2CL_2, *F*w = 1350.62, 0.23×0.15×0.06 mm^3, colourless block, triclinic, $P\bar{1}$, *a* = 10.1833(8), *b* = 14.1275(2), *c* = 18.9026(3)Å, α = 72.7975(8)°, β = 84.8815(8)°, γ = 73.2814(8)°, *V* = 2487.93(7) Å^3, *Z* = 2, *D*x = 1.803 gcm^{-3}, μ = 6.209 mm^{-1}. 58377 reflections were measured by using a Bruker-AXS smart CCD area detector diffractometer (MoKα radiation, λ = 0.71073 Å)[155] up to a resolution of $(\sin\theta/\lambda)_{max}$ = 0.63 Å^{-1} at a temperature of T = 100 K. The reflections were corrected for absorption and scaled on the basis of multiple measured reflections by using the SADABS program[155] (0.39–0.53 correction range). 8408 reflections were unique (R_{int} = 0.061). Using ShelXle[158], the structures were solved with SHELXS-2014 by using direct methods and refined with SHELXL-2014 on *F*2 for all reflections.[156] Non-hydrogen atoms were refined by using anisotropic displacement parameters. The positions of the hydrogen atoms were calculated for idealized positions. 604 parameter were refined without restraints. R_1 = 0.028 for 8408 reflections with $I>2\sigma(I)$ and wR_2 = 0.062 for 10224 reflections, *S* = 1.029, residual electron density was between -1.08 and 1.74 eÅ^{-3}. Geometry calculations and checks for higher symmetry were performed with the PLATON program.[157]

X-ray Crystal Structure Determination of 3.68

Crystals suitable for X-ray diffraction were obtained by slow evaporation of a concentrated solution in DCM at T = -35 °C. *Crystallographic data*: $C_{30}H_{33}AuPCL_3Si_2$, *F*w = 784.03, 0.13×0.11×0.04 mm^3, colourless irregular, orthorhombic, *Pnma*, *a* = 17.6549(3), *b* = 15.2371(1), *c* = 11.9627(2) Å, *V* = 3218.08(10) Å^3, *Z* = 4, *D*x = 1.618 gcm^{-3}, μ = 4.963 mm^{-1}. 82143 reflections were measured by using a Bruker-AXS smart CCD area detector diffractometer (MoKα radiation, λ = 0.71073 Å)[155] up to a resolution of $(\sin\theta/\lambda)_{max}$ = 0.65 Å^{-1} at a temperature of T = 173 K. The reflections were corrected for absorption and scaled on the basis of multiple measured reflections by using the SADABS program[155] (0.05–0.15 correction range). 3526 reflections were unique (R_{int} = 0.064). Using ShelXle[158], the structures were solved with SHELXS-2014 by using direct methods and refined with SHELXL-2014 on *F*2 for all reflections.[156] Non-hydrogen atoms were refined by using anisotropic displacement parameters. The positions of the hydrogen atoms were calculated for idealized positions. 189 parameter were refined without restraints. R_1 = 0.032 for 3526

reflections with $I>2\sigma(I)$ and wR_2 = 0.08 for 3842 reflections, S = 1.066, residual electron density was between -2.35 and 2.47 eÅ^{-3}. Geometry calculations and checks for higher symmetry were performed with the PLATON program.[157]

X-ray Crystal Structure Determination of 3.69

Crystals suitable for X-ray diffraction were obtained by slow evaporation of a concentrated solution in DCM at T = -35 °C. *Crystallographic data*: $C_{27}H_{17}AuCLPF_6$, *F*w = 718.80, 0.60×0.10×0.09 mm^3, colourless rod, triclinic, $P\bar{1}$, a = 8.6440(2), b = 10.0254(2), c = 14.5537(3)Å, α = 81.7475(8)°, β = 87.4505(8)°, 73.0847(7)°, V = 1194.15(4) Å^3, Z = 2, Dx = 1.999 gcm^{-3}, μ = 6.401 mm^{-1}. 20118 reflections were measured by using a Bruker-AXS smart CCD area detector diffractometer (MoKα radiation, λ = 0.71073 Å)[155] up to a resolution of $(\sin\theta/\lambda)_{max}$ = 0.63 Å^{-1} at a temperature of T = 100 K. The reflections were corrected for absorption and scaled on the basis of multiple measured reflections by using the SADABS program[155] (0.06–0.10 correction range). 4374 reflections were unique (R_{int} = 0.051). Using ShelXle[158], the structures were solved with SHELXS-2014 by using direct methods and refined with SHELXL-2014 on $F2$ for all reflections.[156] Non-hydrogen atoms were refined by using anisotropic displacement parameters. The positions of the hydrogen atoms were calculated for idealized positions. 325 parameter were refined without restraints. R_1 = 0.031 for 4374 reflections with $I>2\sigma(I)$ and wR_2 = 0.069 for 4867 reflections, S = 1.149, residual electron density was between -1.06 and 1.18 eÅ^{-3}. Geometry calculations and checks for higher symmetry were performed with the PLATON program.[157]

X-ray Crystal Structure Determination of 3.71

Crystals suitable for X-ray diffraction were obtained by slow evaporation of a concentrated solution in THF. *Crystallographic data*: $C_{58}H_{42}P_2CLCu$, *F*w = 899.86, 0.18×0.09×0.06 mm^3, colourless cube, triclinic, $P\bar{1}$, a = 10.6222(3), b = 13.4612(3), c = 18.3551(5)Å, α = 82.3313(9)°, β = 84.5796(9)°, γ = 74.1664(9)°, V = 2497.75(11) Å^3, Z = 2, Dx = 1.196 gcm^{-3}, μ = 0.59 mm^{-1}. 45604 reflections were measured by using a Bruker-AXS smart CCD area detector diffractometer (MoKα radiation, λ = 0.71073 Å)[155] up to a resolution of $(\sin\theta/\lambda)_{max}$ = 0.63 Å^{-1} at a temperature of T = 100 K. The reflections were corrected for absorption and scaled on the basis of multiple measured reflections by using the SADABS

program[155] (0.85–0.91 correction range). 8007 reflections were unique (R_{int} = 0.061). Using ShelXle[158], the structures were solved with SHELXS-2014 by using direct methods and refined with SHELXL-2014 on *F*2 for all reflections.[156] Non-hydrogen atoms were refined by using anisotropic displacement parameters. The positions of the hydrogen atoms were calculated for idealized positions. 559 parameter were refined without restraints. R_1 = 0.043 for 8007 reflections with $I>2\sigma(I)$ and wR_2 = 0.094 for 10236 reflections, *S* = 1.027, residual electron density was between -0.46 and 0.54 eÅ^{-3}. Geometry calculations and checks for higher symmetry were performed with the PLATON program.[157]

SQUEEZE RESULTS (Version = 50315)[226]
Note: Data are Listed for all Voids in the P1 Unit Cell
i.e. Centre of Gravity, Solvent Accessible Volume,
Recovered number of Electrons in the Void and
Details about the Squeezed Material
_platon_squeeze_void_nr
_platon_squeeze_void_average_x
_platon_squeeze_void_average_y
_platon_squeeze_void_average_z
_platon_squeeze_void_volume
_platon_squeeze_void_count_electrons
_platon_squeeze_void_content
1 -0.022 0.000 0.000 465 175 ' '
_platon_squeeze_void_probe_radius 1.20
_platon_squeeze_details

The general procedure has been described in more detail as the "BYPASS procedure".[227]

X-ray Crystal Structure Determination of 3.72

Crystals suitable for X-ray diffraction were obtained from a hot solution in acetonitrile. *Crystallographic data*: $C_{60}H_{45}Cl_2Cu_2NP_2$, *F*w = 1039.91, 0.30×0.24×0.10 mm^3, colourless block, monoclinic, *P21/c*, *a* = 17.4324(15), *b* = 14.0893(12), *c* = 19.4541(17) Å, α = 90°, β = 101.264(3)°, γ = 90°, *V* = 4686.1(7) Å^3, *Z* = 4, *D*x = 1.474 gcm^{-3}, μ = 1.133 mm^{-1}. 57184 reflections were measured by using a Bruker-AXS smart CCD area detector diffractometer (MoKα radiation, λ = 0.71073Å)[155] up to a resolution of $(\sin\theta/\lambda)_{max}$ = 0.60 Å^{-1} at a temperature of T = 100 K. The reflections were corrected for absorption and scaled on the basis of multiple measured reflections by using the SADABS program[155] (0.69–0.84 correction range). 9331 reflections were unique (R_{int} = 0.0364). Using ShelXle[158], the structures were solved with SHELXS-2014 by using direct methods and refined with SHELXL-2014 on *F*2 for all

reflections.[156] Non-hydrogen atoms were refined by using anisotropic displacement parameters. The positions of the hydrogen atoms were calculated for idealized positions. 605 parameter were refined without using restraints. R_1 = 0.0356 for 7831 reflections with $I>2\sigma(I)$ and wR_2 = 0.1037 for 9331 reflections, S = 1.060, residual electron density was between -0.63 and 1.30 eÅ^{-3}. Geometry calculations and checks for higher symmetry were performed with the PLATON program.[157]

4. Phosphasemibullvalenes

Part of this chapter has been published in:

"Expanding the Phosphorus-Carbon Analogy: Formation of an Unprecedented 5-Phosphasemibullvalene Derivative" - M. Rigo, M. Weber, C. Müller, *Chem. Commun*. **2016**, *52*, 7090.

Tetiana Krachko, Emmanuel Nicolas, Andreas Ehlers and Chris Slootweg (Universiteit van Amsterdam) are kindly acknowledged for the DFT calculations reported in this chapter.

4.1 Introduction

4.1.1 Barrelene and Semibullvalene

Bicyclo-[2,2,2]-2,5,7-octatriene (**4.1**) is a bicyclic hydrocarbon with the chemical formula C_8H_8. Formally, it is the Diels-Alder adduct of benzene and acetylene and shows three ethylene units connected by two methinic bridgehead atoms. First postulated in 1955, it has been synthesized by Zimmerman *et al.* in 1960, using α-pyrone and methyl-vinyl ketone as starting materials. The arrangement of the p-orbitals of the three double bonds, which partially overlap forming a "barrel shaped electron cloud", led to the name "barrelene" (Figure 38).[228,229] Because of the overlap of orbital lobes with opposite sign and the presence of 6 π-electrons, the structure presents Möbius antiaromaticity.[230–233]

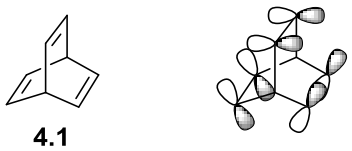

Figure 38. Bicyclo-[2,2,2]-2,5,7-octatriene (**4.1**) and its p-orbitals.

Among the remarkable characteristics of barrelene, the most interesting is the photorearrangement to semibullvalene. This reaction was described by Zimmerman *et al.* in 1966, when the first semibullvalene derivative was reported.[234] Irradiating a 1-2% solution of **4.1** in isopentane containing 3-8% of acetone as photosensitizer with UV-light, afforded 25-40% of semibullvalene **4.2** and 1-2% of cyclooctatetraene (**4.3**) as side product (Scheme 39). In the absence of a triplet photosensitizer, **4.3** was obtained as only product, as the reaction follows a singlet mechanism.[235,236]

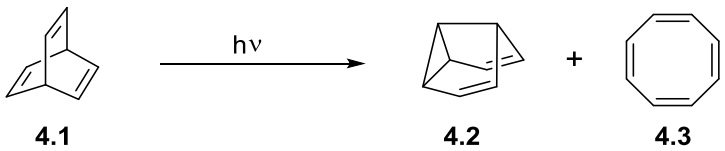

Scheme 39. Photoisomerization of **4.1** to **4.2** and **4.3**.

The presence of semibullvalene **4.2** was confirmed by elemental analysis, mass spectrometry, hydrogenation (to the known tricyclo-[5.1.0.0^{4-8}]octane), and NMR analysis.[234] This compound is a fluxional molecule in equilibrium with its valence tautomer *via* a degenerate

Cope rearrangement. This is a very fast process even at very low temperatures.[237] In fact the ^{1}H NMR spectrum only shows three distinct resonances relative to the α-, β- and γ-protons of **4.2** (Figure 39 a). The transition state is predicted to have a delocalized, bishomoaromatic C_{2v}-symmetric structure (Figure 39 b).[238]

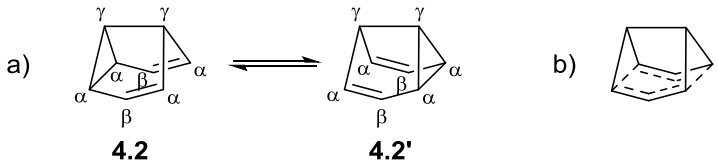

Figure 39. Degenerate Cope rearrangement in semibullvalene (a) and bishomoaromatic transition state (b).

The mechanism of the photoisomerization of barrelene to semibullvalene was investigated by the same group. This was done by irradiating a solution of deuterated barrelene bearing protons only at the methinic positions. Since α-, β- and γ-protons in semibullvalene give rise to distinct resonances in the ^{1}H NMR spectra, it was possible to determine the mechanism by simply checking in which of these positions the methinic protons were to be found at the end of the irradiation.[235,238] This reaction can be classified as a special case of the di-π-methane rearrangement, which was described for a number of different systems.[239,240] This photochemical reaction involves molecules that contain two π-systems separated by a saturated carbon atom (*i. e.* a 1,4-diene or an allyl-substituted aromatic ring), to form an ene- (or aryl-) substituted cyclopropane. The rearrangement formally consists of a 1,2 shift of one ene (or aryl) group and a bond formation between the lateral carbons of the non-migrating moiety (Scheme 40, top). The same mechanism can be drawn for the photoisomerization of barrelene to semibullvalene (Scheme 40, bottom), and has been supported by DFT calculations.[241,242]

The reaction starts with the light-induced homolytic fission of two double bonds and proceeds *via* the formation of two different biradical species (BR1 and BR2), which then yield the products **4.2** and **4.2′** (Scheme 40). The biradical species are reaction intermediates and can help to understand and predict reaction courses, regioselectivity, and general reaction trends.[240]

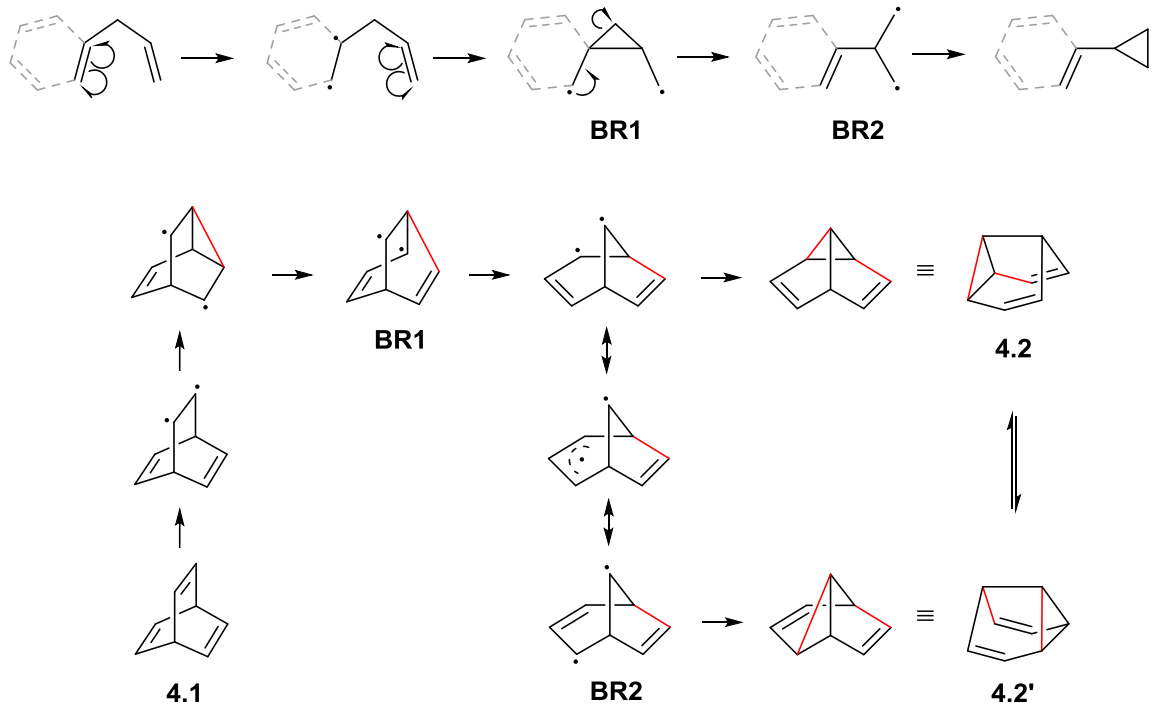

Scheme 40. Di-π-methane rearrangement of a generic diene (top) and of barrelene (bottom).

As expected from the general mechanism described above, also annulated barrelenes (*e.g.* benzo- and dibenzobarrelenes), are reported to undergo di-π-methane rearrangement by irradiation with UV-light and in the presence of a triplet photosensitizer (Scheme 41).[243–245]

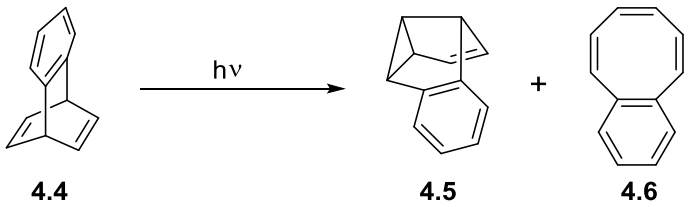

Scheme 41. Photoisomerization of **4.4** to **4.5** and **4.6**.

In this case, the biradical species can involve vinyl-vinyl or benzo-vinyl bridging, according to the positions where the radical forms, but only the former has been observed.[246] For benzosemibullvalenes, the degenerate Cope-rearrangement has neither been observed nor reported. Together with experimental data, DFT calculations support the proposed di-π-methane rearrangement for the photoisomerization of benzobarrelenes. [241,247–249]

As shown above, the high symmetry of **4.1** (D_{3h}) leads to the formation of a single product (two degenerated isomers in equilibrium). However, as one might expect, the presence of substituents on the barrelene (or the benzobarrelene) backbone leads to regioselectivity problems. The position of the radicals in the biradical intermediates and their stabilization can

be influenced by changing the position and the nature of the substituents on the barrelene backbone. Therefore it is possible to modify the selectivity of the photoisomerization and to achieve differently substituted regioisomers. In this respect, for substituted benzo- and dibenzobarrelenes, the regioselectivity was found to be dependent on the stabilizing (or destabilizing) effect of the substituents, which determines the biradical species involved in the di-π-methane rearrangement.[240,245,250,251]

In the past, some efforts have been devoted to the study of trifluoromethyl-substituted barrelenes.[252,253] These compounds, obtained from the cycloaddition between benzene and hexafluoro-2-butyne, undergo di-π-methane rearrangement to a number of different products, as depicted in Scheme 42. Due to the effect of the trifluoromethyl groups, the products are obtained in a non-statistical mixture and in the photoisomerization of **4.7** only three of the possible products were actually observed. **4.8**, **4.10** and **4.9** were obtained in a 4:2:1 ratio, and most likely **4.9′** and **4.10′** are not detected because they are less stable than the isomers they are in equilibrium with.

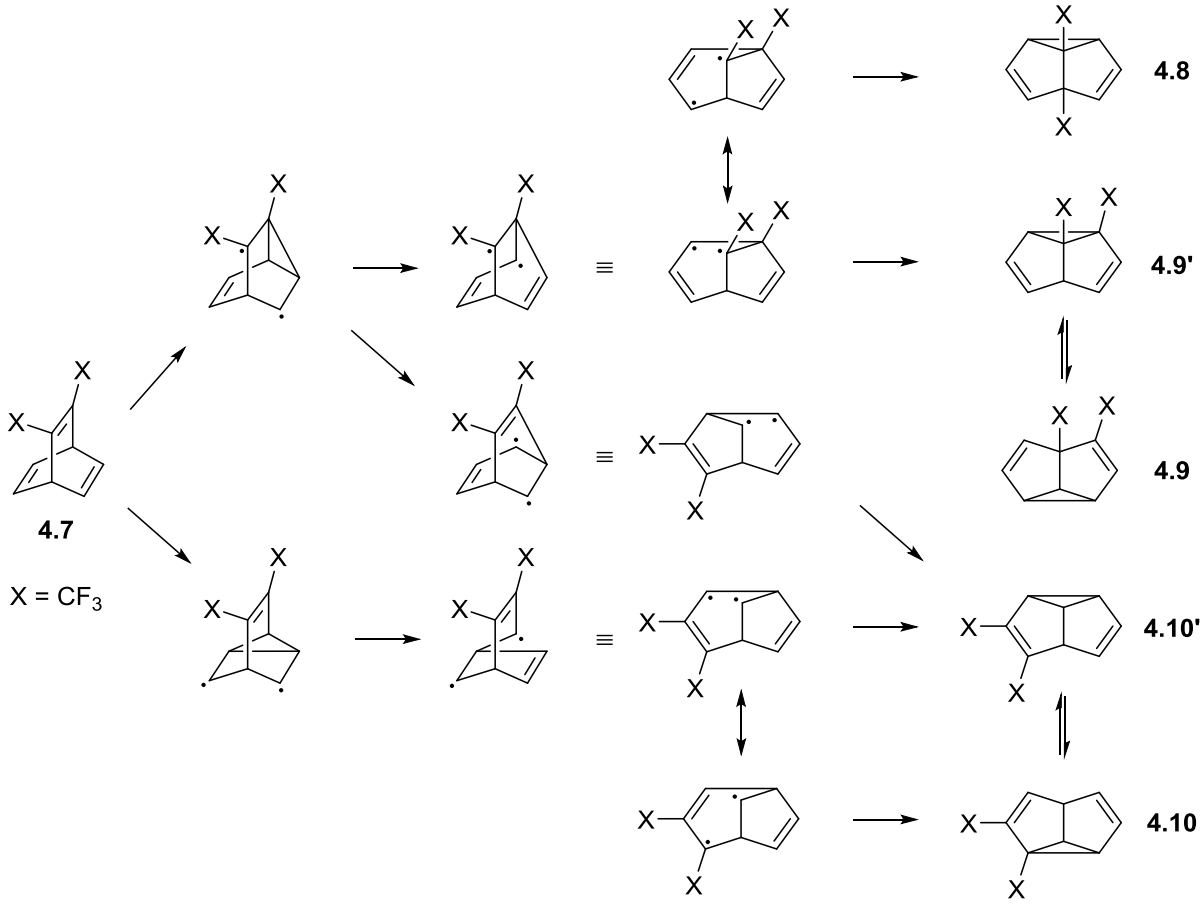

Scheme 42. Complete scheme of the rearrangement of bis(trifluoromethyl)bicyclo[2.2.2]octa-2,5,7-triene **4.7**.

4.1.2 Phosphasemibullvalenes

Phosphorus-containing semibullvalene derivatives are known, but only a few examples have been described in the literature up to now. The first one was reported by Regitz *et al.* in 1997 while investigating cycloaddition reactions between *t*BuCP and tropone, as a cyclotetramerization byproduct (Scheme 43a).[254] With an unclarified mechanism, thermal cyclotetramerization occurs and tetraphosphasemibullvalene **4.12** is obtained in 4.9 % yield after workup. One year later a similar compound was reported by Binger *et al.*, who reacted 2,4,6-tri-*tert*-butyl-1,3,5-triphosphabenzene (**4.13**) with diisopropylaminophosphaethine in the attempt of synthesizing an asymmetrically substituted tetraphosphabarrelene (Scheme 43b).[202] The molecular structure in the crystal of **4.14** was determined by X-ray diffraction, confirming the tetraphosphasemibullvalene structure. The same groups reported also on triphosphasemibullvalene **4.16**, obtained by photoisomerization of a triphosphabishomoprismane derivative (Scheme 43c).[255] The only monophosphorus-containing semibullvalene described until now is dibenzo-1-phosphasemibullvalene (**4.18**), reported by Grützmacher *et al.* in 2003. The compound was synthesized *via* a multistep procedure, starting from 5-chloro-5H-dibenzo[a,d]cycloheptene (**4.17**) and $P(SiMe_3)_3$ (Scheme 43d). Its molecular structure was confirmed by single crystal X-ray diffraction of the tungsten complex [(**4.18**)$W(CO)_5$].[256]

No Cope rearrangement was reported for any of these derivatives, and all but **4.16** turned out to be thermally unstable, and decompose if stored at room temperature. For this reason, most likely, investigations on these interesting phosphorus cages stopped, and up to now, no other phosphasemibullvalene derivative is known. Also, no state-of-the-art procedure is known for the synthesis of differently substituted phosphorus-containing semibullvalenes, thus limiting the amount of molecules available and their substitution patterns.

In order to better investigate the properties of this ligand class, a versatile synthetic path leading to the formation of differently substituted phosphasemibullvalenes is desirable. Following the photochemical approach that led to the first synthesis of semibullvalene, we decided to investigate the reactivity of 1-phosphabarrelenes towards UV light.

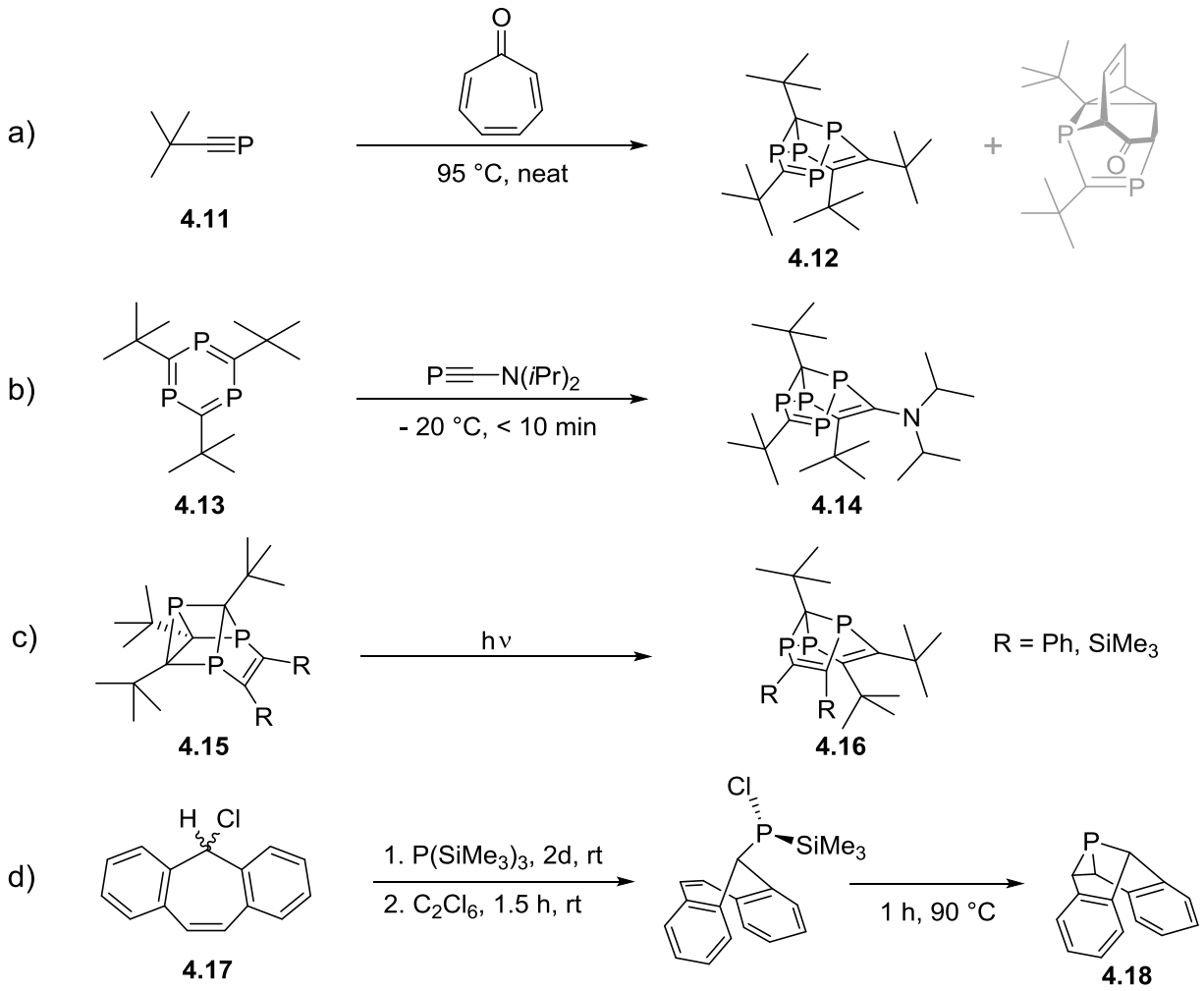

Scheme 43. Synthetic routes to known phosphasemibullvalene derivatives.

4.2 Results and discussion

In this chapter the synthesis of the first 5-phosphasemibullvalene derivatives is described. An investigation of the mechanism of this hitherto unknown reaction is presented and the first coordination compounds are reported.

4.2.1 Mechanism and Selectivity

At first, a solution of phosphabarrelene **3.12** in THF was irradiated with UV light, and the reaction progress was monitored by means of $^{31}P\{^{1}H\}$ NMR spectroscopy. Gradually, the

resonance relative to the starting material (δ = -69.8 ppm) decreases in intensity, while a new resonance appears at δ = 33.1 ppm. Over the course of 15 h the reaction is complete and only the resonance corresponding to the product can be detected, suggesting a quantitative conversion to a new species (Figure 40).

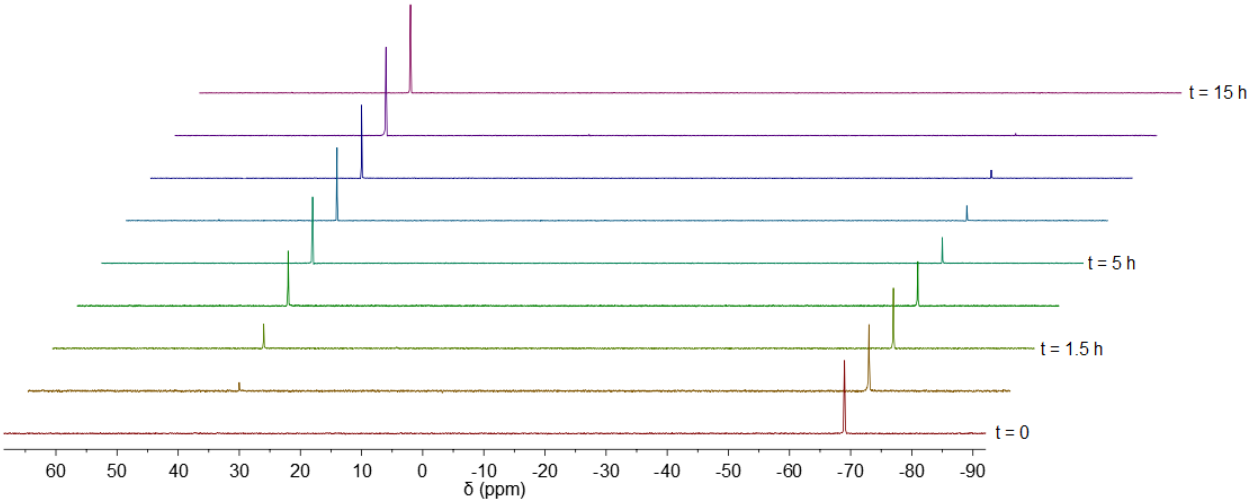

Figure 40. Time-dependent $^{31}P\{^{1}H\}$ NMR spectra during the irradiation of **3.12** in THF.

The ^{1}H NMR spectrum of the reaction mixture shows only one set of sharp signals, in agreement with the quantitative formation of a single species (Figure 41). The appearance of different resonances relative to single protons suggest that the symmetry found in the starting material is lost. Moreover, while in phosphabarrelene **3.12** all the protons are bound to sp^2-hybridized carbon atoms, the chemical shift of the most upfield signal (δ = 4.19 ppm) suggests the presence of a proton bound to an sp^3-hybridized carbon atom.

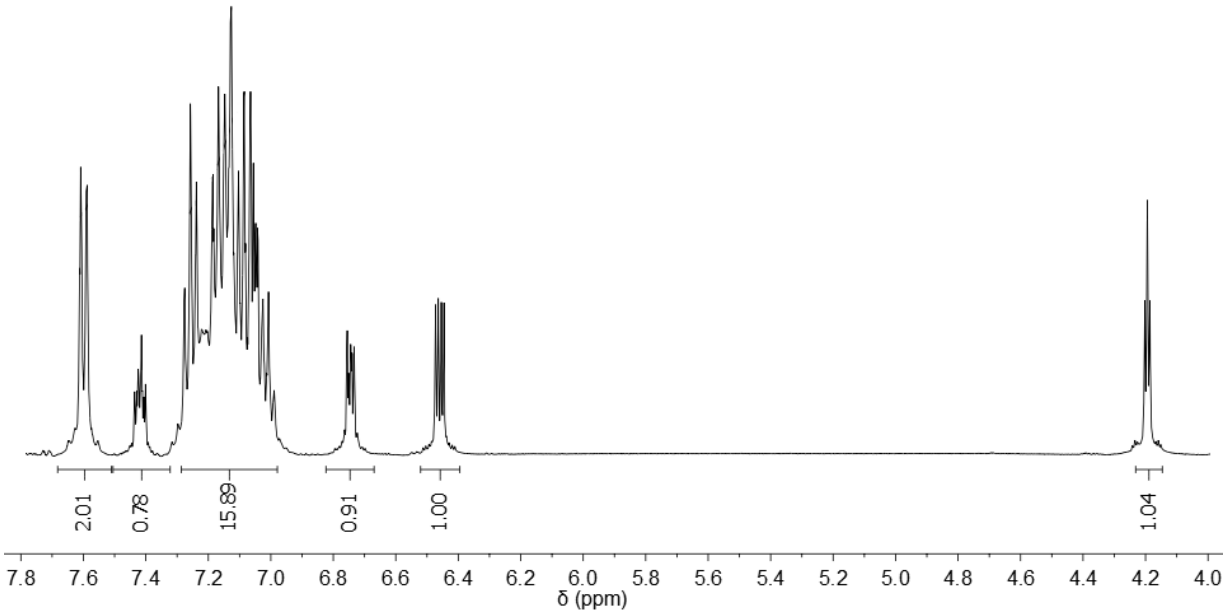

Figure 41. ^{1}H NMR spectrum of the reaction mixture in THF-d_8 (400 MHz).

In this respect, ^{13}C NMR spectroscopy provides very good indications for a defined reaction. While the starting material only presents one sp^3-hybridized carbon atom, three resonances can now be detected in the aliphatic region at δ = 47.8, 60.4 and 63.7 ppm respectively, suggesting the presence of a cyclopropane ring included in the desired phosphasemibullvalene derivative.

Finally, a mass spectrum (ESI-TOF) proved the identical molecular weight of both the starting material and the product, confirming the successful photoisomerization of **3.12** to **4.19**, the first reported 5-phosphasemibullvalene derivative (Scheme 44).

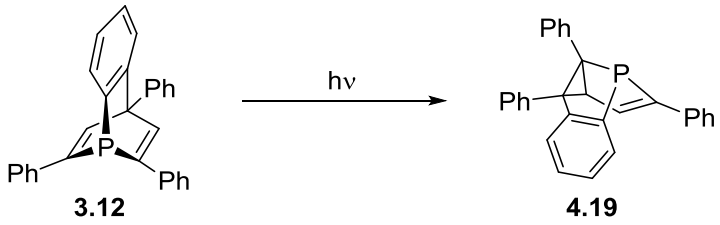

Scheme 44. Photorearrangement of **3.12** to **4.19**.

Unfortunately, no single crystals suitable for X-ray diffraction were obtained from the product, but the identity of this unprecedented phosphorus-containing cage was unambiguously confirmed by single crystal X-ray diffraction of a number of metal complexes and derivatives (*vide infra*).

The compound proved to be stable for days in refluxing toluene, showing very high stability compared to known phosphasemibullvalenes. In addition to this, and differently from the all-carbon semibullvalenes, extended UV irradiation over 7 days did not lead to any further reactions or decomposition. Also, as for benzosemibullvalenes, no Cope rearrangement was detected with variable temperature NMR experiments between T = -80 °C and T = 100 °C in toluene for **4.19**. DFT calculations confirm that the Cope rearrangement is a disfavored process, most likely due to the loss of aromaticity of the benzynic bridge (Scheme 45).

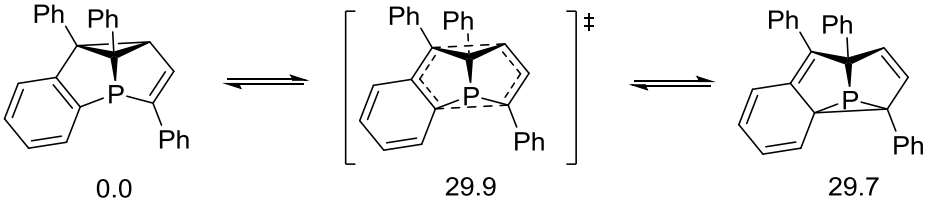

Scheme 45. Cope rearrangement for **4.19**. The energy values are expressed in kcal/mol and have been calculated on the #um062x / 6-31G (d) level.

Interestingly, the reaction does not need a triplet photosensitizer. Nevertheless it proceeds roughly three time faster in the presence of acetone.

In order to investigate the mechanism, DFT calculations have also been performed. As in the case of barrelene **4.1**, we assumed that the photoisomerization of **3.12** would follow a di-π-methane rearrangement mechanism. According to the calculations, the most favorable pathway involves two biradical species stabilized by the phenyl groups at the phosphabarrelene skeleton (Scheme 46). In this case, the activation barrier that leads to BR2 starting from BR1 is fairly small (9.6 kcal/mol). In fact, radicals are stabilized by resonance in benzylic positions and by adjacent heteroatoms with lone pairs (the P atom in this case). Calculations also suggest that a pathway involving radicals on the β-carbons is not favored energetically.

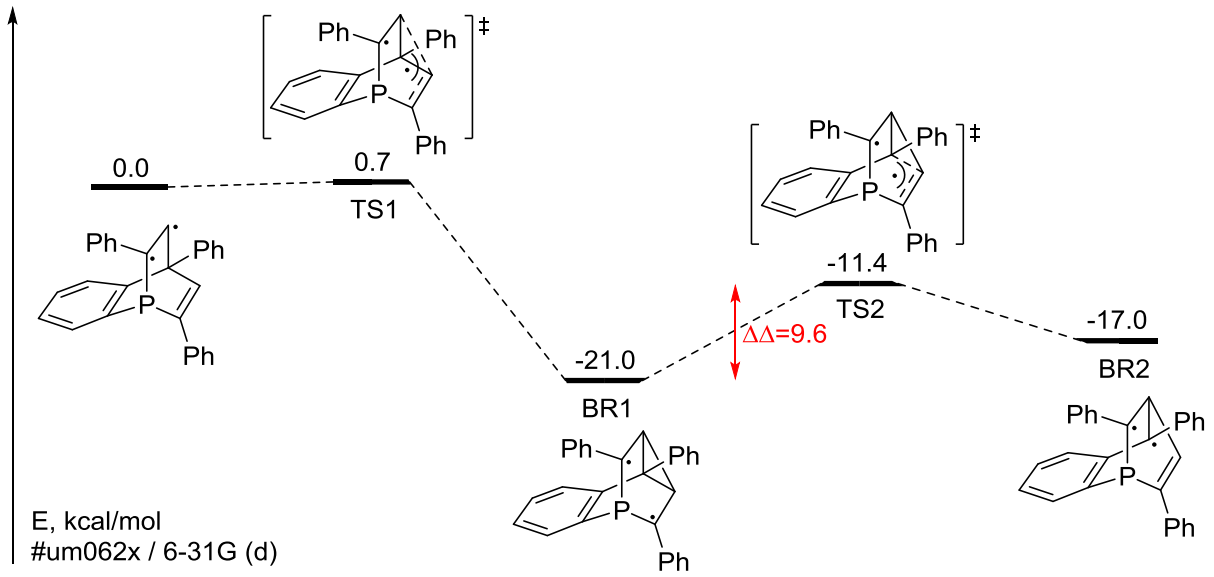

Scheme 46. Photoisomerization of **3.12** to **4.19**. Triplet surface.

As one can see from Scheme 46, the formation of BR2 is a stereogenic step. The phosphabarrelene has a symmetry plane and only one of the benzylic positions will be occupied by the radicals in BR2 which is, *de facto*, chiral. Hence, the reaction leads to the formation of a racemic mixture in which each enantiomer has four stereocenters: three carbon atoms and the phosphorus, which cannot undergo inversion due to the rigid character of the molecule (Figure 42). Unless specified, the 5-phosphasemibullvalenes will always be meant as racemic mixtures throughout this manuscript.

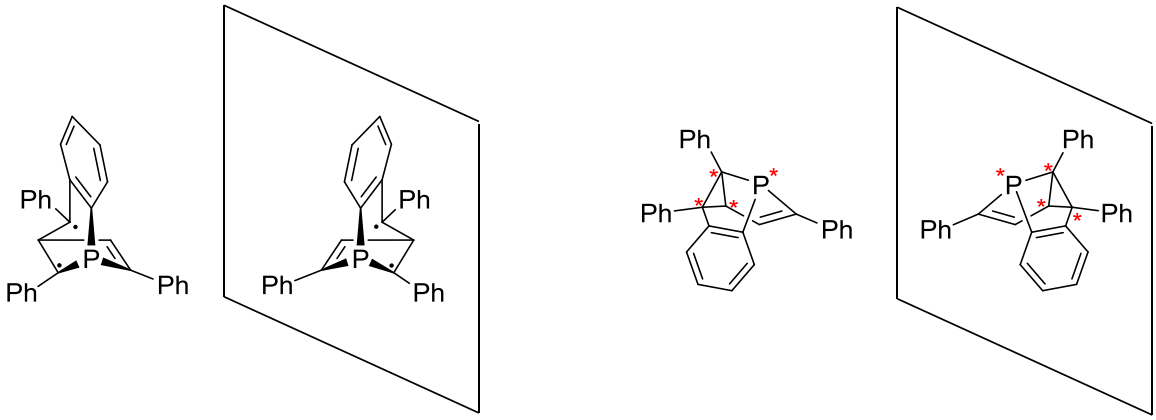

Figure 42. Two enantiomers of BR2 and of ***rac*-4.19**.

To support the calculated mechanism, an experimental proof is needed. This can be achieved by marking one of the substituents on the phosphabarrelene, and by verifying subsequently its position in the final product. For this reason, a phosphabarrelene substituted with a tolyl-group (**4.20**) was synthesized and photoisomerized to the corresponding 5-phosphasemibullvalene **4.21** (Scheme 47). The product, similarly to **4.19**, shows a sharp single resonance at δ = 33.3 ppm in the $^{31}P\{^{1}H\}$ NMR spectrum and was obtained as a pale-yellow foamy solid in quantitative yield.

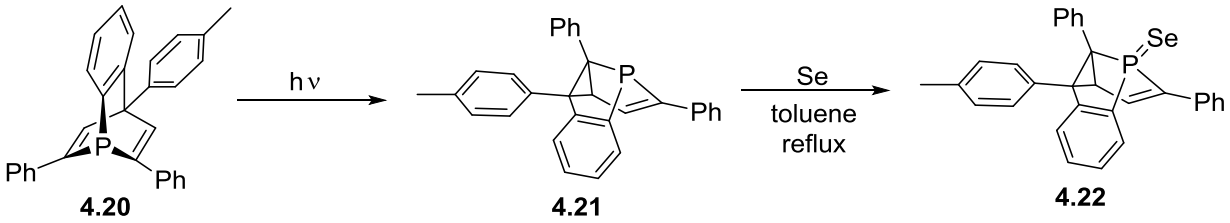

Scheme 47. Photoisomerization of **4.20** to **4.21** and oxidation to **4.22**.

Unable to grow single crystals of phosphasemibullvalenes in order to finally proof the structure of **4.21**, the product was converted into the corresponding selenide, since this air-stable compound might crystallize more easily. The conversion was performed with an excess of grey selenium in refluxing toluene to yield **4.22** quantitatively after removing the excess of selenium by filtration (Scheme 47). The $^{31}P\{^{1}H\}$ NMR spectrum of the product shows one single resonance at δ = 57.5 ppm with characteristic satellites due to a $^{1}J_{P\text{-}Se}$ coupling. Single crystals suitable for X-ray diffraction could be obtained by slow evaporation of the solvent. The crystallographic characterization confirms that the tolyl-group is found on the cyclopropane ring, adjacent to the benzynic bridge, in the position suggested by the predicted mechanism (Figure 43).

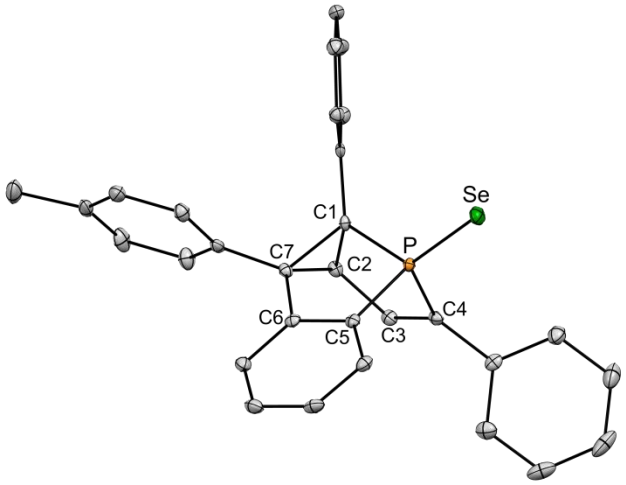

Figure 43. Molecular structure of **4.22** in the crystal. Displacement ellipsoids are shown at the 50% probability level. Hydrogen atoms are omitted for clarity. Selected bond lengths (Å) and angles (°): P–C1: 1.849(2); P–C4: 1.820(9); P–C5: 1.799(2); P–Se: 2.081(1); C1–C2: 1.515(2); C1–C7: 1.541(3); C2–C7: 1.564(3); C2–C3: 1.482(9); C3–C4: 1.341(1); C5–C6: 1.403(1); C6–C7: 1.497(3); C1–P–C5: 94.52(2); C1–P–C4: 94.52(9); C4–P–C5: 97.97(2).

As this is the first reported molecular structure of a 5-phosphasemibullvalene derivative, its features deserve a few remarks. First of all, it appears that the phosphorus center is strongly pyramidalized, with C-P-C angles as small as 94.52 and 97.97°. Furthermore, the P-C and C-C single and double bonds within the cage are rather short, while the C-C bonds in the cyclopropane moiety are slightly longer than in other substituted three-membered rings.[257] This deformation can be attributed to the rigid polycyclic nature of the cage compound. Unfortunately, a comparison with the known tetraphosphasemibullvalenes is not meaningful due to the considerable difference in the molecular structure of the compounds.

At this stage, the effect of the substituents was studied. In fact, this can affect the formation of the biradical species and therefore the phosphasemibullvalenes. For this reason, an asymmetrically substituted phosphabarrelene was synthesized. Two different BR2 species are envisaged, and the different effect of the substituents on the stabilization of the radicals leads to regioselectivity. In order to destabilize one of the two BR2 species, a phenyl ring was substituted by a methyl group, which has a less pronounced stabilizing effect. A suitable precursor for this reaction was reported in Chapter 3. Hence, a solution of the asymmetrically substituted phosphabarrelene 3.42 was exposed to UV light. According to the proposed mechanism, two different 5-phosphasemibullvalenes as well as their respective enantiomers can be obtained (Scheme 48).

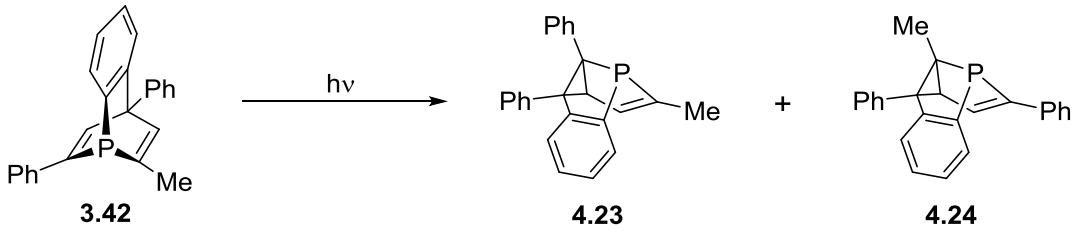

Scheme 48. Photoisomerization of **3.42** to **4.23** and **4.24** (only one enantiomer is shown).

Two different BR2 species are involved in this reaction, and due to the different stabilization deriving from the phenyl and methyl groups, one major product is expected. Indeed, two resonances were observed in the $^{31}P\{^{1}H\}$ NMR spectrum of the reaction mixture after irradiation. A HH COSY NMR spectrum showing a cross peak between the methyl protons and the adjacent vinylic protons, suggests **4.23** as the major product (95% yield by NMR). This observation supports the proposed mechanism, since the benzylic radical is much more stable than the vinylic one. The finding was also confirmed by DFT calculations which, comparing the two different biradical species, suggest **4.23** as the thermodynamic product (Scheme 49).

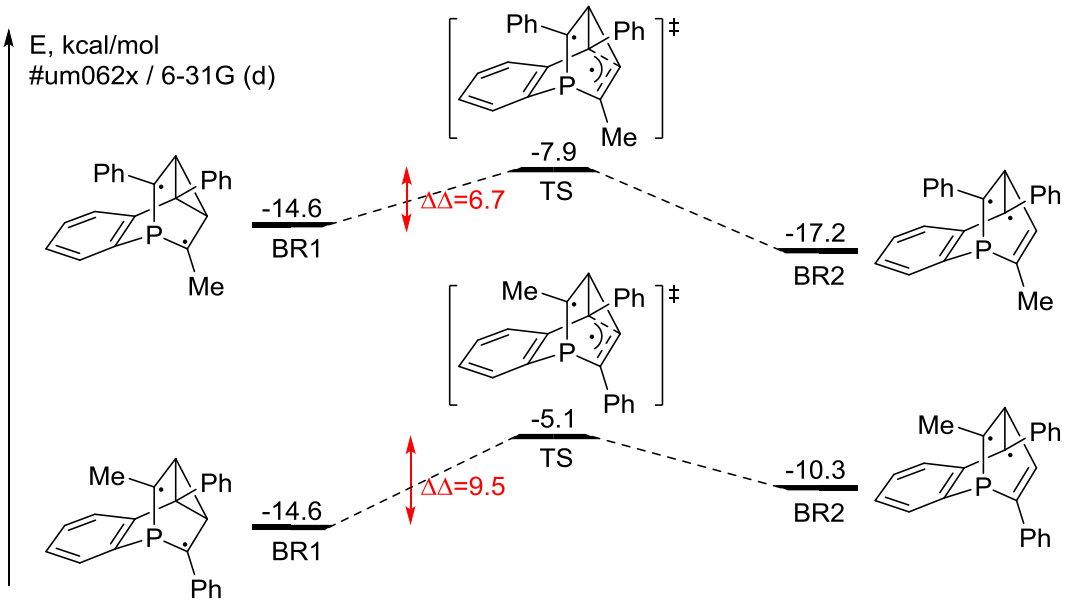

Scheme 49. Photoisomerization of **3.42** to **4.23** and **4.24**. Triplet surface. Biradicals involved in the reaction.

Again, in order to grow crystals and prove the identity of the major product, the compounds were oxidized. Therefore, the product mixture was treated with an excess of grey selenium in refluxing toluene to obtain the corresponding selenides in quantitative yield. Finally, it was possible to obtain single crystals suitable for X-ray diffraction of the main product **4.25** by slow evaporation of a saturated toluene solution. The X-ray analysis confirms that the phenyl

group of the main product is located on the cyclopropane ring, as predicted by DFT calculations. Interestingly, both enantiomers are present in the unit cell and are depicted in Figure 44, giving additional confirmation of the synthesis of a racemic mixture of products.

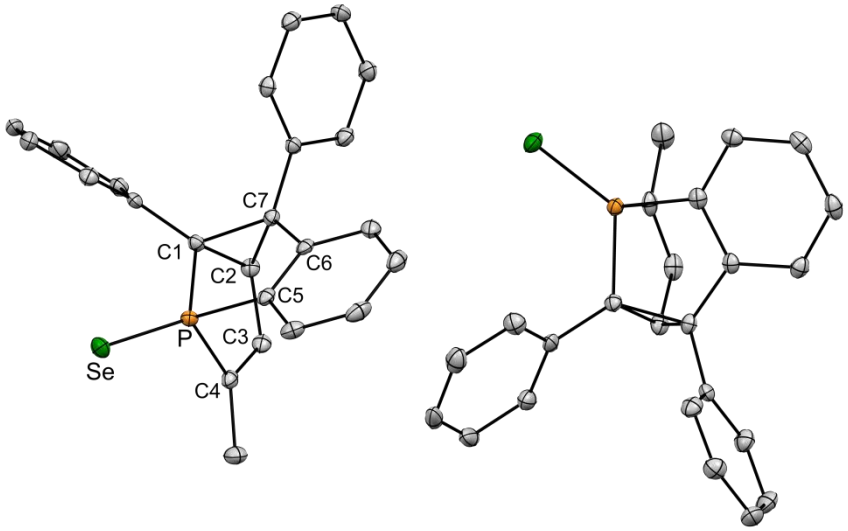

Figure 44. Molecular structure of **4.25** in the crystal. Displacement ellipsoids are shown at the 50% probability level. Hydrogen atoms are omitted for clarity. Two enantiomers are shown in the unit cell. Selected bond lengths (Å) and angles (°): P–C1: 1.852(2); P–C4: 1.818(1); P–C5: 1.800(1); P–Se: 2.090(3); C1–C2: 1.515(2); C1–C7: 1.542(7); C2–C7: 1.568(2); C2–C3: 1.479(3); C3–C4: 1.335(1); C5–C6: 1.401(2); C6–C7: 1.491(4); C1–P–C5: 94.85(2); C1–P–C4: 94.92(1); C4–P–C5: 95.97(2).

To further extend the substrate scope of the reaction to differently substituted phosphabarrelenes, the di-π-methane rearrangement was verified on the trimethylsilyl-substituted derivative **3.45**, reported in Chapter 3. In principle, the β-silicon effect and the presence of phenyl groups could destabilize the radicals in α-position to the P atom. The resulting BR2 species, where the radicals are in β-position, can yield a 2-phosphasemibullvalene derivative, which includes the heteroatom in the cyclopropane ring. However, this reaction does not take place, and unexpectedly 5-phosphasemibullvalene **4.28** is obtained following the same mechanism discussed above (Scheme 50).

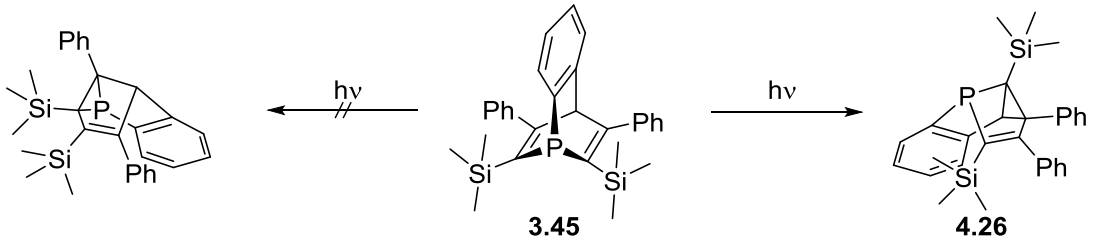

Scheme 50. Photoisomerization of **3.45** to **4.26**.

The product shows a sharp single resonance at δ = 49.0 ppm in the $^{31}P\{^{1}H\}$ NMR spectrum and was obtained as a pale-yellow foamy solid in quantitative yield. As observed for **3.12**, the photoisomerization of **3.45** causes a loss of symmetry in the molecule which is reflected in the NMR spectra of **4.26**. This phenomenon is particularly evident in the ^{1}H, $^{13}C\{^{1}H\}$ and $^{29}Si\{^{1}H\}$ NMR spectra, where two signals can now be detected for the unequal trimethylsilyl groups. Again, to verify the connectivity of **4.26**, the product was converted into the corresponding selenide, and then crystallized. The conversion was performed with an excess of grey selenium in refluxing toluene, to yield **4.27** quantitatively after removing the excess of selenium by filtration. The $^{31}P\{^{1}H\}$ NMR spectrum of the compound shows one single resonance at δ = 69.1 ppm, with characteristic satellites due to $^{1}J_{P\text{-}Se}$ coupling. Single crystals suitable for X-ray diffraction were obtained by slow evaporation from a saturated solution in toluene, and the molecular structure in the crystal is depicted in Figure 45.

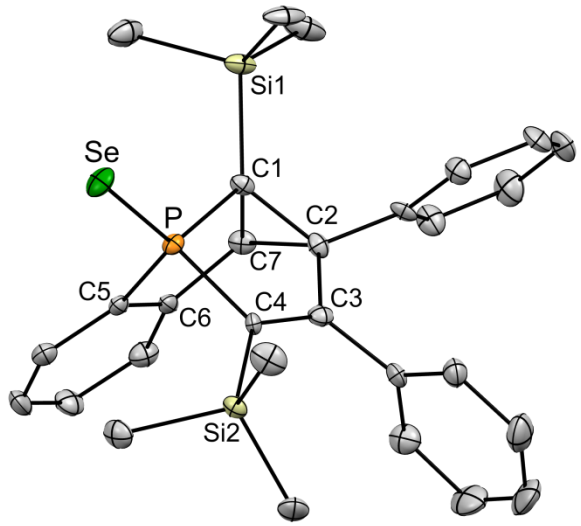

Figure 45. Molecular structure of **4.27** in the crystal. Displacement ellipsoids are shown at the 50% probability level. Hydrogen atoms are omitted for clarity. Selected bond lengths (Å) and angles (°): P–C1: 1.839(6); P–C4: 1.816(5); P–C5: 1.804(5); P–Se: 2.098(1); C1–C2: 1.526(7); C1–C7: 1.526(6); C1–Si1: 1.880(2); C2–C7: 1.552(7); C2–C3: 1.496(8); C3–C4: 1.361(7); C4-Si2: 1.877(1); C5–C6: 1.399(7); C6–C7: 1.498(7); C1–P–C5: 94.84(2); C1–P–C4: 96.25(1); C4–P–C5: 98.68(2).

Since unexpectedly, the trimethylsilyl groups in **3.45** led to the stabilization of the radicals in α-position, the photoisomerization was attempted on compound **3.47** (see Chapter 3), from which these group have been removed. In this way the reaction may be forced through a BR2 species bearing radicals in β-position to the P atom, finally leading to 2-phosphasemibullvalenes (Scheme 51).

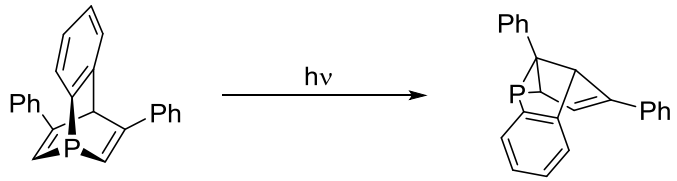

3.47 **4.28**

Scheme 51. Reaction of **3.47** wit UV light.

The UV irradiation leads to full consumption of the starting material, and three new resonances are observed in the $^{31}P\{^{1}H\}$ NMR spectrum of the reaction mixture (Figure 46).

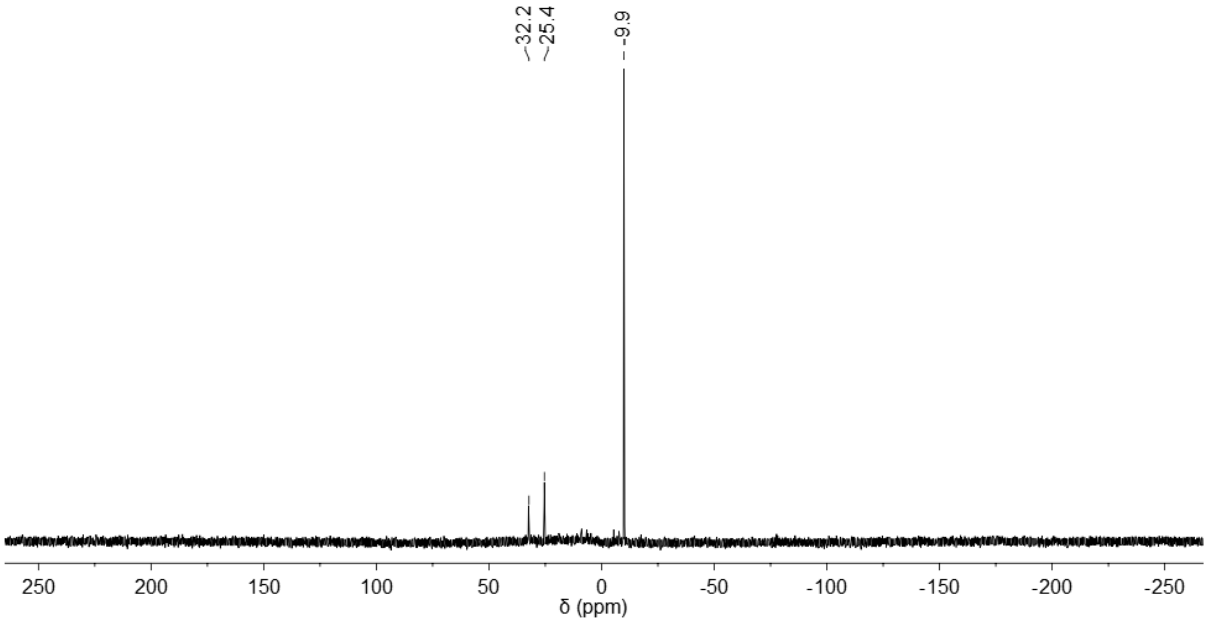

Figure 46. $^{31}P\{^{1}H\}$ NMR spectrum of the photoisomerization of **3.47**.

According to reported data on semibullvalenes including P atoms in the cyclopropane ring, the main resonance at δ = -9.9 ppm could be assigned to **4.28**.[202,254–256] Alternatively, a side reaction can be envisaged, since 2-phosphasemibullvalenes are polycyclic vinyl-phosphiranes. These molecules are known since more than three decades and are reported to undergo rearrangement upon heating or photochemical activation, leading to 5-membered phospholenes.[258] However, separation and characterization of the products is still in progress.

In order to extend the substrate scope to other compounds than benzo-phosphabarrelenes, the reactivity of trifluoromethyl-substituted derivatives towards UV light was investigated (Scheme 52).

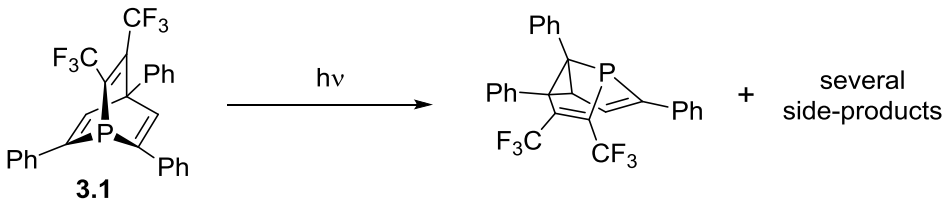

Scheme 52. Reaction of **3.1** with UV light.

Irradiation of a THF solution of **3.1** with UV light, though, led to the formation of a mixture of different products, which were not possible to separate. The $^{31}P\{^{1}H\}$ NMR spectrum of the reaction mixture shows five different quartets (Figure 47).

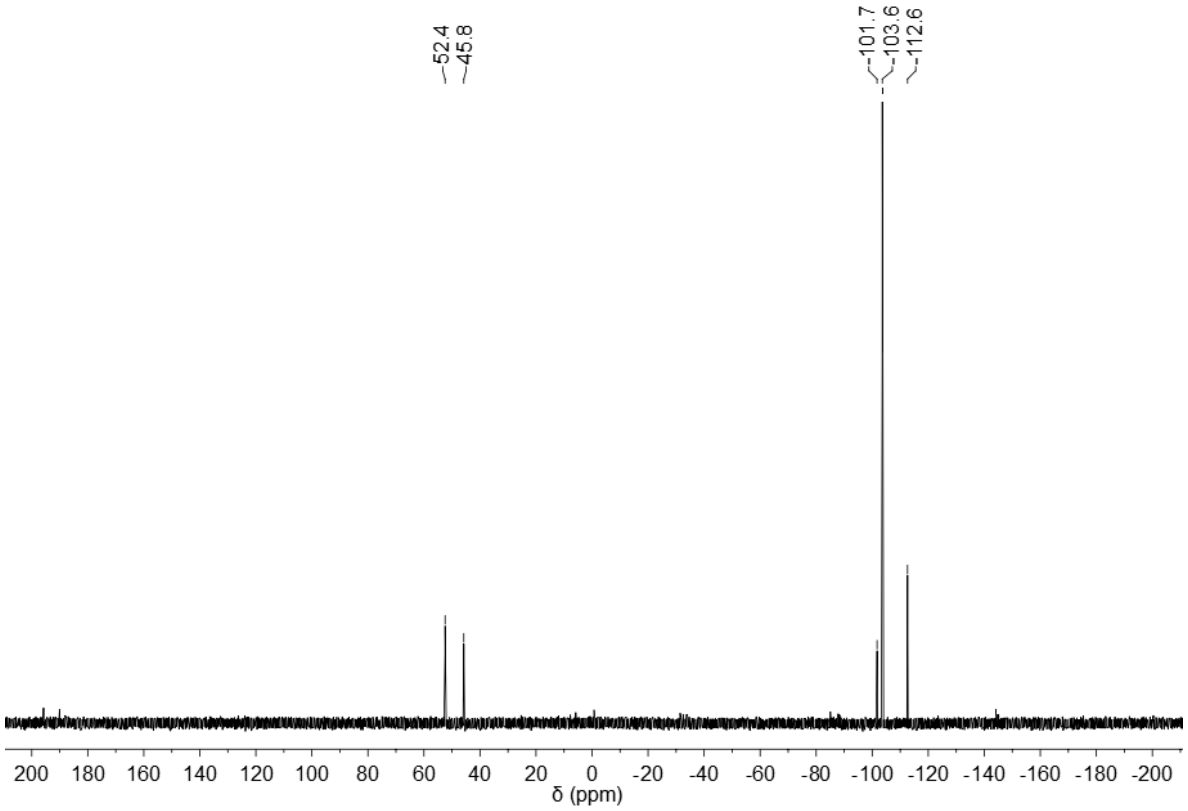

Figure 47. $^{31}P\{^{1}H\}$ NMR spectrum of the photoisomerization of **3.1**.

In this case, also the double bond which links the CF_3 groups can be cleaved homolytically, resulting in more potential products according to the proposed mechanism. Thanks to the previous reported work on the photoisomerization of bis(trifluoromethyl)bicyclo[2.2.2]octa-2,5,7-triene (see Scheme 42), it is possible to speculate on the structure of the products, which are depicted in Scheme 53.[252,253]

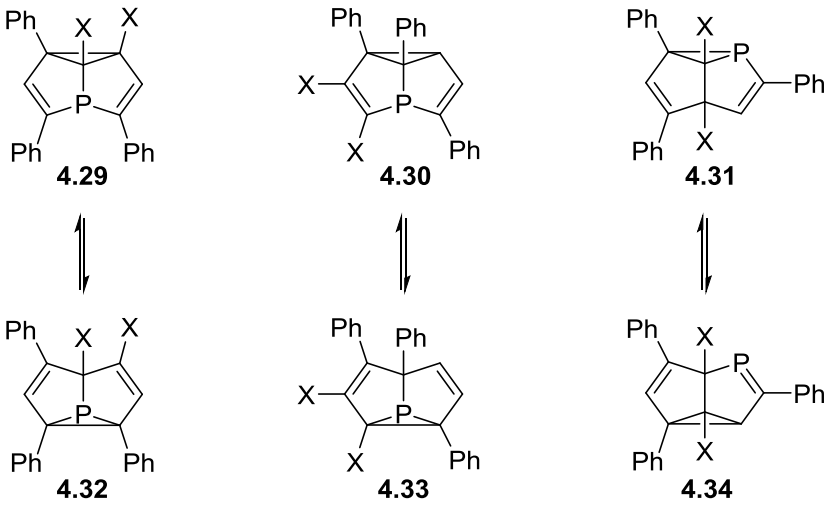

Scheme 53. Possible products of the photoisomerization of **3.1** and their Cope rearrangement equilibria (X = CF_3).

According to the assignments done for the signals in the $^{31}P\{^1H\}$ NMR spectrum in known phosphasemibullvalene derivatives, it is possible to identify the possible isomers in solution.[202,254–256] The two resonances at lower field (δ = 54.8 ppm and δ = 48.2 ppm) can most likely be assigned to products **4.29** and **4.30**, while the remaining three (at δ = -99.3, -101.2, -110.2 ppm, respectively) probably correspond to molecules **4.31**, **4.32** and **4.33**, which include the phosphorus atom in the cyclopropane ring. For **4.34**, a shift to much lower field is expected, considering the $\lambda^3\sigma^2$ nature of the P atom. However, only two small resonances are observed in the area. Variable temperature NMR experiments could actually clarify this, since coalescence between the Cope isomers would be expected at higher temperatures. In fact, DFT calculations confirm that the activation barrier for the isomerization of these derivatives, differently from the benzobarrelenes, is fairly low (Scheme 54). Similar results were obtained for ligand **3.46**.

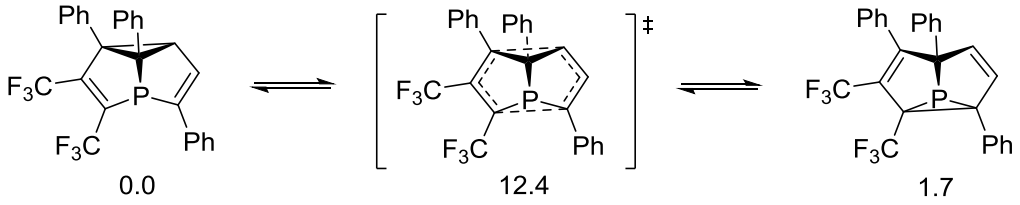

Scheme 54. Cope rearrangement between **4.32** and **4.35**. The energy values are expressed in kcal/mol and have been calculated on the #um062x / 6-31G (d) level.

4.2.2 Oxidation

As anticipated, like most phosphines, 5-phosphasemibullvalenes are prone to oxidation with chalcogens. Two alternative ways to obtain these derivatives were found. One can either oxidize the 5-phosphasemibullvalene or, alternatively, irradiate directly the oxidized phosphabarrelene, described in Chapter 3 (Scheme 55).

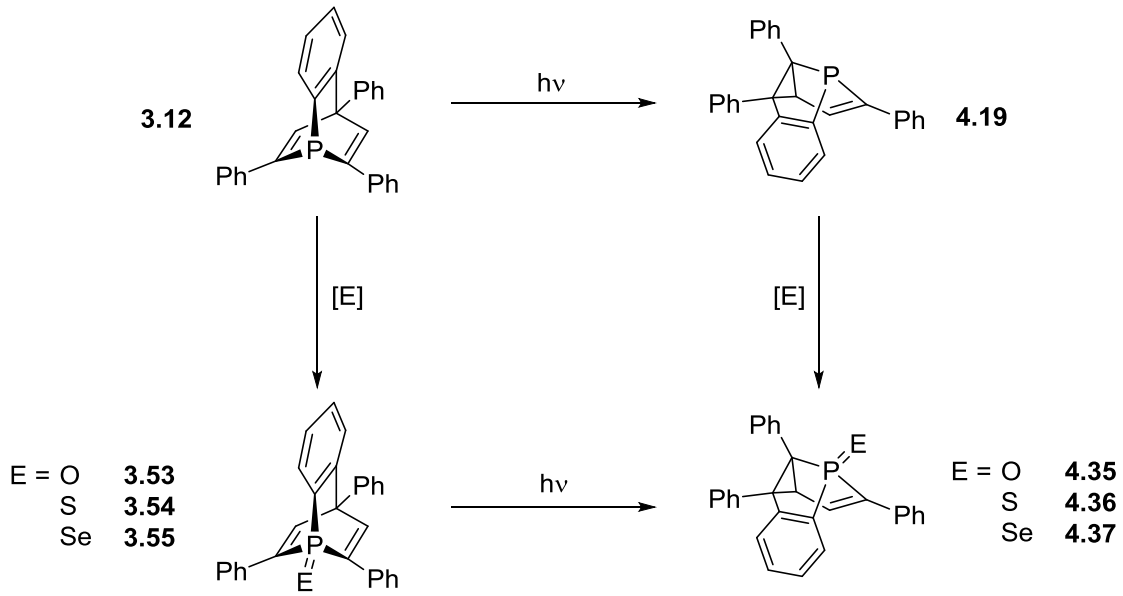

Scheme 55. Synthetic paths to oxidized 5-phosphasemibullvalene derivatives.

Oxidation with oxygen can easily be achieved, since 5-phosphasemibullvalenes oxidize in air. After stirring a solution of the appropriate ligand overnight in the presence of atmospheric oxygen, only one resonance can be detected in the $^{31}P\{^{1}H\}$ NMR spectrum. However, as confirmed by the ^{1}H NMR spectrum, oxidation leads to partial decomposition of the starting material, therefore workup is needed. After removing the volatiles and washing twice the remaining solid with pentane, the 5-phosphasemibullvalene oxides was obtained as a white solid. Oxidation with sulfur and selenium, as for phosphabarrelenes, can be achieved using elemental sulfur and DBU or grey selenium, respectively (see Chapter 3). The easiest way to obtain these derivatives, though, is to perform the photoisomerization starting from oxidized barrelenes, since the reaction is quantitative and phosphabarrelenes are usually more stable and easier to handle.

In general, the rate of the photoisomerization of phosphabarrelenes and their derivatives depends on several factors, such as concentration of the sample, distance from the UV light source and solvent. While investigating the photoisomerization of the oxidized derivatives, a

marked difference in the rate of conversion was noticed. In fact, the phosphabarrelene selenides reacted much faster compared to the other derivatives. Hence, the rates for the photoisomerization of **3.12**, **3.53**, **3.54** and **3.55** have been studied adopting the same experimental conditions. For this, four J-Young NMR tubes, containing an equally concentrated solution in THF of the above mentioned molecules, were positioned 20 cm away from the UV light source and irradiated until full conversion. The reaction was followed by means of $^{31}P\{^{1}H\}$ NMR spectroscopy, and the complete photoisomerization required 6 h for **3.12**, 5 h for **3.53**, 3 h for **3.54**, but only 40 min for **3.55**. However, DFT calculations run for a generic unsubstituted benzobarrelene, do not show a clear difference in the energy levels of the different transition states and biradicals formed in the different reactions (see Scheme 56 and Table 9).

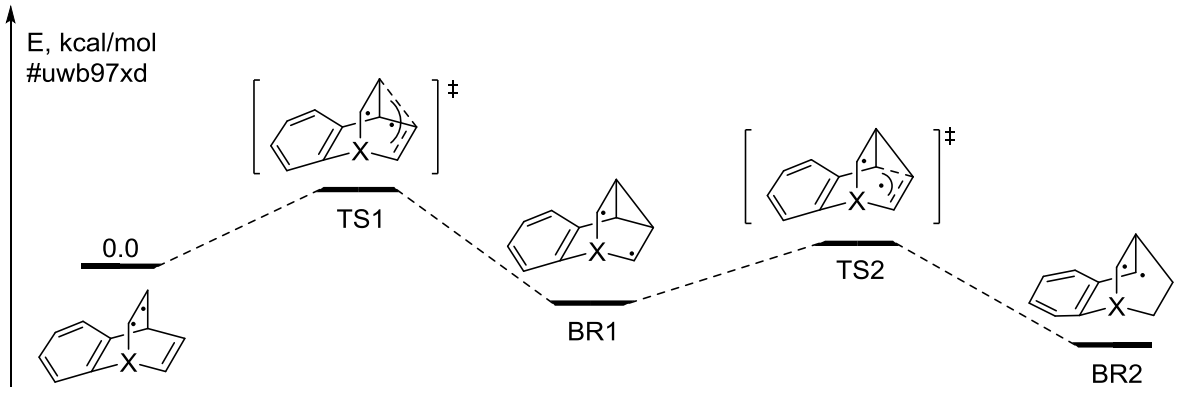

Scheme 56. Photoisomerization of **3.12**, **3.53**, **3.54** and **3.55**, with X = P:, P=O, P=S and P=Se respectively. Triplet surface.

Table 9. Energy values (in kcal/mol) for transition states and biradicals in the photoisomerization of **3.12**, **3.53**, **3.54** and **3.55**, with X = P:, P=O, P=S and P=Se respectively.

X	TS1	BR1	TS2	BR2
P:	3.6	-15.2	-6.1	-13.4
P=O	3.9	-13.1	-5.2	-14.8
P=S	3.7	-13.5	-5.2	-14.3
P=Se	3.6	-13.5	-5.4	-14.1

Hence, the reason for the difference in the rate of the rearrangement does not lay in the energetic profile of the reactions, but has other causes. For example, a more extended π-system, derived from an additional double bond between the phosphorus and the chalcogen

atom, could account for a better absorption of the UV radiation and be the reason for the faster reaction. In the case of **3.55**, the reaction is much faster compared to the others. The explanation for this is most likely related to the presence of selenium, a heavy atom that due to enhanced spin-orbit coupling, favors the intersystem crossing between the singlet and triplet state, thus increasing the rate of the reaction.[236,259]

As for the free 5-phosphasemibullvalenes, no Cope rearrangement was detected for **4.35** with variable temperature NMR experiments between T = -80 °C and T = 100 °C in toluene. In addition to this, the molecule is thermally stable in refluxing toluene for days. Single crystals suitable for X-ray diffraction were obtained by slow evaporation from a saturated solution of the corresponding compound in toluene. The molecular structure in the crystal of **4.35**, **4.36** and **4.37** are depicted in Figure 48, and selected bond lengths and angles are reported in Table 10.

Table 10. Selected bond lengths (Å) and angles (°) for **4.35**, **4.36** and **4.37**, with E = O, S, Se respectively.

Bond (Å) /angle (°)	**4.35**	**4.36**	**4.37**
P-C1	1.818(5)	1.848(2)	1.843(2)
P-C4	1.809(5)	1.816(2)	1.816(2)
P-C5	1.819(6)	1.802(1)	1.801(2)
P-E	1.491(4)	1.937(1)	2.081(1)
C1-C2	1.519(7)	1.508(2)	1.504(3)
C1-C7	1.564(7)	1.539(2)	1.536(3)
C2-C7	1.560(7)	1.563(2)	1.559(3)
C2-C3	1.485(7)	1.482(2)	1.479(3)
C3-C4	1.350(7)	1.339(2)	1.341(3)
C5-C6	1.379(7)	1.398(2)	1.402(3)
C6-C7	1.496(7)	1.501(2)	1.504(2)
C1-P-C5	95.50(2)	94.14(7)	94.77(9)
C1-P-C4	95.60(2)	94.52(7)	94.60(9)
C4-P-C5	97.20(2)	99.88(7)	96.62(9)

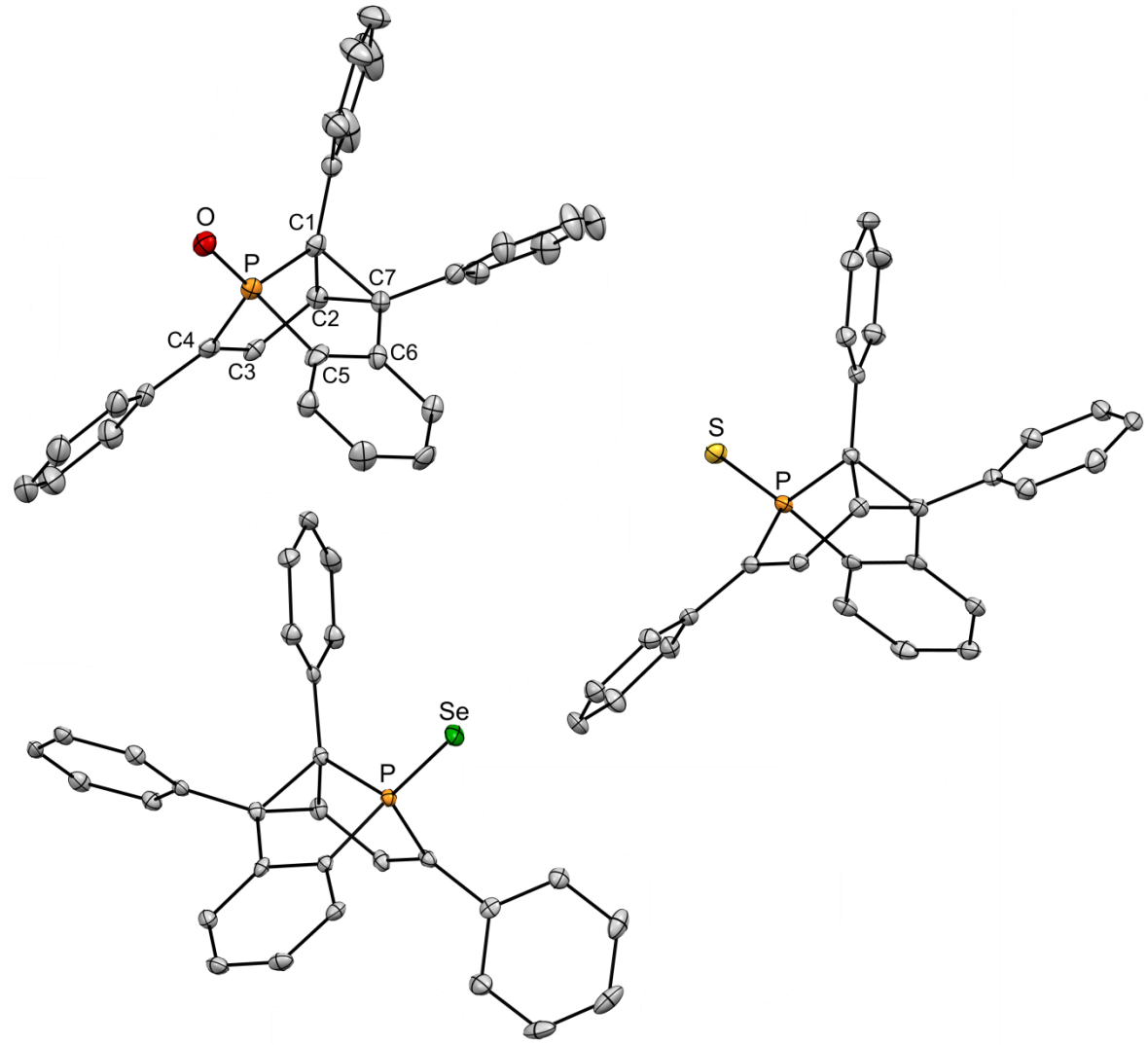

Figure 48. Molecular structure of **4.35**, **4.36** and **4.37** in the crystal. Displacement ellipsoids are shown at the 50% probability level. Hydrogen atoms, solvent molecules and enantiomers are omitted for clarity. Selected bond lengths (Å) and angles (°) are reported in Table 10.

Given the stability of the oxidized 5-phosphasemibullvalenes, they were employed to demonstrate that the photoisomerization of phosphabarrelenes leads to the formation of a racemic mixture. This is suggested by the proposed mechanism, and found confirmation for the presence of two enantiomers in the unit cell of the molecular structures of some compounds (*vide supra*). Hence, a sample of **4.37** was prepared and the enantiomers were separated by means of chiral HPLC, using isopropanol as eluent at room temperature. As expected, the chromatogram shows two peaks with equal area, proving the presence of a racemic mixture (Figure 49).

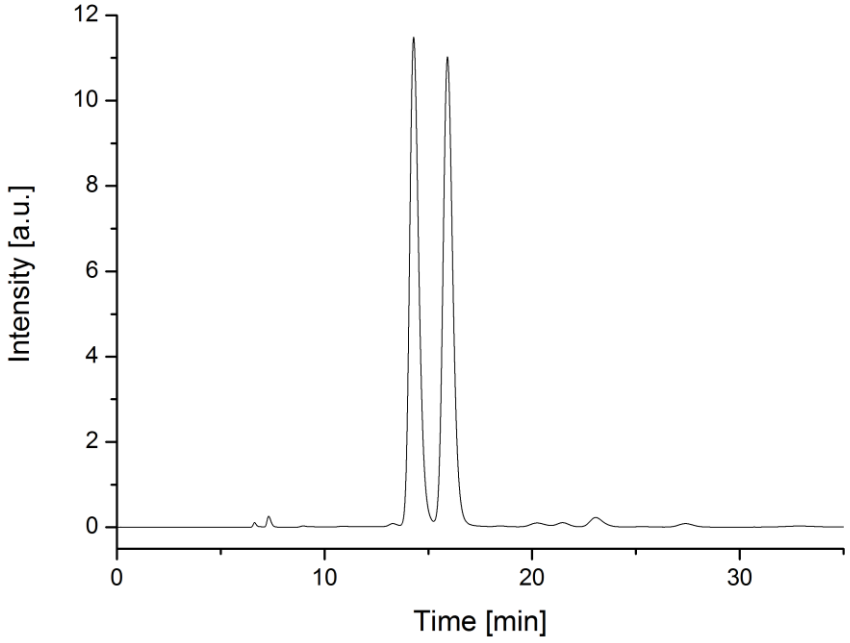

Figure 49. Enantiomeric resolution of **4.37**: HPLC chromatogram in isopropanol.

Finally, since the direct irradiation of **3.1** led to the formation of a complex mixture, the photoisomerization of the phosphabarrelene oxide **3.57** was attempted, hoping that the double bond would have a stabilizing effect on the radicals α to the phosphorus atom, thus leading more selectively to the 5-phosphasemibullvalene derivatives. In fact, when **3.57** was irradiated with UV light in THF, only two resonances at δ = 49.4 ppm and δ = 53.5 ppm were observed in the $^{31}P\{^{1}H\}$ NMR spectrum, suggesting the exclusive formation of the possible 5-phosphasemibullvalene oxides in a 15:85 ratio. However, it was so far not possible to isolate the products due to the small difference in polarity. Moreover, when the reaction was performed on a larger scale, reproducibility issues unfortunately occurred.

4.2.3 Coordination chemistry

Since these compounds are being reported for the first time, no coordination compound is so far known for 5-phosphasemibullvalenes. To test their properties as ligands, a few metal complexes were synthesized. First, tungsten and nickel carbonyl complexes were synthesized in order to evaluate the electronic properties of the ligands. In fact, metal-carbonyls can be used as probes for the evaluation and comparison of the electronic properties of a ligand, since the stretching frequency of the CO bands in the infrared spectra is proportional to the

net-donation of electron density from the ligand to the metal center. More precisely, the higher the net-donation, the lower the frequency of the stretching vibration. The tungsten complex **4.38** was prepared by mixing equimolar amounts of **4.19** and the metal precursor [(THF)W(CO)$_5$] in THF (Scheme 57). The $^{31}P\{^1H\}$ NMR spectrum of the reaction mixture shows one single resonance at δ = 61.6 ppm with characteristic satellites due to $^1J_{P\text{-}W}$ coupling, in agreement with the quantitative formation of **4.38**, which was characterized by means of NMR and IR spectroscopy. The IR spectrum of the obtained solid shows four CO stretching bands at $\tilde{\nu}$ = 2071, 1982, 1924 and 1908 cm^{-1}.

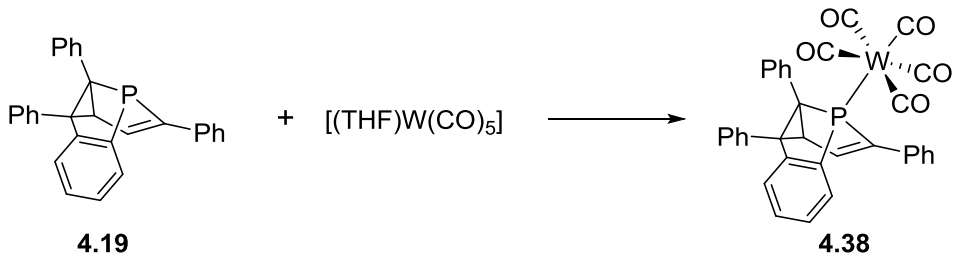

Scheme 57. Synthesis of **4.38**.

As discussed in the next chapter, [LNi(CO)$_3$] type complexes are the best probes to investigate the electronic properties of a ligand. To prepare them, an excess of [Ni(CO)$_4$] was condensed at T = -196 °C onto a solution with the appropriate ligand in a J-Young NMR tube with a condensation line (Scheme 58). Upon thawing of the solution and shaking, a violent gas evolution was observed in the NMR tube. In the $^{31}P\{^1H\}$ NMR spectra, a downfield shift suggested full conversion to the nickel complex. Evaporation of the volatiles yielded the compounds as yellow solids quantitatively. The IR spectra were measured in DCM and show the expected pattern for [LNi(CO)$_3$] type complexes. The value of the A_1 stretching band for complexes **4.39** and **4.40** is $\tilde{\nu}$ = 2074.0 and 2069.0 cm^{-1}, respectively.

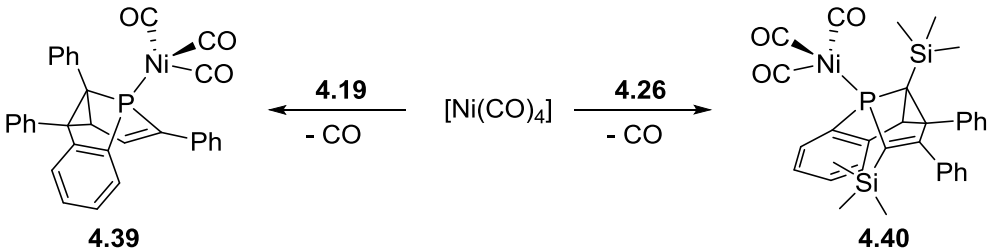

Scheme 58. Synthesis of **4.39** and **4.40**.

In order to evaluate the properties of 5-phosphasemibullvalenes as ligands in homogeneous catalysis (see Chapter 5), [LAuCl] type gold complexes were synthesizes starting from [AuCl(SMe$_2$)] in DCM at room temperature (Scheme 59).

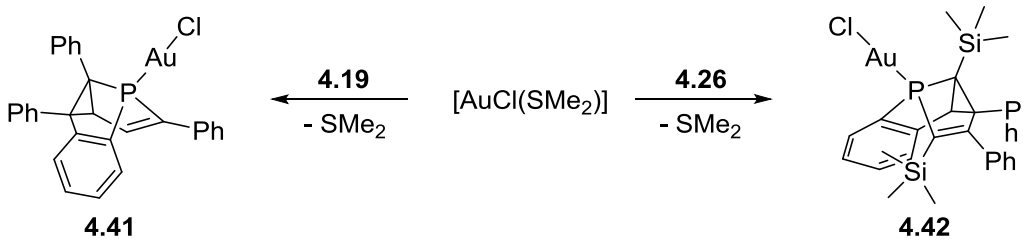

Scheme 59. Synthesis of **4.41** and **4.42**.

Quantitative formation of complexes **4.41** and **4.42** was observed in the $^{31}P\{^{1}H\}$ NMR spectra, where a single downfield-shifted resonance was observed. Evaporation of the volatiles yielded the compounds as pale-yellow solids quantitatively. To completely remove dimethylsulfide it was necessary to dissolve the complex again and remove the volatiles for a couple of times. The best results were obtained by dissolving the complex in the smallest amount of DCM and precipitate it with diethyl ether or pentane. In this way the obtained pale-yellow solid could be more easily thoroughly dried in vacuum. If needed, washing with diethyl ether or pentane was helpful. Single crystals suitable for X-ray diffraction were obtained by slow evaporation of DCM at T = -35 °C, and the molecular structure of **4.41** in the crystal is depicted in Figure 50.

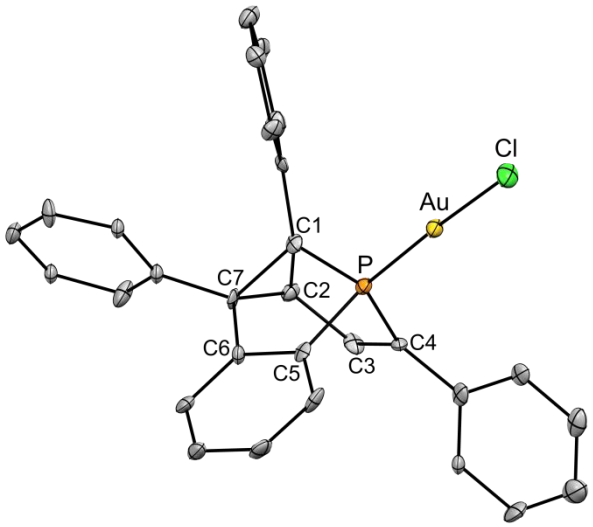

Figure 50. Molecular structure of **4.41** in the crystal. Displacement ellipsoids are shown at the 50% probability level. Hydrogen atoms and enantiomer are omitted for clarity. Selected bond lengths (Å) and angles (°): P–C1: 1.853(5); P–C4: 1.827(1); P–C5: 1.795(2); P–Au: 2.211(3); Au–Cl: 2.277(1); C1–C2: 1.508(3); C1–C7: 1.522(9); C2–C7: 1.558(1); C2–C3: 1.514(10); C3–C4: 1.331(2); C5–C6: 1.410(1); C6–C7: 1.492(1); C1–P–C5: 94.1(5); C1–P–C4: 94.5(5); C4–P–C5: 95.8(5).

In the molecular structure of compound **4.41**, the P–C and C–C bonds in the polycyclic cage have similar bond lengths compared to the oxidized derivatives reported above. Moreover, the P–Au distance was found to be almost identical to the one found in complex **3.67**.

Finally, after proving the ability of 5-phosphasemibullvalenes to form stable coordination compounds with different metals, the di-π-methane rearrangement was also investigated for phosphabarrelenes in the coordination sphere of a transition metal. Obviously, a different precursor from the ones discussed above was needed, because metal-carbonyls might dissociate CO molecules and gold complexes tend to decompose upon UV irradiation. Therefore copper complex **3.71** was prepared (see Chapter 3) and was irradiated with UV light in THF (Scheme 60).

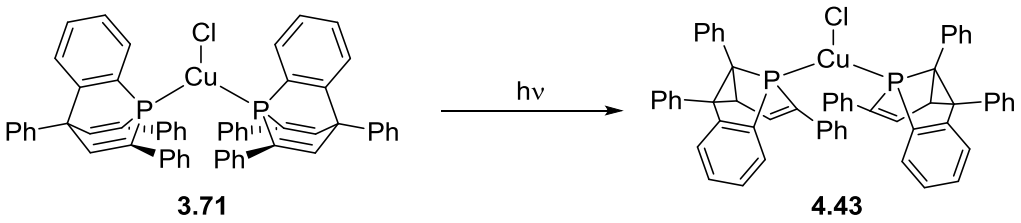

Scheme 60. Photoisomerization of **3.71** to **4.43**.

Gradually the broad resonance relative to the starting material disappears and a new, broad resonance appears at δ = 31.4 ppm. The ^{1}H NMR spectrum of the reaction mixture shows a single set of sharp signals in accordance with the quantitative formation of compound **4.43**, which was fully characterized by means of NMR spectroscopy.

An additional proof was obtained by photoisomerization of complex **3.72** in MeCN, reported in Scheme 61.

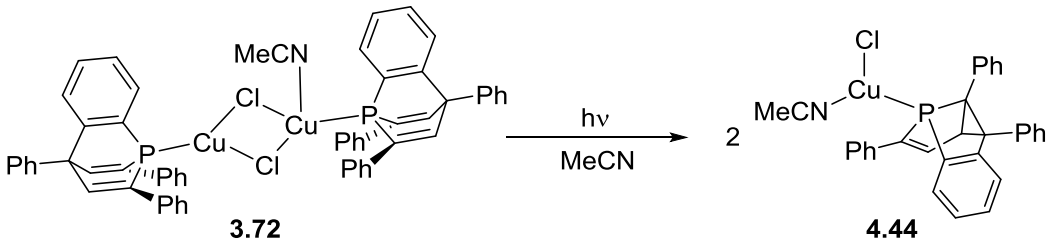

Scheme 61. Photoisomerization of **3.72** to **4.44**.

Interestingly, the dimer **3.72** undergoes photoisomerization and two equivalents of complex **4.44** are obtained, as confirmed by single crystal X-ray diffraction. The molecular structure in the crystal confirms the successful photoisomerization to the corresponding phosphasemibullvalene derivative, which is coordinated to a Cu(I) center together with a molecule of acetonitrile in a trigonal planar fashion (Figure 51). As in the case of the starting material, also **4.44** is rather insoluble and the characterization in solution is limited to ^{1}H NMR spectroscopy.

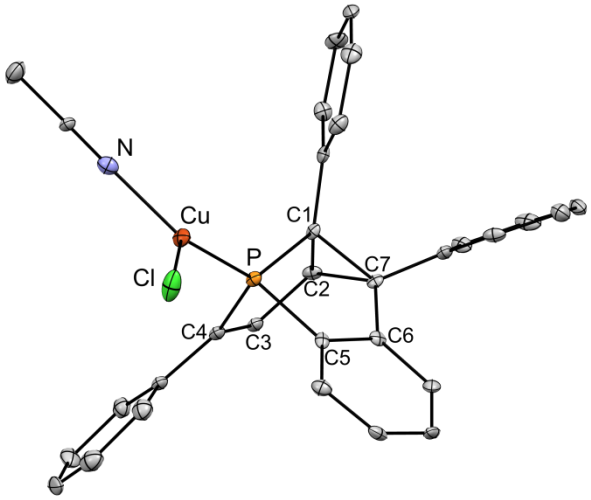

Figure 51. Molecular structure of **4.44** in the crystal. Displacement ellipsoids are shown at the 50% probability level. Hydrogen atoms are omitted for clarity. Selected bond lengths (Å) and angles (°): P–C1: 1.858(5); P–C4: 1.843(5); P–C5: 1.822(5); P–Cu: 2.172(1); Cu–Cl: 2.230(1); Cu–N: 1.977(4); C1–C2: 1.505(7); C1–C7: 1.551(6); C2–C7: 1.565(6); C2–C3: 1.476(7); C3–C4: 1.337(7); C5–C6: 1.405(6); C6–C7: 1.490(6); C1–P–C5: 92.5(2); C1–P–C4: 92.9(2); C4–P–C5: 95.8(2); P–Cu–Cl: 121.60(5); P–Cu–N: 133.3(1); Cl–Cu–N: 107.4(1).

After proving that the photoisomerization can be performed directly in a coordination compound, the photoisomerization of metal complexes containing ligand **3.1** was investigated, since **3.1** alone yielded multiple products upon direct irradiation. In theory, the π-backdonation from the filled metal orbitals to the phosphabarrelene could stabilize some of the BR2 species over the others. Unfortunately, the complexes reported for **3.1** (see Chapter 3) are not suitable for photoisomerization due to light-sensitivity or low stability. For this reason, an attempt was made to synthesize the complex [(**3.1**)$_2$Rh(CO)Cl], starting from [Rh(CO)$_2$Cl]$_2$ and 4 equivalents of phosphabarrelene **3.1** in DCM, in analogy to **3.61**. After addition of the solvent, the solution turned immediately dark and gas evolution was observed, indicating loss of CO. However, the ^{31}P{^{1}H} NMR spectrum showed several unidentified products. Single crystals suitable for X-ray analysis were obtained by slow evaporation of the solvent. Surprisingly, even though no UV irradiation was involved in the process, the crystallographic characterization of **4.45** shows two molecules of the phosphasemibullvalene **4.30** bound to a Rh(CO)Cl fragment, in a *trans* fashion (Figure 52). However, this reaction is still matter of investigation and was so far not reproduced.

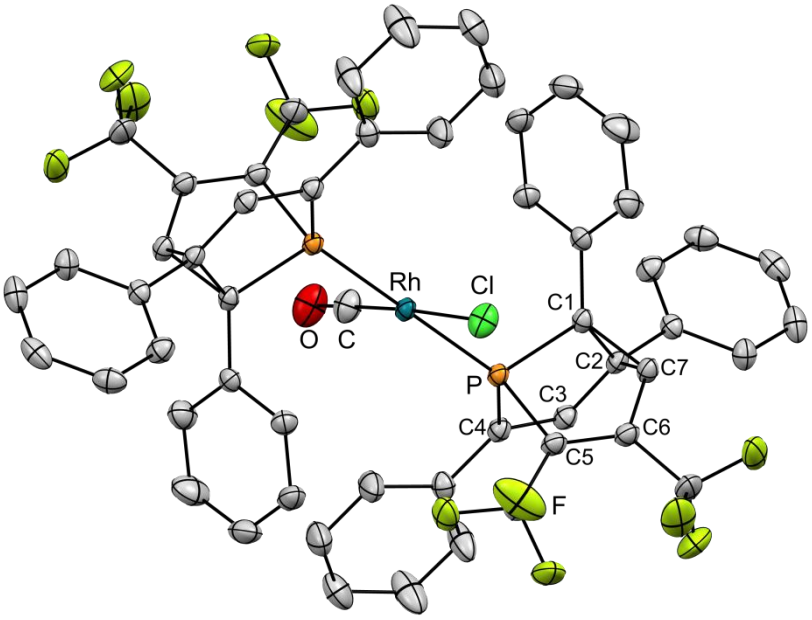

Figure 52. Molecular structure of **4.45** in the crystal. Displacement ellipsoids are shown at the 50% probability level. Hydrogen atoms are omitted for clarity. Selected bond lengths (Å) and angles (°): P–C1: 1.852(5); P–C4: 1.835(2); P–C5: 1.837(5); P–Rh: 2.288(5); Rh–Cl: 2.333(3); Rh–C: 1.808(8); C–O: 1.143(3); C1–C2: 1.531(7); C1–C7: 1.501(5); C2–C7: 1.598(5); C2–C3: 1.469(1); C3–C4: 1.358(1); C5–C6: 1.338(3); C6–C7: 1.466(1); C1–P–C5: 92.00(10); C1–P–C4: 94.05(10); C4–P–C5: 93.27(10); P–Rh–Cl: 96.39(10); P–Rh–C: 93.37(10).

4.3 Conclusions

The first 5-phosphasemibullvalene derivatives have been described, and a synthetic path for this new class of chiral molecules based on the skeleton of 2,4,6-triarylsubstituted phosphinines has been presented. Phosphabarrelenes, their oxidized derivatives and metal complexes undergo quantitative di-π-methane rearrangement upon irradiation with UV light. The reaction mechanism was investigated by means of DFT calculations, which are supported by several experiments, giving an insight in the selectivity of the reaction in the case of asymmetrically-substituted phosphabarrelenes. The substrate scope has been extended to differently substituted benzobarrelenes and the photoisomerization of trifluoromethyl-substituted molecules was investigated.

The oxidation of 5-phosphasemibullvalenes has been reported and some chalcogenide derivatives have been fully characterized.

Differently from other reported derivatives, 5-phosphasemibullvalenes proved to be thermally stable and suitable for coordination to metal centers. The first metal complexes have been

reported and fully characterized. Some of these complexes have been employed in catalytic transformations, which are described in the following chapter.

4.4 Experimental part

General remarks

Unless otherwise stated, all the experiments were performed under an inert argon atmosphere using modified Schlenk techniques or in a MBraun glovebox. All common chemicals were commercially available and were used as received. Dry or deoxygenated solvents were prepared using standard techniques or used from a MBraun solvent purification system. The NMR spectra were recorded on a JEOL ECX400 (400 MHz) spectrometer and chemical shifts are reported relative to the residual resonance in the deuterated solvents. IR spectra were measured on a Nicolet iS10 FTIR-ATR spectrometer by Thermo Scientific in the solid state and on a FT-IR spectrometer Vertex 70 by Bruker in dichloromethane. For reactions under UV irradiation, a UVP High intensity 100 Watt B-100AP Mercury Vapor Lamp without filter was used. HPLC equipment consisted of a Shimadzu LC-20 AD pump, a Shimadzu SPD-20 A UV/Vis detector and a Shimadzu CTO-20AC oven with column selector. Column and analysis specifications: Chiralpak IA (250x4.6 mm, particle size = 5 μm, purchased from Daicel), eluent = 2-propanol, column temperature = 25 °C, flow rate = 0.5 mL/min, λ=254 nm (UV detector), injection volume = 10 μL. The mass characterizations have been performed on an Agilent 6210 ESI-TOF instrument by Agilent Technologies, Santa Clara, CA, USA with standard settings of 5 L/min, 4 kV and 15 psi.

[2,10-diphenyl-4-tolyl-4H-1,4-ethenophosphinoline], (4.20)

The tolyl-barrelene was synthesized according to a literature procedure.[185,171] *o*-Fluorobromobenzene (2.07 g, 11.82 mmol) was added dropwise at rt to magnesium (0.287 g, 11.82 mmol) and *p*-tolylphosphinine (2.00 g, 5.91 mmol) in 20 mL of THF. The solution turned dark violet. After the addition the mixture was heated to reflux for 3 hours. After cooling, 2 mL of water were added and then the volatiles were removed. The residue was extracted with 100 mL of toluene and the organic phase was washed 3 times with 50 mL of

water. The aqueous phase was then extracted twice with 50 mL of toluene. The combined organic phases were dried and the solvent was removed *in vacuo*. The residue was dissolved in DCM and adsorbed on 50 g of silica gel, that was stored for one week under air. Afterwards the loaded silica was eluted with DCM through another silica pad (100 g). The solvent was finally evaporated *in vacuo* and the residue was recrystallized from hot methanol. Filtration, washing with cold methanol and drying *in vacuo* yielded the barrelene (0.337 g, 14%) as an off-white powder.

^{1}H NMR (acetone-d_6, 400 MHz): δ = 2.48 (s, 3H, Me), 6.56 (m, 1H), 7.05 (m, 2H), 7.28 (m, 2H), 7.37 (m, 4H), 7.48 (m, 2H), 7.79 (m, 7H), 8.23 (d, *J* = 6.1 Hz, 2H).

^{13}C{^{1}H} NMR (acetone-d_6, 101 MHz): δ = 21.1 (s), 64.7 (s), 125.0 (d, *J* = 13.2 Hz), 125.2 (d, *J* = 1.3 Hz), 126.7 (s), 126.8 (s), 128.1 (d, *J* = 1.6 Hz), 128.6 (d, *J* = 1.7 Hz), 129.5 (d, *J* = 1.1 Hz), 129.9 (s), 130.6 (s), 132.2 (s), 132.6 (s), 138.0 (s), 138.9 (s), 139.5 (d, *J* = 24.8 Hz), 141.9 (d, *J* = 11.2 Hz), 148.7 (d, *J* = 4.8 Hz), 153.2 (d, *J* = 15.6 Hz), 156.5 (d, *J* = 3.4 Hz).

^{31}P{^{1}H} NMR (acetone-d_6, 162 MHz): δ = -70.6 (s) ppm.

General procedure for the synthesis of 5-phosphasemibullvalenes

A solution of phosphabarrelene in THF (or DCM or toluene) in a J-Young NMR tube was exposed to UV light until full conversion, following the reaction by means of ^{31}P{^{1}H} NMR. The reaction time is dependent on the concentration, the solvent and the distance from the light source. During this process, the solution usually turns from colourless to yellow, due to residual grease impurities. Afterwards, the volatiles were removed, yielding the product as a pale-yellow foamy solid in quantitative yield.

Compound 4.19

^{1}H NMR (THF-d_8, 400 MHz): δ = 4.20 (m, 1H), 6.47 (dd, *J* = 7.4, 3.4 Hz, 1H), 6.75 (m, 1H), 7.18 (m, 15H), 7.43 (m, 1H), 7.61 (d, *J* = 8.3 Hz, 2H) ppm.

^{13}C{^{1}H} NMR (THF-d_8, 101 MHz): δ = 47.8 (d, *J* = 3.5 Hz), 60.4 (d, *J* = 8.9 Hz), 63.7 (d, *J* = 2.1 Hz), 124.2 (d, *J* = 1.7 Hz), 124.6 (s), 124.7 (s), 124.8 (s), 124.9 – 125.0 (m), 125.1 (s), 125.3 (d, *J* = 1.3 Hz), 125.4 (s), 125.7 (d, *J* = 2.1 Hz), 125.8 (s), 125.9 (s), 126.0 (s), 126.1 (s), 126.4 (s), 129.4 (s), 133.8 (d, *J* = 18 Hz), 136.3 (d, *J* = 23.2 Hz), 136.9 (s), 143.8 (d, *J* = 15.6 Hz), 146.6 (d, *J* = 3.1 Hz), 147.6 (d, *J* = 21.5 Hz) ppm.

^{31}P{^{1}H} NMR (THF-d_8, 162 MHz): δ = 33.1 (s) ppm.

Compound 4.21

^{1}H NMR (THF-d_8, 400 MHz): δ = 2.23 (s, 3H, CH_3), 4.16 (t, *J* = 3.2 Hz, 1H), 6.45 (dd, *J* = 7.4, 3.4 Hz, 1H), 6.73 (m, 1H), 7.09 (m, 12H), 7.25 (dd, *J* = 8.2, 6.8 Hz, 2H), 7.41 (m, 1H), 7.60 (d, *J* = 8.4 Hz, 2H) ppm.

^{13}C{^{1}H} NMR (THF-d_8, 101 MHz): δ = 20.1 (s), 49.6 (d, *J* = 3.4 Hz), 62.2 (d, *J* = 8.5 Hz), 65.2 (d, *J* = 2.2 Hz), 125.9 (d, *J* = 1.7 Hz), 126.4 (d, *J* = 7.7 Hz), 126.5 (s), 126.8 (d, *J* = 10.0 Hz), 127.1 (s), 127.2 (s), 127.6 (d, *J* = 2.3 Hz), 127.6 (s), 127.7 (s), 127.7 (s), 127.8 (s), 128.2 (s), 128.52(s), 131.0 (s), 135.5 (s), 135.7 (s), 136.2 (s), 138.2 (d, *J* = 22.9 Hz), 145.5 (d, *J* = 15.6 Hz), 148.7 (d, *J* = 3.0 Hz), 149.2 (d, *J* = 21.3 Hz) ppm.

^{31}P{^{1}H} NMR (THF-d_8, 162 MHz): δ = 32.4 (s) ppm.

Compound 4.26

^{1}H NMR (THF-d_8, 400 MHz): δ = -0.23 (d, *J* = 0.5 Hz, 9H, CH_3), -0.20 (d, *J* = 0.7 Hz, 9H, CH_3), 3.96 (d, *J* = 4.7 Hz, 1H), 6.55 (m, 2H), 6.89 (m, 3H), 7.03 (m, 2H), 7.15 (m, 3H), 7.28 (m, 2H), 7.50 (m, 1H), 7.76 (m, 1H) ppm.

^{13}C{^{1}H} NMR (THF-d_8, 101 MHz): δ = -1.6 (d, *J* = 4.2 Hz, CH_3), 1.5 (d, *J* = 5.0 Hz, CH_3), 48.1 (d, *J* = 36.2 Hz), 51.0 (d, *J* = 4.6 Hz), 73.1 (d, *J* = 1.7 Hz), 126.7 (d, *J* = 1.2 Hz), 126.8 (d, *J* = 6.9 Hz), 127.5 (d, *J* = 35.8 Hz), 127.9 (s), 128.7 (bs), 128.9 (bs), 129.0 (d, *J* = 0.7 Hz), 129.1 (bs), 141.4 (d, *J* = 4.2 Hz), 141.9 (d, *J* = 3.6 Hz), 142.1 (d, *J* = 45.5 Hz), 146.9 (s), 151.6 (d, *J* = 26.4 Hz), 160.4 (d, *J* = 3.6 Hz) ppm.

^{29}Si{^{1}H} NMR (79 MHz, THF-d_8): δ = -6.9 (d, $^{2}J_{P\text{-}Si}$ = 17.4 Hz), 1.1 (d, $^{2}J_{P\text{-}Si}$ = 10.5 Hz) ppm.

^{31}P{^{1}H} NMR (THF-d_8, 162 MHz): δ = 49.0 (s, $^{2}J_{P\text{-}Si}$ = 25.3, 34.0 Hz) ppm.

Reaction of 3.42 with UV light

This material was used for the next reaction without purification.

^{31}P{^{1}H} NMR (THF-d_8, 162 MHz): δ = 35.3 (s), 44.2 (s) ppm.

General procedure for the synthesis of 5-phosphasemibullvalene oxides

The compounds can be synthesized following one of two different procedures:

Method A: A solution of the given ligand (0.075 mmol) in 5 mL THF was left overnight with air contact. Afterwards the solution was concentrated to roughly 0.2 mL and the product was precipitated adding 3 mL of pentane. The liquid phase was then removed by decanting and the

solid was washed two more times with pentane. After drying in high vacuum, the product was obtained as a pale-yellow powder.

Method B: A solution of phosphabarrelene oxide in THF was exposed to UV light and the reaction was followed by ^{31}P NMR spectroscopy until completion. The solution slowly turned from colourless to pale-yellow. Afterwards the volatiles were removed, yielding the product as an off-white powder in quantitative yield.

Compound 4.35

Yield = 42%.

^{1}H NMR (THF-d_8, 400 MHz): δ = 4.39 (dd, *J* = 10.1, 4.1 Hz, 1H), 6.70 (dd, *J* = 39.8, 4.1 Hz, 1H), 6.85 (m, 1H), 7.20 (m, 15H), 7.66 (m, 1H), 7.81 (d, *J* = 8.0 Hz, 2H) ppm.

^{13}C{^{1}H} NMR (THF-d_8, 101 MHz): δ = 46.8 (d, *J* = 11.2 Hz), 61.5 (s), 65.7 (d, *J* = 5.8 Hz), 126.1 (d, *J* = 8.0 Hz), 127.8 (d, *J* = 4.6 Hz), 127.8 (s), 127.8 (s), 128.3 (d, *J* = 10.6 Hz), 128.5 (s), 128.7 (d, *J* = 11.0 Hz), 128.8 (s), 129.2 (s), 129.3 (s), 129.5 (s), 129.8 (d, *J* = 4.6 Hz), 132.3 (d, *J* = 2.4 Hz), 133.2 (d, *J* = 3.7 Hz), 133.9 (d, *J* = 10.7 Hz), 138.9 (m), 139.9 (s), 143.2 (d, *J* = 23.5 Hz), 144.5 (d, *J* = 90.5 Hz) ppm.

^{31}P{^{1}H} NMR (THF-d_8, 162 MHz): δ = 52.5 ppm.

General procedure for the synthesis of 5-phosphasemibullvalene sulfides

The compounds can be synthesized following one of two different procedures:

Method A: A solution of phosphabarrelene (0.075 mmol) in 2 mL of toluene was refluxed overnight together with 1.1 eq. of elemental sulfur and a 5-fold excess of DBU. Afterwards the volatiles were removed and the solution was eluted through a plug of silica (4 cm) with a 3:2 mixture of DCM/pentane. The volatiles where again removed and the remaining solid was washed a couple of times with pentane. After drying in high vacuum, the product was obtained as a white powder.

Method B: A solution of phosphabarrelene sulfide in THF was exposed to UV light and the reaction was followed by ^{31}P NMR spectroscopy until completion. The solution slowly turned from colourless to pale-yellow. Afterwards the volatiles were removed, yielding the product as an off-white powder in quantitative yield.

Compound 4.36

Yield = 71%.

^{1}H NMR (THF-d_8, 400 MHz): δ = 4.48 (dd, *J* = 9.7, 4.1 Hz, 1H), 6.65 (dd, *J* = 39.0, 4.0 Hz, 1H), 6.85 (m, 1H), 6.89 (m, 1H), 7.17 (m, 6H), 7.30 (m, 9H), 7.70 (m, 1H), 7.79 (d, *J* = 7.9 Hz, 2H) ppm.

^{13}C{^{1}H} NMR (THF-d_8, 101 MHz): δ = 47.2 (d, *J* = 9.0 Hz), 64.8 (m), 65.5 (s), 126.0 (d, *J* = 9.8 Hz), 128.2 (m), 128.4 (d, *J* = 11.2 Hz), 128.5 (d, *J* = 4.3 Hz), 128.6 (s), 129.1 (d, *J* = 1.7 Hz), 130.8 (d, *J* = 4.5 Hz), 131.8 (d, *J* = 21.5 Hz), 132.0 (bs), 132.0 (d, *J* = 2.5 Hz), 132.8 (d, *J* = 4.8 Hz), 133.9 (d, *J* = 11.3 Hz), 138.6 (d, *J* = 1.9 Hz), 141.2 (d, *J* = 82.5 Hz), 144.1 (d, *J* = 71.7 Hz), 144.4 (d, *J* = 19.5 Hz) ppm.

^{31}P{^{1}H} NMR (THF-d_8, 162 MHz): δ = 65.8 ppm.

General procedure for the synthesis of 5-phosphasemibullvalene selenides

The compounds can be synthesized following one of two different procedures:

Method A: To a solution of the appropriate phosphasemibullvalene in toluene, an excess of grey selenium was added and the solution was heated up to reflux overnight. Afterwards the solution was filtered over celite and the solvent was removed *in vacuo*, yielding the product as an off-white powder quantitatively.

Method B: A solution of phosphabarrelene selenide in THF was exposed to UV light and the reaction was followed by ^{31}P NMR spectroscopy until completion. The solution slowly turned from colourless to pale-yellow. Afterwards the volatiles were removed, yielding the product as an off-white powder in quantitative yield.

Compound 4.37

^{1}H NMR (THF-d_8, 400 MHz): δ = 4.46 (dd, *J* = 9.3, 4.1 Hz, 1H), 6.63 (dd, *J* = 38.0, 4.0 Hz, 1H), 6.87 (m, 1H), 7.24 (m, 15H), 7.65 (dd, *J* = 10.9, 6.9 Hz, 1H), 7.76 (m, 2H) ppm.

^{13}C{^{1}H} NMR (THF-d_8, 101 MHz): δ = 48.1 (d, *J* = 7.9 Hz), 65.0 (s), 65.2 (d, *J* = 4.2 Hz), 68.3 (s), 126.6 (d, *J* = 10.6 Hz), 128.5 (d, *J* = 2.1 Hz), 128.6 (m), 128.7 (m), 128.8 (s), 129.0 (s), 129.2 (s), 131.2 (d, *J* = 4.5 Hz), 132.1 (m), 132.6 (d, *J* = 19.5 Hz), 133.3 (d, *J* = 5.5 Hz), 134.0 (d, *J* = 11.8 Hz), 138.6 (d, *J* = 1.6 Hz), 141.0 (d, *J* = 73.6 Hz), 143.6 (d, *J* = 61.6 Hz), 145.3 (d, *J* = 17.2 Hz) ppm.

^{31}P{^{1}H} NMR (THF-d_8, 162 MHz): δ = 57.2 (s, $^{1}J_{P\text{-}Se}$ = 824.9 Hz) ppm.

Table 11. Enantiomeric resolution of **4.37**.

Peak	Retention time (min)	Area (%)
1	14.29	50.15
2	15.92	49.85

Compound 4.22

^{1}H NMR ($CDCl_3$, 400 MHz): δ = 2.26 (s, 3H), 4.25 (dd, *J* = 9.3, 4.0 Hz, 1H), 7.04 (d, *J* = 7.9 Hz, 2H), 7.27 (m, 15H), 7.72 (m, 3H) ppm.

^{13}C{^{1}H} NMR ($CDCl_3$, 101 MHz): δ = 21.1 (d, *J* = 1.1 Hz), 47.2 (d, *J* = 8.2 Hz), 63.4 (s), 63.8 – 64.1 (m), 125.3 (s), 125.7 (d, *J* = 10.6 Hz), 127.7 (d, *J* = 5.4 Hz), 127.8 (s), 128.0 (d, *J* = 2.2 Hz), 128.0 (s), 128.1 (d, *J* = 1.6 Hz), 128.4 (m), 129.1 (d, *J* = 7.4 Hz), 130.1 (t, *J* = 4.2 Hz), 130.5 (m), 131.7 (d, *J* = 5.3 Hz), 134.0 (s), 137.6 (s), 139.0 (d, *J* = 74.1 Hz), 142.6 (d, *J* = 61.7 Hz), 144.2 (d, *J* = 17.6 Hz) ppm.

^{31}P{^{1}H} NMR ($CDCl_3$, 162 MHz): δ = 57.5 (s, $^{1}J_{P\text{-}Se}$ = 805.1 Hz) ppm.

Compound 4.27

^{1}H NMR (THF-d_8, 400 MHz): δ = -0.10 (s, 9H, CH_3), -0.09 (s, 9H, CH_3), 4.14 (d, *J* = 11.7 Hz, 1H), 6.30 (bs, 1H), 6.94 (bs, 4H), 7.07 (m, 2H), 7.20 (m, 2H), 7.40 (tdd, *J* = 7.5, 3.6, 1.1 Hz, 1H), 7.50 (m, 2H), 7.68 (m, 1H), 7.81 (dd, *J* = 7.6, 2.7, 1H) ppm.

^{13}C{^{1}H} NMR (THF-d_8, 101 MHz): δ = -1.1 (d, *J* = 1.8 Hz, CH_3), 1.3 (d, *J* = 1.9 Hz, CH_3), 49.9 (d, *J* = 2.1 Hz), 51.1 (d, *J* = 25.9 Hz), 71.6 (d, *J* = 11.1 Hz), 127.4 (d, *J* = 9.6 Hz), 127.5 (d, *J* = 9.2 Hz), 127.8 (d, *J* = 10.9 Hz), 127.9 (s), 128.1 (bs), 128.1 (s), 128.7 (s), 129.0 (d, *J* = 0.7 Hz), 130.3 (d, *J* = 2.3 Hz), 131.8 (d, *J* = 2.7 Hz), 133.1 (s), 137.6 (d, *J* = 22.5 Hz), 140.1 (d, *J* = 21.4 Hz), 140.5 (d, *J* = 6.5 Hz), 142.3 (d, *J* = 21.2 Hz), 144.4 (d, *J* = 66.5 Hz), 161.3 (d, *J* = 7.5 Hz) ppm.

^{29}Si{^{1}H} NMR (79 MHz, THF-d_8): δ = -6.9 (d, $^{2}J_{P\text{-}Si}$ = 17.4 Hz), 1.1 (d, $^{2}J_{P\text{-}Si}$ = 10.5 Hz) ppm.

^{31}P{^{1}H} NMR (THF-d_8, 162 MHz): δ = 69.1 (s, $^{2}J_{P\text{-}Si}$ = 10.3 Hz, $^{1}J_{P\text{-}Se}$ = 784.3 Hz) ppm.

Compounds 4.25

^{1}H NMR (THF-d_8, 400 MHz): δ = 1.93 (d, *J* = 14.1 Hz, 3H, CH_3), 4.11 (dd, *J* = 9.5, 3.7 Hz, 1H), 6.06 (ddd, *J* = 40.2, 3.7, 1.7 Hz, 1H), 6.88 (dd, *J* = 7.3, 3.4 Hz, 1H), 7.20 (m, 10H), 7.35 (tt, *J* = 7.4, 1.6 Hz, 1H), 7.43 (tdd, *J* = 7.4, 3.6, 1.1 Hz, 1H), 7.74 (ddt, *J* = 10.7, 7.6, 0.7 Hz, 1H) ppm.

$^{13}C\{^{1}H\}$ NMR (THF-d_8, 101 MHz): 12.6 (d, J = 14.1 Hz), 47.0 (d, J = 9.6 Hz), 62.9 (d, J = 60.4 Hz), 63.3 (d, J = 3.8 Hz), 125.3 (d, J = 10.5 Hz), 127.7 (s), 127.8 (m), 127.9 (d, J = 15.4 Hz), 128.1 (s), 128.3 (s), 129.6 (d, J = 4.6 Hz), 129.8 (d, J = 20.0 Hz), 130.9 (s), 131.4 (d, J = 2.5 Hz), 131.7 (d, J = 5.3 Hz), 137.1 (d, J = 1.4 Hz), 139.6 (d, J = 72.6 Hz), 141.2 (d, J = 62.1 Hz), 143.8 (d, J = 17.4 Hz).

$^{31}P\{^{1}H\}$ NMR (THF-d_8, 162 MHz): δ = 60.3 (s, $^{1}J_{P\text{-}Se}$ = 818.1 Hz) ppm.

Compound 4.38

A solution of **4.19** (30 mg, 0.075 mmol) in THF was added dropwise to a solution of $[W(CO)_5(THF)]$ (1 eq.) and heated up to reflux for t = 3 h. Afterwards the volatiles were removed, yielding the product as a pale yellow solid in quantitative yield.

^{1}H NMR (THF-d_8, 400 MHz): δ = 4.45 (dd, J = 6.5, 3.7 Hz, 1H), 6.46 (dd, J = 22.9, 3.7 Hz, 1H), 6.96 (d, J = 7.8 Hz, 1H), 7.22 (m, 12H), 7.39 (m, 1H), 7.41 (m, 1H), 7.47 (m, 3H), 7.97 (t, J = 8.0 Hz, 1H) ppm.

$^{13}C\{^{1}H\}$ NMR (THF-d_8, 101 MHz): δ = 51.2 (d, J = 2.5 Hz), 65.5 (s), 68.4 (s), 69.9 (d, J = 34.1 Hz), 128.1 (d, J = 14.7 Hz), 128.5 (s), 128.7 (d, J = 9.6 Hz), 128.8 (s), 128.9 (s), 129.0 (d, J = 4.9 Hz), 129.1 (s), 129.2 (d, J = 2.6 Hz), 129.3 (s), 129.5 (d, J = 1.5 Hz), 129.7 (d, J = 4.7 Hz), 131.4 (s), 131.8 (d, J = 3.2 Hz), 131.9-132.5 (bm), 133.9 (d, J = 7.2 Hz), 136.7 (d, J = 12.0 Hz), 137.0 (d, J = 14.0 Hz), 138.9 (s), 145.9 (d, J = 35.1 Hz), 148.4 (d, J = 5.2 Hz), 148.6 (d, J = 26.9 Hz), 196.4 (d, $^{2}J_{C\text{-}P}$ = 7.3 Hz, $^{1}J_{C\text{-}W}$ = 124.8 Hz, CO_{cis}), 198.9 ppm (d, $^{2}J_{C\text{-}P}$ = 24.2 Hz, CO_{trans}).

$^{31}P\{^{1}H\}$ NMR (THF-d_8, 162 MHz): δ = 61.6 (s, $^{1}J_{P\text{-}W}$ = 251.1 Hz) ppm.

IR (solid state): 2071 (m); 1982 (w); 1924 (sh); 1908 (s) cm^{-1}.

General procedure for the synthesis of $[(L)Ni(CO)_3]$ complexes

Caution: $[Ni(CO)_4]$ is highly toxic and potentially carcinogenic. It can be absorbed through the skin or inhaled due to its high volatility. Vapors of $[Ni(CO)_4]$ can autoignite. All manipulations must be done with extreme care in a well-ventilated fumehood.

In a J-Young NMR tube 0.6 mL of THF containing the appropriate ligand were degassed by freeze and thaw technique. Afterwards, an excess of $[Ni(CO)_4]$ was condensed in the same tube using a condensation line. The tube was slowly warmed up to room temperature, and the reaction progress was monitored by ^{31}P NMR spectroscopy, degassing the tubes until full conversion. The volatiles were removed *in vacuo*, yielding the product quantitatively. IR spectra were measured in DCM.

Compound 4.39

^{1}H NMR (THF-d_8, 400 MHz): δ = 4.37 (dd, *J* = 6.1, 3.6 Hz, 1H), 6.42 (dd, *J* = 19.4, 3.5 Hz, 1H), 6.91 (m), 7.19 (m, 13H), 7.43 (m, 4H), 7.63 (m, 1H) ppm.

^{13}C{^{1}H} NMR (THF-d_8, 101 MHz): δ = 50.4 (s), 64.0 (s), 65.6 (d, *J* = 28.2 Hz), 67.1 (s), 126.2 (s), 126.3 (s), 127.0 (s), 127.1 (m), 127.4 (s), 127.5 (d, *J* = 5.6 Hz), 127.7 (d, *J* = 3.5 Hz), 127.9 (m), 135.1 (d, *J* = 15.1 Hz), 136.0 (d, *J* = 14.5 Hz), 138.1 (s), 144.0 (d, *J* = 26.7 Hz), 146.6 (d, *J* = 17.8 Hz), 147.0 (d, *J* = 2.7 Hz), 195.0 (s, CO) ppm.

^{31}P{^{1}H} NMR (THF-d_8, 162 MHz): δ = 73.9 (s) ppm.

IR (DCM): 2074.2 (m), 2001.6 (bs) cm^{-1}.

Compound 4.40

^{31}P{^{1}H} NMR (No solvent, 162 MHz): δ = 75.3 (s) ppm.

IR (DCM): 2069.0 (m), 1995.4 (bs) cm^{-1}.

General procedure for the synthesis of [(L)AuCl] complexes

A solution of the appropriate ligand (0.075 mmol) in DCM or THF was added dropwise to a solution of [AuCl(SMe$_2$)] (1 eq.) and stirred for t = 1 h at room temperature. Afterwards the solvent was removed, and the residue was dried thoroughly in high vacuum, yielding the product as a pale yellow solid in quantitative yield. To remove completely dimethylsulfide, the product was dissolved in the smallest amount of DCM and then precipitated using pentane, subsequently removing the volatiles and drying thoroughly.

Compound 4.41

^{1}H NMR (THF-d_8, 400 MHz): δ = 4.60 (dd, *J* = 8.3, 3.7 Hz, 1H), 6.79 (dd, *J* = 29.5, 3.7 Hz, 1H), 6.91 (m, 1H), 7.16 (m, 6H), 7.35 (m, 9H), 7.79 (m, 3H) ppm.

^{13}C{^{1}H} NMR (THF-d_8, 101 MHz): δ = 50.5 (d, *J* = 4.6 Hz), 64.7 (d, *J* = 55.4 Hz), 68.4 (s), 128.2 (d, *J* = 14.4 Hz), 128.4 (d, *J* = 7.7 Hz), 128.8 (d, *J* = 1.9 Hz), 128.8 (s), 129.0 (d, *J* = 11.1 Hz), 129.3 (s), 129.4 (d, *J* = 6.7 Hz), 129.4 (d, *J* = 0.9 Hz), 129.6 (d, *J* = 1.0 Hz), 129.8 (s), 129.9 (d, *J* = 6.0 Hz), 132.1 (s), 132.2 (d, *J* = 2.2 Hz), 133.4 (d, *J* = 11.5 Hz), 133.9 (d, *J* = 13.2 Hz), 135.1 (d, *J* = 10.1 Hz), 138.1 (d, *J* = 1.8 Hz), 138.9 (d, *J* = 55.6 Hz), 143.6 (d, *J* = 46.3 Hz), 147.6 (d, *J* = 10.0 Hz) ppm.

^{31}P{^{1}H} NMR (THF-d_8, 162 MHz): δ = 63.7 (s) ppm.

Compound 4.42

^{1}H NMR (THF-d_8, 400 MHz): δ = -0.06 (s, 9H, CH_3), -0.05 (s, 9H, CH_3), 4.30 (d, *J* = 10.9 Hz, 1H), 6.59 (bs, 2H), 6.97 (m, 3H), 7.11 (m, 2H), 7.24 (m, 3H), 7.41 (m, 1H), 7.47 (m, 1H), 7.55 (tdd, *J* = 7.5, 1.8, 1.2 Hz, 1H), 7.75 (m, 1H), 7.92 (m, 1H) ppm.

^{13}C{^{1}H} NMR (THF-d_8, 101 MHz): δ = -1.4 (d, *J* = 2.4 Hz, CH_3), 1.6 (d, *J* = 2.8 Hz, CH_3), 49.5 (d, *J* = 16.6 Hz), 51.6 (d, *J* = 3.2 Hz), 73.5 (d, *J* = 7.5 Hz), 128.61(bs), 128.3 (s), 128.3 (bs), 128.3 (s), 128.4 (s), 128.4 (bs), 128.6 (s), 129.0 (s), 129.1 (s), 129.2 (s), 130.4 (s), 132.1 (d, *J* = 2.3 Hz), 133.0 (s), 135.2 (d, *J* = 9.0 Hz), 139.7 (d, *J* = 17.6 Hz), 140.0 (d, *J* = 6.1 Hz), 143.1 (d, *J* = 50.5 Hz), 144.5 (d, *J* = 13.8 Hz), 164.4 (d, *J* = 1.9 Hz) ppm.

^{29}Si{^{1}H} NMR (79 MHz, THF-d_8): δ = -8.1 (d, $^{2}J_{P\text{-}Si}$ = 18.6 Hz), -0.3 (d, $^{2}J_{P\text{-}Si}$ = 15.9 Hz) ppm.

^{31}P{^{1}H} NMR (THF-d_8, 162 MHz): δ = 67.3 (s, with ^{29}Si satellites, $^{2}J_{P\text{-}Si}$ = 16.1, 19.2 Hz) ppm.

Compound 4.43

A solution of **3.71** (30 mg, 0.066 mmol) in THF in a NMR tube was exposed to UV light for t = 6 h, and was shaken from time to time. The solution turned from colourless to pale-yellow. Afterwards the volatiles were removed, yielding the product as a pale yellow solid in quantitative yield.

^{1}H NMR (THF-d_8, 400 MHz): δ = 4.33 (dd, *J* = 5.5, 3.5 Hz, 1H), 6.54 (dd, *J* = 18.5, 3.6 Hz, 1H), 6.77 (d, *J* = 7.7 Hz, 1H), 6.89 (m, 4H), 7.11 (m, 7H), 7.26 (m, 4H), 7.89 (d, *J* = 7.5 Hz, 2H), 7.94 (m, 1H) ppm.

^{13}C{^{1}H} NMR (THF-d_8, 101 MHz): δ = 49.5 (s), 64.1 (d, *J* = 28.5 Hz), 66.5 (s), 127.4 (s), 128.0 (s), 128.1 (s), 128.2 (d, *J* = 3.5 Hz), 128.4 (s), 128.8 (m), 129.2 (m), 129.7 (d, *J* = 6.6 Hz), 130.0 (s), 130.2 (s), 132.2 (s), 135.0 (d, *J* = 15.0 Hz), 136.3 (d, *J* = 15.1 Hz), 139.3 (s), 142.8 (d, *J* = 27.4 Hz), 147.0 (d, *J* = 17.4 Hz), 148.1 (d, *J* = 2.3 Hz) ppm.

^{31}P{^{1}H} NMR (THF-d_8, 162 MHz): δ = 31.4 (bs) ppm.

Compound 4.44

A solution of **3.72** (30 mg, 0.029 mmol) in MeCN in a NMR tube was exposed to UV light and the reaction was followed by means of ^{1}H NMR until full conversion. Crystals suitable for X-ray diffraction were found in the NMR tube.

^{1}H NMR (MeCN-d_3, 400 MHz): δ = 4.32 (dd, *J* = 5.5, 3.6 Hz, 1H), 6.58 (dd, *J* = 17.3, 3.6 Hz, 1H), 6.80 (m, 1H), 7.22 (m, 15H), 7.67 (m, 1H), 7.75 (m, 1H) ppm.

4.4.1 DFT Calculations

Density functional calculations were performed with the Gaussian09 suite of software, revision D.01,[260] using the (U)M06-2X functional,[261] the 6-31G(d)** basis set.[262–264] All geometries have been computed and optimized in the gas phase. The stationary points were characterized by full vibration frequencies calculations as minima (no imaginary frequency) or transition states (one single imaginary frequency). When necessary, final proof for the position of the transition state was obtained by an IRC calculation. For more informations, see attachments.

4.4.2 X-ray crystal structure determination

X-ray crystal structure determination of 4.22

Crystals suitable for X-ray diffraction were obtained by slow evaporation from a saturated solution in toluene. *Crystallographic data*: $C_{30}H_{23}PSe$, *F*w 493.41, 0.34×0.30×0.10 mm^3, colourless block, triclinic, $P\bar{1}$, a = 9.4028(2), b = 11.0259(2), c = 13.3343(2)Å, α = 81.0914(6)°, β = 87.5909(7)°, γ = 72.4935(7)°, V = 1302.48(4) $Å^3$, Z = 2, Dx = 1.258 gcm^{-3}, μ = 1.517 mm^{-1}. 22643 reflections were measured by using a Bruker-AXS smart CCD area detector diffractometer (MoKα radiation, λ = 0.71073 Å)[155] up to a resolution of $(\sin\theta/\lambda)_{max}$ = 0.61 $Å^{-1}$ at a temperature of T = 100 K. The reflections were corrected for absorption and scaled on the basis of multiple measured reflections by using the SADABS program[155] (0.65–0.75 correction range). 4721 reflections were unique (R_{int} = 0.030). Using ShelXle[158], the structures were solved with SHELXS-2014 by using direct methods and refined with SHELXL-2014 on *F*2 for all reflections.[156] Non-hydrogen atoms were refined by using anisotropic displacement parameters. The positions of the hydrogen atoms were calculated for idealized positions. 290 parameter were refined without restraints. R_1 = 0.026 for 4721 reflections with $I>2\sigma(I)$ and wR_2 = 0.066 for 5011 reflections, S = 1.065, residual electron density was between -0.45 and 0.36 $eÅ^{-3}$. Geometry calculations and checks for higher symmetry were performed with the PLATON program.[157]

SQUEEZE RESULTS (APPEND TO CIF)[226]
Note: Data are Listed for all Voids in the P1 Unit Cell
i.e. Centre of Gravity, Solvent Accessible Volume,

```
# Recovered number of Electrons in the Void and
# Details about the Squeezed Material
  _platon_squeeze_void_nr
  _platon_squeeze_void_average_x
  _platon_squeeze_void_average_y
  _platon_squeeze_void_average_z
  _platon_squeeze_void_volume
  _platon_squeeze_void_count_electrons
  _platon_squeeze_void_content
   1  0.000  0.500  0.500       189       46 ' '
_platon_squeeze_details
```

The general procedure has been described in more detail as the "BYPASS procedure".[227]

X-ray crystal structure determination of 4.25

Crystals suitable for X-ray diffraction were obtained by slow evaporation from a saturated solution in toluene. *Crystallographic data*: $C_{24}H_{19}PSe$, *F*w = 417.32, 0.23×0.19×0.06 mm^3, colourless block, monoclinic, $P2_1/c$, a = 16.8430(3), b = 18.0440(3), c = 13.2789(11) Å, $\alpha = 90°$, β = 107.7201(6)°, $\gamma = 90°$, V = 3844.19(11) $Å^3$, Z = 8, Dx = 1.442 gcm^{-3}, μ = 2.041 mm^{-1}. 46767 reflections were measured by using a Bruker-AXS smart CCD area detector diffractometer (MoKα radiation, λ = 0.71073 Å)[155] up to a resolution of $(\sin\theta/\lambda)_{max}$ = 0.61 $Å^{-1}$ at a temperature of T = 100 K. The reflections were corrected for absorption and scaled on the basis of multiple measured reflections by using the SADABS program[155] (0.66–0.79 correction range). 6493 reflections were unique (R_{int} = 0.048). Using ShelXle[158], the structures were solved with SHELXS-2014 by using direct methods and refined with SHELXL-2014 on *F*2 for all reflections.[156] Non-hydrogen atoms were refined by using anisotropic displacement parameters. The positions of the hydrogen atoms were calculated for idealized positions. 471 parameter were refined without restraints. R_1 = 0.029 for 6493 reflections with $I>2\sigma(I)$ and wR_2 = 0.064 for 7886 reflections, S = 1.016, residual electron density was between -0.40 and 0.37 $eÅ^{-3}$. Geometry calculations and checks for higher symmetry were performed with the PLATON program.[157]

X-ray crystal structure determination of 4.27

Crystals suitable for X-ray diffraction were obtained by slow evaporation from a saturated solution in toluene. *Crystallographic data*: $C_{29}H_{33}PSeSi_2$, *F*w = 547.66, 0.26×0.20×0.18 mm^3,

colourless block, orthorhombic, $P2_12_12_1$, a = 9.9355(3), b = 14.2567(3), c = 19.3825(6) Å, α = 90°, β = 90°, γ = 90°, V = 2745.48(13) Å^3, Z = 4, Dx = 1.325 gcm^{-3}, μ = 1.529 mm^{-1}. 14832 reflections were measured by using a Bruker-AXS smart CCD area detector diffractometer (MoKα radiation, λ = 0.71073 Å)[155] up to a resolution of $(\sin\theta/\lambda)_{max}$ = 0.63 Å^{-1} at a temperature of T = 100 K. The reflections were corrected for absorption and scaled on the basis of multiple measured reflections by using the SADABS program[155] (0.75–0.90 correction range). 4636 reflections were unique (R_{int} = 0.073). Using ShelXle[158], the structures were solved with SHELXS-2014 by using direct methods and refined with SHELXL-2014 on $F2$ for all reflections.[156] Non-hydrogen atoms were refined by using anisotropic displacement parameters. The positions of the hydrogen atoms were calculated for idealized positions. 304 parameter were refined without restraints. R_1 = 0.044 for 4687 reflections with $I>2\sigma(I)$ and wR_2 = 0.084 for 5564 reflections, S = 1.008, residual electron density was between -0.48 and 1.08 eÅ^{-3}. Geometry calculations and checks for higher symmetry were performed with the PLATON program.[157] (Flack x parameter = 0.042(8)).[265]

X-ray crystal structure determination of 4.35

Crystals suitable for X-ray diffraction were obtained by slow evaporation from a saturated solution in toluene. *Crystallographic data*: $C_{29}H_{21}OP$, Fw = 416.43, 0.44×0.21×0.13 mm^3, colourless block, orthorhombic, $P2_12_12_1$, a = 8.31950(10), b = 12.1199(2), c = 42.2796(8)Å, α = 90°, β = 90°, γ = 90°, V = 4263.12(12) Å^3, Z = 8, Dx = 1.298 gcm^{-3}, μ = 0.148 mm^{-1}. 21816 reflections were measured by using a Bruker-AXS smart CCD area detector diffractometer (MoKα radiation, λ = 0.71073 Å)[155] up to a resolution of $(\sin\theta/\lambda)_{max}$ = 0.61 Å^{-1} at a temperature of T = 100 K. The reflections were corrected for absorption and scaled on the basis of multiple measured reflections by using the SADABS program[155] (0.89–0.96 correction range). 7445 reflections were unique (R_{int} = 0.035). Using ShelXle[158], the structures were solved with SHELXS-2014 by using direct methods and refined with SHELXL-2014 on $F2$ for all reflections.[156] Non-hydrogen atoms were refined by using anisotropic displacement parameters. The positions of the hydrogen atoms were calculated for idealized positions. 543 parameter were refined without restraints. R_1 = 0.063 for 7445 reflections with $I>2\sigma(I)$ and wR_2 = 0.147 for 8076 reflections, S = 1.074, residual electron density was between -0.57 and 0.85 eÅ^{-3}. Geometry calculations and checks for higher symmetry were performed with the PLATON program.[157] (Flack x parameter = 0.59(18)).[265]

X-ray crystal structure determination of 4.36

Crystals suitable for X-ray diffraction were obtained by slow evaporation from a saturated solution in toluene. *Crystallographic data*: $C_{29}H_{21}PS$, C_7H_8, *F*w = 524.62, 0.31×0.29×0.08 mm^3, colourless platelet, monoclinic, $P2_1/c$, a = 15.7212(3), b = 13.3889(2), c = 13.5092(3) Å, α = 90°, β = 96.1249(9)°, γ = 90°, V = 2827.31(9) $Å^3$, Z = 4, Dx = 1.232 gcm^{-3}, μ = 0.19 mm^{-1}. 33341 reflections were measured by using a Bruker-AXS smart CCD area detector diffractometer (MoKα radiation, λ = 0.71073 Å)[155] up to a resolution of $(\sin\theta/\lambda)_{max}$ = 0.63 $Å^{-1}$ at a temperature of T = 100 K. The reflections were corrected for absorption and scaled on the basis of multiple measured reflections by using the SADABS program[155] (0.85–0.97 correction range). 4792 reflections were unique (R_{int} = 0.049). Using ShelXle[158], the structures were solved with SHELXS-2014 by using direct methods and refined with SHELXL-2014 on *F*2 for all reflections.[156] Non-hydrogen atoms were refined by using anisotropic displacement parameters. The positions of the hydrogen atoms were calculated for idealized positions. 344 parameter were refined without restraints. R_1 = 0.036 for 4792 reflections with $I>2\sigma(I)$ and wR_2 = 0.089 for 5802 reflections, S = 1.029, residual electron density was between -0.32 and 0.40 $eÅ^{-3}$. Geometry calculations and checks for higher symmetry were performed with the PLATON program.[157]

X-ray crystal structure determination of 4.37 CCDC - 1438074

Crystals suitable for X-ray diffraction were obtained by slow evaporation from a saturated solution in toluene. *Crystallographic data*: $C_{29}H_{21}PSe$; *F*w=479.39; 0.38×0.20×0.07 mm^3; colourless block, triclinic; P-1; a= 9.4639(2), b= 10.1522(2), c=14.1214(3) Å; α=77.6074(8)°, β=86.1247(9), γ=71.6074(7)°; V=1257.47(5) $Å^3$; Z=2; Dx=1.266 gcm^{-3}; μ=1.569 mm^{-1}. 23201 reflections were measured by using a D8 Venture, Bruker Photon CMOS Detector (MoKα radiation; λ = 0.71073 Å)[155] up to a resolution of $(\sin\theta/\lambda)_{max}$= 0.60 $Å^{-1}$ at a temperature of T = 100.0 K. 74381 reflections were unique (R_{int} = 0.054). The structures were solved with SHELXS-2013 by using direct methods and refined with SHELXL-2013 on *F*2 for all reflections.[156] Non-hydrogen atoms were refined by using anisotropic displacement parameters. The positions of the hydrogen atoms were calculated for idealized positions. 280 parameter were refined with one restraint. R_1 = 0.033 for 4381 reflections with $I>2\sigma(I)$ and wR_2 = 0.076 for 5154 reflections, S = 1.029, residual electron density was between -0.31 and 0.45 $eÅ^{-3}$. Geometry calculations and checks for

higher symmetry were performed with the PLATON program.[157] The hkl were squeezed with PLATON, because the solvents were not identified.[226]

SQUEEZE RESULTS (APPEND TO CIF)
Note: Data are Listed for all Voids in the P1 Unit Cell i.e. Centre of Gravity, Solvent Accessible Volume, Recovered number of Electrons in the Void and Details about the Squeezed Material

```
loop_
  _platon_squeeze_void_nr
  _platon_squeeze_void_average_x
  _platon_squeeze_void_average_y
  _platon_squeeze_void_average_z
  _platon_squeeze_void_volume
  _platon_squeeze_void_count_electrons
_platon_squeeze_void_content
   1  0.000  0.500  0.500       200       47 ' '
```

The general procedure has been described in more detail as the "BYPASS procedure".[227]

X-ray crystal structure determination of 4.41

Crystals suitable for X-ray diffraction were obtained by slow evaporation from a saturated solution in DCM at T = -35 °C. *Crystallographic data*: $C_{29}H_{21}PAuCL$, *F*w = 632.85, 0.20×0.05×0.04 mm^3, colourless needle, triclinic, $P\bar{1}$, a = 10.4332(2), b = 15.2583(3), c = 15.9246(4)Å, α = 98.9170(8)°, β = 98.1137(8)°, γ = 109.0312(8)°, V = 2317.15(9) $Å^3$, Z = 4, Dx = 1.814 gcm^{-3}, μ = 6.548 mm^{-1}. 31635 reflections were measured by using a Bruker-AXS smart CCD area detector diffractometer (MoKα radiation, λ = 0.71073Å)[155] up to a resolution of $(\sin\theta/\lambda)_{max}$ = 0.60 $Å^{-1}$ at a temperature of T = 100 K. The reflections were corrected for absorption and scaled on the basis of multiple measured reflections by using the SADABS program[155] (0.63–0.75 correction range). 6978 reflections were unique (R_{int} = 0.041). Using ShelXle[158], the structures were solved with SHELXS-2014 by using direct methods and refined with SHELXL-2014 on $F2$ for all reflections.[156] Non-hydrogen atoms were refined by using anisotropic displacement parameters. The positions of the hydrogen atoms were calculated for idealized positions. 529 parameter were refined without restraints. R_1 = 0.054 for 6978 reflections with $I>2\sigma(I)$ and wR_2 = 0.155 for 8154 reflections, S = 1.066, residual electron density was between -2.79 and 6.60 $eÅ^{-3}$. Geometry calculations and checks for higher symmetry were performed with the PLATON program.[157]

SQUEEZE RESULTS (Version = 50315)[226]

```
# Note: Data are Listed for all Voids in the P1 Unit Cell
# i.e. Centre of Gravity, Solvent Accessible Volume,
# Recovered number of Electrons in the Void and
# Details about the Squeezed Material
  _platon_squeeze_void_nr
  _platon_squeeze_void_average_x
  _platon_squeeze_void_average_y
  _platon_squeeze_void_average_z
  _platon_squeeze_void_volume
  _platon_squeeze_void_count_electrons
  _platon_squeeze_void_content
   1  0.315  0.679  0.698        9        0 ' '
   2  0.684  0.321  0.302        9        0 ' '
_platon_squeeze_void_probe_radius              1.20
_platon_squeeze_details
```

The general procedure has been described in more detail as the "BYPASS procedure".[227]

X-ray crystal structure determination of 4.44

Crystals suitable for X-ray diffraction were obtained from by slow evaporation from a solution in THF/acetonitrile. *Crystallographic data*: $C_{31}H_{24}ClCuNP$, *Fw* = 540.47, 0.17×0.12×0.07 mm^3, colourless block, orthorhombic, *Pna2₁*, *a* = 17.0577(8), *b* = 8.4718(4), *c* = 16.9486(6) Å, $\alpha = 90°$, $\beta = 90°$, $\gamma = 90°$, *V* = 2449.23(18) $Å^3$, *Z* = 4, *D*x = 1.466 gcm^{-3}, μ = 1.088 mm^{-1}. 16075 reflections were measured by using a Bruker-AXS smart CCD area detector diffractometer (MoKα radiation, λ = 0.71073Å)[155] up to a resolution of $(\sin\theta/\lambda)_{max}$ = 0.60 $Å^{-1}$ at a temperature of T = 100 K. The reflections were corrected for absorption and scaled on the basis of multiple measured reflections by using the SADABS program[155] (0.89–0.94 correction range). 4286 reflections were unique (R_{int} = 0.067). Using ShelXle[158], the structures were solved with SHELXS-2014 by using direct methods and refined with SHELXL-2014 on *F*2 for all reflections.[156] Non-hydrogen atoms were refined by using anisotropic displacement parameters. The positions of the hydrogen atoms were calculated for idealized positions. 293 parameter were refined using one restraint. R_1 = 0.0340 for 3789 reflections with $I>2\sigma(I)$ and wR_2 = 0.0646 for 4286 reflections, *S* = 1.036, residual electron density was between -0.31 and 0.27 $eÅ^{-3}$. Geometry calculations and checks for higher symmetry were performed with the PLATON program.[157]

X-ray crystal structure determination of 4.45

Crystals suitable for X-ray diffraction were obtained by slow evaporation from a saturated solution in DCM. *Crystallographic data*: $C_{55}H_{34}F_{12}CLOP_2Rh$, *F*w = 1139.12, 0.46×0.33×0.30 mm^3, yellow block, tetragonal, $I4_1/a$, a = 26.5933(1), b = 26.5933(1), c = 14.1953(3) Å, α = 90°, β = 90°, γ = 90°, V = 10039.0(2) $Å^3$, Z = 8, Dx = 1.507 gcm^{-3}, μ = 0.541 mm^{-1}. 56830 reflections were measured by using a Bruker-AXS smart CCD area detector diffractometer (MoKα radiation, λ = 0.71073 Å)[155] up to a resolution of $(\sin\theta/\lambda)_{max}$ = 0.63 $Å^{-1}$ at a temperature of T = 100 K. The reflections were corrected for absorption and scaled on the basis of multiple measured reflections by using the SADABS program[155] (0.65–0.75 correction range). 5502 reflections were unique (R_{int} = 0.043). Using ShelXle[158], the structures were solved with SHELXS-2014 by using direct methods and refined with SHELXL-2014 on $F2$ for all reflections.[156] Non-hydrogen atoms were refined by using anisotropic displacement parameters. The positions of the hydrogen atoms were calculated for idealized positions. 341 parameter were refined without restraints. R_1 = 0.036 for 5502 reflections with $I>2\sigma(I)$ and wR_2 = 0.098 for 6490 reflections, S = 1.117, residual electron density was between -0.46 and 0.45 $eÅ^{-3}$. Geometry calculations and checks for higher symmetry were performed with the PLATON program.[157]

SQUEEZE RESULTS (APPEND TO CIF)[226]
Note: Data are Listed for all Voids in the P1 Unit Cell
i.e. Centre of Gravity, Solvent Accessible Volume,
Recovered number of Electrons in the Void and
Details about the Squeezed Material
_platon_squeeze_void_nr
_platon_squeeze_void_average_x
_platon_squeeze_void_average_y
_platon_squeeze_void_average_z
_platon_squeeze_void_volume
_platon_squeeze_void_count_electrons
_platon_squeeze_void_content
1 0.000 0.250 0.125 259 61 ' '
2 0.000 0.750 0.875 259 62 ' '
3 0.500 0.250 0.375 259 62 ' '
4 0.500 0.750 0.625 259 61 ' '
_platon_squeeze_details

The general procedure has been described in more detail as the "BYPASS procedure".[227]

5. Catalysis

Part of this chapter has been published in:

"Phosphinines versus Mesoionic Carbenes: A Comparison of Structurally Related Ligands in Au(I)-Catalysis" - M. Rigo, L. Hettmancyzk, F. J. L. Heutz, S. Hohloch, M. Lutz, B. Sarkar, C. Müller, Dalton Trans. **2017**, *46,* 86.

Evi Habraken, Andreas Ehlers and Chris Slootweg (Universiteit van Amsterdam) are kindly acknowledged for the DFT calculations reported in this chapter.

5.1 Introduction

As mentioned in Chapter 1, homogeneous catalysis is one of the fields where phosphorus-containing molecules have been employed the most. In this respect, the choice of the ligand is fundamental for the implementation of the right properties of the catalyst. The overall characteristics of a ligand depend on a number of different features. For the majority of the ligands, the most important ones are certainly steric and electronic properties. Since these do influence each other, it is virtually impossible to completely separate them. However, a large number of models that approximate their effects are available nowadays. In the next paragraphs, the main methodologies for the evaluation of these properties of monodentate ligands will be illustrated.

5.1.1 Steric properties

In the last decades, several parameters have been introduced for the quantification of the steric bulk of ligands.[266,267] Introduced by Tolman, the most widely applied concept is the cone angle (θ).[268,269] This is the angle of a cone that embraces all the atoms in the ligand (Figure 53, left). In this calculation, an average P-Ni distance of 2.28 Å is taken as P-M distance. The method is also available for asymmetrically substituted ligands and for those with particularly high steric demand[49] and the parameter can be determined starting from crystallographic parameters.[270] To overcome the inaccuracy of Tolman's method, White *et al.* introduced the concept of the so-called solid angle.[271] This is the area of the "shadow" that the atomic spheres representing the substituents would project on the van der Waals surface of the metal center (Figure 53, right).[272,273]

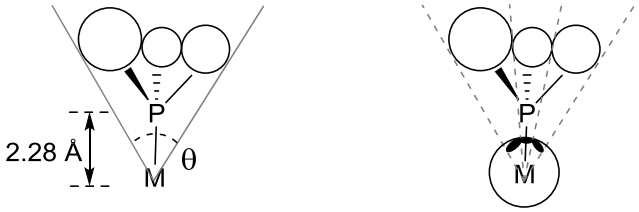

Figure 53. Tolman's definition of the cone angle (left), White's definition of the solid angle (right).

Entirely theoretical methods have also been developed. Brown *et al.* reported on the computation of energy-minimized structures of $[Cr(CO)_5L]$ type complexes. A new steric

parameter, the so-called ligand repulsive energy (E_R), is obtained by computing the van der Waals repulsive force acting between the L and $Cr(CO)_5$ fragments along the Cr-P axis. This value is then multiplied for the equilibrium Cr-P distance (r_e) to give E_R. The fact that the computation is performed on a metal complex allows for a better description of the steric bulk of a ligand in the coordination sphere of a metal.[274]

An additional computational method was developed by Suresh and co-workers. This is based on calculations of the molecular electrostatic potential (MESP), which represents the "lone pair strength" and is correlated to the steric demand of the substituents. In fact, the larger the substituents, the wider the R-P-R angles resulting in a larger p-character of the phosphorus lone pair. A steric parameter deriving from these calculations (θ_{MESP}) showed good correlation to other experimental methods.[275,276]

The most recent method for the evaluation of the steric hindrance of ligands is the buried volume (%V_{bur}). This descriptor, developed by the groups of Nolan and Cavallo, is the amount of volume which is occupied by the atoms of the ligand (van der Waals radii) in a sphere of r = 3.5 Å. The ligand is computed at a 2.00 or 2.28 Å distance from the metal center without taking into account the hydrogen atoms (Figure 54).[277,278]

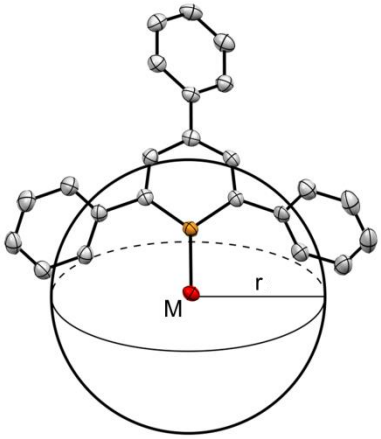

Figure 54. Percent buried volume %V_{Bur}.

This method can be used for both planar and three-dimensional ligands, allowing a better comparison between structurally different ligands. A large number of data for common phosphorus-containing ligands and N-heterocyclic carbenes have been reported, obtained from the corresponding gold complexes of the type [LAuCl].[279] These values can be calculated using a software developed by Cavallo *et al.*, which is also able to calculate topographic steric maps.[280,281]

The steric properties of phosphinines have so far only been evaluated using the occupancy angles (see Chapter 2).[51] This method only allows for the estimation of the steric bulk of flat heterocycles, so is not suitable for a comparison with classical phosphine ligands. Even though they are regarded as bulky ligands, so far the steric properties of phosphabarrelenes have not been studied and compared. The same applies to 5-phosphasemibullvalenes, which is a completely new class of ligands.

5.1.2 Electronic properties

As for the steric properties, different parameters and methodologies have been developed to quantify the electronic properties of phosphorus ligands. However, these are more difficult to study. In fact, according to the Dewar-Chatt-Duncanson model, they are the result of two main contributions, namely the σ-donation and the π-back donation.[282–284]

To evaluate these properties, different experimental methodologies have been developed involving techniques, such as electrochemical measurements, UV-vis or NMR spectroscopy.[285] In the case of phosphorus ligands, different approaches exploiting the latter are known. They are based, for example, on the chemical shift in the NMR spectra or on the magnitude of the coupling constants between P and other NMR active nuclei.[286–288] In particular, comparing the magnitude of $^{1}J_{\text{P-Se}}$ in phosphine-selenides allows for an estimation of their σ-donor properties. In fact, the coupling constant is proportional to the s-character of the orbital hosting the lone pair. A higher s-character and therefore a less directional orbital implies a less efficient donation.[287,289]

The main strategy is a result of the pioneering studies of Cotton and Strohmeier.[290–294] It exploits the shift of the carbonyl bands in the IR spectra of metal-carbonyl complexes of the type $[LM(CO)_x]$, which is proportional to the net-donation of the ligand. This is made of two components. More precisely, the σ-donation regards the effective dative donation from an occupied molecular orbital (MO) of the ligand (L) to a vacant MO of the metal, while the π-back donation regards the donation in the opposite direction, from an occupied MO of the metal to an empty orbital of the ligand (Figure 55).

Figure 55. σ-donation (left) and π-back donation (right) contributions to the M-L bond in a M-CO complex.

The stretching frequency of the CO bands in the infrared spectra is directly proportional to the strength of the C≡O bond. If L is a strong σ-donor, more electron density will flow to the metals d-orbitals, and a more efficient π-back donation will be possible to the π* orbitals of CO, thus weakening the C-O bond. On the other hand, if L is a strong π-acceptor, the π-back donation contribution into the π* orbitals of CO will be lower, and the C-O bond will be strengthened.

The first, and still commonly used electronic parameter was introduced by Tolman in the seventies.[49,268,269] Also known as χ, Tolman's electronic parameter (TEP) is based on the infrared stretching frequency of the A_1 band in $[LNi(CO)_3]$ type complexes. At the beginning defined as the difference between this frequency and the corresponding one in the reference complex $[P(t\text{Bu})_3Ni(CO)_3]$, it is nowadays more often expressed as the wavenumber $\tilde{\nu}$ itself in cm^{-1}. As most experimental parameters, TEP takes into account both the σ- and π-contributions, thus describing the net-donation of a given ligand.[49,268,269]

Similar methods have been developed with the aim to avoid the use of $[Ni(CO)_4]$ which, as a drawback, is rather dangerous. Crabtree *et al.* reported on similar methods using Mo-, Rh- and Ir-carbonyl complexes. These linearly correlate with TEP and are valid alternatives to it.[295,296] On the other hand, the L-M bond in these complexes could be more affected by the steric properties of the ligand. For this reason a larger library of ligands has been characterized using the Ni-based system.[49]

Some methodologies allow for the qualitative estimation of the different contributions, yet they are not widely used.[297,298] The reason lies in the fact that an *a priori* determination of the electronic properties of a ligand is virtually impossible. According to the metal, its charge and the number and nature of the remaining ancillary ligands, the σ- and π-contributions will change.[299] Therefore, the real properties of the ligand depend on the coordination compound which is examined. To overcome this problem and trying to rationalize the ligand properties, ligand databases are being compiled, aiming to predict their reactivity.[221,267]

In this respect, a large number of theoretical methods have been developed. These allow for the separation of the σ- and π-contribution and for a qualitative estimation of their single contributions to the bond.[300] A number of theoretical methods for the fulfillment of this task are available.[301–303]

Very little is known about the electronic properties of phosphinines and phosphabarrelenes. Phosphinines are known to be strong π-acceptors, even though their electronic properties have not been related to those of other P-containing ligands. A few studies have been reported, suggesting the phosphabarrelenes to be stronger donors than phosphinines but weaker than triphenylphosphine.[56,171,187] However, a systematic analysis is still missing.

5.1.3 Phosphinines and phosphabarrelenes in homogeneous catalysis

Even though phosphinines are known for half a century, the investigation of their properties as ligands in homogeneous catalysis only started in the last 20 years. Still, only a few examples are reported in the literature.

The first examples of phosphinines as ligand in catalytic reactions date back to the late 1990's and involve Fe(0)-catalyzed cyclooligomerization reactions. Two similar half-sandwich complexes featuring a η^6-coordinated phosphinine were employed in the formation of pyridines starting from nitriles and alkynes, and in the cyclodimerization of butadiene. However, low selectivities and activities were found for both reactions.[304,305]

The hydrosilylation of alkynes has been investigated as well. It is the only example of a catalytic reaction involving a biphosphinine. Thanks to the electron-withdrawing properties of the ligand, it was possible to selectively produce vinylsilanes in moderate to high yields using an iridium-based catalyst.[306] A related example reports the palladium-catalyzed hydrosilylation of alkenes using chiral phosphinine ligands. Unfortunately, only low enantioselectivities were achieved (up to 27% *ee*).[307]

Also in other reactions the π-accepting properties of phosphinines have been exploited. In the cycloisomerization of dieneynes, a combination of 2,4,6-triphenylphosphinine and [Ni(COD)$_2$] has been used.[51]

The most interesting example that has been reported concerns hydroformylation reactions. 2,4,6,-Substituted phosphinines, as rather bulky and monodentate ligands, can compete with

common phosphines and phosphites in the hydroformylation of terminal and internal alkenes. The strong π-accepting properties of phosphinines are thought to favour the dissociation of a carbonyl ligand from a rhodium catalytic species, thus creating an active site for the hydroformylation process. For example, in the Rh-catalyzed hydroformylation of styrene a clear selectivity for the branched product was observed.[110,308,309] Good results were also obtained with more challenging substrates, such as 2-octene or tetra-substituted alkenes. A screening of differently substituted ligands proved that steric bulk is a fundamental feature for the achievement of high turnover frequencies, as it allows for the formation of a monoligated Rh species. In particular, the best results have been obtained with compound **5.1** (Figure 56).[56] So far, attempts involving the application of chiral bidentate phosphinines in this reaction did not lead to satisfactory results.[110]

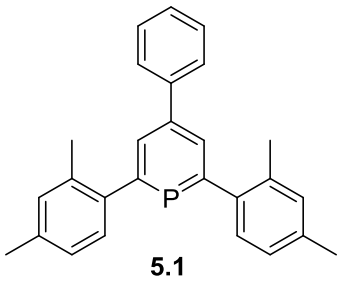

5.1

Figure 56. Ligand **5.1**, which has been employed in some of the described catalytic applications.

The same ligand was successfully employed by another group in combination with the rhodium precursor ($[Rh(norbornadiene)_2]BF_4$) for the isomerisation of allylic alcohols to saturated carbonyl compounds.[310]

Asymmetric hydrogenations have also been investigated. Reetz *et al.* tested mixtures of ligand **5.1** and an axially chiral phosphonite in combinatorial catalysis. Interestingly, in the Rh-catalyzed hydrogenation of acetamidoacrylate, the heterocombination of these ligands led to an inversion of the enantioselectivity compared to the homocombination of the chiral phosphonite.[311] Bidentate phosphinine-phosphite ligands were employed in the Rh-catalyzed hydrogenation of different substrates by Müller and co-workers.[312]

Finally, the same group reported on the cerium ammonium nitrate driven water oxidation in 2015. A cyclometalated phosphinine-iridium(III) catalyst was employed in this reaction, resulting in TOFs which were comparable to the most active catalysts reported in the literature.[124]

Similarly to phosphinines, also phosphabarrelenes are known for a long time. Also their application in homogeneous catalysis is limited to a few publications. Among the reported examples, cross coupling reactions are the ones that have been explored the most.

Ligand **3.20** has been employed in Pd-catalyzed Negishi coupling reactions for the synthesis of biphenyls. Excellent results were obtained using a low catalyst loading at room temperature. The mechanism has been investigated by means of DFT calculations and one intermediate of the catalytic cycle has been isolated and characterized crystallographically.[188]

The same ligand was also used for other cross coupling reactions. Two Pd complexes in different oxidation states (Pd(II) for **3.21** and Pd(0) for **3.22**, respectively) were successfully employed in the Suzuki–Miyaura coupling of different aryl chlorides with phenylboronic acid at room temperature. High conversions were obtained with a relatively low catalyst loading (0.2 mol-%) and a good tolerance for functional groups was observed.[187] In addition to this, the mechanism of the reaction has been studied with DFT calculations, and a Pd(0) intermediate of the catalytic cycle has been trapped.[189] The same reaction was investigated using a neutral and a cationic Pd(II)-complex of the bidentate ligand **3.31**. These complexes, **5.2** and **5.3**, proved to be very active and excellent conversions and TON were achieved for the synthesis of biphenyl derivatives (Figure 57). More interestingly, complex **5.3** has also been efficiently employed in the allylation of secondary amines.[162,313]

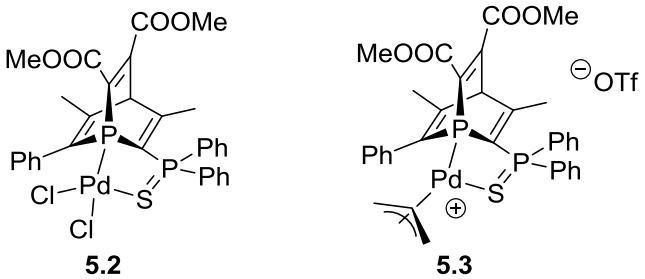

5.2 **5.3**

Figure 57. Pd complexes **5.2** and **5.3**.

Only one example has been reported for phosphatriptycenes in homogeneous catalysis. In this work, good results have been obtained in the catalytic Stille coupling and Heck reaction thanks to the weak σ-donor properties of the ligand.[182]

Similar to **3.22**, the Pt(0)-based compound **3.23** was tested in the hydrosilylation of alkynes. High regioselectivities were achieved for terminal alkynes under mild conditions at low catalyst loadings, both for complex **3.23** and for an *in situ* formed catalyst.[190]

The most prominent example of a phosphabarrelene-based catalyst has been reported by Breit and co-workers. A bulky ligand bearing xylyl substituents (**3.26**) was successfully employed in the hydroformylation of internal alkenes.[171,185] First, cyclic olefins (cyclopentene and cyclohexene) have been applied in the reaction, since these substrate are not disturbed by alkene isomerization. In both cases, ligand **3.26** had the best performance with a turnover frequency of up to 12000 h^{-1}, which is ten times faster than the corresponding phosphinine. More interesting results were obtained in the hydroformylation of 2-octene, which was successfully achieved using the same ligand. Almost no isomerization was observed (Scheme 62). Similarly, the hydroformylation of 2,5-dihydrofuran and N-Boc-pyrroline, which are known to easily isomerize, proceeded with a low amount of isomerization.

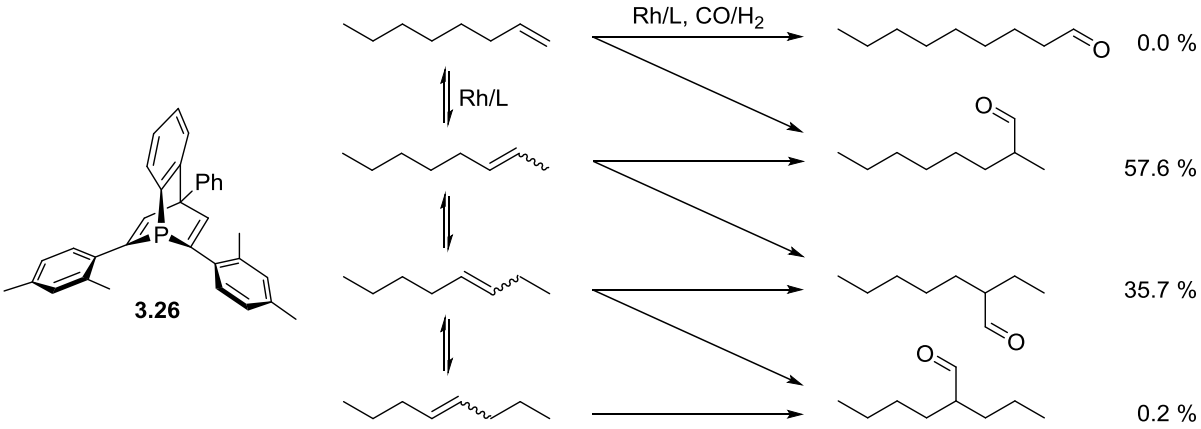

Scheme 62. Hydroformylation of 2-octene with **3.26** as ligand.

An example of a tandem hydroformylation-cyclization reaction on an imidazole derivative was reported by Müller *et al.* (Scheme 63).[186] The use of phosphabarrelene **3.19** resulted in much higher yields of the aldehyde compared to its phosphinine precursor (32% *vs* 98% conversion) and led to the almost quantitative formation (93%) of the final bicyclic product.

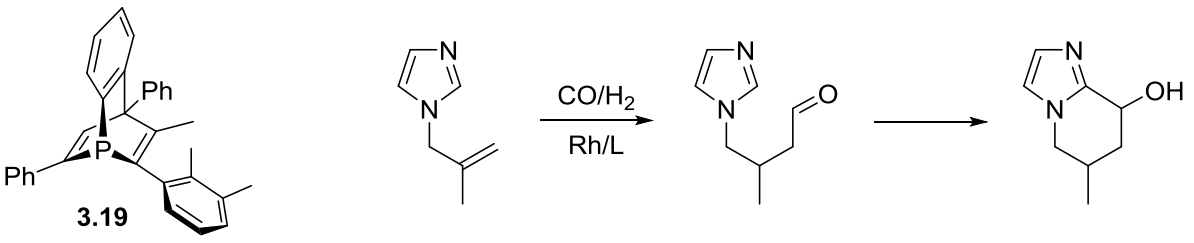

Scheme 63. Phosphabarrelene **3.19** and the tandem hydroformylation-cyclization reaction.

Only one example of asymmetric homogeneous catalysis has been reported. In this work, chiral mono- and bidentate phosphabarrelene-phosphites have been prepared and tested in the

asymmetric hydrogenation of the methyl ester of itaconic acid and two different acetamidoacrylates.[181] Even though full conversion was reached in relatively short times, the monodentate ligands did not allow for high enantiomeric excess. On the other hand, one of the phosphito-phosphabarrelene chelating ligands yielded up to 90% *ee* for the acetamidoacrylates.

5.2 Results and discussion

It is clear that the properties of phosphinines and phosphabarrelenes have not been studied in detail. Also, nothing is known about the properties of 5-phosphasemibullvalenes. These could be particularly interesting for applications in asymmetric catalysis, as a large number of examples featuring configurationally rigid chiral phosphines has been reported.[9,314–322] In this chapter the steric and electronic properties of these compounds will be investigated and the ligands will be employed in Au(I)-catalyzed cycloisomerization reactions.

5.2.1 Steric properties

The steric properties of the ligands reported in this work have been evaluated by calculations of the buried volume. This methodology allows for a comparison between phosphinines, phosphabarrelenes and 5-phosphasemibullvalenes, even though they have rather different shapes. The calculations have been performed using a specific software.[281] In Figure 58 the values corresponding to the buried volume of a ligand located at d = 2.28 Å from the center of a sphere with r = 3.50 Å are reported.

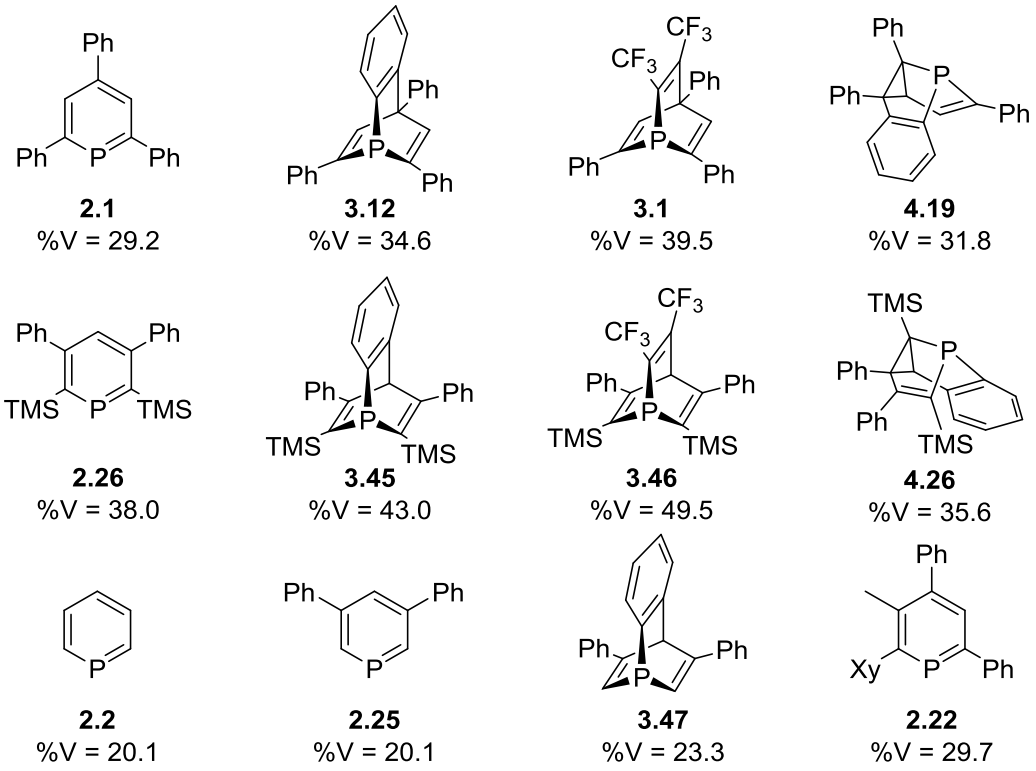

Figure 58. $\%V_{Bur}$ for selected ligands at d = 2.28 Å.

In the first row of Figure 58, 2,4,6-triphenylphosphinine (**2.1**) and its derivatives are shown. These are the corresponding phosphabarrelenes obtained *via* cycloaddition with benzyne and hexafluoro-2-butyne (**3.12** and **3.1**, repectively) and phosphasemibullvalene **4.19**, which is the photoisomerization product of **3.12**. The buried volume of **2.1** is similar to that of PPh_3 (29.2 *vs* 29.6%)[279]. As one might expect, phosphabarrelenes **3.12** and **3.1** have larger buried volumes, as they are not flat as phosphinines (34.6 and 39.5%, respectively). Finally, the value for phosphasemibullvalene **4.19** is lower than that of its precursor **3.12** (31.8 *vs* 34.6%). In fact, in 5-membered rings the internal angles are smaller, therefore the substituents on the α-carbons are less directed to the metal center.

In the second row of Figure 58, a similar group of derivatives based on phosphinine **2.26** is reported. The same trend is observed for these compounds, but the values are much higher due to the prensence of TMS-groups on the α-carbon atoms. For example, phosphabarrelenes **3.45** and **3.46** have larger buried volumes than extremely bulky phosphines, such as P(*o*-Tol)$_3$ and P(Mes)$_3$ (43.0 and 49.5% *vs* 41.4 and 47.6%, respectively)[279].

The last row of Figure 58 shows four additional ligands. Interestingly, the buried volume of the parent compound **2.2** and phosphinine **2.25** have the same value, proving that only substituents in positions 2 and 6 of the heterocycle directly contribute to the steric hindrance

of the ligand. Also, this value is rather small due to the absence of substituents, being even smaller than PMe_3 (20.1 *vs* 22.2%)[279]. This is also evident by comparing the buried volume of **3.45** and **3.47** (43.0 *vs* 23.3%). Finally, ligand **2.22** has a similar buried volume to **2.1**. In fact, the methyl group in position 3 and the methyl groups on the xylyl ring do not contribute significantly, since the aryl ring is located almost perpendicular with respect to the phosphinine plane (see Figure 14).[139]

5.2.2 Electronic properties

For the evaluation of the electronic properties of the ligands, Tolman's electronic parameter of [LNi(CO)$_3$] type metal complexes has been measured, as reported in the previous chapters. Some of the ligands are reported together with their TEP in Figure 59, ordered by increasing net-donation. These values are being reported here for the first time and can be compared with the large library that has been compiled by Tolman.[49]

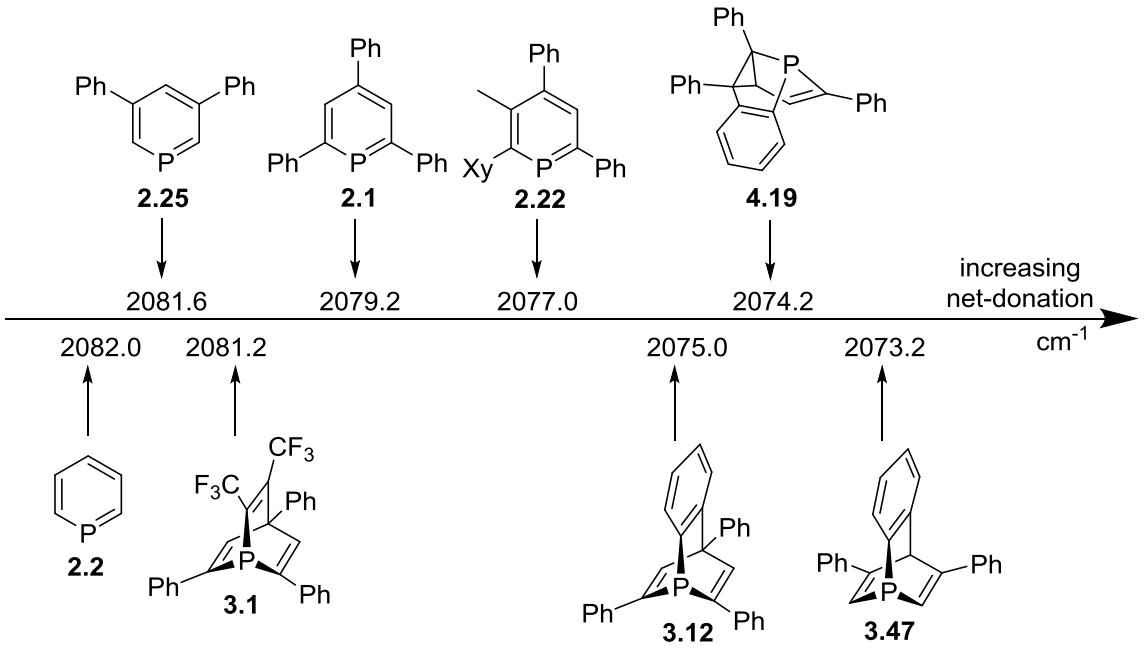

Figure 59. TEP parameter for selected ligands.

First of all, the parent phosphinine (**2.2**) appears as the weakest donor, with a TEP similar to PH_3 (2082.0 *vs* 2083.2 cm^{-1})[49]. The other phosphinines can be found in the same area, with TEP values which are typical for strongly π-accepting phosphites (TEP for P(OMe)$_3$ is 2079.5 cm^{-1})[49]. As one might expect, the net-donation increases due to the introduction of phenyl rings in positions 3 and 5 or even more in positions 2, 4 and 6 of the heterocycle. A methyl

group, which has a stronger +I effect, has a greater influence on the net-donation (see ligand **2.22**). The properties of phosphabarrelenes are dependent on the alkyne which is employed in their synthesis. In fact, benzophosphabarrelenes show higher net-donation, while trifluoromethyl-substituted derivatives are weaker donors than phosphinines (**3.12** and **3.1** *vs* **2.1**). Surprisingly, ligand **3.47** is a better donor than **3.12**, probably because of the lower steric bulk resulting in better coordination properties (%V_{Bur} = 23.3 *vs* 34.6). Finally, 5-phosphasemibullvalenes only show slightly higher net-donation than the corresponding phosphabarrelene isomers. Similarly, this trend was observed for trimethylsilyl-substituted derivatives **3.45** and **4.26**, which have TEP values of 2069.5 and 2069.0 cm^{-1}, respectively, similar to the moderate donor PPh_3 (TEP for PPh_3 is 2068.9 cm^{-1})[49].

Ligands **2.26** and **3.46** did not react with [$Ni(CO)_4$], most likely because of the steric hindrance deriving from the TMS-substituents. In fact, it is known that 2,6-disubstituted TMS-phosphinines prefer π-coordination *via* the aromatic ring towards a metal fragment, rather than σ-coordination.[93] For this reason, the TEP of these ligands has been obtained by means of DTF calculations. To verify the reliability of the experimental data just discussed, TEP values have been calculated for the selected ligands, as summarized in Table 12.

Table 12. Experimental and calculated values of TEP for selected ligands.

Ligand	$\nu(CO)_{exp}$	$\nu(CO)_{calc}$	$\Delta_{calc-exp}$
2.1	2079.2	2080.5	1.3
2.2	2082.0	2084.6	2.6
2.25	2081.6	2083.4	1.8
2.26	-	2073.6	-
3.1	2081.2	2080.7	-0.5
3.12	2075.0	2075.3	0.3
3.45	2069.5	2068.5	-1.0
3.46	-	2075.3	-
3.47	2073.2	2075.9	2.7
4.19	2074.2	2073.4	-0.8
4.26	2069.0	2068.2	-0.8

As one can see from Table 12, the DFT calculations are a good approximation of the experimental values, and allow to assign a TEP value to ligands **2.26** and **3.46** of 2073.6 and 2075.3 cm^{-1}, respectively. These values suggest that the ligands are fairly weak net-donors, with properties similar to secondary phosphine $PHPh_2$ (TEP for $PHPh_2$ is 2073.3 cm^{-1})[49].

From the overall data, it appears clear that the trend is the same for the two sets of differently substituted ligands (those based on **2.1** and those based on **2.26**). However, the derivatives of phosphinine **2.26** are stronger net-donors, as expected due to the +I effect of the TMS groups.[323–327]

Additional information can be obtained from theoretical calculations. In particular, ETS-NOCV is a powerful tool for the quantitative analysis of chemical bonds, combining the extended transition state (ETS) method for energy decomposition analysis with the natural orbitals for chemical valence (NOCV) theory.[328] With this method, the energy contributions to the total bond energy is calculated for each specific orbital interaction between the ligand and the metal fragment. In this way, it is possible to decompose the bond into its different components (such as σ, π, δ), providing the corresponding energy contributions to the total bond energy. Calculating the contributions for a set of ligands bound to the same metal fragment allows for a precise comparison of their electronic properties. An extensive overview of the donor and acceptor ability of phosphines obtained by applying ETS-NOCV calculations has recently been reported by Brenna and co-workers.[329]

In this work, these calculations have been performed for two different metal systems, $[LNi(CO)_3]$ and [LAuCl], and the results are consistent. The results for σ- and π-contributions in [LAuCl] type complexes are summarized in Figure 60 (top and bottom, respectively), in which differently colored columns correspond to different ligand classes. The L-M distance is also an important parameter because it reflects the overlap between the ligand and the metals orbitals, which affects the efficiency of the donation.

From the diagrams it appears clear that phosphinines in general are the weakest σ-donors and the strongest π-acceptors. Thanks to the effect of methyl and trimethylsilyl donor groups, **2.22** and **2.26** have a stronger σ-contribution. Surprisingly, **2.25** is also a stronger donor than **2.1**. This could be due to the lack of substituents in the α-positions, which hinder the coordination to the metal center (this is also reflected in the L-Ni distance in $[LNi(CO)_3]$ type complexes, see experimental part). Benzophosphabarrelenes (**3.12**, **3.45** and **3.47**) are stronger σ-donors than phosphinines, but weaker π-acceptors. However, they have a smaller σ- and a larger π-contribution than PPh_3. Trifluoromethyl-substituted phosphabarrelenes (**3.1** and **3.46**) are weaker σ-donors compared to the benzo-substituted counterparts, however they are much stronger π-acceptors. The remarkable steric bulk around the P atom in these ligands could be the reason why their TEP values are even lower than those of the corresponding phosphinines

(this is also reflected in the L-Ni distance in [$LNi(CO)_3$] type complexes, see experimental part). 5-Phosphasemibullvalenes **4.19** and **4.26** are stronger σ-donors and π-acceptors compared to the corresponding phosphabarrelenes. However, as suggested by the TEP values, the increase in the donation is higher, so overall they behave as stronger net-donors. Finally, it has to be noted that all the selected ligands are weaker σ-donors and stronger π-acceptors than PPh_3. Also, it is evident that the presence of trimethylsilyl groups increases the σ- and decreases the π-contribution (see **2.25** *vs* **2.26**, **3.45** *vs* **3.47** and **4.26** *vs* **4.19**), as suggested by the TEP values reported above. This is consistent with the +I effect of these substituents, but unexpectedly in disagreement with their hyperconjugating effect, which should increase the π-accepting properties.[330]

To conclude, phosphinines are strong π-acceptors and weak σ-donors. The properties of the corresponding phosphabarrelenes are dependent on the alkyne which is employed in their synthesis. Electron-poor trifluoromethyl-substituted phosphabarrelenes are stronger π-acceptors while benzophosphabarrelenes are stronger σ-donors. The corresponding 5-phosphasemibullvalenes are slightly stronger donors. In general these ligands have electronic-properties which range among differently substituted phosphites.

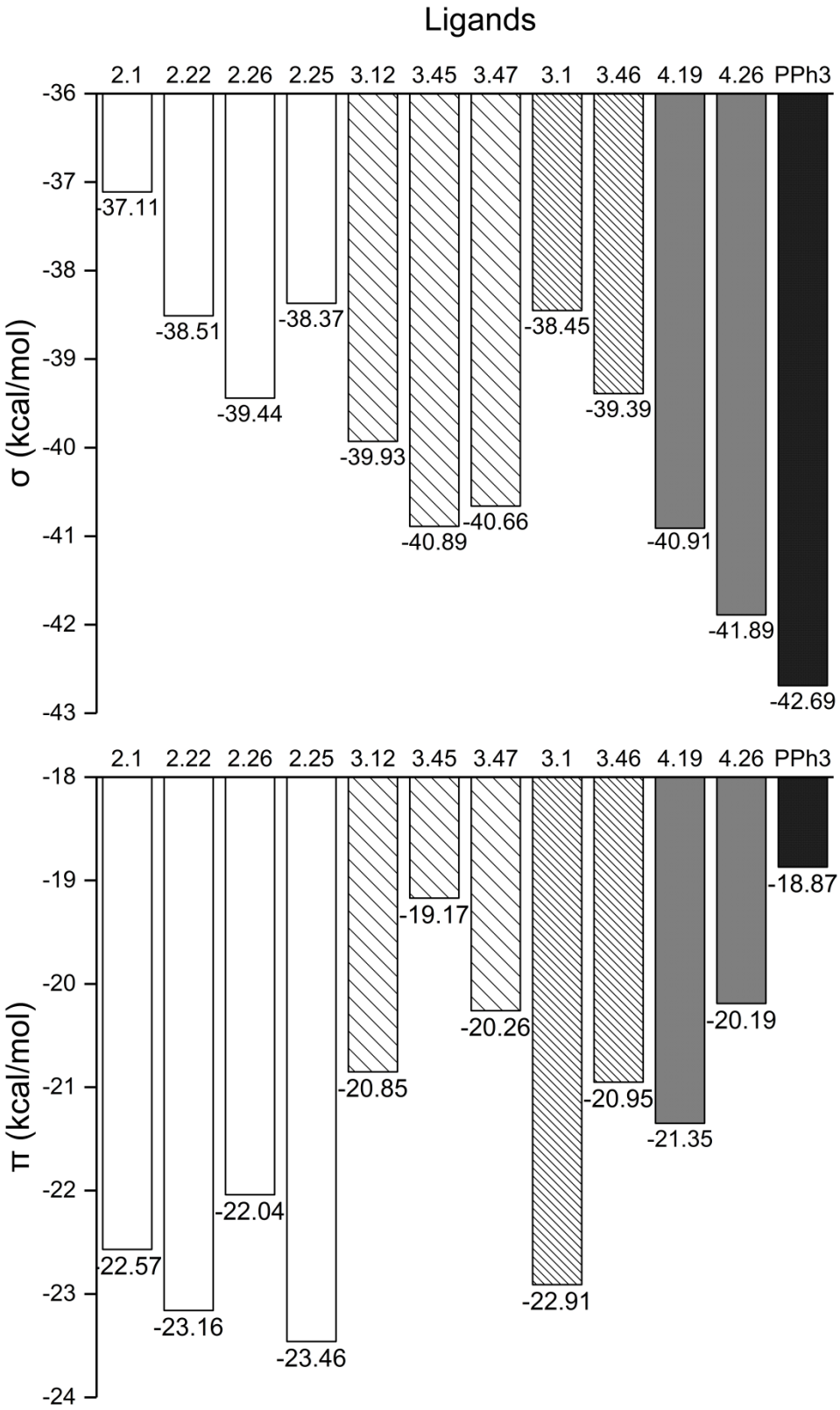

Figure 60. Calculated σ- (top) and π-contribution (bottom) to the L-Au bond in [LAuCl] type complexes. Different colors correspond to different ligand classes: from left to right are reported the values for phosphinines, benzophosphabarrelenes, trifluoromethyl-substituted phosphabarrelenes, 5-phosphasemibullvalenes and reference ligands. See experimental part for details.

These findings find confirmation in the molecular orbital schemes of the ligands. In Figure 61 the energy values for the orbitals from LUMO to HOMO-5 for compounds **2.1**, **3.12**, **3.1** and **4.19** are visualized.

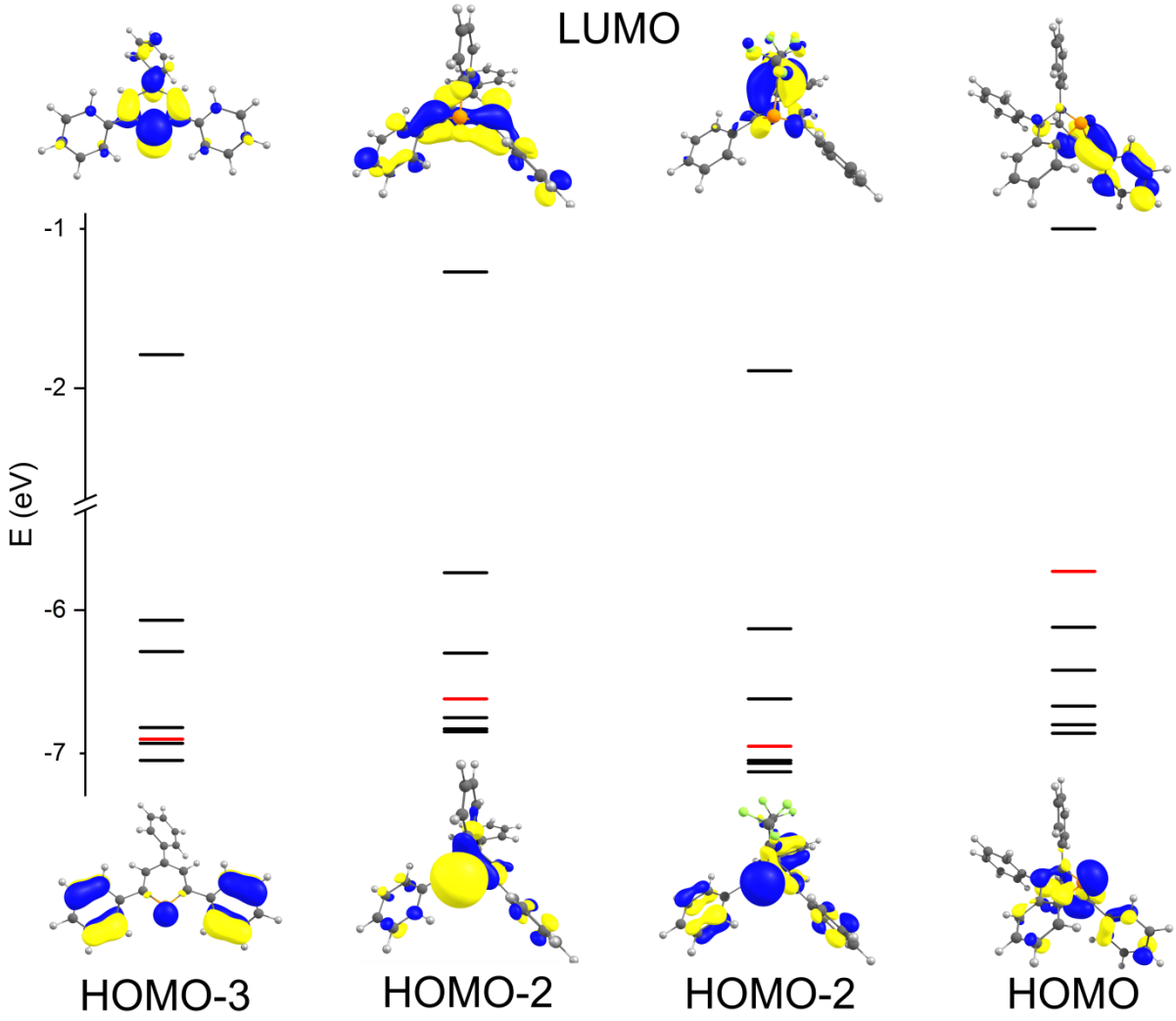

Figure 61. Molecular orbital (MO) scheme for **2.1**, **3.12**, **3.1**, **4.19** (from left to right). Orbitals from LUMO to HOMO-5 are reported. The highest MO which represents the lone pair is marked in red.
For the shape of all other MOs, see attachment.

The lone pair of 2,4,6-triphenylphosphinine (**2.1**) is represented by the HOMO-3 and HOMO-6 orbitals. In fact, this is the weakest donor of the series. **3.1** is slightly stronger, while the difference is more marked for **3.12** and **4.19**, which are the strongest σ-donors of the series (see Figure 60). The trend is confirmed also for the LUMO orbitals. Ligand **2.1** and **3.1** have strong π-acceptor properties and the energy level of their lowest unoccupied molecular orbitals are similar and low in energy. Ligand **3.12** and **4.19** are weaker acceptors, therefore the LUMO orbitals are located higher in energy. As expected for phosphine derivatives, the

LUMOs of phosphabarrelenes and phosphasemibullvalenes correspond to the σ*-orbitals of the P-C bonds.

5.2.3 Gold-catalyzed cycloisomerization reactions

Gold-catalyzed reactions have had a major development in the last decades.[331] Reactivity of Au(I) species, which for a long time were neglected, is the main focus of a large number of reviews.[332–337] These reports mostly deal with reactions where an electrophilic, usually cationic, gold center activates a C-C multiple bond by coordinating to it, allowing for a nucleophilic attack on the otherwise unreactive substrate. The cationic gold species is usually formed from the corresponding [LAuCl] type complex and a chloride abstractor, such as a silver salt. This approach has been extended to intramolecular reactions, such as cycloisomerizations.[332–338]

The choice of the ancillary ligands is crucial, as the putative cationic gold species needs to be stabilized by relatively bulky strong donors, such as phosphines or carbenes.[334,339] However, strong π-accepting phosphites in combination with Au(I)-precursors often show remarkable catalytic activities in such reactions.[340–343] So far, none of the ligands described in this work have ever been employed in a gold-catalyzed transformation. Since their electronic properties are rather similar to those of phosphites, it is interesting to test them in these reactions.

The first reaction that was investigated in this work is the cycloisomerization of the 1,6-enyne dimethyl 2-(3-methylbut-2-enyl)-2-(prop-2-ynyl)malonate (**5.5**) towards the cyclopentene-derivatives **5.6** and **5.7** in dichloromethane at room temperature and under the exclusion of light (Scheme 64).[338]

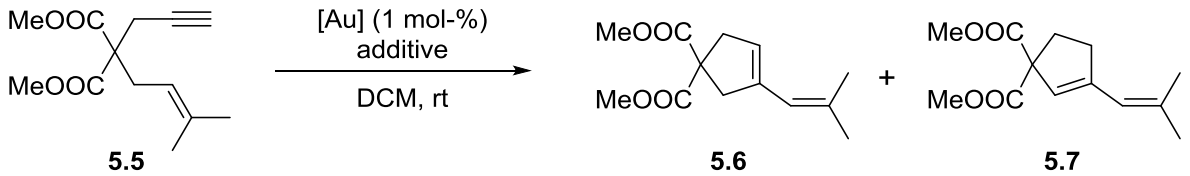

Scheme 64. Cycloisomerization of **5.5** towards **5.6** and **5.7**.

This is a typical benchmark reaction in Au(I) catalysis, in which several phosphorus-containing ligands have been employed.[344–347] Also low-coordinate phosphorus species have been employed in this reaction. Yoshifuji and Ito have successfully applied phosphaalkenes as ligands in this transformation, even without any additive.[348–350] Apparently, the highly π-

accepting properties of these compounds are beneficial for increasing the Lewis acidity of the gold centers. As phosphinines are π-accepting low-coordinate phosphorus compounds, it is indeed interesting to employ them in the same reaction.

In a comparison study with a structurally related mesoionic carbene, precatalysts containing phosphinines **2.1** and **2.22** have been tested in the presence of different additives.[142] The results, compared with those of benchmark catalysts based on PPh_3 and tris(2,4-di-tert-butylphenyl)phosphite (**5.8**), are summarized in Table 13.

Table 13. Results for the catalytic cycloisomerization of substrate **5.5** to **5.6** and **5.7**. Conditions: catalyst precursor: 1 mol-%, additives: 1 mol-% [$AgSbF_6$], 5 mol-% [$Cu(OTf)_2$], dichloromethane, room temperature.

Entry	Precatalyst	Additive	Time	Conversion [%]	Product ratio (5.6 : 5.7)
1	-	[$AgSbF_6$]	24 h	0	-
2	-	[$Cu(OTf)_2$]	24 h	98	1 : 0
3	[$AuCl(SMe_2)$]	-	24 h	75	1 : 0
4	[$AuCl(SMe_2)$]	[$AgSbF_6$]	8 h	>99	1 : 2
5	[AuCl(**2.22**)]	-	24 h	75	1 : 0
6	[AuCl(**2.1**)]	[$AgSbF_6$]	**5 min**	**>99**	**1 : 0**
7	[AuCl(**2.22**)]	[$AgSbF_6$]	**5 min**	**>99**	**1 : 0**
8	[AuCl(**2.22**)]	[$AgSbF_6$]	15 min	>99	2 : 3
9	[AuCl(**2.22**)]	[$Cu(OTf)_2$]	30 min	>99	1 : 0
10	[$AuCl(PPh_3)$]	[$AgSbF_6$]	30 min	>99	1 : 0
11	[AuCl(**5.8**)]	[$AgSbF_6$]	5 min	>99	Mixture

First of all, the gold-precursor as well as the additives have been tested alone in the catalytic reaction. The standard additive [$AgSbF_6$] does not lead to any conversion within 24 h (Table 13, entry 1). In contrast, additive [$Cu(OTf)_2$] leads almost quantitatively and exclusively to product **5.6** within 24 h (entry 2).[351,352] The gold-precursor [$AuCl(SMe_2)$] catalyzes the reaction in the absence of any additive, with 75% conversion within 24 h (entry 3). A combination of this compound and [$AgSbF_6$] leads to a moderately active catalyst which, however, shows poor selectivity (entry 4). No difference in activity or selectivity was observed between [$AuCl(SMe_2)$] alone and [AuCl(**2.22**)] (entries 3 and 5).

The presence of the additive [$AgSbF_6$] causes a drastic increase in the performance of the precatalysts. In fact, both phosphinine-based coordination compounds [AuCl(**2.1**)] and [AuCl(**2.22**)] led to the selective and almost quantitative transformation of the substrate into **5.6** only after 5 min (entries 6 and 7). No difference was detected in the activity of the two

phosphinine-based catalysts. As reported in other studies, longer reaction times lead to isomerization of the product (entry 8).[353] In the presence of additive [$Cu(OTf)_2$], only product **5.6** was obtained quantitatively (>99%), but the reaction was much slower (30 *vs* 5 min, entry 9). Finally, the same reaction was carried out using the benchmark precatalysts [$AuCl(PPh_3)$] and [AuCl(**5.8**)] under the same reaction conditions. Using PPh_3 as a ligand generates a much less active catalyst (entry 10). On the other hand, the system based on the bulky phosphite **5.8** proved to be rather active (entry 11), but a mixture of **5.7** and other unidentified products was obtained. Interestingly, in comparison with the standard precursors, both phosphinine-based catalysts show a better performance in terms of activity and selectivity, similarly to literature known systems.[344–347]

Unfortunately, the facile conversion of dimethyl 2-(3-methylbut-2-enyl)-2-(prop-2-ynyl)malonate (**5.5**) to the corresponding vinylcyclopentenes does not allow for a comparison between the activities of differently substituted ligands, as very fast conversion was observed for the two different phosphinine-based catalysts. Hence, a different, more challenging reaction was envisaged.

Consequently, *N*-2-propyn-1-ylbenzamide (**5.9**) was chosen as a substrate for testing phosphinines, phosphabarrelenes and phosphasemibullvalenes in the same Au(I)-catalyzed cycloisomerization reaction. Hashmi *et al*. showed that **5.9** can be converted both to the corresponding oxazoline (**5.10**) and oxazole (**5.11**), using Au(I) and Au(III) catalysts, respectively (Scheme 65).[354,355] Since then, a few publications about phosphorus-containing ligands employed in this reaction have been reported.[356–360]

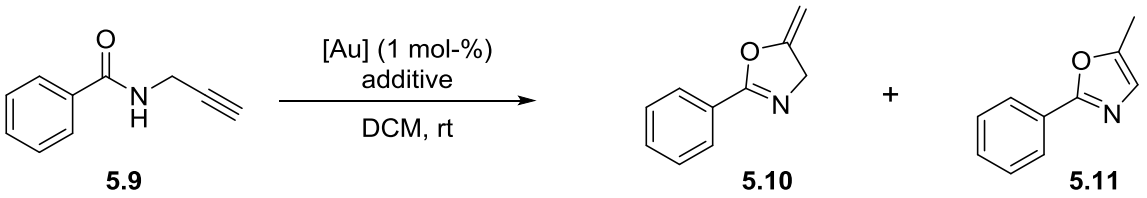

5.9 **5.10** **5.11**

Scheme 65. Cycloisomerization of **5.9** towards **5.10** and **5.11**.

Even though amides are very weak acids, the N-H functionality of the substrate could react with the P=C double bond of the phosphinine ligands.[112,361] To exclude this, an equimolar amount of the substrate and [AuCl(**2.22**)] were stirred in DCM at room temperature. As expected, the $^{31}P\{^1H\}$ NMR spectrum did not show any reaction between the substrate and the coordinated ligand after 16 h. With this verified, phosphinine-containing gold complexes were employed in the cycloisomerization of **5.9**, and the results are summarized in Table 14.

Table 14. Results for the catalytic cycloisomerization of substrate **5.9** to **5.10** and **5.11**. Conditions: catalyst precursor: 1 mol-%, additives: 1 mol-% [$AgSbF_6$], 5 mol-% [$Cu(OTf)_2$], dichloromethane, room temperature.

Entry	Precatalyst	Additive	Time [h]	Conversion [%]	Product ratio (5.10 : 5.11)
1	-	$AgSbF_6$	24	0	-
2	-	$Cu(TfO)_2$	24	5	1 : 0
3	[$AuCl(SMe_2)$]	-	24	0	-
4	[$AuCl(SMe_2)$]	$AgSbF_6$	24	85	9 : 1
5	[AuCl(**2.1**)]	-	24	25	0 : 1
6	[AuCl(**2.1**)]	$AgSbF_6$	24	40	4 : 1
7	[AuCl(**2.22**)]	-	24	15	1 : 3
8	[AuCl(**2.22**)]	$AgSbF_6$	**3**	**>99**	**98 : 2**
9	[AuCl(**2.22**)]	$Cu(OTf)_2$	8	>99	98 : 2
10	[AuCl(**2.26**)]	-	24	40	9 : 1
11	[AuCl(**2.26**)]	$AgSbF_6$	6	>99	9 : 1
12	[$AuCl(PPh_3)$]	[$AgSbF_6$]	7	>99	96 : 4
13	[AuCl(**5.8**)]	[$AgSbF_6$]	11	>99	98 : 2

At first, the reactivity of the substrate in the presence of additives and precursors was investigated. No reaction was detected with [$AgSbF_6$], while only a low conversion was achieved in the presence of [$Cu(OTf)_2$] after 24 h (Table 14, entries 1 and 2). Also the Au(I)-complex [$AuCl(SMe_2)$] does not show any reactivity towards **5.9** (entry 3). A combination of this precursor and [$AgSbF_6$] leads to a high conversion, but the reaction is rather slow (24 h) and unselective (entry 4).

In the absence of any additive, the neutral Au(I)-complexes containing phosphinines **2.1**, **2.22** and **2.26** only show low catalytic activity in the cycloisomerization of **5.9** (entries 5, 7 and 10). However, a clear contrast between the three phosphinine-based complexes was observed in the presence of an additive. In combination with [$AgSbF_6$], a very active catalytic species is formed using **2.22** as ligand, and high conversion (>99%) and a good selectivity towards the oxazoline **5.10** is achieved already after 3 h (entry 8). On the other hand, the catalysts based on phosphinine **2.1** and **2.26** are less active. In particular, the first one only yields 40% of a mixture of products within 24 h, while the latter achieves full conversion of the substrate in 6 h with a product ratio of 9 : 1 (entries 6 and 11). Using the additive [$Cu(OTf)_2$] with the best performing system, again leads to full conversion of the substrate and high selectivity, even though the reaction is much slower, as reported above for substrate **5.5** (entry 9).

In contrast to the observations made for substrate **5.5**, the catalytic activities and selectivities of [AuCl(PPh_3)]/[$AgSbF_6$] and [AuCl(**5.8**)]/[$AgSbF_6$] are similar to each other, and the reactions are slower compared to the catalyst based on **2.22** (entries 12 and 13 *vs* entry 8).

It is clear that the cycloisomerization of **5.9** is indeed much more difficult to achieve compared to **5.5**. At this point, the evaluation of the electronic properties reported above can help to shed light on the obtained results. It is reasonable to assume that 2,4,6-triphenylphosphinine (**2.1**) forms a kinetically less stable Au(I) complex compared to ligand **2.22**, most likely due to electronic effects, as the steric bulk is rather similar (29.2 *vs* 29.7 %V_{Bur}). The ETS-NOCV analysis suggests that phosphinine **2.22**, as a stronger donor, is able to better stabilize the putative cationic gold species involved in the catalytic cycle (Figure 60). In contrast, the lower reactivity of **2.26**-based complex can be ascribed to the steric bulk deriving from the trimethylsilyl groups, which is reflected in the buried volume of the ligand (38.0 %V_{Bur}) and in the distortions observed in the crystallographic characterization of gold complex **2.34**.

The cycloisomerization of **5.9** was also used to test the catalytic properties of phosphabarrelenes and phosphasemibullvalenes, which have never been tested in Au(I)-catalyzed reactions before. Six different ligands have been employed: two benzophosphabarrelene derivatives (**3.12** and **3.45**), two trifluoromethyl-substituted phosphabarrelenes (**3.1** and **3.46**) and two 5-phosphasemibullvalene derivatives (**4.19** and **4.26**). The results are summarized in Table 15.

In the absence of [$AgSbF_6$], some of the catalysts are completely inactive and some show only low catalytic activity in the cycloisomerization of **5.9** (see entries 3, 7 and 9 *vs* entries 1, 5 and 11). On the other hand, a much higher activity for all the Au(I) complexes was observed in the presence of the additive. Catalysts based on benzophosphabarrelenes **3.12** and **3.45** performed similarly, and reached full conversion of the substrate selectively towards oxazoline **5.10** within 2.5 h (entries 2 and 4). Likewise, trifluoromethyl-substituted derivatives **3.1** and **3.46** yielded active and selective catalytic species with very high conversions (96% and >99%, respectively; entries 6 and 8). Finally, phosphasemibullvalenes **4.19** and **4.26** reacted similarly to the corresponding benzobarrelenes, fully converting the substrate to **5.10** in only slightly longer time (3 h *vs* 2.5 h; entries 10 and 12).

Table 15. Results for the catalytic cycloisomerization of substrate **5.9** to **5.10** and **5.11**. Conditions: catalyst precursor: 1 mol-%, additives: 1 mol-% [$AgSbF_6$], dichloromethane, room temperature.

Entry	Precatalyst	Additive	Time [h]	Conversion [%]	Product ratio (5.10 : 5.11)
1	[AuCl(**3.12**)]	-	24	50	92 : 8
2	[AuCl(**3.12**)]	$AgSbF_6$	**2.5**	**>99**	**1 : 0**
3	[AuCl(**3.45**)]	-	24	0	-
4	[AuCl(**3.45**)]	$AgSbF_6$	**2.5**	**>99**	**1 : 0**
5	[AuCl(**3.1**)]	-	24	65	3 : 1
6	[AuCl(**3.1**)]	$AgSbF_6$	6	96	98 : 2
7	[AuCl(**3.46**)]	-	24	0	-
8	[AuCl(**3.46**)]	$AgSbF_6$	5	>99	1 : 0
9	[AuCl(**4.19**)]	-	24	0	-
10	[AuCl(**4.19**)]	$AgSbF_6$	**3**	**>99**	**1 : 0**
11	[AuCl(**4.26**)]	-	24	62	98 : 2
12	[AuCl(**4.26**)]	$AgSbF_6$	**3**	**>99**	**1 : 0**

Interestingly, if the reaction mixture gets exposed to air for 16 h, the kinetic product **5.10** is converted into the thermodynamic product **5.11** (ΔE = -25.6 and -42.9 kcal/mol, respectively). This can be rationalized by the oxidation of Au(I) to Au(III), with the latter species being responsible for the cycloiosomerization of **5.9** to its oxazole isomer.[354] For this reason it is necessary to properly separate the gold species from the products, which can be done by filtrating the mixture over a small plug of silica using diethyl ethers as eluent.

Benzophosphabarrelenes **3.12** and **3.45** and the corresponding phosphasemibullvalenes **4.19** and **4.26** showed similar activities (2.5 and 3 h to full conversion), yet differences in the electronic properties have been observed, mainly between aryl- and TMS-substituted derivatives (Figure 60). In fact, the latter are both stronger σ-donors and weaker π-acceptors than the arylic-substituted counterparts. This results in a higher net-donation in the corresponding [$LNi(CO)_3$] complexes. The difference in the catalytic activity seems to be related to the steric bulk of the ligands, which is lower for 5-phosphasemibullvalenes (34.6 and 43.0 *vs* 29.9 and 35.6 %V_{Bur}). In fact, this could lead to less kinetically stable gold-complexes. Finally, trifluoromethyl-substituted phosphabarrelenes are suitable ligands for the selective conversion of **5.9** to oxazoline **5.10**, even though the substrate takes longer to be fully converted. The longer reaction time could be due to the weaker σ-donation of these ligands, which is comparable to that of phosphinines.

Interestingly, the comparison between benzophosphabarrelene **3.12** and trifluoromethyl-derivative **3.46** shows that even though the electronic properties of these ligands are almost identical (Table 12, Figure 60) a different reactivity is observed (full conversion in 2.5 *vs* 5 h). This can only be ascribed to the considerably different steric bulk of the two ligands (34.6 *vs* 49.5 %V_{Bur}).

In the literature, the reactivity of cationic Au(I) species is considered to strongly correlate with the stabilization of cationic intermediates by means of π-backbonding from the gold atom.[362] However, some theoretical studies state that this contribution has a marginal effect.[363,364] The results presented here suggest that the σ-donor properties of the ancillary ligands are the most important contribution for the achievement of a kinetically stable catalytic species. On the other hand, the big difference in the π-backdonation properties of the selected ligands is not reflected in the catalytic activity. This data suggest that the π-accepting properties of the ligand have a secondary role in this reaction, while the σ-donation and the steric bulk seem to be the most important.

A complex interplay between this two characteristics appears to be the key to a successful stabilization of the catalytic species. In this respect, bulky benzophosphabarrelene and related semibullvalenes are good candidates for this kind of reactions.

Finally, the cycloisomerization of **5.9** was followed over time for the best performing catalytic systems (based on **2.22**, **3.12** and **4.19**, respectively) and the conversion of the substrate was ascertained by means of ^{1}H NMR spectroscopy during specific time intervals. The corresponding conversion-time plot is depicted in Figure 62.

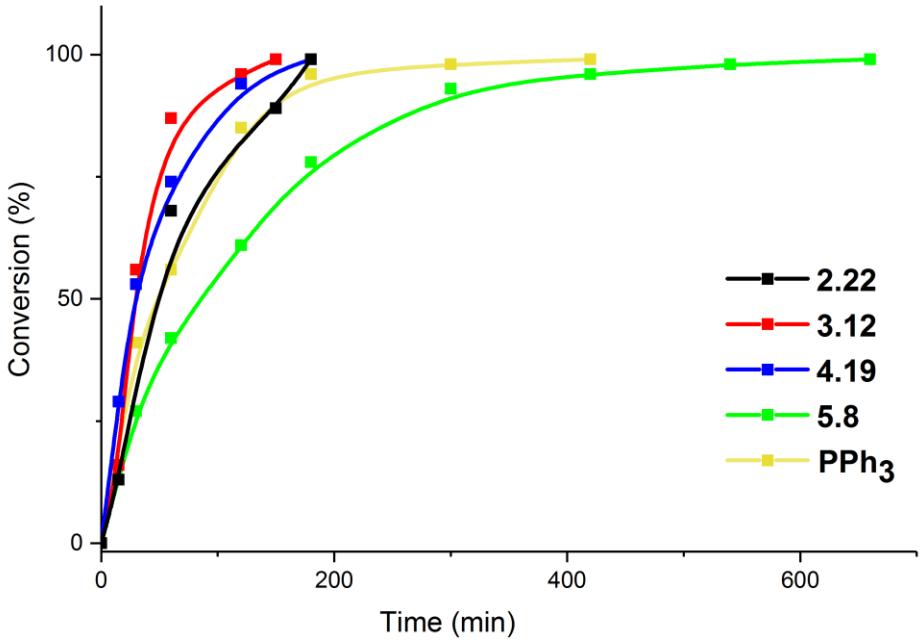

Figure 62. Conversion *vs* time plot for the catalytic systems based on **2.22**, **3.12**, **4.19** and the reference catalysts.

From the plot is it possible to extrapolate the turnover frequencies (TOF) values for these catalysts at 20% conversion, which are reported in Table 16.

Table 16. TOF values for the catalytic systems based on **2.22**, **3.12**, **4.19** and the reference catalysts.

Ligand	**TOF [h^{-1}]**
2.22	91
3.12	98
4.19	104
5.8	49
PPh_3	91

These values show that the activity of the catalytic systems described in this work are comparable with the reported data of state-of-the-art cationic phosphorus-based gold catalysts used for this particular substrate.[357,360,365] In particular, the highest value was observed for the 5-phosphasemibullvalene system (TOF = 104 h^{-1}).

5.3 Conclusions

The steric properties of phosphinines, phosphabarrelenes and 5-phosphasemibullvalenes have been evaluated in terms of their buried volume. For phosphinines the steric bulk is strongly related to the substituents on the α-carbon atoms, and not dependent from the substituents in the other positions. The corresponding phosphabarrelenes are remarkably sterically demanding, trifluoromethyl-substituted derivatives having the highest $\%V_{Bur}$. In contrast, 5-phosphasemibullvalenes are less bulky and have buried volume values which are similar to those of the corresponding phosphinine precursors.

The electronic properties of the ligands have been evaluated both experimentally and by using theoretical methods. The Tolman electronic parameter has been measured and calculated for a number of selected ligands, allowing for a comparison of the net-donation of the ligand classes. Trifluoromethyl-substituted phosphabarrelenes are the weakest donors, followed by phosphinines. The net-donation of phosphabarrelenes and phosphasemibullvalenes is higher and very similar, making them the strongest donors among the ligands of this work. ETS-NOCV calculations on $[LNi(CO)_3]$ and [LAuCl] complexes allowed for the evaluation of the single σ- and π-contributions to the L-M bond, thus giving a deeper insight in the electronic properties of these ligand classes.

Phosphinines, phosphabarrelenes and 5-phosphasemibullvalenes have been successfully employed for the first time in Au(I) catalyzed reactions. At least one compound from each ligand class was able to quantitatively and selectively perform the cycloisomerization of *N*-2-propyn-1-ylbenzamide towards its oxazoline constitutional isomer in a short time. The reported catalysts are faster and more efficient than those obtained from commercial ligands, such as triphenylphosphine. The results are comparable to the best catalyst which are known today.

Even though the strong π-accepting properties of these ligands could be beneficial for the formation of strongly electrophilic Au^+ centers, it seems like these properties have a minor role for the successful conversion of propargyl amides to oxazoline derivatives. The stabilization of the catalytic species appears to benefit from a relatively strong donation (stronger than regular phosphinines but weaker than regular phosphines) and large steric bulk.

5.4 Experimental part

General Remarks

Unless otherwise stated, all the experiments were performed under an inert argon atmosphere using modified Schlenk techniques or in a MBraun glovebox. The catalytic reactions were run in a MBraun glovebox in glass vials. All common chemicals were commercially available and were used as received. Dry or deoxygenated solvents were prepared using standard techniques or used from a MBraun solvent purification system. The NMR spectra were recorded on a JEOL ECX400 (400 MHz) spectrometer and chemical shifts are reported relative to the residual resonance in the deuterated solvents. IR spectra were measured on a Nicolet iS10 FTIR-ATR spectrometer by Thermo Scientific in the solid state and on a FT-IR spectrometer Vertex 70 by Bruker in dichloromethane.

The syntheses of the complexes discussed above have been reported in the previous chapters.

Calculations of %Vbur

The buried volume (%V_{bur}) was calculated according to literature and the values are reported in Table 17.[281] The recommended parameters have been used: 3.50 Å was selected as the value for the sphere radius, both 2.00 and 2.28 Å were considered as distances for the metal–ligand bond, hydrogen atoms were omitted, mesh spacing was set to 0.10 and scaled Bondi radii were used. The coordinates of the ligands were obtained from the crystal structures of the gold complexes. The coordinates of **3.46** were obtained from the crystal structure of the free ligand. The coordinates of **3.47** were obtained from the crystal structure of **3.45**. The coordinates of **4.26** were obtained from the crystal structure of its selenide. The coordinates of **2.2** and **2.25** were obtained from the crystal structure of [(**2.26**)AuCl] deleting the appropriate atoms. Coordinates of phosphite **5.8** were obtained from its crystal structure.[366]

Table 17. %V_{bur} at different L-M distances for the given ligands.

Ligand	**2.1**	**2.2**	**2.22**	**2.25**	**2.26**	**3.1**	**3.12**	**3.45**	**3.46**	**3.47**	**4.19**	**4.26**	**5.8**
2.28 Å	29.2	20.1	29.7	20.1	38.0	39.5	34.6	43.0	49.5	23.3	31.8	35.6	42.7
2.00 Å	33.1	23.1	33.8	23.1	42.3	44.4	39.3	48.1	54.7	27.3	36.6	40.8	47.6

5.4.1 DFT calculations

Additional informations can be found in the attachment.

Products 5.10 and 5.11

DFT calculations were performed at the B3PW91[367,368]/6-31G*[369,370] level using Gaussian09 (Revision D.01).[260]

Ni

Density functional calculations were performed with Gaussian 09[260], Revision D01 at the B3PW91[367,368]-6-31G(d)[369,370] level. For Ni: LanL2DZ[371] was used with an additional f-polarization function[372]. Frequency analyses were performed at the same level of theory and for the CO vibration with A_1 symmetry a scaling factor of 0.9753[373] was applied. The ETS-NOCV[328] analyses were performed at the PW91/TZ2P[374–377] level of theory using ADF2016.102[378–380], after an optimization at the PW91/TZ2P level of theory using ADF2016.105.

Table 18. ETS-NOCV results for $LNi(CO)_3$ complexes using PW91/TZ2P (kcal mol^{-1}).

Ligand	Ni-P (Å)	ΔE_{total}	ΔE_{Pauli}	ΔE_{elstat}	ΔE_{orb}	σ	$\pi^{\parallel}$	$\pi^{\square}$	π_{total}
P*t*Bu$_3$	2.301	-37.90	104.91	-95.70	-47.10	-27.94	-5.76	-5.75	-11.51
2.2	2.201	-32.24	97.80	-83.96	-46.08	-22.01	-9.51	-7.58	-17.09
2.1	2.210	-31.06	97.39	-81.51	-46.94	-21.32	-9.94	-7.74	-17.67
2.26	2.266	-30.15	93.40	-78.28	-45.28	-21.67	-8.73	-6.50	-15.23
2.25	2.194	-32.40	100.58	-86.04	-46.94	-22.49	-9.61	-7.65	-17.26
3.19	2.235	-34.58	102.62	-90.10	-47.09	-24.31	-7.57	-7.63	-15.20
3.45	2.264	-33.81	104.18	-91.52	-46.48	-24.98	-6.68	-6.72	-13.41
3.47	2.214	-36.56	108.32	-97.54	-47.34	-26.30	-7.34	-7.06	-14.40
3.1	2.228	-31.24	98.16	-82.73	-46.67	-21.24	-9.12	-8.20	-17.33
3.46	2.283	-30.24	93.09	-79.94	-43.39	-21.02	-7.39	-6.83	-14.22
4.19	2.217	-36.27	104.22	-91.98	-48.51	-25.08	-8.43	-7.39	-15.82
4.28	2.246	-36.15	102.91	-91.82	-47.24	-25.11	-7.63	-6.43	-14.06

Au

The density functional calculations, the geometry optimization and ETS-NOCV[328] analyses were performed at the ZORA-PW91/TZ2P[374–377] level of theory using ADF2016.105[378–380] and ADF2016.102 respectively.

Table 19. ETS-NOCV results using ZORA-PW91/TZ2P for LAuCl (kcal mol^{-1}).

Ligand	Au-P (Å)	ΔE_{total}	ΔE_{Pauli}	ΔE_{elstat}	ΔE_{orb}	σ	$\pi^{\parallel}$	$\pi^{\perp}$	π_{total}
2.1	2.240	-56.86	170.92	-151.71	-76.07	-37.11	-12.46	-10.11	-22.57
2.26	2.278	-62.13	174.70	-161.11	-75.72	-39.44	-12.21	-9.83	-22.04
2.25	2.212	-58.96	163.77	-150.48	-72.25	-38.37	-12.75	-10.71	-23.46
3.19	2.280	-64.65	177.74	-169.04	-73.35	-39.93	-10.45	-10.40	-20.85
3.45	2.243	-68.27	187.8	-181.84	-74.23	-40.89	-9.69	-9.48	-19.17
3.47	2.227	-66.15	177.64	-172.31	-71.47	-40.66	-10.20	-10.06	-20.26
3.1	2.230	-58.68	169.37	-154.02	-74.04	-38.45	-11.82	-11.09	-22.91
3.46	2.239	-63.06	181.91	-170.11	-74.87	-39.39	-10.73	-10.22	-20.95
4.19	2.229	-65.53	175.34	-166.46	-74.41	-40.91	-11.18	-10.17	-21.35
4.28	2.233	-68.92	182.66	-176.70	-74.88	-41.89	-10.49	-9.69	-20.19
PPh_3	2.247	-66.47	174.70	-168.05	-73.12	-42.69	-9.44	-9.43	-18.87

General procedure for the catalytic cycloisomerization with phosphinine complexes

A solution of [LAuCl] (0.0084 mmol, 1 mol-%) and the additive [$AgSbF_6$] (1 equiv.) or [$Cu(OTf)_2$] (5 equiv.) in dichloromethane was added to the substrate (0.84 mmol) in CH_2Cl_2 (5 mL in total). The solution was stirred at room temperature in the dark for the given time. Samples were taken after different reaction times. For that, a little sample was taken with a syringe and filtered over a little plug of silica in case of [$Cu(OTf)_2$], or Celite in case of [$AgSbF_6$] and the plugs were eluted with dichloromethane. The solvent was removed *in vacuo* and conversions were detected by ^1H NMR spectroscopy.

General procedure for the catalytic cycloisomerization with phosphabarrelene and phosphasemibullvalene complexes

A solution of [LAuCl] (0.0084 mmol, 1 mol-%) and the additive [$AgSbF_6$] (1 equiv.) or [$Cu(OTf)_2$] (5 equiv.) in dichloromethane was added to the substrate (0.84 mmol) in CH_2Cl_2 (4 mL in total). The solution was stirred at room temperature in the dark for the given time. Samples were taken after different reaction times. For that, a little sample was taken with a syringe and filtered over Celite. The solvent was removed *in vacuo* and conversions were

detected by ^{1}H NMR spectroscopy. To isolate pure product **5.10** and prevent isomerization to **5.11**, the crude mixture was purified by filtration over a plug of silica (4 cm, in a pipette) using diethyl ether as eluent.

6. Summary and Outlook

This Ph.D. thesis deals with the synthesis and characterization of new phosphinine-based ligands and their application in homogeneous catalysis.

In Chapter 2 an improved synthesis of 2,4,6-triarylphosphinines is presented. Starting from pyrylium salts, the use of a strong nucleophile in the O^+/P exchange in combination with salt elimination resulted in higher yields. By optimizing the reaction conditions it was found that $LiP(TMS)_2$ is the best candidate for the synthesis of these heterocycles (Scheme 66). Also, parameters such as time, temperature, solvent, stoichiometry and counterion have been screened and the best reaction conditions have been found.

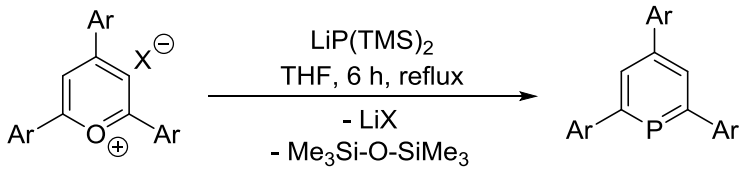

Scheme 66. Synthesis of phosphinines using $LiP(TMS)_2$ as phosphorus source.

In Chapter 3, new phosphabarrelene derivatives have been synthesized via [4+2] cycloaddition reaction between a phosphinine ring and an alkyne, namely hexafluoro-2-butyne or *in situ* generated benzyne (Scheme).

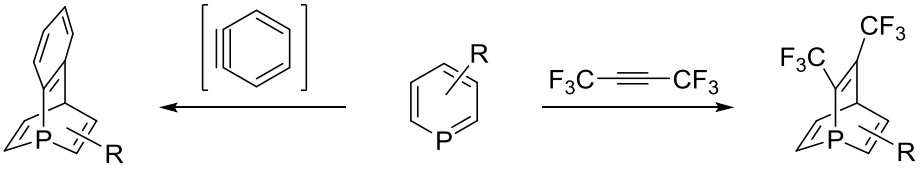

Scheme 67. [4+2] cycloaddition of a phosphinine to a phosphabarrelene.

Different benzyne precursors were tested, in order to establish new functional group tolerant pathways. In this respect, iodophenylsulfonates were found to be suitable. This allowed for further mechanistic insights. The reaction proceeds *via* a concerted Diels-Alder reaction of an aryne with a phosphinine ring, and no λ^4-phosphinine intermediate is involved in the process.

Some phosphabarrelene derivatives showed to be prone to cycloreversion reactions, yielding new phosphinine derivatives. Among these, an asymmetrically substituted phosphinine was obtained in high yields. This electron-poor compound showed interesting properties for the activation of small molecules at the low-coordinate P center (Figure 63). Interestingly, this is a rare example of small molecule activation by main group elements. Meticulous studies on the electronic properties of this phosphinine are envisaged. Also, a deep investigation of the

scope of the activation of small molecules is the objective of the future studies. In this respect, the activation of substrates such as ammonia, amines and alcohols is particularly interesting.

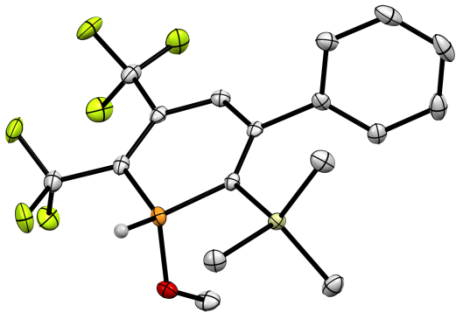

Figure 63. Activation of MeOH by a phosphinine derivative.

The oxidation of phosphabarrelenes was investigated. Oxidized benzophosphabarrelene derivatives with O, S, Se have been synthesized, fully characterized and compared structurally. Trifluoromethyl-substituted phosphabarrelenes are more difficult to oxidize with chalcogens and only oxides were obtained.

Chapter 4 is about 5-phosphasemibullvalenes. These derivatives have been described in here for the first time. A synthetic path for the synthesis of this new class of chiral molecules based on the skeleton of 2,4,6-triarylsubstituted phosphinines has been presented. Phosphabarrelenes, their oxidized derivatives and metal complexes undergo quantitative di-π-methane rearrangement upon irradiation with UV light (Scheme).

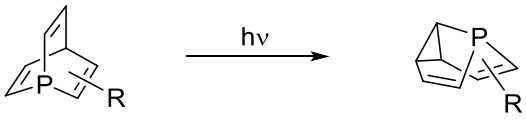

Scheme 68. Photoisomerization of phosphabarrelene to phosphasemibullvalene.

The reaction mechanism was investigated by means of DFT calculations, which are supported by several experiments, giving an insight in the selectivity of the reaction in the case of asymmetrically-substituted phosphabarrelenes. The substrate scope has been extended to differently substituted benzobarrelenes and the photoisomerization of trifluoromethyl-substituted molecules was investigated. Different substitution patterns can be investigated in the future to assess the selectivity of the reaction.

The oxidation of 5-phosphasemibullvalenes has been reported and some chalcogenide derivatives have been fully characterized.

Differently from other similar molecules, 5-phosphasemibullvalenes proved to be thermally stable and suitable for coordination to metal centers. The first metal complexes have been reported and fully characterized.

Finally, in Chapter 5 the properties of phosphinines, phosphabarrelenes and 5-phosphasemibullvalenes have been studied and compared.

The steric properties were evaluated in terms of buried volume. The electronic properties of the ligands have been assessed both experimentally and by using theoretical methods. Metal-carbonyl complexes of W(0) and Ni(0) were synthesized, in order to evaluate and compare the electronic properties by means of IR spectroscopy. The Tolman electronic parameter was measured and calculated for a number of selected ligands, allowing for a comparison of the net-donation among the ligand classes. ETS-NOCV calculations on $[LNi(CO)_3]$ and [LAuCl] complexes allowed for the estimation of the single σ- and π-contributions to the L-M bond, thus giving a deeper insight in the electronic properties of these compounds.

New gold complexes have been synthesized and fully characterized. Phosphinines, phosphabarrelenes and 5-phosphasemibullvalenes have been successfully employed for the first time in Au(I) catalyzed reactions. At least one compound from each ligand class was able to quantitatively and selectively perform the cycloisomerization of *N*-2-propyn-1-ylbenzamide towards its oxazoline constitutional isomer in a short time. The reported catalysts are faster and more efficient than those obtained from commercial ligands, such as triphenylphosphine. The results are comparable to the best catalyst which are known today.

From the obtained results, it appears that the stabilization of the catalytic species benefits from a relatively strong donation (stronger than regular phosphinines but weaker than regular phosphines) and large steric bulk, while the π-contribution has a minor role.

To conclude, phosphinines, phosphabarrelenes and 5-phosphasemibullvalenes are promising ligands for catalytic applications. Even though only a few examples have been reported in the literature, these ligands proved to be able to achieve unprecedented results in homogeneous catalysis. In particular, 5-phosphasemibullvalenes are a new class of chiral ligands. Chiral resolution of the enantiomers is currently being performed, in order to employ the enantiomerically pure ligands in asymmetric homogeneous catalysis. As phosphinines and phosphabarrelenes have been successfully employed in hydroformylation reactions, these will be the objective of the next studies.

7. References

(1) *Ullmann's Encyclopedia of Industrial Chemistry - Phosphate Fertilizers*; John Wiley & Sons, **2000**.
(2) Kollár, L.; Keglevich, G.; Kolla, L. *Chem. Rev.* **2010**, *110* (7), 4257.
(3) Lüssem, B.; Riede, M.; Leo, K. *Phys. status solidi* **2013**, *210* (1), 9.
(4) Priegert, A. M.; Rawe, B. W.; Serin, S. C.; Gates, D. P. *Chem. Soc. Rev.* **2016**, *45* (4), 922.
(5) Hissler, M.; Lescop, C.; Réau, R. *J. Organomet. Chem.* **2005**, *690* (10), 2482.
(6) Hissler, M.; Lescop, C.; Réau, R. *Pure Appl. Chem.* **2007**, *79* (2), 201.
(7) Müller, C. *et al.* in *Phosphorus Ligands in Asymmetric Catalysis*; Wiley, **2008**.
(8) Müller, C. *et al.* in *Phosphorus Compounds: Advanced Tools in Catalysis and Material Sciences*; Peruzzini, M., Gonsalvi, L., Eds.; Springer, **2011**.
(9) Müller, C. *et al.* in *Phosphorus(III) Ligands in Homogeneous Catalysis*; Kamer, P. C. J., van Leeuwen, P. W. N. M., Eds.; John Wiley & Sons, **2012**.
(10) List, B. *Chem. Rev.* **2007**, *107* (12), 5413.
(11) Methot, J. L.; Roush, W. R. *Adv. Synth. Catal.* **2004**, *346* (9–10), 1035.
(12) Wei, Y.; Shi, M. *Chem. - Asian J.* **2014**, *9* (10), 2720.
(13) Xiao, Y.; Sun, Z.; Guo, H.; Kwon, O. *Beilstein J. Org. Chem.* **2014**, *10*, 2089.
(14) Hissler, M.; Dyer, P. W.; Reau, R. *Top. Curr. Chem.* **2005**, *250*, 127.
(15) Baumgartner, T.; Réau, R. *Chem. Rev.* **2006**, *106* (11), 4681.
(16) Ren, Y.; Baumgartner, T. *Dalton Trans.* **2012**, *41* (26), 7792.
(17) He, X.; Baumgartner, T. *RSC Adv.* **2013**, *3* (29), 11334.
(18) Baumgartner, T. *Acc. Chem. Res.* **2014**, *47* (5), 1613.
(19) Duffy, M. P.; Bouit, P.-A.; Geffroy, B.; Tondelier, D.; Hissler, M. *Phosphorus Sulfur Silicon Relat. Elem.* **2015**, *190* (5–6), 845.
(20) Reus, C.; Baumgartner, T. *Dalton Trans.* **2016**, *45* (5), 1850.
(21) Shameem, M. A.; Orthaber, A. *Chem. - Eur. J.* **2016**, *22* (31), 10718.
(22) Mathey, F. *Angew. Chem. Int. Ed.* **2003**, *42* (14), 1578.
(23) Corriu, R. J. P.; Dutheil, J. P.; Lanneau, G. F. *J. Am. Chem. Soc.* **1984**, *106* (4), 1060.
(24) Lanneau, G. F. *Phosphorous Sulfur Relat. Elem.* **1986**, *27* (1–2), 43.
(25) Corriu, R. J. P.; Lanneau, G. F.; Leclercq, D. *Tetrahedron* **1989**, *45* (7), 1959.
(26) Mathey, F. *et al.* in *Phosphorus: the Carbon Copy*; Dillon, K. B., Mathey, F., Nixon, J. F., Eds.; John Wiley & Sons, **1998**.
(27) *CRC Handbook of Chemistry and Physics*; Haynes, W. M., Ed.; CRC Press, Taylor & Francis, **2016**.
(28) Mathey, F. in *Phosphorus-Carbon Heterocyclic Chemistry: The Rise of a New Domain*; Mathey, F., Ed.; Pergamon, **2001**.
(29) Mathey, F. *Dalton Trans.* **2007**, No. 19, 1861.
(30) Aktaş, H.; Slootweg, J. C.; Lammertsma, K. *Angew. Chem. Int. Ed.* **2010**, *49* (12), 2102.
(31) Liu, L.; Ruiz, D. A.; Munz, D.; Bertrand, G. *Chem* **2016**, *1* (1), 147.
(32) Markovski, L. N.; Romanenko, V. D. *Tetrahedron* **1989**, *45* (19), 6019.
(33) Regitz, M. *Chem. Rev.* **1990**, *90* (1), 191.
(34) Le Floch, P. *Coord. Chem. Rev.* **2006**, *250* (3), 627.
(35) Mathey, F. *Chem. Rev.* **1988**, *88* (2), 429.
(36) Märkl, G. *Angew. Chem. Int. Ed.* **1966**, *5* (9), 846.
(37) Märkl, G.; Lieb, F. *Angew. Chem. Int. Ed.* **1968**, *7* (9), 733.
(38) Jutzi, P. *Angew. Chem. Int. Ed.* **1975**, *14* (4), 232.
(39) Ashe III, A. J. *J. Am. Chem. Soc.* **1971**, *93* (13), 3293.
(40) Baldridge, K. K.; Gordon, M. S. *J. Am. Chem. Soc.* **1988**, *110* (13), 4204.

(41) Chamizo, J. A.; Morgado, J.; Sosa, P. *Organometallics* **1993**, *12* (12), 5005.
(42) Frison, G.; Sevin, A.; Avarvari, N.; Mathey, F.; Le Floch, P. *J. Org. Chem.* **1999**, *64* (15), 5524.
(43) Bart, J. C. J. *Angew. Chem. Int. Ed.* **1968**, *7* (9), 730.
(44) Batich, C.; Heilbronner, E.; Hornung, V.; Ashe, A. J.; Clark, D. T.; Cobley, U. T.; Kilcast, D.; Scanlan, I. *J. Am. Chem. Soc.* **1973**, *95* (3), 928.
(45) Mézailles, N.; Mathey, F.; Le Floch, P. *Progress in Inorganic Chemistry*, **2001**, 455.
(46) Pham-Tran, N.-N.; Bouchoux, G.; Delaere, D.; Nguyen, M. T. *J. Phys. Chem. A* **2005**, *109* (12), 2957.
(47) Loibl, A.; de Krom, I.; Pidko, E. A.; Weber, M.; Wiecko, J.; Müller, C. *Chem. Commun.* **2014**, *50* (64), 8842.
(48) Müller, C.; Sklorz, J. A. W.; de Krom, I.; Loibl, A.; Habicht, M.; Bruce, M.; Pfeifer, G.; Wiecko, J. *Chem. Lett.* **2014**, *43* (9), 1390.
(49) Tolman, C. A. *Chem. Rev.* **1977**, *77* (3), 313.
(50) Müller, C.; Broeckx, L. E. E.; de Krom, I.; Weemers, J. J. M. *Eur. J. Inorg. Chem.* **2013**, *2*, 187.
(51) DiMauro, E. F.; Kozlowski, M. C. *J. Chem. Soc. Perkin Trans. 1* **2002**, 3, 439.
(52) Nakajima, K.; Takata, S.; Sakata, K.; Nishibayashi, Y. *Angew. Chem. Int. Ed.* **2015**, *54* (26), 7597.
(53) Märkl, G.; Lieb, F.; Merz, A. *Angew. Chemie* **1967**, *79* (10), 475.
(54) Paciello, R.; Zeller, E.; Breit, B.; Röper, M. (to BASF). DE 19743197 A1, 1999.
(55) Mackewitz, T.; Röper, M. (to BASF). EP 1036796 A1, 2000.
(56) Breit, B.; Winde, R.; Mackewitz, T. *Chem. - Eur. J.* **2001**, *7* (14), 3106.
(57) Märkl, G.; Lieb, F.; Merz, A. *Angew. Chem. Int. Ed.* **1967**, *6* (11), 944.
(58) Arnold, P. L.; Petrukhina, M. A.; Bochenkov, V. E.; Shabatina, T. I.; Zagorskii, V. V.; Sergeev, G. B.; Cloke, F. G. N. *J. Organomet. Chem.* **2003**, *688* (1–2), 49.
(59) Balaban, T. S.; Balaban, A. T. *Sci. Synth.* **2003**, *14*, 11.
(60) Rösch, W.; Regitz, M. *Zeitschrift für Naturforsch. B* **1986**, *41* (7), 524.
(61) Regitz, M.; Binger, P. *Angew. Chem. Int. Ed.* **1988**, *27* (11), 1484.
(62) Chen, X.; Alidori, S.; Puschmann, F. F.; Santiso-Quinones, G.; Benkő, Z.; Li, Z.; Becker, G.; Grützmacher, H.-F.; Grützmacher, H. *Angew. Chem. Int. Ed.* **2014**, *53* (6), 1641.
(63) Chen, X.; Li, Z.; Yanan, F.; Grützmacher, H. *Eur. J. Inorg. Chem.* **2016**, *5*, 633.
(64) Habicht, M. H.; Wossidlo, F.; Weber, M.; Müller, C. *Chem. - Eur. J.* **2016**, *22* (36), 12877.
(65) Märkl, G.; Dörges, C.; Riedl, T.; Klärner, F.-G.; Lodwig, C. *Tetrahedron Lett.* **1990**, *31* (32), 4589.
(66) Avarvari, N.; Le Floch, P.; Mathey, F. *J. Am. Chem. Soc.* **1996**, *118* (47), 11978.
(67) Avarvari, N.; Le Floch, P.; Ricard, L.; Mathey, F. *Organometallics* **1997**, *16* (19), 4089.
(68) Zhang, Y.; Tham, F. S.; Nixon, J. F.; Taylor, C.; Green, J. C.; Reed, C. A. *Angew. Chem. Int. Ed.* **2008**, *47* (20), 3801.
(69) Hettche, A.; Dimroth, K. *Chem. Ber.* **1973**, *106* (3), 1001.
(70) Dimroth, K. in *Phosphorus-Carbon Double Bonds*; Fortschritte der Chemischen Forschung; Springer, **1973**.
(71) Dimroth, K.; Städe, W. *Angew. Chem. Int. Ed.* **1968**, *7* (11), 881.
(72) Pfeifer, G.; Müller, C., *unpublished results.*
(73) Moores, A.; Cantat, T.; Ricard, L.; Mézailles, N.; Le Floch, P. *New J. Chem.* **2007**, *31* (8), 1493.
(74) Pfeifer, G.; Ribagnac, P.; Le Goff, X.-F.; Wiecko, J.; Mézailles, N.; Müller, C. *Eur. J. Inorg. Chem.* **2015**, *2*, 240.
(75) Kanter, H.; Mach, W.; Dimroth, K. *Chem. Ber.* **1977**, *110* (2), 395.
(76) Papke, M.; Müller, C., *unpublished results*.

(77) Dimroth, K.; Steuber, F. W. *Angew. Chem.* **1967**, *79* (9), 410.
(78) Dimroth, K.; Greif, N.; Perst, H.; Steuber, F. W.; Sauer, W.; Duttka, L. *Angew. Chemie* **1967**, *79* (1), 58.
(79) Gerson, F.; Merstetter, P.; Pfenninger, S.; Märkl, G. *Magn. Reson. Chem.* **1997**, *35* (6), 384.
(80) Choua, S.; Dutan, C.; Cataldo, L.; Berclaz, T.; Geoffroy, M.; Mézailles, N.; Moores, A.; Ricard, L.; Le Floch, P. *Chem. - Eur. J.* **2004**, *10* (16), 4080.
(81) Märkl, G.; Lieb, F.; Merz, A. *Angew. Chemie* **1967**, *79* (1), 59.
(82) Bruce, M.; Meissner, G.; Weber, M.; Wiecko, J.; Müller, C. *Eur. J. Inorg. Chem.* **2014**, *10*, 1719.
(83) Moores, A.; Ricard, L.; Le Floch, P. *Angew. Chem. Int. Ed.* **2003**, *42* (40), 4940.
(84) Le Floch, P.; Mathey, F. *Coord. Chem. Rev.* **1998**, *178*, 771.
(85) Le Floch, P. *Coord. Chem. Rev.* **2006**, *250* (5–6), 627.
(86) Mézailles, N.; Le Floch, P.; Waschbüsch, K.; Ricard, L.; Mathey, F.; Kubiak, C. P. *J. Organomet. Chem.* **1997**, *541* (1–2), 277.
(87) Floch, P. Le. In *Topics in Heterocyclic Chemistry* **2008**, *10*, 147.
(88) Mathey, F.; Le Floch, P. *Sci. Synth.* **2005**, *15*, 1097.
(89) Deberitz, J.; Nöth, H. *J. Organomet. Chem.* **1973**, *49* (2), 453.
(90) Vahrenkamp, H.; Nöth, H. *Chem. Ber.* **1973**, *106* (7), 2227.
(91) Deberitz, J.; Nöth, H. *Chem. Ber.* **1970**, *103* (8), 2541.
(92) Vahrenkamp, H.; Nöth, H. *Chem. Ber.* **1972**, *105* (4), 1148.
(93) Doux, M.; Ricard, L.; Mathey, F.; Floch, P. Le; Mézailles, N. *Eur. J. Inorg. Chem.* **2003**, *4*, 687.
(94) Elschenbroich, C.; Baer, F.; Bilger, E.; Mahrwald, D.; Nowotny, M.; Metz, B. *Organometallics* **1993**, *12* (8), 3373.
(95) Nainan, K. C.; Sears, C. T. *J. Organomet. Chem.* **1978**, *148* (3), C31.
(96) Mao, Y.; Lim, K. M. H.; Li, Y.; Ganguly, R.; Mathey, F. *Organometallics* **2013**, *32* (12), 3562.
(97) Reetz, M. T.; Bohres, E.; Goddard, R.; Holthausen, M. C.; Thiel, W. *Chem. - Eur. J.* **1999**, *5* (7), 2101.
(98) Schmid, B.; Venanzi, L. M.; Albinati, A.; Mathey, F. *Inorg. Chem.* **1991**, *30* (25), 4693.
(99) Bruce, M.; Müller, C., *unpublished results*.
(100) Arce, A. J.; Deeming, A. J.; Sanctis, Y. De; Manzur, J. *J. Chem. Soc. Chem. Commun.* **1993**, *5* (3), 325.
(101) Rosa, P.; Le Floch, P.; Ricard, L.; Mathey, F. *J. Am. Chem. Soc.* **1997**, *119* (40), 9417.
(102) Shiotsuka, M.; Matsuda, Y. *Chem. Lett.* **1994**, *23* (2), 351.
(103) Giese, S.; Müller, C., *unpublished results*.
(104) Roesch, P.; Nitsch, J.; Lutz, M.; Wiecko, J.; Steffen, A.; Müller, C. *Inorg. Chem.* **2014**, *53* (18), 9855.
(105) Müller, C.; Broeckx, L. E. E.; de Krom, I.; Weemers, J. J. M. *Eur. J. Inorg. Chem.* **2013**, *2*, 187.
(106) Müller, C.; Wasserberg, D.; Weemers, J. J. M.; Pidko, E. A.; Hoffmann, S.; Lutz, M.; Spek, A. L.; Meskers, S. C. J.; Janssen, R. A. J.; van Santen, R. A.; Vogt, D. *Chem. - Eur. J.* **2007**, *13* (16), 4548.
(107) Alcaraz, J.-M.; Breque, A.; Mathey, F. *Tetrahedron Lett.* **1982**, *23* (15), 1565.
(108) Breque, A.; Santini, C. C.; Mathey, F.; Fischer, J.; Mitschler, A. *Inorg. Chem.* **1984**, *23* (22), 3463.
(109) Schmid, B.; Venanzi, L. M.; Gerfin, T.; Gramlich, V.; Mathey, F. *Inorg. Chem.* **1992**, *31* (24), 5117.
(110) Breit, B. *J. Mol. Catal. A Chem.* **1999**, *143* (1–3), 143.
(111) Carrasco, A. C.; Pidko, E. A.; Masdeu-Bultó, A. M.; Lutz, M.; Spek, A. L.; Vogt, D.; Müller,

C. *New J. Chem.* **2010**, *34* (8), 1547.
(112) Campos-Carrasco, A.; Broeckx, L. E. E.; Weemers, J. J. M.; Pidko, E. A.; Lutz, M.; Masdeu-Bultó, A. M.; Vogt, D.; Müller, C. *Chem. - Eur. J.* **2011**, *17* (8), 2510.
(113) de Krom, I.; Broeckx, L. E. E.; Lutz, M.; Müller, C. *Chem. - Eur. J.* **2013**, *19* (11), 3676.
(114) de Krom, I.; Pidko, E. A.; Lutz, M.; Müller, C. *Chem. - Eur. J.* **2013**, *19* (23), 7523.
(115) de Krom, I.; Lutz, M.; Müller, C. *Dalton Trans.* **2015**, *44* (22), 10304.
(116) Müller, C.; Pidko, E. a.; Lutz, M.; Spek, A. L.; Vogt, D. *Chem. - Eur. J.* **2008**, *14* (29), 8803.
(117) Doux, M.; Mézailles, N.; Melaimi, M.; Ricard, L.; Le Floch, P. *Chem. Commun.* **2002**, *377* (15), 1566.
(118) Doux, M.; Bouet, C.; Mézailles, N.; Ricard, L.; Le Floch, P. *Organometallics* **2002**, *21* (13), 2785.
(119) Doux, M.; Mézailles, N.; Ricard, L.; Le Floch, P. *Eur. J. Inorg. Chem.* **2003**, *21*, 3878.
(120) Dochnahl, M.; Doux, M.; Faillard, E.; Ricard, L.; Le Floch, P. *Eur. J. Inorg. Chem.* **2005**, *1*, 125.
(121) Broeckx, L. E. E.; Lutz, M.; Vogt, D.; Müller, C. *Chem. Commun.* **2011**, *47* (7), 2003.
(122) Broeckx, L. E. E.; Delaunay, W.; Latouche, C.; Lutz, M.; Boucekkine, A.; Hissler, M.; Müller, C. *Inorg. Chem.* **2013**, *52* (19), 10738.
(123) Broeckx, L. E. E.; Güven, S.; Heutz, F. J. L.; Lutz, M.; Vogt, D.; Müller, C. *Chem. - Eur. J.* **2013**, *19* (39), 13087.
(124) Broeckx, L. E. E.; Bucci, A.; Zuccaccia, C.; Lutz, M.; Macchioni, A.; Müller, C. *Organometallics* **2015**, *34* (12), 2943.
(125) Juris, A.; Balzani, V.; Barigelletti, F.; Campagna, S.; Belser, P.; von Zelewsky, A. *Coord. Chem. Rev.* **1988**, *84*, 85.
(126) Le Floch, P.; Carmichael, D.; Ricard, L.; Mathey, F. *J. Am. Chem. Soc.* **1991**, *113* (2), 667.
(127) Trauner, H.; Le Floch, P.; Lefour, J.-M.; Ricard, L.; Mathey, F. *Synthesis - Stuttgart* **1995**, *6*, 717.
(128) Le Floch, P.; Ricard, L.; Mathey, F. *Bull. Soc. Chim. Fr.* **1994**, *131* (3), 330.
(129) Holand, S.; Ricard, L.; Mathey, F. *J. Org. Chem.* **1991**, *56* (12), 4031.
(130) Rosa, P.; Mézailles, N.; Mathey, F.; Le Floch, P. *J. Org. Chem.* **1998**, *63* (14), 4826.
(131) Mathey, F.; Le Floch, P. *Chem. Ber.* **1996**, *129* (3), 263.
(132) Rosa, P.; Ricard, L.; Mathey, F.; Le Floch, P. *Organometallics* **1999**, *18* (17), 3348.
(133) Choua, S.; Sidorenkova, H.; Berclaz, T.; Geoffroy, M.; Rosa, P.; Mézailles, N.; Ricard, L.; Mathey, F.; Le Floch, P. *J. Am. Chem. Soc.* **2000**, *122* (49), 12227.
(134) Rosa, P.; Mézailles, N.; Ricard, L.; Mathey, F.; Le Floch, P.; Jean, Y. *Angew. Chem. Int. Ed.* **2001**, *40* (7), 1251.
(135) Heift, D.; Benkő, Z.; Grützmacher, H. *Dalton Trans.* **2014**, *43* (15), 5920.
(136) Jupp, A. R.; Geeson, M. B.; McGrady, J. E.; Goicoechea, J. M. *Eur. J. Inorg. Chem.* **2016**, *5*, 639.
(137) Fritz, G.; Hölderich, W. *Z. Anorg. Allg. Chem.* **1976**, *422* (2), 104.
(138) Uhlig, F.; Gremler, S.; Dargatz, M.; Scheer, M.; Herrmann, E. *Z. Anorg. Allg. Chem.* **1991**, *606* (1), 105.
(139) Müller, C.; Pidko, E. A.; Totev, D.; Lutz, M.; Spek, A. L.; van Santen, R. A.; Vogt, D. *Dalton Trans.* **2007**, *46*, 5372.
(140) Müller, C.; Pidko, E. a.; Staring, A. J. P. M.; Lutz, M.; Spek, A. L.; Van Santen, R. a.; Vogt, D. *Chem. - Eur. J.* **2008**, *14* (16), 4899.
(141) Stott, J.; Bruhn, C.; Siemeling, U. *Zeitschrift für Naturforsch. B* **2013**, *68* (8), 2.
(142) Rigo, M.; Hettmanczyk, L.; Heutz, F. J. L.; Hohloch, S.; Lutz, M.; Sarkar, B.; Müller, C. *Dalton Trans.* **2017**, *46* (1), 86.
(143) Mézailles, N.; Ricard, L.; Mathey, F.; Le Floch, P. *Eur. J. Inorg. Chem.* **1999**, *1999* (12), 2233.

(144) Bhattacharyya, K.; Mézailles, N., *unpublished results*.
(145) Rigo, M.; Sklorz, J. A. W.; Hatje, N.; Noack, F.; Weber, M.; Wiecko, J.; Müller, C. *Dalton Trans.* **2016**, *45* (5), 2218.
(146) Schäfer, H.; Fritz, G.; Hölderich, W. *Z. Anorg. Allg. Chem.* **1977**, *428* (1), 222.
(147) Hendriksen, J. H.; Gruetzmacher, H. *PhD thesis* **2012**.
(148) Suter, R.; Benkő, Z.; Grützmacher, H. *Chem. - Eur. J.* **2016**, *22* (42), 14979.
(149) Allspach, T.; Regitz, M.; Becker, G.; Becker, W. *Synthesis - Stuttgart* **1986**, *1986* (1), 31.
(150) Mansell, S. M.; Green, M.; Kilby, R. J.; Murray, M.; Russell, C. A. *C. R. Chim.* **2010**, *13* (8–9), 1073.
(151) Strohmeier, W.; Shönuer, G. *Chem. Ber.* **1961**, *94* (5), 1346.
(152) Dash, K. C.; Eberlein, J.; Schmidbaur, H. *Syn. React. Inorg. Met.* **1973**, *3* (4), 375.
(153) Heutz, F. J. L.; Müller, C., *unpublished results*.
(154) Strohmeier, W.; Müller, F.-J. *Chem. Ber.* **1969**, *102* (10), 3608.
(155) Bruker, Bruker AXS Inc., Madison, Wisconsin, USA.
(156) Sheldrick, G. M. *Acta Crystallogr. A* **2008**, *64* (1), 112.
(157) Spek, A. L. *Acta Crystallogr. D* **2009**, *65* (2), 148.
(158) Hübschle, C. B.; Sheldrick, G. M.; Dittrich, B. *J. Appl. Crystallogr.* **2011**, *44* (6), 1281.
(159) Ashe, A. J.; Gordon, M. D. *J. Am. Chem. Soc.* **1970**, *10*, 7596.
(160) Märkl, G.; Lieb, F.; Martin, C. *Tetrahedron Lett.* **1971**, *12* (17), 1249.
(161) Märkl, G.; Heier, K. H. *Tetrahedron Lett.* **1974**, *15* (49–50), 4369.
(162) Piechaczyk, O.; Doux, M.; Ricard, L.; le Floch, P. *Organometallics* **2005**, *24* (6), 1204.
(163) Alcaraz, J.; Mathey, F. *J. Chem. Soc. Chem. Commun.* **1984**, *1984* (8), 508.
(164) Bansal, R. K.; Gupta, N.; Kumawat, S. K. *Z. Naturforsch. B* **2008**, *63* (3), 321.
(165) Tanaka, H.; Motoki, S. *Bull. Chem. Soc. Jpn.* **1986**, *59* (6), 2047.
(166) Dietz, J.; Renner, J.; Bergsträßer, U.; Binger, P.; Regitz, M. *Eur. J. Org. Chem.* **2003**, *3*, 512.
(167) Alcaraz, J.-M.; Mathey, F. *Tetrahedron Lett.* **1984**, *25* (2), 207.
(168) Märkl, G.; Beckh, H.-J. *Tetrahedron Lett.* **1987**, *28* (30), 3475.
(169) Blug, M.; Mézailles, N. *PhD thesis* **2009**.
(170) Horgen, D. A.; Garner, C. M. *PhD thesis* **2014**.
(171) Fuchs, E.; Keller, M.; Breit, B. *Chem. - Eur. J.* **2006**, *12* (26), 6930.
(172) Chen, C.-F.; Ma, Y.-X. *Iptycenes Chemistry: From Synthesis to Applications*; Springer, **2013**.
(173) Ishii, A.; Takaki, I.; Nakayama, J.; Hoshino, M. *Tetrahedron Lett.* **1993**, *34* (51), 8255.
(174) Jongsma, C.; de Kleijn, J. P.; Bickelhaupt, F. *Tetrahedron* **1974**, *30* (18), 3465.
(175) Hellwinkel, D.; Schenk, W. *Angew. Chem. Int. Ed.* **1969**, *8* (12), 987.
(176) Weinberg, K. G.; Whipple, E. B. *J. Am. Chem. Soc.* **1971**, *93* (7), 1801.
(177) Tsuji, H.; Inoue, T.; Kaneta, Y.; Sase, S.; Kawachi, A.; Tamao, K. *Organometallics* **2006**, *25* (26), 6142.
(178) Kobayashi, J.; Agou, T.; Kawashima, T. *Chem. Lett.* **2003**, *32* (12), 1144.
(179) Agou, T.; Kobayashi, J.; Kawashim, T. *Heteroatom Chem.* **2004**, *15* (6), 437.
(180) Kobayashi, J.; Agou, T.; Kawashima, T. *Phosphorus Sulfur Silicon Relat. Elem.* **2004**, *179* (4–5), 959.
(181) Breit, B.; Fuchs, E. *Synthesis - Stuttgart* **2006**, *13*, 2121.
(182) Agou, T.; Kobayashi, J.; Kawashima, T. *Chem. Lett.* **2004**, *33* (8), 1028.
(183) Wallis, C.; Edwards, P. G.; Hanton, M.; Newman, P. D.; Stasch, A.; Jones, C.; Tooze, R. P. *Dalton Trans.* **2009**, *12*, 2170.
(184) Mézailles, N.; Ricard, L.; Mathey, F.; Le Floch, P. *Eur. J. Inorg. Chem.* **1999**, *12*, 2233.
(185) Breit, B.; Fuchs, E. *Chem. Commun.* **2004**, *6*, 694.
(186) Bäuerlein, P. S.; Gonzalez, I. A.; Weemers, J. J. M.; Lutz, M.; Spek, A. L.; Vogt, D.; Müller, C. *Chem. Commun.* **2009**, *33*, 4944.

(187) Blug, M.; Guibert, C.; Le Goff, X.-F.; Mézailles, N.; Le Floch, P. *Chem. Commun.* **2008**, *210* (2), 201.
(188) Ribagnac, P.; Blug, M.; Villa-Uribe, J.; Le Goff, X.-F.; Gosmini, C.; Mézailles, N. *Chem. - Eur. J.* **2011**, *17* (51), 14389.
(189) Ortiz, D.; Blug, M.; Le Goff, X.-F.; Le Floch, P.; Mézailles, N.; Maître, P. *Organometallics* **2012**, *31* (17), 5975.
(190) Blug, M.; Le Goff, X.-F.; Mézailles, N.; Le Floch, P. *Organometallics* **2009**, *28* (8), 2360.
(191) Welfelé, S.; Mézailles, N.; Maigrot, N.; Ricard, L.; Mathey, F.; Le Floch, P. *New J. Chem.* **2001**, *25* (10), 1264.
(192) Annen, U.; Regitz, M. *Tetrahedron Lett.* **1987**, *28* (43), 5141.
(193) Krespan, C. G.; McKusick, B. C.; Cairns, T. L. *J. Am. Chem. Soc.* **1960**, *82* (6), 1515.
(194) Krespan, C. G. *J. Am. Chem. Soc.* **1961**, *83* (16), 3432.
(195) Kobayashi, Y.; Kumadaki, I.; Ohsawa, A.; Hamana, H. *Tetrahedron Lett.* **1977**, *18* (10), 867.
(196) Kobayashi, Y.; Hamana, H.; Fujino, S.; Ohsawa, A.; Kumadaki, I. *J. Org. Chem.* **1979**, *44* (26), 4930.
(197) Kobayashi, Y.; Hamana, H.; Fujino, S.; Ohsawa, A.; Kumadaki, I. *J. Am. Chem. Soc.* **1980**, *102* (1), 252.
(198) Peters, C.; Stutzmann, S.; Disteldorf, H.; Werner, S.; Bergsträßer, U.; Krüger, C.; Binger, P.; Regitz, M. *Synthesis - Stuttgart* **2000**, *4*, 529.
(199) Peters, C.; Disteldorf, H.; Fuchs, E.; Werner, S.; Stutzmann, S.; Bruckmann, J.; Krüger, C.; Binger, P.; Heydt, H.; Regitz, M. *Eur. J. Org. Chem.* **2001**, 3425.
(200) Binger, P.; Glaser, G.; Gabor, B.; Mynott, R. *Angew. Chem. Int. Ed.* **1995**, *34* (1), 81.
(201) Binger, P.; Stannek, J.; Gabor, B.; Mynott, R.; Bruckmann, J.; Krüger, C.; Leininger, S. *Angew. Chem. Int. Ed.* **1995**, *34* (20), 2227.
(202) Binger, P.; Stutzmann, S.; Bruckmann, J.; Krüger, C.; Grobe, J.; Le Van, D.; Pohlmeyer, T. *Eur. J. Inorg. Chem.* **1998**, *12*, 2071.
(203) Bachrach, S. M.; Magdalinos, P. *J. Mol. Struct. Theochem* **1996**, *368*, 1.
(204) Jones, C.; Schulten, C.; Stasch, A. *Dalton Trans.* **2007**, *19*, 1929.
(205) Cloke, F. G. N.; Hitchcock, P. B.; Nixon, J. F.; Vickers, D. M. *J. Organomet. Chem.* **2001**, *635* (1–2), 212.
(206) Himeshima, Y.; Sonoda, T.; Kobayashi, H. *Chem. Lett.* **1983**, *12* (8), 1211.
(207) Kitamura, T.; Yamane, M. *J. Chem. Soc. Chem. Commun.* **1995**, *983* (9), 983.
(208) Sanz, R. *Org. Prep. Proced. Int.* **2008**, *40* (3), 215.
(209) Yoshida, S.; Uchida, K.; Hosoya, T. *Chem. Lett.* **2015**, *44* (5), 691.
(210) Yoshida, S.; Hosoya, T. *Chem. Lett.* **2015**, *44* (11), 1450.
(211) Chen, Q.; Yu, H.; Xu, Z.; Lin, L.; Jiang, X.; Wang, R. *J. Org. Chem.* **2015**, *80* (13), 6890.
(212) Sundalam, S. K.; Nilova, A.; Seidl, T. L.; Stuart, D. R. *Angew. Chem. Int. Ed.* **2016**, *55* (29), 8431.
(213) Wentrup, C. *Aust. J. Chem.* **2010**, *63* (7), 979.
(214) Sapountzis, I.; Lin, W.; Fischer, M.; Knochel, P. *Angew. Chem. Int. Ed.* **2004**, *43* (33), 4364.
(215) Knochel, P.; Dohle, W.; Gommermann, N.; Kneisel, F. F.; Kopp, F.; Korn, T.; Sapountzis, I.; Vu, V. A. *Angew. Chem. Int. Ed.* **2003**, *42* (36), 4302.
(216) Palau, C.; Berchadsky, Y.; Chalier, F.; Finet, J.-P.; Gronchi, G.; Tordo, P. *J. Phys. Chem.* **1995**, *99* (1), 158.
(217) Märkl, G.; Dietl, S.; Ziegler, M. L.; Nuber, B. *Angew. Chem. Int. Ed.* **1988**, *27* (3), 389.
(218) Klebach, T. C.; Turkenburg, L. A. N.; Bickelhaupt, F. *Tetrahedron Lett.* **1978**, *19* (12), 1099.
(219) Blug, M.; Piechaczyk, O.; Fustier, M.; Mézailles, N.; Le Floch, P. *J. Org. Chem.* **2008**, *73* (8), 3258.
(220) Dunn, N. L.; Ha, M.; Radosevich, A. T. *J. Am. Chem. Soc.* **2012**, *134* (28), 11330.
(221) Fey, N.; Papadouli, S.; Pringle, P. G.; Ficks, A.; Fleming, J. T.; Higham, L. J.; Wallis, J. F.;

Carmichael, D.; Mézailles, N.; Müller, C. *Phosphorus Sulfur Silicon Relat. Elem.* **2015**, *190* (5–6), 706.
(222) Pickardt, J.; Rösch, L.; Schumann, H. *Z. Anorg. Allg. Chem.* **1976**, *426* (1), 66.
(223) Gao, J.; Pan, X.; Liu, J.; Lai, J.; Chang, L.; Yuan, G. *RSC Adv.* **2015**, *5* (35), 27439.
(224) Dong, C.-G.; Hu, Q.-S. *Org. Lett.* **2006**, *8* (22), 5057.
(225) Durden, J. A.; Crosby, D. G. *J. Org. Chem.* **1965**, *30* (5), 1684.
(226) Spek, A. L. *Acta Crystallogr. C* **2015**, *71* (1), 9.
(227) Van der Sluis, P.; Spek, A. L. *Acta Crystallogr. A* **1990**, *46* (3), 194.
(228) Hine, J.; Brown, J. A.; Zalkow, L. H.; Gardner, W. E.; Hine, M. *J. Am. Chem. Soc.* **1955**, *77* (3), 594.
(229) Zimmerman, H. E.; Paufler, R. M. *J. Am. Chem. Soc.* **1960**, *82* (6), 1514.
(230) Heilbronner, E. *Tetrahedron Lett.* **1964**, *5* (29), 1923.
(231) Zimmerman, H. E. *J. Am. Chem. Soc.* **1966**, *88* (7), 1564.
(232) Zimmerman, H. E.; Grunewald, G. L.; Paufler, R. M.; Sherwin, M. A. *J. Am. Chem. Soc.* **1969**, *91* (9), 2330.
(233) Rzepa, H. S. *Chem. Rev.* **2005**, *105* (10), 3697.
(234) Zimmerman, H. E.; Grunewald, G. L. *J. Am. Chem. Soc.* **1966**, *88* (1), 183.
(235) Zimmerman, H. E.; Binkley, R. W.; Givens, R. S.; Grunewald, G. L.; Sherwin, M. A. *J. Am. Chem. Soc.* **1969**, *91* (12), 3316.
(236) Zhao, J.; Wu, W.; Sun, J.; Guo, S. *Chem. Soc. Rev.* **2013**, *42* (12), 5323.
(237) Cheng, A. K.; Anet, F. A. L.; Mioduski, J.; Meinwald, J. *J. Am. Chem. Soc.* **1974**, *96* (9), 2887.
(238) Zimmerman, H. E.; Binkley, R. W.; Givens, R. S.; Sherwin, M. A. *J. Am. Chem. Soc.* **1967**, *89* (15), 3932.
(239) Zimmerman, H. E.; Mariano, P. S. *J. Am. Chem. Soc.* **1969**, *91* (7), 1718.
(240) Zimmerman, H. E.; Armesto, D. *Chem. Rev.* **1996**, *96*, 3065.
(241) Zimmerman, H. E.; Sulzbach, H. M.; Tollefson, M. B. *J. Am. Chem. Soc.* **1993**, *115* (15), 6548.
(242) Zimmerman, H. E.; Kutateladze, A. G.; Maekawa, Y.; Mangette, J. E. *J. Am. Chem. Soc.* **1994**, *116* (21), 9795.
(243) Ciganek, E. *J. Am. Chem. Soc.* **1966**, *88* (12), 2882.
(244) Rabideau, P. W.; Hamilton, J. B.; Friedman, L. *J. Am. Chem. Soc.* **1968**, *90* (16), 4465.
(245) Ramaiah, D.; Sajimon, M. C.; Joseph, J.; George, M. V. *Chem. Soc. Rev.* **2005**, *34* (1), 48.
(246) Zimmerman, H. E.; Givens, R. S.; Pagni, R. M. *J. Am. Chem. Soc.* **1968**, *90* (22), 6096.
(247) Adam, W.; Lucchi, O. De. *J. Am. Chem. Soc.* **1982**, *2*, 5747.
(248) Matute, R. A.; Houk, K. N. *Angew. Chem. Int. Ed.* **2012**, *51* (52), 13097.
(249) Jiménez-Osés, G.; Liu, P.; Matute, R. A.; Houk, K. N. *Angew. Chem. Int. Ed.* **2014**, *53* (33), 8664.
(250) Chen, J.; Scheffer, J. R.; Trotter, J. *Tetrahedron* **1992**, *48* (16), 3251.
(251) Matute, R. A.; Garcia-Garibay, M. A.; Houk, K. N. *Org. Lett.* **2014**, *16* (19), 5232.
(252) Liu, R. S. H. *J. Am. Chem. Soc.* **1968**, *90* (1), 215.
(253) Liu, R. S. H.; Krespan, C. G. *J. Org. Chem.* **1969**, *34* (5), 1271.
(254) Mack, A.; Breit, B.; Wettling, T.; Bergsträsser, U.; Leininger, S.; Regitz, M. *Angew. Chem. Int. Ed.* **1997**, *36* (12), 1337.
(255) Binger, P.; Günther, K.; Regitz, M. *Synthesis - Stuttgart* **1999**, *8*, 1363.
(256) Geier, J.; Frison, G.; Grützmacher, H. *Angew. Chem. Int. Ed.* **2003**, *42* (33), 3955.
(257) Allen, F. H.; Kennard, O.; Watson, D. G.; Brammer, L.; Orpen, A. G.; Taylor, R. *J. Chem. Soc. Perkin Trans. 2* **1987**, *12*, S1.
(258) Richter, W. J. *Chem. Ber.* **1983**, *116* (10), 3293.
(259) Koziar, J. C.; Cowan, D. O. *Acc. Chem. Res.* **1978**, *11* (9), 334.

(260) Frisch, M. J.; Trucks, G. W.; Schlegel, H. B.; Scuseria, G. E.; Robb, M. A.; Cheeseman, J. R.; Scalmani, G.; Barone, V.; Mennucci, B.; Petersson, G. A.; Nakatsuji, H.; Caricato, M.; Li, X.; Hratchian, H. P.; Izmaylov, A. F.; Bloino, J.; Zheng, G.; Sonnenberg, J. L.; Hada, M.; Ehara, M.; Toyota, K.; Fukuda, R.; Hasegawa, J.; Ishida, M.; Nakajima, T.; Honda, Y.; Kitao, O.; Nakai, H.; Vreven, T.; Montgomery, J. A., J.; Peralta, J. E.; Ogliaro, F.; Bearpark, M.; Heyd, J. J.; Brothers, E.; Kudin, K. N.; Staroverov, V. N.; Kobayashi, R.; Normand, J.; Raghavachari, K.; Rendell, A.; Burant, J. C.; Iyengar, S. S.; Tomasi, J.; Cossi, M.; Rega, N.; Millam, J. M.; Klene, M.; Knox, J. E.; Cross, J. B.; Bakken, V.; Adamo, C.; Jaramillo, J.; Gomperts, R.; Stratmann, R. E.; Yazyev, O.; Austin, A. J.; Cammi, R.; Pomelli, C.; Ochterski, J. W.; Martin, R. L.; Morokuma, K.; Zakrzewski, V. G.; Voth, G. A.; Salvador, P.; Dannenberg, J. J.; Dapprich, S.; Daniels, A. D.; Farkas, Ö.; Foresman, J. B.; Ortiz, J. V; Cioslowski, J.; Fox, D. J. Gaussian Inc.: Wallingford CT 2009,.
(261) Zhao, Y.; Truhlar, D. G. *Theor. Chem. Acc.* **2008**, *120* (1–3), 215.
(262) Hariharan, P. C.; Pople, J. A. *Theor. Chim. Acta* **1973**, *28* (3), 213.
(263) Hehre, W. J.; Ditchfield, R.; Pople, J. A. *J. Chem. Phys.* **1972**, *56* (5), 2257.
(264) Francl, M. M.; Pietro, W. J.; Hehre, W. J.; Binkley, J. S.; Gordon, M. S.; DeFrees, D. J.; Pople, J. A. *J. Chem. Phys.* **1982**, *77* (7), 3654.
(265) Flack, H. D. *Acta Crystallogr. A* **1983**, *39* (6), 876.
(266) Brown, T. L.; Lee, K. J. *Coord. Chem. Rev.* **1993**, *128* (1–2), 89.
(267) Fey, N.; Orpen, A. G.; Harvey, J. N. *Coord. Chem. Rev.* **2009**, *253* (5–6), 704.
(268) Tolman, C. A. *J. Am. Chem. Soc.* **1970**, *92* (10), 2956.
(269) Tolman, C. A.; Seidel, W. C.; Gosser, L. W. *J. Am. Chem. Soc.* **1974**, *96* (1), 53.
(270) Müller, T. E.; Mingos, D. M. P. *Transit. Metal Chem.* **1995**, *20* (6), 533.
(271) White, D.; Taverner, B. C.; Leach, P. G. L.; Coville, N. J. *J. Comput. Chem.* **1993**, *14* (9), 1042.
(272) White, D.; Tavener, B. C.; Leach, P. G. L.; .Coville, N. J. *J. Organomet. Chem.* **1994**, *478* (1–2), 205.
(273) White, D.; Taverner, B. C.; Coville, N. J.; Wade, P. W. *J. Organomet. Chem.* **1995**, *495* (1–2), 41.
(274) Brown, T. L. *Inorg. Chem.* **1992**, *31* (7), 1286.
(275) Suresh, C. H.; Koga, N. *Inorg. Chem.* **2002**, *41* (6), 1573.
(276) Suresh, C. H. *Inorg. Chem.* **2006**, *45* (13), 4982.
(277) Cavallo, L.; Correa, A.; Costabile, C.; Jacobsen, H. *J. Organomet. Chem.* **2005**, *690* (24–25), 5407.
(278) Poater, A.; Ragone, F.; Giudice, S.; Costabile, C.; Dorta, R.; Nolan, S. P.; Cavallo, L. *Organometallics* **2008**, *27* (12), 2679.
(279) Clavier, H.; Nolan, S. P. *Chem. Commun.* **2010**, *46* (6), 841.
(280) Poater, A.; Cosenza, B.; Correa, A.; Giudice, S.; Ragone, F.; Scarano, V.; Cavallo, L. *Eur. J. Inorg. Chem.* **2009**, *13*, 1759.
(281) Falivene, L.; Credendino, R.; Poater, A.; Petta, A.; Serra, L.; Oliva, R.; Scarano, V.; Cavallo, L. *Organometallics* **2016**, *35* (13), 2286.
(282) Dewar, M. J. S. *Bull. Soc. Chim. Fr.* **1951**, *18*, C71.
(283) Chatt, J.; Duncanson, L. A. *J. Chem. Soc.* **1953**, 2939.
(284) Chatt, J.; Duncanson, L. a.; Venanzi, L. M. *J. Chem. Soc.* **1955**, 4456.
(285) Canac, Y.; Lepetit, C. *Inorg. Chem.* **2017**, *56* (1), 667.
(286) Bodner, G. M.; May, M. P.; McKinney, L. E. *Inorg. Chem.* **1980**, *19* (7), 1951.
(287) Allen, D. W.; Taylor, B. F. *J. Chem. Soc. Dalton* **1982**, *1*, 51.
(288) Kühl, O.; Olaf, K. *Coord. Chem. Rev.* **2005**, *249* (5–6), 693.
(289) Beckmann, U.; Süslüyan, D.; Kunz, P. C. *Phosphorus Sulfur Silicon Relat. Elem.* **2011**, *186* (10), 2061.

(290) Cotton, F. a; Kraihanzel, C. S. *J. Am. Chem. Soc.* **1962**, *84* (23), 4432.
(291) Kraihanzel, C. S.; Cotton, F. A. *Inorg. Chem.* **1963**, *2* (3), 533.
(292) Cotton, F. A. *Inorg. Chem.* **1964**, *3* (5), 702.
(293) Strohmeier, W.; Guttenberger, J. F. *Chem. Ber.* **1964**, *97* (7), 1871.
(294) Strohmeier, W.; Müller, F. J. *Chem. Ber.* **1967**, *100* (9), 2812.
(295) Anton, D. R.; Crabtree, R. H. *Organometallics* **1983**, *2* (2), 621.
(296) Chianese, A.; Li, X.; Janzen, M.; Faller, J.; Crabtree, R. *Organometallics* **2003**, *22*, 1663.
(297) Golovin, M. N.; Rahman, M. M.; Belmonte, J. E.; Giering, W. P. *Organometallics* **1985**, *4* (11), 1981.
(298) Wilson, M. R.; Prock, A.; Giering, W. P.; Fernandez, A. L.; Haar, C. M.; Nolan, S. P.; Foxman, B. M. *Organometallics* **2002**, *21* (13), 2758.
(299) Landis, C. R.; Feldgus, S.; Uddin, J.; Wozniak, C. E.; Moloy, K. G. *Organometallics* **2000**, *19* (23), 4878.
(300) Frenking, G.; Fröhlich, N. *Chem. Rev.* **2000**, *100* (2), 717.
(301) Perrin, L.; Clot, E.; Eisenstein, O.; Loch, J.; Crabtree, R. H. *Inorg. Chem.* **2001**, *40*, 5806.
(302) Kalescky, R.; Kraka, E.; Cremer, D. *Inorg. Chem.* **2014**, *53* (1), 478.
(303) Setiawan, D.; Kalescky, R.; Kraka, E.; Cremer, D. *Inorg. Chem.* **2016**, *55* (7), 3713.
(304) Knoch, F.; Kremer, F.; Schmidt, U.; Zenneck, U.; Le Floch, P.; Mathey, F. *Organometallics* **1996**, *15*, 2713.
(305) Le Floch, P.; Knoch, F.; Kremer, F.; Mathey, F.; Scholz, J.; Scholz, W.; Thiele, K.-H.; Zenneck, U. *Eur. J. Inorg. Chem.* **1998**, *1998* (1), 119.
(306) Miyake, Y.; Isomura, E.; Iyoda, M. *Chem. Lett.* **2006**, *35* (8), 836.
(307) Bell, J. R.; Franken, A.; Garner, C. M. *Tetrahedron* **2009**, *65* (45), 9368.
(308) Breit, B. *Chem. Commun.* **1996**, *17*, 2071.
(309) Breit, B.; Winde, R.; Harms, K. *J. Chem. Soc. Perkin Trans. 1* **1997**, *4* (18), 2681.
(310) Reetz, M.; Guo, H. *Synlett* **2006**, *13*, 2127.
(311) Reetz, M. T.; Mehler, G. *Tetrahedron Lett.* **2003**, *44* (24), 4593.
(312) Müller, C.; López, L. G.; Kooijman, H.; Spek, A. L.; Vogt, D. *Tetrahedron Lett.* **2006**, *47* (12), 2017.
(313) Doux, M.; Piechaczyk, O.; Cantat, T.; Mézailles, N.; Le Floch, P. *C. R. Chim.* **2007**, *10*, 573.
(314) Hamada, Y.; Seto, N.; Ohmori, H.; Hatano, K. *Tetrahedron Lett.* **1996**, *37* (42), 7565.
(315) Robin, F.; Mercier, F.; Ricard, L.; Mathey, F.; Spagnol, M. *Chem. - Eur. J.* **1997**, *3* (8), 1365.
(316) Chen, Z.; Jiang, Q.; Zhu, G.; Xiao, D.; Cao, P.; Guo, C.; Zhang, X. *J. Org. Chem.* **1997**, *62*, 4521.
(317) Jiang, Q.; Xiao, D.; Zhang, Z.; Cao, P.; Zhang, X. *Angew. Chem. Int. Ed.* **1999**, *38* (4), 516.
(318) Gilbertson, S. R.; Genov, D. G.; Rheingold, A. L. *Org. Lett.* **2000**, *2* (18), 2885.
(319) Clochard, M.; Mattmann, E.; Mercier, F.; Ricard, L.; Mathey, F. *Org. Lett.* **2003**, *5* (17), 3093.
(320) Henry, C. E.; Xu, Q.; Fan, Y. C.; Martin, T. J.; Belding, L.; Dudding, T.; Kwon, O. *J. Am. Chem. Soc.* **2014**, *136*, 11890.
(321) Lee, A.; Kim, H. *J. Am. Chem. Soc.* **2015**, *137* (35), 11250.
(322) Zagidullin, A.; Miluykov, V.; Sinyashin, O.; Hey-Hawkins, E. *Catal. Today* **2017**, *279*, 142.
(323) Roberts, J. D.; McElhill, E. A.; Armstrong, R. *J. Am. Chem. Soc.* **1949**, *71* (8), 2923.
(324) Roberts, J. D.; Regan, C. M. *J. Am. Chem. Soc.* **1953**, *75* (16), 4102.
(325) Benkeser, R. A.; Krysiak, H. R. *J. Am. Chem. Soc.* **1953**, *75* (10), 2421.
(326) Gassman, P. G.; Deck, P. A.; Winter, C. H.; Dobbs, D. A.; Cao, D. H. *Organometallics* **1992**, *11* (2), 959.
(327) Ferro, V. R.; Omar, S.; González-Jonte, R. H.; García de la Vega, J. M. *Heteroatom Chem.* **2003**, *14* (2), 160.
(328) Mitoraj, M. P.; Michalak, A.; Ziegler, T. *J. Chem. Theory Comput.* **2009**, *5* (4), 962.

(329) Ardizzoia, G. A.; Brenna, S. *Phys. Chem. Chem. Phys.* **2017**, *19* (8), 5971.
(330) Adcock, W.; Aldous, G. L.; Kitching, W. *Tetrahedron Lett.* **1978**, *19* (36), 3387.
(331) Echavarren, A. M.; Hashmi, A. S. K.; Toste, F. D. *Adv. Synth. Catal.* **2016**, *358* (9), 1347.
(332) Hashmi, A. S. K.; Hutchings, G. J. *Angew. Chem. Int. Ed.* **2006**, *45* (47), 7896.
(333) Hashmi, A. S. K. *Chem. Rev.* **2007**, *107* (7), 3180.
(334) Marion, N.; Nolan, S. P. *Chem. Soc. Rev.* **2008**, *37* (9), 1776.
(335) Gorin, D. J.; Sherry, B. D.; Toste, F. D. *Chem. Rev.* **2008**, *108* (8), 3351.
(336) Hashmi, A. S. K.; Rudolph, M. *Chem. Soc. Rev.* **2008**, *37* (9), 1766.
(337) Rudolph, M.; Hashmi, A. S. K. *Chem. Soc. Rev.* **2012**, *41* (6), 2448.
(338) Jiménez-Núñez, E.; Echavarren, A. M. *Chem. Rev.* **2008**, *108* (8), 3326.
(339) Dorel, R.; Echavarren, A. M. *Chem. Rev.* **2015**, *115* (17), 9028.
(340) Tarselli, M. A.; Gagné, M. R. *J. Org. Chem.* **2008**, *73* (6), 2439.
(341) Suárez-Pantiga, S.; Hernández-Díaz, C.; Piedrafita, M.; Rubio, E.; González, J. M. *Adv. Synth. Catal.* **2012**, *354* (9), 1651.
(342) Delpont, N.; Escofet, I.; Pérez-Galán, P.; Spiegl, D.; Raducan, M.; Bour, C.; Sinisi, R.; Echavarren, A. M. *Catal. Sci. Technol.* **2013**, *3* (11), 3007.
(343) Blanco Jaimes, M. C.; Rominger, F.; Pereira, M. M.; Carrilho, R. M. B.; Carabineiro, S. A. C.; Hashmi, a S. K. *Chem. Commun.* **2014**, *50* (38), 4937.
(344) Nieto-Oberhuber, C.; Muñoz, M. P.; Buñuel, E.; Nevado, C.; Cárdenas, D. J.; Echavarren, A. M. *Angew. Chem. Int. Ed.* **2004**, *43* (18), 2402.
(345) Nieto-Oberhuber, C.; López, S.; Echavarren, A. M. *J. Am. Chem. Soc.* **2005**, *127* (17), 6178.
(346) Mézailles, N.; Ricard, L.; Gagosz, F. *Org. Lett.* **2005**, *7* (19), 4133.
(347) Nieto-Oberhuber, C.; Muñoz, M. P.; López, S.; Jiménez-Núñez, E.; Nevado, C.; Herrero-Gómez, E.; Raducan, M.; Echavarren, A. M. *Chem. - Eur. J.* **2006**, *12* (6), 1677.
(348) Freytag, M.; Ito, S.; Yoshifuji, M. *Chem. – An Asian J.* **2006**, *1* (5), 693.
(349) Ito, S.; Kusano, S.; Morita, N.; Mikami, K.; Yoshifuji, M. *J. Organomet. Chem.* **2010**, *695* (2), 291.
(350) Ito, S.; Zhai, L.; Mikami, K. *Chem. - Asian J.* **2011**, *6* (11), 3077.
(351) Guérinot, A.; Fang, W.; Sircoglou, M.; Bour, C.; Bezzenine-Lafollée, S.; Gandon, V. *Angew. Chem. Int. Ed.* **2013**, *52* (22), 5848.
(352) Fang, W.; Presset, M.; Guérinot, A.; Bour, C.; Bezzenine-Lafollée, S.; Gandon, V. *Chem. - Eur. J.* **2014**, *20* (18), 5439.
(353) Wright, J. R.; Young, P. C.; Lucas, N. T.; Lee, A.; Crowley, J. D. *Organometallics* **2013**, *32* (23), 7065.
(354) Hashmi, a S. K.; Weyrauch, J. P.; Frey, W.; Bats, J. W. *Org. Lett.* **2004**, *6* (23), 4391.
(355) Hashmi, A. S. K.; Rudolph, M.; Schymura, S.; Visus, J.; Frey, W. *Eur. J. Org. Chem.* **2006**, *21*, 4905.
(356) Hashmi, A. S. K.; Loos, A.; Littmann, A.; Braun, I.; Knight, J.; Doherty, S.; Rominger, F. *Adv. Synth. Catal.* **2009**, *351* (4), 576.
(357) Doherty, S.; Knight, J. G.; Hashmi, A. S. K.; Smyth, C. H.; Ward, N. A. B.; Robson, K. J.; Tweedley, S.; Harrington, R. W.; Clegg, W. *Organometallics* **2010**, *29* (18), 4139.
(358) Hashmi, A. S. K.; Loos, A.; Doherty, S.; Knight, J. G.; Robson, K. J.; Rominger, F. *Adv. Synth. Catal.* **2011**, *353* (5), 749.
(359) Hashmi, A. S. K.; Blanco Jaimes, M. C.; Schuster, A. M.; Rominger, F. *J. Org. Chem.* **2012**, *77* (15), 6394.
(360) Biasiolo, L.; Del Zotto, A.; Zuccaccia, D. *Organometallics* **2015**, *34* (9), 1759.
(361) de Krom, I.; Broeckx, L. E. E.; Lutz, M.; Müller, C. *Chem. - Eur. J.* **2013**, *19* (11), 3676.
(362) Gorin, D. J.; Toste, F. D. *Nature* **2007**, *446* (7134), 395.
(363) Hertwig, R. H.; Koch, W.; Schröder, D.; Schwarz, H.; Hrušák, J.; Schwerdtfeger, P. *J. Phys. Chem.* **1996**, *100* (30), 12253.

(364) Nechaev, M. S.; Rayón, V. M.; Frenking, G. *J. Phys. Chem. A* **2004**, *108* (15), 3134.
(365) Doherty, S.; Knight, J. G.; Perry, D. O.; Ward, N. A. B.; Bittner, D. M.; McFarlane, W.; Wills, C.; Probert, M. R. *Organometallics* **2016**, *35* (9), 1265.
(366) Crous, R.; Datt, M.; Foster, D.; Bennie, L.; Steenkamp, C.; Huyser, J.; KirstenCurrent address: Dept Chemis, L.; Steyl, G.; Roodt, A. *Dalton Trans.* **2005**, *8* (6), 1108.
(367) Becke, A. D. *J. Chem. Phys.* **1993**, *98* (7), 5648.
(368) Perdew, J. P.; Wang, Y. *Phys. Rev. B* **1992**, *45* (23), 13244.
(369) Petersson, G. A.; Bennett, A.; Tensfeldt, T. G.; Al-Laham, M. A.; Shirley, W. A.; Mantzaris, J. *J. Chem. Phys.* **1988**, *89* (4), 2193.
(370) Petersson, G. A.; Al-Laham, M. A. *J. Chem. Phys.* **1991**, *94* (9), 6081.
(371) Hay, P. J.; Wadt, W. R. *J. Chem. Phys.* **1985**, *82* (1), 299.
(372) Ehlers, A. W.; Böhme, M.; Dapprich, S.; Gobbi, A.; Höllwarth, A.; Jonas, V.; Köhler, K. F.; Stegmann, R.; Veldkamp, A.; Frenking, G. *Chem. Phys. Lett.* **1993**, *208* (1–2), 111.
(373) Scott, A. P.; Radom, L. *J. Phys. Chem.* **1996**, *100* (41), 16502.
(374) Van Lenthe, E.; Baerends, E. J. *J. Comput. Chem.* **2003**, *24* (9), 1142.
(375) Van Lenthe, E.; Baerends, E. J.; Snijders, J. G. *J. Chem. Phys.* **1994**, *101* (11), 9783.
(376) Van Lenthe, E.; Ehlers, A.; Baerends, E.-J. *J. Chem. Phys.* **1999**, *110* (18), 8943.
(377) Van Lenthe, E.; Baerends, E. J.; Snijders, J. G. *J. Chem. Phys.* **1993**, *99* (6), 4597.
(378) Velde, G.; Bickelhaupt, F. M.; Baerends, E. J.; Fonseca Guerra, C.; van Gisbergen, S. J. a.; Snijders, J. G.; Ziegler, T. *J. Comput. Chem.* **2001**, *22* (9), 931.
(379) Fonseca Guerra, C.; Snijders, J. G.; te Velde, G.; Baerends, E. J. *Theor. Chem. Acc.* **1998**, *99* (6), 391.
(380) ADF2016, SCM, Theoretical Chemistry, Vrije Universiteit: Amsterdam, The Netherlands.